National Library
of Canada

Canadian Theses Service

Ottawa, Canada
K1A 0N4

Bibliothèque nationale
du Canada

Service des thèses canadiennes

NOTICE

The quality of this microform is heavily dependent upon the quality of the original thesis submitted for microfilming. Every effort has been made to ensure the highest quality of reproduction possible.

If pages are missing, contact the university which granted the degree.

Some pages may have indistinct print especially if the original pages were typed with a poor typewriter ribbon or if the university sent us an inferior photocopy.

Reproduction in full or in part of this microform is governed by the Canadian Copyright Act, R.S.C. 1970, c. C-30, and subsequent amendments.

AVIS

La qualité de cette microforme dépend grandement de la qualité de la thèse soumise au microfilmage. Nous avons tout fait pour assurer une qualité supérieure de reproduction.

S'il manque des pages, veuillez communiquer avec l'université qui a conféré le grade.

La qualité d'impression de certaines pages peut laisser à désirer, surtout si les pages originales ont été dactylographiées à l'aide d'un ruban usé ou si l'université nous a fait parvenir une photocopie de qualité inférieure.

La reproduction, même partielle, de cette microforme est soumise à la Loi canadienne sur le droit d'auteur, SRC 1970, c. C-30, et ses amendements subséquents.

NL-339 (r. 88/04) c

Canada

National Library
of Canada

Bibliothèque nationale
du Canada

Canadian Theses Service

Service des thèses canadiennes

Ottawa, Canada
K1A 0N4

The author has granted an irrevocable non-exclusive licence allowing the National Library of Canada to reproduce, loan, distribute or sell copies of his/her thesis by any means and in any form or format, making this thesis available to interested persons.

L'auteur a accordé une licence irrévocable et non exclusive permettant à la Bibliothèque nationale du Canada de reproduire, prêter, distribuer ou vendre des copies de sa thèse de quelque manière et sous quelque forme que ce soit pour mettre des exemplaires de cette thèse à la disposition des personnes intéressées.

The author retains ownership of the copyright in his/her thesis. Neither the thesis nor substantial extracts from it may be printed or otherwise reproduced without his/her permission.

L'auteur conserve la propriété du droit d'auteur qui protège sa thèse. Ni la thèse ni des extraits substantiels de celle-ci ne doivent être imprimés ou autrement reproduits sans son autorisation.

ISBN 0-315-55616-1

Canadä

THE UNIVERSITY OF ALBERTA

QUANTITATIVE REFLECTANCE SPECTROSCOPY OF MIXTURES CONTAINING MAFIC SILICATES WITH APPLICATIONS TO PLANETARY GEOLOGY

by

EDWARD ANTHONY CLOUTIS ©

A THESIS
SUBMITTED TO THE FACULTY OF GRADUATE STUDIES AND RESEARCH
IN PARTIAL FULFILMENT OF THE REQUIREMENTS FOR THE DEGREE
OF DOCTOR OF PHILOSOPHY

DEPARTMENT OF GEOLOGY

EDMONTON, ALBERTA
FALL 1989

THE UNIVERSITY OF ALBERTA

RELEASE FORM

NAME OF AUTHOR EDWARD ANTHONY CLOUTIS

TITLE OF THESIS QUANTITATIVE REFLECTANCE SPECTROSCOPY OF MIXTURES CONTAINING MAFIC SILICATES WITH APPLICATIONS TO PLANETARY GEOLOGY

DEGREE FOR WHICH THESIS WAS PRESENTED DOCTOR OF PHILOSOPHY

YEAR THIS DEGREE GRANTED FALL 1989

Permission is hereby granted to THE UNIVERSITY OF ALBERTA LIBRARY to reproduce single copies of this thesis and to lend or sell such copies for private, scholarly or scientific research purposes only.

The author reserves other publication rights, and neither the thesis nor extensive extracts from it may be printed or otherwise reproduced without the author's written permission.

(SIGNED) ....

PERMANENT ADDRESS:

Department of Geology
University of Alberta
Edmonton, Alberta T6G 2E3

DATED ....July 11.... 1989

THE UNIVERSITY OF ALBERTA

FACULTY OF GRADUATE STUDIES AND RESEARCH

The undersigned certify that they have read, and recommend to the FACULTY OF GRADUATE STUDIES AND RESEARCH, for acceptance, a thesis entitled QUANTITATIVE REFLECTANCE SPECTROSCOPY OF MIXTURES CONTAINING MAFIC SILICATES WITH APPLICATIONS TO PLANETARY GEOLOGY submitted by EDWARD ANTHONY CLOUTIS in partial fulfilment of the requirements for the degree of DOCTOR OF PHILOSOPHY in GEOLOGY.

....

Supervisor

....

J. Donald Eyton

R.S.j.Lambert

....

External Examiner

Date: June 1, 1989

ABSTRACT

The reflectance spectra of mixtures of mafic silicates with various accessory phases can be used to interpret remotely sensed spectra of many bodies in the solar system. Application of the deconvolution techniques derived from the laboratory spectra of mafic silicate + metal mixtures suggests that the S-class asteroid, (8) Flora, has a surface composed of 50 wt. % metal, 40 % olivine ($Fa=35\pm30$), 10 % orthopyroxene ($Fs=30^{+15}_{-15}$) and a few percent clinopyroxene, corresponding most closely to the pallasite and lodranite meteorites. Similar analysis of the A-class asteroid (446) Aeternitas indicates a surface composed of 35 wt. % metal, 55 % olivine ($Fa=20\pm10$), 3 % orthopyroxene ($Fs<45$), and 7 % clinopyroxene ($Fs<17$). The Eagle Station sub-group of pallasites are the closest meteorite analogues to Aeternitas.

The reflectance spectra of materials which show no distinct absorption bands in the 0.3-2.6μm spectral region display measureable differences in spectral slope. The abundances of carbon and magnetite required to suppress completely mafic silicate absorption bands are quite high. Most dark asteroids should display weak, but resolvable, absorption bands if they are compositionally similar to some dark meteorites such as carbonaceous chondrites and ureilites.

The observational data for an M-class asteroid, (16) Psyche, are largely consistent with a surface composed largely of fine-grained metal. The observational data for an E-class asteroid, (44) Nysa, are consistent with an enstatite achondrite-like surface mineralogy. The main asteroid groups prevalent in the inner part of the main belt to be differentiated objects. If this is the case, theories suggesting widespread and intense heating of the inner main asteroid belt are essentially correct.

Laboratory reflectance spectra of glass-rich mineral mixtures are largely applicable to lunar spectral remote sensing, and perhaps to some asteroids. Current spectrum analysis procedures are not completely satisfactory for determining mafic silicate compositions from absorption band wavelength positions. These procedures could be strengthened by a more

accurate knowledge of the actual continuum slope which affects lunar surface and sample spectra.

ACKNOWLEDGEMENTS

As with any major piece of work, it is difficult to properly thank all the people who knowingly or unknowingly contributed to its completion. My most heartfelt thanks to Dr. Michael Gaffey for your inspiration, support, guidance, and wisdom, and for showing me all the qualities which a true scientist should embody. Special thanks to the committee members- Drs. Dorian Smith, Richard Lambert, Ron Eyton, and Doug Hube- for having enough confidence in me and my work to let it happen, in particular to Drs. Smith and Lambert for the crucial day-to-day support and advice. An additional kudos to Dr. Smith for his help in obtaining the early, crucial financial support to launch this project.

On a more practical note, many thanks to Dr. Roger N. Clark and Greg Swayze at the U.S. Geological Survey for providing access to their spectrometer facility; Dr. E.D. Ghent and John Machacek at the University of Calgary microprobe laboratory for their generous help in obtaining the chemical analyses of the various samples; Paul Wagner and David Tomlinson at the University of Alberta microprobe facility for the crucial last minute data; and Alex Stelmack for help with chemical analyses often on short notice. Extra special thanks to Dr. Carle Pieters and Stephen Pratt of the NASA RELAB spectrometer facility for kindly making their laboratory available for my use time after time and putting up with my various self-imposed deadlines.

Grateful thanks to the staff at the various granting agencies who saw fit to invest scarce research dollars in this project- the Sigma Xi Foundation, the Central Research Fund of the University of Alberta, and the Geological Society of America. I hope to able to properly thank you someday. Thanks also to Dr. John Sampron White and Peter Dunn of the Smithsonian Institution for providing some key mineral samples long ago.

A big "hi kids" to the gang of the Geology Department who were there to share, or buy me, a beer or two after an allegedly long hard day, and for our good times in general. I hesitate to name names because I may inadvertently omit someone.

My deepest love to my parents and family- I can't even begin to thank you for all you have done for me. I will love you always.

To my wife, companion, and friend- Rosemarie- your love and support are still priceless to me.

Table of Contents

Chapter Page

ABSTRACT iv

ACKNOWLEDGEMENTS vi

LIST OF TABLES ix

LIST OF FIGURES x

I. INTRODUCTION 1

A. REFERENCES 5

II. METAL-SILICATE MIXTURES: SPECTRAL PROPERTIES AND APPLICATIONS TO ASTEROID TAXONOMY 7

A. REFERENCES 45

III. REFLECTANCE SPECTRA OF "FEATURELESS" MATERIALS AND THE SURFACE MINERALOGIES OF M- AND E-CLASS ASTEROIDS 55

A. REFERENCES 87

IV. REFLECTANCE SPECTRA OF MAFIC SILICATE-OPAQUE ASSEMBLAGES WITH APPLICATIONS TO METEORITE SPECTRA 95

A. REFERENCES 127

V. REFLECTANCE SPECTRA OF GLASS-BEARING MAFIC SILICATE MIXTURES AND SPECTRAL DECONVOLUTION PROCEDURES 140

A. REFERENCES 173

VI. CONCLUSION 179

A. REFERENCES 184

VII. APPENDIX 187

A. REFERENCES 192

LIST OF TABLES

Table Page

II-1. Chemical analyses of olivine (OLV003), pyroxenes (PYX032, PYX117), and meteoritic metal (MET101) 32

III-1. Chemical analyses of olivine (OLV003), pyroxene (PYX032), magnetite (MAG101), and meteoritic metal (MET101) 74

IV-1. Chemical analyses of olivine (OLV003), pyroxene (PYX032), and magnetite (MAG101) 115

IV-2. Magnetite and carbon abundances in various meteorite classes 116

IV-3. Selected spectral properties for mafic silicate+carbon and mafic silicate+magnetite samples 117

V-1. Chemical analyses of pyroxene (PYX032), plagioclase (PLG108), and glasses (L1, L31, L32) 154

V-2. Mineral and glass abundances in the lunar analogue samples 155

V-3. Selected spectral properties of some lunar analogue samples 156

LIST OF FIGURES

Figure Page

II-1. Absolute reflectance spectra of the 45-90μm sized olivine + meteoritic metal mixtures ... 33

II-2. Wavelength positions of the intersection of a horizontal continuum with the long wavelength wing of Band I for olivine and olivine + metal mixtures ... 34

II-3. Reflectance ratio (1.8μm: Band I minimum) for olivine and olivine + metal mixtures versus grain size ... 35

II-4. Band I center wavelength position after continuum removal for olivine and olivine + metal mixtures versus olivine iron content ... 36

II-5. Band area ratio of orthopyroxene and orthopyroxene + metal mixtures versus metal content ... 37

II-6. Reflectance ratio (0.7μm peak: Band II minimum) of orthopyroxene and orthopyroxene + metal mixtures versus grain size ... 38

II-7. Reflectance ratio (1.4μm peak: Band I minimum) of orthopyroxene and orthopyroxene + metal mixtures versus grain size ... 39

II-8. Band II-Band I minima separation of orthopyroxenes versus Band II minimum wavelength position ... 40

II-9. Band II-Band I minima separation of orthopyroxenes and orthopyroxene + metal mixtures versus Band II minimum wavelength position ... 41

II-10. Absolute reflectance spectra of 45-90μm sized samples of olivine, orthopyroxene, metal, and various combinations of the three ... 42

II-11. Normalized reflectance spectra of Flora and a possible laboratory analogue ... 43

II-12. Normalized reflectance spectra of Nysa and a possible laboratory analogue ... 44

III-1. Absolute and normalized reflectance spectra of a number of metal powders ... 75

III-2. Absolute and normalized reflectance spectra of different size fractions of meteoritic metal (MET101) 76

III-3. Absolute and normalized reflectance spectra of metal and 99.5/0.5 metal/carbon 77

III-4. Absolute reflectance spectrum of the acid-insoluble fraction of the Happy Canyon E7 enstatite chondrite 78

III-5. Reflectance ratio (1.8μm: 0.7μm peak) of metal, enstatite, and various meteorites 79

III-6. Absolute and normalized reflectance spectra of olivine+carbon mixtures 80

III-7. Absolute and normalized reflectance spectra of orthopyroxene+carbon mixtures 81

III-8. Absolute reflectance spectra of olivine+magnetite mixtures 82

III-9. Absolute reflectance spectra of Psyche, meteoritic metal and meteoritic enstatite 83

III-10. Reflectance ratio (1.6μm: 0.56μm) versus 2.2μm: 0.56μm reflectance ratio for enstatite- and metal-rich meteorites and some asteroids 84

III-11. Reflectance ratio (2.5μm: 1.0μm) versus 1.0μm: 0.35μm reflectance ratio for metal powder and Psyche reflectance spectra 85

III-12. Normalized reflectance spectra of Nysa and meteoritic enstatite 86

IV-1. Normalized reflectance spectra of olivine+magnetite mixtures 118

IV-2. Normalized reflectance spectra of 90/10 olivine/magnetite mixtures 119

IV-3. Absolute reflectance spectrum of amorphous carbon 120

IV-4. Normalized reflectance spectra of orthopyroxene+carbon mixtures 121

IV-5. Normalized reflectance spectra of olivine+carbon mixtures 122

IV-6. Band depth versus carbon content for mafic silicate+carbon spectra 123

IV-7. Absolute reflectance spectrum of Band I area of 99.5/0.5 olivine/carbon mixture..... 124

IV-8. Normalized reflectance spectra of meteoritic metal+carbon mixtures 125

IV-9. Absolute reflectance spectrum of wustite 126

V-1. Absolute reflectance spectrum of ilmenite 157

V-2. Absolute reflectance spectra of plagioclase (PLG108) and orthopyroxene (PYX032).. 158

V-3. Absolute reflectance spectra of samples L1, L2, and L3.................................. 159

V-4. Straight line continuum-divided L1 and L3 spectra 160

V-5. L1 and L3 spectra after division by scaled L2 spectra.. 161

V-6. Absolute reflectance spectra of samples L1 and L8 162

V-7. Absolute reflectance spectra of samples L3 and L9.. 163

V-8. Absolute reflectance spectra of samples L1, L2, L3, L26, and L27 164

V-9. Normalized reflectance spectra of samples L1, L2, L3, L26, and L27..................... 165

V-10. Reflectance ratio (0.400μm: 0.565μm) versus TiO_2 content for lunar and laboratory samples 166

V-11. Straight line continuum-divided L1, L3, L26, and L27 spectra 167

V-12. L1, L3, L26, and L27 spectra after division by scaled L2 spectra 168

V-13. Absolute reflectance spectra of samples L1 and L29 169

V-14. Absolute reflectance spectra of samples L2 and L32 170

V-15. Absolute reflectance spectra of samples L1 and L28 171

V-16. Absolute reflectance spectra of samples L2 and L31 172

I. INTRODUCTION

Remote sensing is the most cost-effective and viable method of geological information gathering for most bodies in the solar system. Large areas can be imaged quickly and repeatedly by land-based, airborne, and spaceborne sensors. Reflectance spectroscopy is one of the most important aspects of remote sensing, but data interpretation techniques have failed to keep pace with advances made in sensor technology and data acquisition procedures. It is imperative that data interpretation be developed to the highest possible degree of sophistication so that the full benefits of spectroscopic remote sensing can be realized.

Empirical laboratory spectral reflectance studies of geological materials are currently the most effective method for developing spectral interpretation algorithms and revealing the physico-chemical processes controlling the spectral properties of minerals. To date, most laboratory spectral studies have lacked an integrated approach to relating spectral properties to the physical and chemical nature of the materials being examined. Mineral spectra often lack detailed chemical analyses, so that correlations between the spectra and the chemistry of the minerals cannot be substantiated (e.g. Hunt & Salisbury, 1970). These types of studies provide a broad survey of spectral types but are of limited use in detailed geological investigations. Integrated spectro-chemical studies can be directly applied to the analysis of remotely sensed data to determine mineral abundances, certain cation chemistries, and particle sizes of mineral assemblages (e.g. Gaffey, 1984). The direct application of laboratory spectral reflectance data to remotely sensed data is possible because both types of data are normally acquired in an analogous manner.

There are ongoing efforts to understand spectral reflectance from purely theoretical considerations (Hapke, 1981), but the practical applications of these techniques remain to be demonstrated. Semi-empirical approaches are much more promising, but there is as yet no widely accepted procedure for deconvolving spectra (Clark & Roush, 1984). A number of efforts in this area show great potential and may eventually prove to be of value, although it is doubtful that they will ever completely supplant empirical approaches (Johnson *et al.*, 1983;

Huguenin, 1985; Fujii *et al.*, 1986; Mustard *et al.*, 1986).

In the meantime, the business of remote sensing must continue. Empirical studies can provide immediate results and are useful for judging the accuracy of the more theoretical studies. An intelligently constructed empirical laboratory can provide useful information for the interpretation of spectral information from diverse targets (Cloutis, 1985).

An important study by Adams & Filice (1967) investigated the myriad factors which can affect spectral reflectance. They concluded that the most important variables are end member mineral abundances, particle size and mineral composition. Other factors such as particle packing, viewing geometry, particle shape, temperature and instrumentation are of lesser importance.

The differences in reflectnace between packed and unpacked powdered mineral samples (20 % volume change) are on the order of 2-3 %, with the packed powders generally having lower reflectance at longer wavelengths and higher reflectance at shorter wavelengths than the unpacked samples (Adams & Filice, 1967). Such differences are of minor importance when a decrease in mean grain size of 60 % can change overall albedo by a facot of two. Furthermore, the degree of packing does not affect the presence of spectral absoprtion features. In any case, large differences in packing density are not expected on low gravity bodies, airless bodies such as asteroids.

Viewing geometry also has a minor effect on spectral reflectance. Adams & Filice (1967) found that the 0.7μm:0.4μm reflectance ratio varies slightly as the illumination angle changes. The magnitude of the change depends on the type of material. This effect is small over the normal range of phase angles (~30°) at which most inner solar system objects are imaged (Gaffey, 1974). Even large variations do not affect key spectral parameters such as band minimum wavelength positions, while band areas vary by only a few percent (Gradie *et al.*, 1980; Pieters, 1983).

As particles approach spherical shape, the overall reflectance decreases and the 0.7μm:0.4μm ratio increases. In general, very little is known about the effect of particle shape on spectral reflectance, but it is felt that this effect is probably only important in certain sedimentary environments (Adams & Filice, 1967).

Temperature variations can affect key spectral parameters such as band minima wavelength positions and band areas. Normal temperature fluctuations in the inner solar system can be quite large and erroneous mineralogical interpreations may result if this effect is not acknowledged (Roush, 1984). In most cases, the thermal regimes of planetary bodies can be modeled or measured with sufficient precision to compensate for or, at least, recognize the effect of temperature variations.

The two main types of spectral reflectance measured in the laboratory, bidirectional and bihemispherical, do not provide identical spectra. The spectra measured in bidirectional geometry are redder than those obtained using an integrating sphere arrangement (bihemispherical). The degree of difference increases with increasing absolute reflectance. At small phase angles, the integrating sphere measurements provide a better match to spectra expected for planets covered with the same materials (Gradie & Veverka, 1982).

Mafic silicates form the basis of this project for a number of reasons. They are known, or inferred to be, major constituents of the surfaces of most bodies in the inner solar system. They are spectrally distinct and amenable to spectral analysis. In addition, the spectral properties of mafic silicates have been studied by a number of investigators, although the data for mixtures containing mafic silicates are generally lacking. A comprehensive summary of mafic silicate spectral reflectance studies published before 1984 can be found in Cloutis (1985).

In spite of all these studies, there remain problems in spectral interpretation which must be addressed. Mafic silicates (primarily olivine and pyroxene) rarely occur without the presence of accessory phases. Ignoring the diverse terrestrial weathering products, the major accessory phases of cosmic importance are metallic nickel-iron, magnetite, carbon and carbonaceous compounds, plagioclase feldspar, and glass and glass-bonded aggregates (agglutinates). All of these materials are present in varying amounts in almost all terrestrial and extraterresrial occurrences of mafic silicates. The accessory phases are also interesting because they represent the major spectral classes- nickel iron and agglutinates are spectrally red, magnetite, carbon and carbonaceous compounds are spectrally neutral and opaque, while the mafic silicates are strongly featured. The information provided from spectral studies of these materials will provide both an immediately useful data base and a survey of how the spectra of these different classes of materials interact.

In order to characterize the physico-chemical basis of these interactions, a wide variety of disciplines must be brought to bear on the problem, such as metallography, mineralogy, petrology, orbital dynamics, organic chemistry, and other remote sensing techniques. It can be argued that the mineral assemblages on the surfaces of asteroids and the Moon can be determined by matching the spectra of meteorites and returned lunar samples with the remote sensing spectra of the respective bodies. However, this technique will not work for regions of the Moon which are mineralogically distinct from the lunar samples or for asteroids for which no meteorites are available. The laboratory spectra also allow us to investigate whether different materials can have the same spectral properties. Examination of the spectral reflectance properties of mixtures of mafic silicates plus accessory phases in the laboratory will improve our interpretation of remotely sensed data for which precise mineralogical assignments have not yet been made.

The laboratory spectra have been subdivided on the basis of the non-mafic silicate phases. These subdivisions are mafic silicates+metal, spectrally featureless materials, mafic silicates+opaque materials, and mafic silicates+glass. The first three groups are particularly applicable to asteroid remote sensing, while the last group is most relevant to lunar remote sensing.

A. REFERENCES

Adams, J.B., and A.L. Filice, Spectral reflectance 0.4 to 2.0 microns of silicate rock powders. *Jour. Geophys. Res.*, **72**, 5705-5715, 1967.

Clark, R.N., and T.L. Roush 1984, Reflectance spectroscopy: Quantitative analysis techniques for remote sensing applications, *Jour. Geophys. Res.*, **89**, 6329-6340, 1984.

Cloutis, E.A., *Interpretive Techniques for Reflectance Spectra of Mafic Silicates*, M.Sc. thesis, University of Hawaii, Honolulu, 1985.

Fujii, N., H. Azuma, K. Ito, and M. Miyamoto, Effects of grain sizes on the spectral reflectance of mineral mixtures- Towards an inversion problem for three component mixtures, *Lunar Plan. Sci. Conf. XVII*, 245-246, 1986.

Gaffey, M.J., *A Systematic Study of the Spectral Reflectivity Characteristics of the Meteorite Classes With Applications to the Interpretation of Asteroid Spectra for Mineralogical and Petrological Information*, Ph.D. thesis, Massachusetts Institute of Technology, Cambridge, 1974.

Gaffey, M.J., Rotational spectral variations of asteroid (8) Flora: Implications for the nature of the S-type asteroids and for the parent bodies of the ordinary chondrites, *Icarus*, **60**, 83-114, 1984.

Gradie, J., and J. Veverka, When are spectral reflectance curves comparable?, *Icarus*,**49**, 109-119, 1982.

Gradie, J., J. Veverka, and B. Buratti, The effects of scattering geometry on the spectrophotometric properties of powdered materials, *Proc. Lunar Plan. Sci. Conf. 11th*, 799-815, 1980.

Hapke, B., Bidirectional reflectance spectroscopy, 1, Thoery, *Jour. Geophys. Res.*, **86**, 3039-3054, 1981.

Huguenin, R., Primary minerals on Mars: Detection by high order derivative spectroscopy, *Lunar Plan. Sci. Conf. XVI*, 378-379, 1985.

Hunt, G.R., and J.W. Salisbury, Visible and near-infrared spectra of minerals and rocks: I. Silicate minerals, *Mod. Geol.*, **1**, 283-300, 1970.

Johnson, P.E., M.O. Smith, S. Taylor-George, and J.B. Adams, A semiempirical method for analysis of the reflectance spectra of binary mineral mixtures, *Jour. Geophys. Res.*, **88**, 3557-3561, 1983.

Mustard, J.F., C.M. Pieters, and S.F. Pratt, Deconvolution of spectra for intimate mixtures, *Lunar Plan. Sci. Conf. XVII*, 593-594, 1986.

Pieters, C.M., Sterngth of mineral absorption features in the transmitted component of near-infrared reflected light: First results from RELAB,*Jour. Geophys. Res.*, **88**, 9534-9544, 1983.

Roush, T.L., *Effects of Temperature on Remotely Sensed Mafic Mineral Absorption Features*, M.Sc. thesis, University of Hawaii, Honolulu, 1984.

II. METAL-SILICATE MIXTURES: SPECTRAL PROPERTIES AND APPLICATIONS TO ASTEROID TAXONOMY[1]

INTRODUCTION

Remote sensing is one of the most effective means for deriving information about the surface compositions of terrestrial and extraterrestrial targets which are inaccessible to direct sampling. Consequently, it is imperative that the maximum amount of compositional information be derived from such studies. Reflectance spectroscopy is one of the most effective tools in remote sensing, and in order to improve the quality and quantity of information derivable from spectral studies, the spectral reflectance properties of mafic silicate-meteoritic metal mixtures have been examined.

These particular assemblages were chosen because accurate, quantitative identification and analysis of these materials has potentially important implications for theories concerning the origin and evolution of the asteroid belt (Gaffey, 1984; 1986), and perhaps the solar system (Bell, 1986; Gaffey, 1988). The S-class asteroids are the most abundant group in the inner part of the main asteroid belt (Gradie & Tedesco, 1982). Their mineralogy, particularly the nature of the metallic phase, is disputed. These objects have been interpreted as being either differentiated objects with affinities to certain "primitive" achondrites (Gaffey, 1984; Gaffey, 1986; Bell & Keil, 1987), or as parent bodies for the ordinary chondrites, and hence undifferentiated (Anders, 1978; Feierberg *et al.*, 1982). The competing interpretations are almost exclusively based on differing interpretations of the telescopic spectral data. Important constraints can be placed on early solar system history depending on which interpretation ultimately proves to be correct.

The recent identification of probable olivine- and metal-rich asteroids also hinges on correct interpretation of the telescopic spectra (Bell *et al.*, 1984a; 1984b; Cruikshank &

---

[1] A version of this chapter has been submitted for publication. Cloutis, E.A., Gaffey, M.J., Smith, D.G.W., and Lambert, R. St J. 1989. Journal of Geophysical Research.

Hartmann, 1984). If these A-class asteroids are differentiated objects, then they are most likely the remnants of once-larger planetesimals whose outer layers have been stripped away by impacts to reveal their core-mantle boundaries, and are mineralogically similar to pallasite meteorites (Buseck, 1977; Bell *et al.*, 1984b). The necessary laboratory spectral studies were undertaken in order to constrain the possible surface mineralogies of these important classes of asteroids.

The spectral reflectance properties of the individual end member phases (olivine, orthopyroxene, and metal) and olivine-orthopyroxene mixtures have been extensively studied. Olivine reflectance spectra in the 0.3-2.6μm wavelength region show a broad asymmetric absorption feature near 1μm, which is composed of three overlapping absorption bands (Burns, 1970a; Roush, 1984). These bands arise from electronic transitions in Fe^{2+} cations located in two distinct crystallographic sites. The band minimum progressively shifts towards longer wavelengths with increasing iron content, and its wavelength position can be used to determine iron content (Cloutis, 1985; King & Ridley, 1987). The only other resolvable, pervasive absorption band is a weak feature situated near 0.65μm whose origin is still unclear (Burns, 1970a; Mao & Bell, 1972; Burns *et al.*, 1973; Runciman *et al.*, 1973; Hazen *et al.*, 1977; Roush, 1984), but seems to be useful for further constraining olivine composition (King & Ridley, 1987). A steep drop-off in reflectance occurs at wavelengths shorter than 0.55μm due to various charge transfer absorptions but does not appear to be diagnostic of any particular composition (Burns, 1970a; Burns *et al.*, 1972).

Low-calcium pyroxene, which will be referred to here as orthopyroxene (OPX), exhibits two main absorption bands in its reflectance spectrum near 1μm and 2μm (Band I and II, respectively). These features are due to crystal field transitions in ferrous iron located in the M2 crystallographic site (Clark, 1957; White & Keester, 1967; Burns, 1970b; Burns *et al.*, 1972; Roush, 1984). As with olivine, the wavelength positions of these bands shift to longer wavelengths with increasing iron content (Adams & McCord, 1972; Adams, 1974; Cloutis, 1985; Cloutis *et al.*, 1986a; 1986b). The presence of the band at 2μm is useful for easily distinguishing pyroxene from olivine.

A number of meteoritic metals and nickel-iron alloys have been spectrally characterized. In almost all cases the various Ni-Fe alloys show a featureless spectrum between 0.3 and 2.7μm with a gradual rise in reflectance towards longer wavelengths (red slope). The spectral slope is dependent on the particle size or surface roughness of the metal, and to a lesser extent, on its chemistry (Watson, 1938; Yolken & Kruger, 1965; Blodgett & Spicer, 1967; Gorban *et al.*, 1973; Johnson & Fanale, 1973; Gorban & Stashchuk, 1974; Gaffey, 1976; Dollfus *et al.*, 1980; Feierberg *et al.*, 1982; McFadden, 1983; Wagner *et al.*, 1987; Britt & Pieters, 1988; Cloutis, 1989, in preparation).

The evidence for comminuted materials on the surfaces of metal-rich asteroids is compelling. Meteorites which presumably resided for a period of time at the surfaces of their parent bodies (solar gas-rich breccias) show comminuted textures (Wilkening, 1983; Williams *et al.*, 1984; 1986; Bell & Keil, 1987; Britt & Pieters, 1987). The available photopolarimetric data for most S-class asteroids are best modelled as a particulate surface layer (Veverka, 1971; Zellner *et al.*, 1977; Barucci *et al.*, 1984) probably composed largely of ~100μm-sized grains (Dollfus & Zellner, 1979). Thermal radiometric models of the larger asteroids tends to support the polarimetric results for a comminuted surface (Morrison & Lebofsky, 1979), and metal-rich surfaces on S-asteroids (Gaffey, 1989). Radar albedos of main-belt S-asteroids, assuming a certain metallic component, seem to indicate particulate regoliths with approximately lunar porosities (Ostro *et al.*, 1985). Computational models of asteroid evolution favor the development of a substantial surface regolith on all but the smallest asteroids (Comerford, 1967; Cintala *et al.*, 1979; Housen *et al.*, 1979a; 1979b; Housen & Wilkening, 1982; King *et al.*, 1984). The reflectance spectra of three A-class asteroids are best simulated by fine-grained olivine scattered on a roughened metal substrate. Large olivine grains, such as those found in pallasites, do not match the spectral data and must be extensively fragmented to provide the necessary match (Bell *et al.*, 1984a).

At the temperatures present in the main asteroid belt, kamacite lies in the brittle-ductile transition region, and may be subject to brittle deformation during impacts (Zukas, 1969; Auten, 1973; Remo & Johnson, 1975). Laboratory impact studies of meteoritic metal show the development of irregular surfaces and the comminution of the metal even at room temperatures (Auten, 1973; Marcus & Hackett, 1974; Matsui & Schultz, 1984). Comminution of differentiated metal may also be facilitated by the presence of exsolved and included phases such as schreibersite/rhabdite, troilite, graphite, and cohenite. These phases could serve as areas of weakness in the metal and facilitate fracturing (Baldanza & Pialla, 1969; Comerford, 1969; Doan & Goldstein, 1969).

EXPERIMENTAL PROCEDURE

Natural and synthetic materials were used in this study. The olivine (OLV003) was separated from large pale green grains from San Carlos, Arizona. The pyroxenes (PYX032, PYX117) are from Ekersund, Norway, and an unspecified locality in India, respectively. Powders were obtained from a single, partial crystal in both cases. The metal (MET101) was ground from a fresh, interior sample of the Odessa, TX coarse octahedrite (Buchwald, 1975).

Chemical analyses of the samples were acquired at the University of Calgary SEMQ microprobe facility and represent an average of six or more point analyses or area scans (Table II-1). The ferrous iron values of the silicates were obtained by wet chemistry, and ferric iron was calculated from the difference between total and ferrous iron. For the meteoritic metal, only the kamacite phase, which forms the bulk of the sample (Buchwald, 1975), was analyzed.

Mafic silicate powders were obtained by crushing in an alumina mortar and pestle. Impurities were removed by a combination of magnetic separation and hand picking. The cleaned samples were repeatedly wet sieved with acetone to ensure well-constrained size fractions. The 0-45 and 45-90μm size ranges were used in the various mixtures. The metal powder was produced by grinding a portion of an alteration-free piece of the iron meteorite on an emery grinder, magnetically separated from the grinding wheel contaminants, and repeatedly wet sieved with acetone. A portion of the metal powder was beaten in the mortar to reduce the metal shavings to a more equidimensional habit, and wet sieved with acetone to the various size fractions. The 45-90μm portion of this material was used in the olivine-metal mixtures. Immediately upon completion of the sieving, the samples were transferred to a dry nitrogen environment for storage. They were briefly removed for incorporation into the mineral mixtures, and returned to the nitrogen environment. In total, the metal powders were exposed to normal atmosphere for a maximum of five days. The various mineral mixtures were made on a weight percent basis with an accuracy of ±0.1%. The olivine-metal (OLV003-MET101), and one of the pyroxene-metal mixtures (PYX117-MET101) were made at 25 weight percent intervals, and the other pyroxene-metal mixture (PYX032-MET101) at 50 wt. % intervals. In addition, a 30:40:30 mixture of OLV003:PYX117:MET101, and its metal-free equivalent (OLV003:PYX117=43:57) were also prepared.

The reflectance spectra were acquired at the NASA RELAB spectrometer facility at Brown University, and at the U.S. Geological Survey spectrometer facility in Denver, CO. Details of the respective instruments can be found in Pieters (1983) and King & Ridley (1987). The samples measured at the RELAB facility (OLV003-MET101 series, OLV003:PYX117, OLV003:PYX117:MET101, and the various end members) were acquired at an incidence angle of 0° and an emission angle of 15°. The PYX-MET mixtures and end members were measured at the U.S. Geological Survey facility using an integrating sphere arrangement. All the spectra were measured relative to halon, a near-perfect diffuse reflector in the wavelength region of interest (0.3-2.7μm; Weidner & Hsia, 1981), corrected for minor (~2%) irregularities in halon's absolute reflectance in the 2μm region, as well as for dark current offsets. The reflectance spectra were processed and analyzed using the Gaffey Spectral Processing System, a PC-compatible version of SPECPR (Clark, 1980). Continuum removal was performed by dividing out a straight line tangent to the reflectance spectrum on either side of an absorption band. Band centers and band minima were calculated by fitting a quadratic equation to ~10 data points on either side of a visually determined minimum or center.

RESULTS

The various spectra have been divided up into three groups- OLV+MET and end members, PYX+MET and end members, and OLV+PYX+MET and OLV+PYX and end members. Each group possesses distinct spectral properties which can be used to identify the particular minerals present in the assemblages, and to constrain some of their physical and chemical properties.

Olivine-Metal Mixtures

Very little spectral data exist for olivine-metal mixtures. Gaffey (1976) in his comprehensive examination of meteorite spectra did not include pallasites (olivine-metal meteorites) because of the difficulties in sample preparation. Bell *et al.* (1984a) measured the reflectance spectra of olivine grains scattered on a roughened metal background and concluded that fine-grained olivine+metal substrate provides the best match to the telescopic data for A-class asteroids, although the overall red slope due to the metal could not be accurately reproduced. Gaffey (1986) cites an unpublished study of very fine-grained iron (3μm) mixed with two sizes of olivine (<45μm and 125-250μm). The very fine-grained iron imparted a red slope to the spectra.

Intimate mixtures of olivine and metal involve the interaction of a mineral with a broad absorption band near 1μm and a relatively flat reflectance slope beyond 1.8μm (olivine), with a material having a featureless, red slope of low overall reflectance (metal). The various olivine-metal mixtures using the 45-90μm sized olivine and the 45-90μm sized beaten metal are shown in Figure II-1. These mixtures are all characterized by a variable strength absorption band near 1μm (Band I) and no band near 2μm (Band II). This is used as an initial criterion for determining whether an olivine-rich assemblage is present and amenable to the spectral deconvolution procedures developed for OLV-MET mixtures.

A large number of olivine spectra are available in the literature, and many of these were included in the search for spectral systematics (Adams, 1975; Hunt & Evarts, 1981;

Miyamoto *et al.*, 1981; Singer, 1981; Miyamoto *et al.*, 1983; Cloutis, 1985; King & Ridley, 1987; Pieters & Mustard, 1988). Progressively increasing amounts of metal added to olivine alter the mafic silicate spectrum in systematic ways. In naturally-occuring olivines, the reflectance from 1.8-2.5μm is essentially constant, with the exception of some iron-rich members (Cloutis, 1989). Metal is substantially redder in this wavelength region, even for the most finely powdered sample (0-45μm). A red slope seems to be characteristic of all nickel-iron alloys with a grain size or surface roughness greater than the wavelength of light (e.g. Gaffey, 1986; Miyamoto, 1987; Britt & Pieters, 1988). OLV-MET spectra fall somewhere between these two extremes and the 2.5/1.8μm reflectance ratio can be used to determine the metal abundance. A four-fold increase in metal grain size would alter the estimate of metal abundance by only 10%. Unfortunately, this calibration is valid only for pyroxene-free samples, as the addition of even a few percent pyroxene dramatically reduces this reflectance ratio.

A more widely applicable calibration involves the width of Band I. Increasing amounts of metal impart a red slope to the olivine, this effect being more pronounced at shorter wavelengths. The width of Band I is measured by the intersection of a horizontal straight line continuum tangent to the local reflectance maximum between ~0.5-0.7μm with the long wavelength side of Band I. The intersection point of this tangent for all olivines, regardless of particle size and chemistry, falls between 1.45 and 1.62μm. The addition of even 25 wt. % metal shifts the intersection point to a value well below the olivine field (Figure II-2). Extrapolating from pure metal spectra (Cloutis *et al.*, 1989), a fourfold increase in metal grain size would result in overestimating metal abundance by ~10 %. At this point no acceptable spectral criterion has been found for determining the grain size of the metal, except for the 2.5/1.8μm reflectance ratio. The intersection point criterion is much less sensitive to small amounts of pyroxene than the 2.5/1.8μm ratio.

The depth of the major ferrous iron olivine absorption band (Band I) measured as the reflectance ratio at 1.8μm divided by the reflectance at the band minimum increases as olivine grain size increases. Reflectance ratios are particularly useful parameters because they are dimensionless and are independent of absolute reflectance, which is unavailable in many cases. The 1.8μm/Band I minimum reflectance ratio increases with increasing grain size to a maximum of ~10, at which point the absorption band becomes saturated. This ratio is severely depressed by the addition of metal, and appears to be relatively independent of metal grain size (Figure II-3). Since the abundance of metal has been determined from the intersection point criterion, correcting for metal abundance will yield the olivine grain size. A series of contours can be constructed on Figure II-3 connecting points of equal metal abundance. These contours are not shown because the necessary samples have not yet been characterized. The reflectance ratio for an unknown spectrum plotted in Figure II-3 for a given metal content will yield the olivine grain size.

The final factor which can be determined is the ferrous iron content of the olivine. In pure olivines, the wavelength position of the band minimum and band center shifts to longer wavelengths with increasing iron content from ~1.05-1.09μm (Figure II-4). The presence of metal causes an apparent shift of the band minimum towards shorter wavelengths. In the mixtures studied, 50 wt. % metal shifts the band minimum and band center downwards by 21 and 6 nm respectively. Extrapolating from the spectra of various sized metal powders, a four fold increase in metal grain size would accelerate the shift in band center by only 1-2nm. The iron content of the olivine can be determined by adding a value to the band minimum or band center equivalent to the amount of metal present, since a straight line continuum is not a completely satisfactory correction for the metal. Failure to correct fully for this discrepancy will provide only the minimum iron content of the olivine.

Pyroxene-Metal Mixtures

Pyroxene- and metal-rich meteorites include lodranites, mesosiderites, siderophyres, and winonaites (Mason, 1962; Powell, 1969, 1971; Mason & Jarosewich, 1973; Prinz *et al.*, 1980; King *et al.*, 1981; Mori *et al.*, 1984). To date there has been very little success in identifying possible parent bodies for these meteorites on the basis of telescopic spectral studies. The pyroxene-metal spectral data may help to overcome this difficulty, and perhaps provide additional information on unsampled asteroid types.

The available spectral data for pyroxene-metal (PYX-MET) mixtures is of variable quality. Gaffey (1976) examined the reflectance spectrum of one mesosiderite (Veramin) which showed two weak absorption bands at the approximate positions expected for pyroxene. A number of enstatite chondrites, containing metal and nearly pure iron-free enstatite were also examined. These meteorites show almost no Fe^{2+} absorption bands (Gaffey, 1976; Miyamoto, 1987) because the pyroxene is almost pure $MgSiO_3$ (Keil, 1968; Watters & Prinz, 1979). As a result they will not be considered here. Feierberg *et al.* (1982) measured partial reflectance spectra (0.85-2.5μm) of a series of pyroxene-metal mixtures and mathematical constructs of areal mixtures. The usefulness of the data is hampered by the lack of chemical data for the pyroxene (probably a pigeonite) and the lack of ultraviolet and visible wavelength data.

Orthopyroxene-metal mixture spectra are characterized by the presence of two major absorption bands in the 0.9-1.0μm (Band I), and 1.75-2.1μm (Band II) regions, both due to Fe^{2+} crystal field transitions in the pyroxene. A large number of available pyroxene spectra were assembled from the literature in addition to those measured in this study to search for spectral systematics (Adams, 1968; Hunt & Salisbury, 1970; Nash & Conel, 1974; Adams, 1974, Pieters, 1974; Adams, 1975; Adams *et al.*, 1979; Singer, 1981; McFadden *et al.*, 1982; Miyamoto *et al.*, 1983; Cloutis, 1985; Mustard *et al.*, 1986). Unfortunately, orthopyroxenes show wide, and as yet unexplained, variations in many spectral parameters such as reflectance ratios. This severely hampers the construction of high quality deconvolution techniques for PYX-MET spectra. The calibrations found for these assemblages are not as comprehensive as those available for OLV-MET spectra.

The addition of meteoritic metal (with its red, featureless spectrum) to orthopyroxene changes a number of properties: overall reflectance is reduced; Band II is reduced in intensity; the reflectance maxima near 0.7μm and 1.4μm (interband maximum) are both suppressed relative to longer wavelengths; and the band minima shift to shorter wavelengths. These effects are also seen in other PYX-MET spectra (Feierberg *et al.*, 1982). All orthopyroxenes, with the exception of the smallest grain sizes (<5μm) have a band area ratio (Band II*/Band I*; Cloutis *et al.*, 1986b) between 0.8 and 1.17. The addition of metal causes a reduction of the Band area ratio (Figure II-5). A 75:25 PYX:MET mixture has an area ratio of 0.78 versus 1.00 for the pure pyroxene. At 50 wt. % metal, for which two different pyroxenes were used, the area ratios are essentially identical. Band area ratio was found to be the most useful parameter for establishing metal content. Although ternary mixtures of pyroxene-metal-plagioclase were not examined in this study, the addition of even large amounts of plagioclase feldspar will not vary these results by more than a few percent (Nash & Conel, 1974; Mustard *et al.*, 1986).

Highly comminuted, metal-free pyroxene shows a low band area ratio, and may be confused with pyroxene-metal mixtures using this criterion alone. However, the smallest pyroxene fractions show a decrease in the reflectance ratio of the interband peak (1.4μm maximum) to the local maximum near 0.7μm. For fine-grained pyroxenes this ratio is <1.2, versus >1.2 for the PYX-MET spectra. This was found to be the sole criterion for separating these two types of assemblages when absolute reflectance is unknown.

Increasing metal content results in an increasingly red slope being imparted to the PYX-MET spectra. This is a potentially useful criterion except for the fact that pyroxene reflectance ratios are highly variable. Increasing metal content causes the intersection of a horizontal continuum tangent to the 1.4μm interband peak with the long wavelength wing of Band II to shift to shorter wavelengths. The addition of metal also tends to reduce most reflectance ratios. The ratio of the Band II minimum reflectance to the local 0.7μm peak reflectance ranges from 1.1 to 3.3 in pure pyroxenes. The addition of 50 wt. % metal reduces the initial ratios in two chemically and spectrally distinct pyroxenes from 3.15 and 1.89 to 0.94 and 0.76, respectively- a substantial decrease in variability (Figure II-6). The grain size of the metal can be roughly constrained using this ratio, in conjunction with the band area ratio for metal abundance. Extrapolating from pure metal spectra, contours can be constructed on Figure II-6 joining points of equal metal content. Plotting the reflectance ratio in the field of Figure II-6 will yield the metal grain size for the previously determined metal content. These construction lines have been omitted because of the lack of data for larger grain size pyroxene-metal mixtures.

The variability in pyroxene spectra is most problematic for particle size determinations, since reflectance ratios are traditionally the most effective means for determining this parameter, assuming absolute reflectance is unknown. Olivine grain size is best determined by the depth or intensity of the major 1μm absorption band. A similar approach to pyroxenes, measuring band depth as the ratio of the reflectance of the interband peak (1.4μm maximum) to the reflectance of the Band I minimum shows a general increase with increasing grain size, although there are a number of exceptions. In general it appears that a peak:minimum ratio of ~5.5 or less indicates a smaller pyroxene grain size (Figure II-7). Corrections for metal content can be made in a manner analogous to the olivines (Figure II-3).

The wavelength positions of the two major Fe^{2+} absorptions near 1μm and 2μm have been shown to shift to longer wavelengths with increasing iron content (Adams & McCord, 1972; Adams, 1974, 1975; Cloutis, 1985; Cloutis *et al.*, 1986a, 1986b; Aoyama *et al.*, 1987). All available orthopyroxene spectral data for which at least major element chemistries are available were re-evaluated. While the sample size is small (15 samples) it appears that the substitution of aluminum for silicon in the tetrahedral sites results in absorption band minima shifting to shorter wavelengths, opposite to the trend found for increasing iron content. Both these trends are consistent with the different ionic radii of Mg^{2+}, Fe^{2+}, Si^{4+}, and Al^{3+}. The shift in the wavelength position of the Band II minimum due to changing iron content is greater than that for Band I. When the separation of the two bands is plotted against the Band II minimum position a very tight linear trend emerges which is very useful for determining iron content (Cloutis, 1985). When higher aluminum content orthopyroxenes are included, the iron content of these samples is seriously underestimated using this criterion. Based on this admittedly small sample size, it appears that for every 1 wt. % increase in Al_2O_3, the ferrosilite (Fs) content is underestimated by ~5 mole %. The Fs contents of four high-aluminum pyroxenes (>4 wt. % Al_2O_3) are shown in Figure II-8. This systematic variation, if it proves to be real, may be of particular significance for lunar remote sensing, since lunar pyroxenes commonly contain some aluminum (Adams & McCord, 1972; Papike *et al.*, 1976). No consistent spectral parameter has been found to differentiate between low- and high-aluminum pyroxenes. Using the wavelength positions of the band minima as indicators of pyroxene chemistry is the most useful criterion, but it provides only a lower limit on pyroxene ferrous iron content.

The presence of red-sloped metal causes both absorption band minima to shift to shorter wavelengths, but to remain very close to the pure pyroxene trend (Figure II-9). Each 25 wt. % increase in metal content shifts the apparent Fe content of the pyroxenes downwards by ~8 %. Since metal content can be determined using other spectral parameters, its effect can be compensated for to yield the minimum Fs content.

The decline in band area ratios (Figure II-5) with increasing metal content mimics a similar trend observed for increasing olivine content in olivine-pyroxene mixtures (Cloutis *et al.*, 1986a). On the basis of this criterion alone, PYX-MET and PYX-OLV assemblages may be confused. The simplest method for distinguishing among them is on the basis of the horizontal tangent intersection point. Pyroxene, and pyroxene-metal mixtures have their intersection point at <~1.1μm, while in PYX-OLV spectra it occurs at ~>1.1μm.

Olivine-Pyroxene-Metal Mixtures

A single olivine-pyroxene-metal (OLV:PYX:MET=30:40:30) mixture and its metal-free counterpart (OLV:PYX=43:57) were spectrally characterized in order to examine briefly the general spectral properties that are present in these ternary assemblages (Figure II-10). The spectral properties of olivine-pyroxene mixtures have been thoroughly examined in Singer (1981), Miyamoto *et al.* (1983), and Cloutis *et al.* (1986b). When metal is added, it acts to largely counteract many of the effects of the olivine in terms of intersection point and band minima wavelength positions. There is no one spectral parameter which can be used to separate OLV-PYX-MET mixtures from OLV-PYX and PYX-MET assemblages.

The spectral properties of the ternary OLV-PYX-MET mixtures can be anticipated from the studies of the various binary mixtures. The predicted effects of the metal- narrowing of absorption bands and shifts of band minima and tangent intercepts to shorter wavelengths, are offset to a large degree by the addition of olivine. Other effects such as reduction of the band area ratio are enhanced by the addition of olivine. These discrepancies in systematic spectral variations can be used to recognize the presence of olivine in a PYX-MET assemblage. The band area ratio can be used to set a very effective upper limit on metal abundance Applying the primary PYX-MET calibration (Figure II-5) to the ternary assemblage indicates a metal abundance of ~60 % (i.e., PYX:MET= 40:60). in ternary assemblages. If the mixture contained only pyroxene and metal, it should have a tangent intercept at 1.015 ± .015μm. It actually occurs at 1.10μm which is at the extreme high end of the pyroxene range, due to the broadening influence of the olivine Band I. The 40:60 PYX:MET spectrum should have a band minimum at 0.896 ± .007μm, but again due to olivine, it occurs at 0.917μm. These latter two calibrations for pyroxene are not shown because they do not form part of the pyroxene + metal calibrations. They show only general trends which are of lower precision than the band area ratio calibration. They are however very useful for reliably establishing the presence of olivine. Olivine also causes a noticeable slope break to appear on the long wavelength wing of Band I at 1.10-1.15μm, in addition to the shift in band minimum and tangent intercept.

Olivine-pyroxene mixtures have band area ratios ranging from 0 to ~1.2- equal to the range for pyroxene-metal (Cloutis *et al.*, 1986b). Enough spectral differences exist to distinguish these two types of assemblages. The horizontal tangent intercept in pyroxenes and PYX-MET spectra occurs between 0.9 and 1.13μm, and in olivines between 1.44 and 1.63μm. Olivine-pyroxene spectra will have an intercept point between these two extremes. In many cases, particularly for approximately equal amounts of olivine and pyroxene, the 0.7μm: interband peak ratio is >1, and the horizontal tangent intersection point misses Band I completely, intersecting the long wavelength wing of Band II. This is seen in the reflectance spectra of many H chondrites which have approximately the same proportions of OLV:PYX:MET as the ternary mixture (Chapman & Salisbury, 1973; Gaffey, 1976). This is probably due to the neutral non-red spectral nature of the metal in ordinary chondrites (Gaffey, 1986). A 0.7 peak: interband peak ratio of <~0.8 seems effectively to encompass metal-rich ternary assemblages, and distinguishes them from metal-free or metal-poor binary OLV-PYX mixtures and ordinary chondrites. The separation is most pronounced when pyroxenes with a low initial 0.7μm peak:interband peak ratio are involved. A low ratio is characteristic of many meteoritic pyroxenes (Gaffey, 1976; McFadden *et al.*, 1982; Miyamoto et al., 1983).

One H chondrite (Tieschitz) has a tangent intersection point on Band I but it lies at ~1.22μm (Gaffey, 1976). The absence of a Band I intersection point or its presence at >~1.1μm is characteristic of metal-free and/or dark and neutral opaque-bearing OLV-PYX assemblages (Cloutis, 1989, in preparation). Other characteristics shown by H chondrites which are inconsistent with metal-rich spectra are an interband peak at the high end or outside the pyroxene range, and a high 0.7μm peak:interband peak ratio. It can perhaps be argued that the carbon in ordinary chondrites may effectively suppress the red slope of the metal. A 99.5:0.5 wt. % mixture of meteoritic metal: amorphous carbon was spectrally characterized to test this hypothesis. The mixture involved 45-90μm meteoritic metal (Odessa coarse octahedrite) and amorphous carbon with a grain size of <0.023μm, thoroughly mixed together. This amount of carbon is comparable to that found in H chondrites (Moore & Lewis, 1967). The albedo of this amorphous carbon (<1 %) is substantially lower than other lampblacks used in mineral mixtures (Clark, 1983). The normalized reflectance spectrum of the mixture matches the pure metal spectrum. The carbon suppresses the overall reflectance but preserves the red slope of the metal.

— Metal grain size is probably also not a viable explanation for the flat overall spectral slope. Lower grade enstatite chondrites have a smaller mean grain size of metal than the higher petrologic grades (Easton, 1983), but show a redder slope than the coarser-grained samples (Salisbury *et al.*, 1975; Gaffey, 1976), even when the metal content is relatively constant (Mason, 1966; Keil, 1968). The amount of fine-grained metal in chondrites can be extrapolated from the results of Dodd (1976). The probable abundance of submicron-sized metal in ordinary chondrites is $<<1\%$. It appears that neither carbon nor comminuted metal can alter the spectral signature of an OLV-PYX-MET assemblage enough to produce an ordinary chondrite-like spectrum. The only feasible mechanism is to comminute a substantial portion of the metal to submicron grain sizes. Such a process, if applied to the entire assemblage, would also fragment the silicate grains to such a small size that their absorption bands would probably be indistinguishable. The original suggestion by Gaffey (1986) that the metal in ordinary chondrites is intrinsically spectrally neutral, is the most feasible explanation for the mismatch between the artificial construct and ordinary chondrite spectra.

Plagioclase-pyroxene spectra may mimic many of the features of the ternary mixture spectra. These binary mixtures are largely outside the scope of this study, but an initial examination of available plagioclase-pyroxene spectra suggests that the slope break on the long wavelength wing of Band I is confined to wavelengths $>1.18\mu m$.

Clinopyroxene-orthopyroxene-metal spectra may also be confused with those of olivine-orthopyroxene-metal. Enough spectral differences probably exist to distinguish these ternary assemblages. Comparing clinopyroxenes and olivines, the former show reflectance maxima near $0.8\mu m$, a second absorption band between 2.15 and $2.40\mu m$, and band minima at wavelengths below $1.06\mu m$, compared with reflectance maxima between 0.5 and $0.7\mu m$, no Band II, and Band I minima at $>1.05\mu m$ in olivines (Adams, 1968; 1974; 1975; Gaffey, 1976; Miyamoto *et al.*, 1983; Cloutis, 1985; Hiroi *et al.*, 1985; Cloutis *et al.*, 1986a).

APPLICATION TO ASTEROID SPECTRA

The spectral deconvolution techniques outlined are applicable to the analysis of reflectance spectra of mafic silicate-metal mixtures. S-class asteroid spectra have been interpreted as olivine-pyroxene-metal assemblages (Gaffey, 1984), while the A-class asteroids appear to be composed almost entirely of olivine and metal (Bell *et al.*, 1984; Cruikshank & Hartmann, 1984). A representative member of each group was selected for interpretation using the spectral deconvolution procedures developed.

S-Class Asteroid (8) Flora

Asteroid (8) Flora is a representative member of the S-asteroid group for which spectral (Chapman & Gaffey, 1979; Feierberg *et al.*, 1982; Gaffey, 1984; Gaffey *et al.*, 1988; Gaffey, 1989), polarimetric (Veverka, 1971; 1973; Morrison & Zellner, 1979), radar (Ostro *et al.*, 1985) and photometric data (Veeder *et al.*, 1978) are available. The reflectance spectrum of Flora shows a number of features which are characteristic of an olivine+pyroxene+metal assemblage (Figure II-11). The average reflectance spectrum has an interband peak wavelength position at the high end of the orthopyroxene field, an inflection point on the long wavelength wing of Band I near 1.10μm, and a Band I tangent intersection point outside the pyroxene field (~1.12μm), all of which are indicative of olivine. The spectrum of Flora also has a high interband peak:0.7μm peak ratio (1.22) and a Band II intersection point at <2.3μm, which are indicative of metal.

The Band I minimum and center wavelength positions, as determined by Gaffey (1984), are at 0.925μm and 1.001μm, respectively. Large metal grains could account for this difference but the interband peak:0.7μm peak ratio and tangent intersection point are indicative of a fine-grained metal (<90μm). The difference between the wavelength position of the Band I minimum and continuum-removed center can be explained by the presence of partially overlapping olivine and orthopyroxene absorption bands of approximately equal intensity. The Band I minimum position (0.925μm) indicates that an orthopyroxene is slightly dominant. Dividing out the red-sloped continuum results in the olivine absorption band appearing slightly more dominant (1.001μm). Olivine and orthopyroxene absorption bands are of approximately equal intensity at 80/20 OLV/PYX (Cloutis, 1985; Cloutis *et al.*, 1986b). The wavelength position of the band center, separation between Band I and Band II, and band area ratio (Band II*/Band I*) are all consistent with this interpretation.

The intersection point of the horizontal continuum for the Flora spectrum is at 1.12μm, but would be at <1.46μm if no metal were present. The calibrations for metal abundances in binary mixtures indicate that either 40 wt. % metal is present (if the assemblage contains only olivine+metal, Figure II-2), or 85 wt. % metal (if the assemblage contains only orthopyroxene+metal, Figure II-5). Given the dominance of olivine over pyroxene, a weighted average of 50 % metal is probable. The interband peak:Band I minimum reflectance ratio of 1.22 indicates a substantial fine-grained (<45μm) mafic silicate component using both the olivine (Figure II-3), and pyroxene (Figure II-7) spectral criteria. The absolute reflectance of Flora (22 % at 0.56μm; Gaffey *et al.*, 1988) is higher than that of the 50/50 OLV/MET laboratory spectrum containing 45-90μm-sized materials. This is further evidence for a significant fine-grained surface component on Flora. The reflectance spectra of mixtures containing a range of particle sizes appear most like spectra of samples containing only fine-grained particles. Both have high overall reflectance because the finest fraction is most effective at scattering rather than absorbing incident radiation (Cloutis, 1985).

The wavelength position of Band II is a useful indicator of pyroxene chemistry because it is unaffected by the presence of olivine (Cloutis, 1985; Cloutis *et al.*, 1986a). After correcting the band minima positions of Flora for 50 % metal and 40 % olivine, the mean orthopyroxene composition is determined to be Fs 30. The uncertainties in the wavelength position of Band II (1.9±0.1μm) bracket a range of Fs contents of 5 to 65 mole %. If clinopyroxene is also present on Flora, as seems likely because of the lack of an appreciable red slope beyond 2.0μm, then the Fs content of the orthopyroxene represents a maximum value. Orthopyroxene+clinopyroxene spectra usually show complex Band II absorption features with the band minimum occuring between the two end member values (Cloutis, 1985). If no clinopyroxene is assumed, and also assuming that the surface assemblage of Flora is an equilibrium mixture, the olivine must be a high-iron variety (Fa=35±10). The olivine composition cannot be independently determined because the Band I position, which is the primary method for determining this parameter, was used to constrain the OLV/PYX ratio.

An olivine+pyroxene+metal assemblage corresponding to that derived for Flora was not spectrally characterized. However an additive mixture of 30 % 50/50 OLV/MET, 60 % 25/75 OLV/MET and 10 % orthopyroxene (PYX117) provides a reasonable match to the low wavelength spectrum of Flora (Figure II-11). Because areal and intimate mixtures are not spectrally equivalent, the data are not directly comparable but do provide a reasonable approximation to an intimate mixture. Since orthopyroxene is a more intense absorber than olivine, the 10 % orthopyroxene in the additive mixture is an upper limit. The simulated spectrum effectively reproduces the broadness of the absorption feature near 1μm and the reflectance drop-off at wavelengths shorter than 0.7μm. The simulated spectrum is consistently brighter than Flora at wavelengths greater than 1.1μm. This discrepancy would be reduced if a smaller grain size metal, which has a less red slope at longer wavelengths than coarser metal were used (Cloutis *et al.*, 1989). A few weight percent of clinopyroxene would also improve the fit at longer wavelengths and in the ultraviolet region.

A fine-grained mafic silicate+metal component on Flora is supported by the polarimetric data. The polarimetric parameters P_{min} and α_0 for Flora (Veverka, 1971; 1973; Zellner *et al.*, 1977; Morrison & Zellner, 1979) lie in the field for fine-grained powders and outside the range for most ordinary chondrites (Zellner *et al.*, 1977; Dollfus *et al.*, 1979; Geake & Dollfus, 1986). A synthesis of the available laboratory polarimetric data suggests that the data for Flora are consistent with an assemblage containing a significant <45μm-sized component. The observational radar data for Flora, while not conclusive, are also consistent with a mafic silicate+metal assemblage of typical lunar regolith porosities (Ostro *et al.*, 1985).

On the basis of available observational data, the surface of Flora seems to be composed of ~50 wt. % metal, ~40 wt. % olivine (Fa=35±10), ~10 wt. % orthopyroxene

($Fs=30^{+11}_{-11}$) and perhaps a few percent clinopyroxene. There are a range of grain sizes present, with a significant fine-grained (<45μm) component. The determined average surface assemblage is in good agreement with earlier interpretations (Gaffey, 1984).

A 50/40/10 MET/OLV/PYX assemblage does not correspond to any known meteorite. Pallasites are similar in terms of metal:olivine ratios and olivine composition, but lack appreciable amounts of pyroxene (Buseck, 1977). The Antarctic lodranite described by Yanai & Kojima (1983) contains an olivine:pyroxene ratio similar to that determined for Flora, but is deficient in metal (13.6 wt. %).This is due in part to terrestrial weathering, but if the original metal content were ~50 wt. %, it would be very similar to Flora in most respects.

A-Class Asteroid (446) Aeternitas

A-class asteroids have been interpreted to be olivine-rich objects with various amounts of metal and perhaps minor amounts of pyroxene (Cruikshank & Hartmann, 1984; Bell *et al.*, 1984a; 1984b). Unlike Flora, no polarimetric or radar data are available for these objects. Asteroid (446) Aeternitas is perhaps the best characterized of this group (Chapman & Gaffey, 1979; Veeder *et al.*, 1983; Bell *et al.*, 1984a; 1984b; Bell *et al.*, 1988; Gaffey *et al.*, 1988; Gaffey, 1989).

The reflectance spectrum of Aeternitas (Figure II-12) has features characteristic of olivine+metal: a prominent absorption band near 1μm; an inflection near 1.25μm; and a high interband peak:0.7μm peak ratio (1.7). A slight pyroxene component is indicated by the flatness of the reflectance spectrum in the 1.6- to 2.4μm interval and the presence of weak absorption bands in this region which are not characteristic of olivine (King & Ridley, 1987).

The wavelength position of Band I can be used to place constraints on pyroxene abundances. If orthopyroxene is the dominant form of pyroxene, the olivine:pyroxene ratio must be >9:1, because more than 10 % orthopyroxene would shift the band I minimum of Aeternitas (1.057μm) to much shorter wavelengths and introduce a significant absorption band near 1.9μm (Cloutis, 1985; Cloutis *et al.*, 1986b). If clinopyroxene is the dominant form of pyroxene, its abundance can be as high as ~30 wt. % before significant spectral alteration is seen.

The mafic silicate + metal spectral calibrations applied to Aeternitas provide some discrepant interpretations. Assuming for the moment that the spectrum of Aeternitas indicates only olivine + metal, the tangent intersection position (Figure II-2) indicates 40 wt. % metal and 60 wt. % olivine. The 1.8μm:1.0μm reflectance ratio (2.00) corresponds to a grain size of ~100-200μm (Figure II-3). The Band I minimum wavelength position is fairly insensitive to small amounts of pyroxene , and after correcting for 40 % metal and 10 % orthopyroxene, is 1.064±0.003μm. This corresponds to an olivine composition of Fa=20±10.

Two weak absorption bands seem to be present at 1.96μm and 2.26μm. A mixture of 25/75 orthopyroxene/clinopyroxene could account for them. A 25/75 orthopyroxene/clinopyroxene ratio is indicated by the fact that both bands are of approximately equal intensity (Cloutis, 1985). The wavelength positions of the bands, uncorrected for metal content, correspond to an orthopyroxene or pigeonite containing 45 mole % Fs and a clinopyroxene containing 17 mole % Fs. This is a roughly equilibrium two-pyroxene assemblage (Robinson, 1980). Orthopyroxene + clinopyroxene spectra often show shifts in Band II minima wavelength positions due to overlaps of their respective bands. Therefore, the calculated Fs contents of the pyroxenes are upper limits.

The reflectance spectrum of Aeternitas bears little superficial resemblance to the 50/50 olivine/metal spectrum. The former has a much more pronounced reflectance drop-off in the ultraviolet, a much higher interband peak:0.7μm peak ratio and a flatter slope in the 1.7μm to 2.5μm region. None of these factors serve as primary spectral calibration parameters but are nevertheless useful for determining whether reflectance spectra are truly binary mafic silicate + metal mixtures.

The absolute reflectance spectrum of Aeternitas is brighter than any of the olivine + metal laboratory spectra (13-26 % at 0.56μm, Figure II-1). Gaffey *et al.* (1988) determined an absolute reflectance of 37 % at 0.56μm, while Veeder *et al.* (1983) determined a geometric albedo of 17 %. If the mean grain size determination for Aeternitas is correct

(100-200μm), then the absolute reflectance of Aeternitas should be lower and not higher than the laboratory spectra, since the albedo of olivine and metal decreases with increasing grain size (King & Ridley, 1987; Britt & Pieters, 1988; Cloutis *et al.*, 1989). This discrepancy may not be as significant as the laboratory data indicate because iron meteorite slabs and powders show large variations in absolute albedo (7-29 % at 0.56μm; Johnson & Fanale, 1973; Gaffey, 1976; Britt & Pieters, 1988; Cloutis *et al.*, 1989).

The meteoritic metal used in this study has a redder spectral slope than metal spectra measured by the other investigators cited above. The reflectance spectrum of Aeternitas, as measured by the interband peak:0.7μm peak, is even redder than the pure metal spectrum. This strongly suggests that an additional phase is present which has a high interband peak:0.7μm peak ratio. The likeliest candidates are orthopyroxene and clinopyroxene because they can also account for the absorption features present in the 2μm region.

Various additive mixtures of OLV/MET with orthopyroxene and clinopyroxene were examined. A good overall match to Aeternitas' spectrum was found for 60 % 50/50 OLV/MET, 20 % 75/25 OLV/MET and 20 % clinopyroxene ($En_{43}Fs_{14}Wo_{43}$), all 45-90μm-sized samples. The only region of mismatch is the 0.35μm to 0.65μm region (Figure II-12). Clinopyroxene in intimate association with olivine+metal would probably show a greater reflectance decline in this region than the mathematical construct because clinopyroxene normally shows a rapid reflectance decline at wavelengths shorter than ~0.65μm which cannot be accurately reproduced by the additive mixtures. The absolute reflectance of the construct (14 % at 0.56μm) is less than Aeternitas. However, the absolute reflectance of olivine and clinopyroxene can be up to a factor of two higher for 0-45μm-sized samples versus 45-90μm-sized samples (Cloutis, 1985) while metal shows a 20 % reflectance increase with a similar diminution in grain size (Cloutis *et al.*, 1989).

The variations in absolute reflectance due to changes in grain size and the variations seen in meteoritic metal measured by different investigators compared to the absolute reflectance of Aeternitas require that the surface of the asteroid possess a significant amount of fine-grained (<45μm) material. This of course is at odds with the grain size determination made earlier, suggesting 100-200μm-sized grains. The grain size determination based on the 1.8μm:1.0μm reflectance ratio (Figure II-3) would give higher values if clinopyroxene were present because clinopyroxenes normally have high 1.8μm:1.0μm reflectance ratios. An overestimate of metal abundance would also result because clinopyroxenes tend to have low reflectances in the region of the 0.7μm peak.

Clinopyroxene+olivine spectra are dominated by the clinopyroxene (Cloutis, 1985). The mathematical construct of Aeternitas thus provides an upper limit on pyroxene abundances. Band depth analysis suggests that in the region of Band I, the clinopyroxene band is approximately twice as intense as the olivine. The orthopyroxene Band I is approximately four times as intense as the olivine Band I (Cloutis, 1985).

When factored in with the previously determined 75/25 clinopyroxene/orthopyroxene ratio and the effect of clinopyroxene on metal content determination, the most consistent surface assemblage for Aeternitas is ~55 wt. % olivine, ~7 % clinopyroxene, ~3 % orthopyroxene, and ~35 % metal. The composition of the olivine appears to be Fa=20±10. If the mafic silicates on Aeternitas represent an equilibrium assemblage, the corresponding pyroxenes would have compositions of ~Fs=15 (orthopyroxene) and ~Fs=5 (clinopyroxene). These values are well within the range previously determined using Band II positions. The mineral abundances determined by Bell *et al.* (1984a; 1984b) for Aeternitas (40 % olivine, 0-10 % pyroxene, 50-60 % metal) are in good agreement with the current interpretation.

There are no known meteorites with mineral assemblages similar to that determined for Aeternitas, but the Eagle Station sub-group of pallasites (Dodd, 1981) are closest in terms of metal:olivine ratio and olivine composition. As was the case for Flora, the pallasites lack the necessary amounts of pyroxene which are required by spectral considerations.

SUMMARY

Olivine-metal, orthopyroxene-metal, and olivine-orthopyroxene-metal mixtures each possess unique spectral properties. A cursory examination of the reflectance spectrum of an unknown is usually sufficient to identify the spectrally significant minerals present. Various spectral parameters which do not rely on a knowledge of the absolute reflectance can be used to place severe constraints on assemblage properties such as phase abundances, major element chemistries of the mafic silicates, and particle sizes. Each of these properties has important implications for unravelling the history of the target. Each type of assemblage must be deconvolved in a systematic manner to obtain the maximum amount of compositional information.

Olivine and olivine-metal assemblages are recognized by the presence of only one major absorption band near 1μm, and a reflectance minimum between 1.0 and 1.1μm. Systematic deconvolution requires determining the horizontal tangent continuum for metal abundance, the 1.8/Band I minimum reflectance ratio for olivine grain size, and the Band I minimum wavelength position for olivine iron content. The parameters determined at each stage are used to correct subsequent calibrations.

Orthopyroxenes show a much wider range of spectral properties than olivine. The derived spectral deconvolution procedures are consequently of lower accuracy. Orthopyroxene and orthopyroxene-metal assemblages are recognized by the presence of absorption bands between 0.8-0.95μm and 1.6-2.0μm, a reflectance maximum between 0.64 and 0.78μm, and a horizontal tangent intersection point between 0.9 and 1.1μm, an interband peak between 1.23 and 1.36μm, and no slope break at 1.10-1.15μm. Systematic deconvolution involves determining the Band II*/Band I* area ratio for metal abundance, the 0.7μm peak/Band II minimum reflectance ratio for metal grain size, the interband peak:Band I minimum reflectance ratio for pyroxene grain size, and the band minima separation versus Band II minimum wavelength position for pyroxene chemistry. The parameters determined at each stage are used to correct subsequent calibration steps.

Olivine-orthopyroxene-metal assemblages show spectral properties intermediate between the three end members. However not all parameters vary to the same degree and these variations can be used to at identify, at a minimu, the spectrally significant phases.

Pyroxene is a much more intense absorber than olivine, and hence tends to dominate silicate absorption features. Away from absorption band minima olivine features such as band broadening, interband maximum wavelength position, and a slope break at 1.10-1.15μm can be recognized. They allow some constraints to be placed on the relative abundances of the various minerals.

The presence of clinopyroxene or plagioclase adds an additional level of complication to the analysis. As yet no effective spectral deconvolution techniques have been developed for quaternary mixtures, but merely identifying the presence of other phases is often sufficient to permit judicious application of the calibrations.

Re-analysis of the reflectance spectra of asteroids (8) Flora (S-class) and (446) Aeternitas (A-class), on the basis of the laboratory spectra, shows that previous interpretations are largely consistent with the new analyses. The surface of Flora seems to consist of ~50 wt. % metal, ~40 wt. % olivine, ~10 wt. % orthopyroxene, and perhaps a few wt. % clinopyroxene. The mafic silicates appear to be high iron varieties. The olivine composition is determined to be $Fa=35\pm10$, while the orthopyroxene is $Fs=30^{+35}_{-25}$. A substantial portion of the surface materials consist of fine-grained (<45μm-sized) particles.

The surface of Aeternitas is interpreted to consist of ~35 wt. % metal, ~55 wt. % olivine, ~7 wt. % clinopyroxene, and ~3 wt. % orthopyroxene. The mafic silicates appear to be more magnesium-rich than those on Flora, although the pyroxene compositions are poorly constrained. The olivine contains 20±10% Fa, the clinopyroxene is constrained to <17 mole % Fs, and the orthopyroxene is constrained to <45 mole % Fs. A significant amount of the surface materials are fine-grained (<45μm-sized particles). The spectral differences between Flora and Aeternitas can be attributed to differences in particle sizes of the surface materials, particularly the metal, and slight differences in pyroxene abundances and compositions. These differences appear to be sufficient to produce large enough variations in spectral properties that these asteroids have been assigned to different taxonomic classes. On the basis of the derived surface assemblages, neither asteroid is a plausible parent body for the ordinary chondrites.

Table II-1. Chemical composition of the minerals used in this study.

Wt. %	OLV003	PYX032	PYX117	Wt. %	MET101
SiO_2	40.64	50.21	53.54	Si	N.D.
FeO	9.25	23.65	16.17	Fe	93.39
Fe_2O_3	0.59	5.11	1.02	--	--
MgO	49.13	17.57	27.53	Mg	0.00
CaO	0.07	1.59	0.35	Ca	N.D.
Al_2O_3	<0.01	1.24	1.54	Al	0.03
NiO	0.33	0.01	0.05	Ni	6.07
TiO_2	0.00	0.19	0.03	Ti	0.00
MnO	0.09	0.53	0.44	Mn	0.00
Cr_2O_3	0.01	0.04	0.07	Cr	0.18
Na_2O	0.00	0.00	0.00	Na	0.00
ZnO	0.00	N.D.	N.D.	Zn	0.11
CoO	0.04	0.06	0.01	Co	0.50
V_2O_5	0.00	<0.01	0.00	V	0.00
K_2O	0.00	N.D.	N.D.	K	N.D.
ZrO_2	N.D.	0.00	0.00	Zr	N.D.
				S	0.00
				P	0.02
				Cu	0.00
				Pb	0.87
TOTAL	100.15	100.20	100.75	--	101.17

Number of Ions on the Basis of 4 or 6 Oxygen[1]

	OLV003	PYX032	PYX117
Si	0.994	1.920	1.931
Al	--	0.056	0.065
V	--	tr.	-
Ti	--	0.005	0.001
Cr	tr.	0.001	0.002
Fe^{3+}	0.011	0.147	0.028
Fe^{2+}	0.190	0.756	0.487
Mg	1.793	1.002	1.480
Ca	0.003	0.065	0.013
Co	0.001	0.002	tr.
Ni	0.006	tr.	0.001
Mn	0.002	0.017	0.013
Zn	--	--	-
Na	--	--	-
TOTAL	2.999	3.972	4.022

[1] Olivine and pyroxene formulae calculated on the basis of 4 and 6 oxygen, respectively.

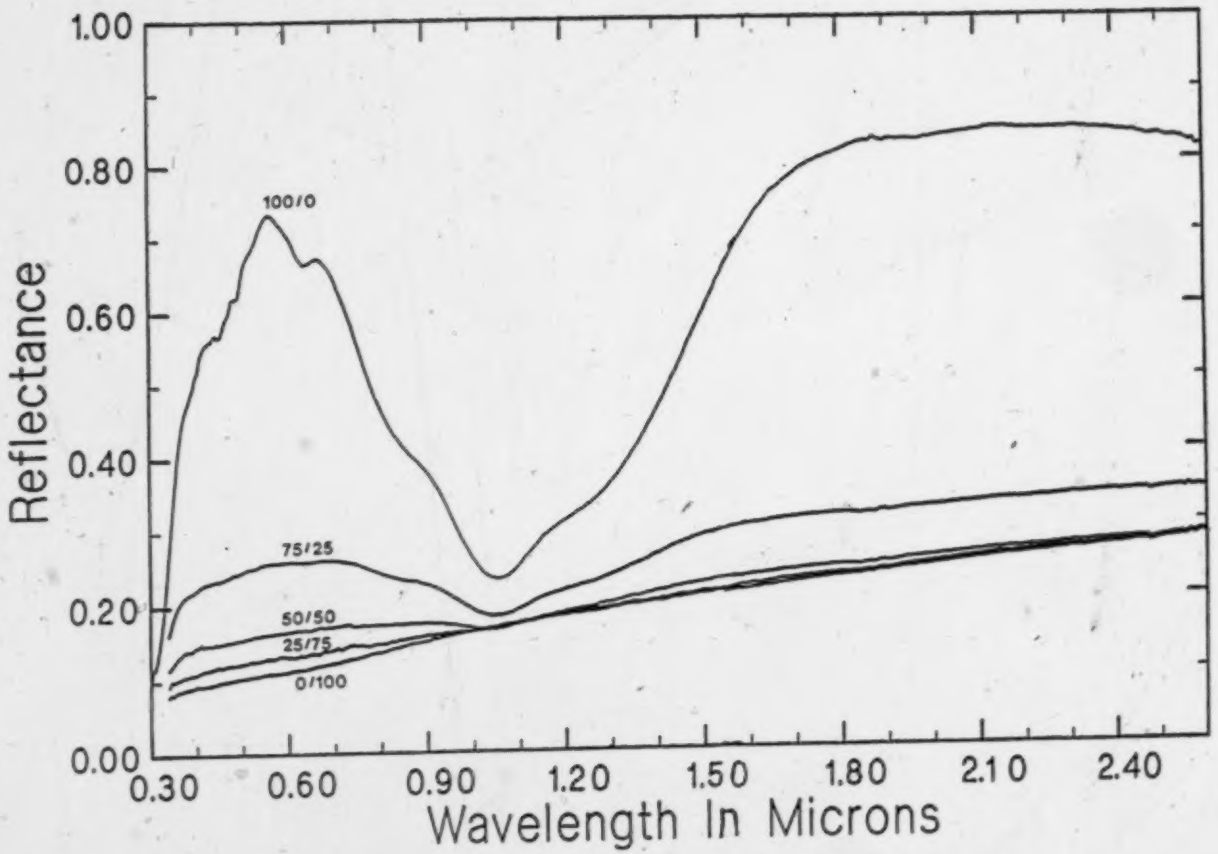

Figure II-1. Absolute reflectance spectra of the 45-90μm sized olivine-meteoritic metal mixtures and end members. Numbers indicate olivine/metal weight percent ratios.

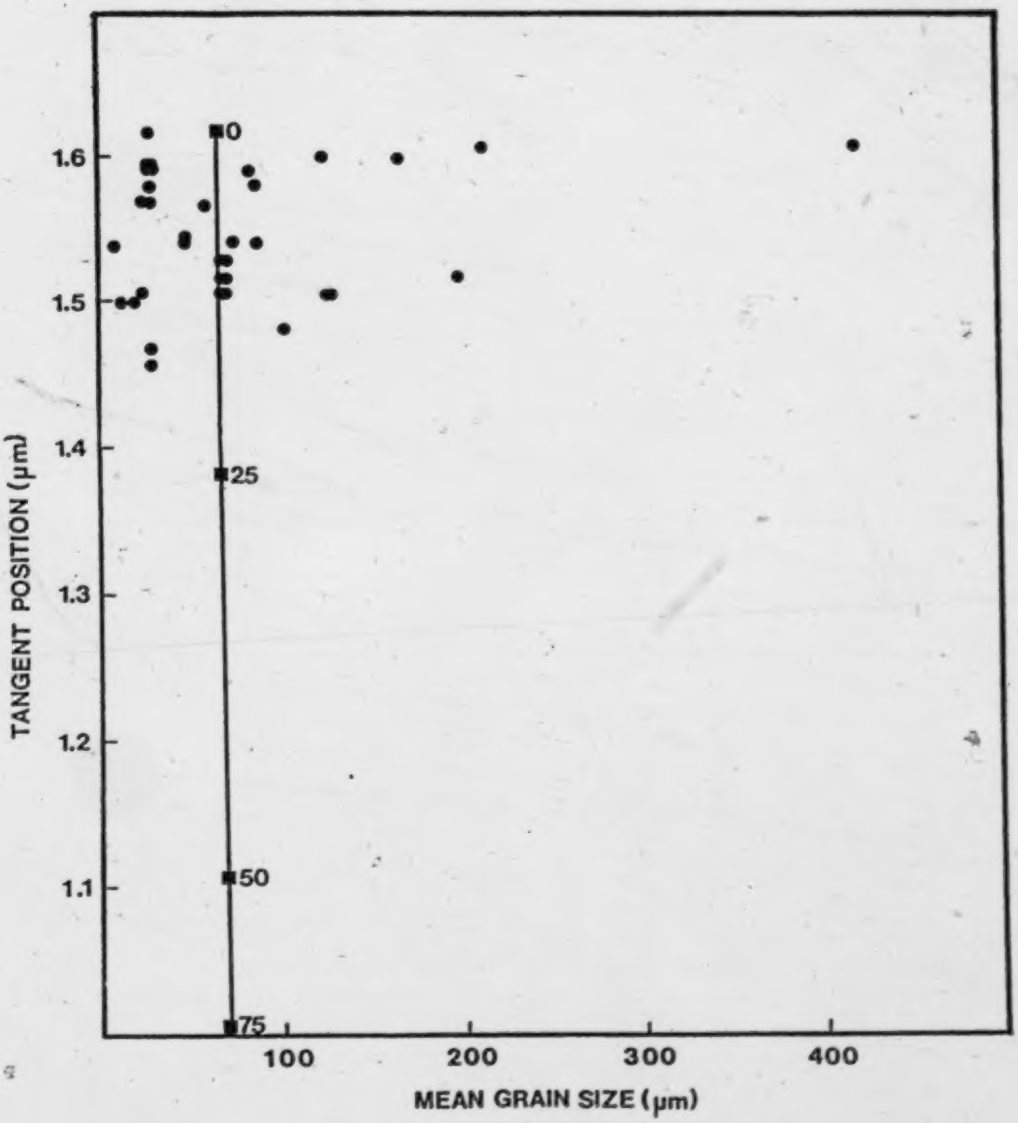

Figure II-2. Wavelength positions of the intersection of a horizontal continuum tangent to the local reflectance maximum near 0.5-0.7μm with the long wavelength wing of the major absorption band (Band I) as a function of mean grain size. Olivines are plotted as circles. Squares indicate olivine-metal mixtures. The numbers refer to the weight percent metal in the mixtures.

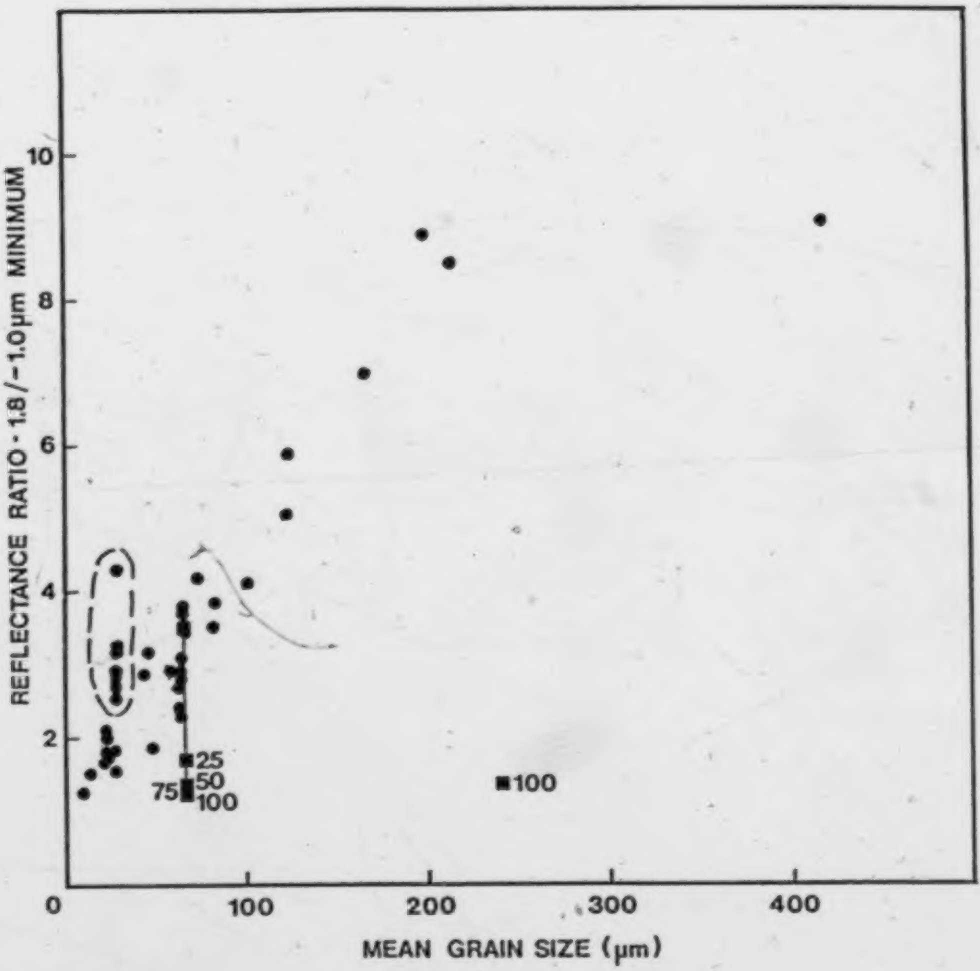

Figure II-3. Ratio of the absolute reflectance at 1.8μm to the reflectance of the Band I minimum near 1μm, as a function of mean grain size. The points surrounded by the dotted line are some iron-rich olivines which fall off the general trend. Symbols are the same as in Figure 2. The isolated square labelled 100 is the reflectance ratio of a larger grain size metal taken at 1.8 and 1.05μm.

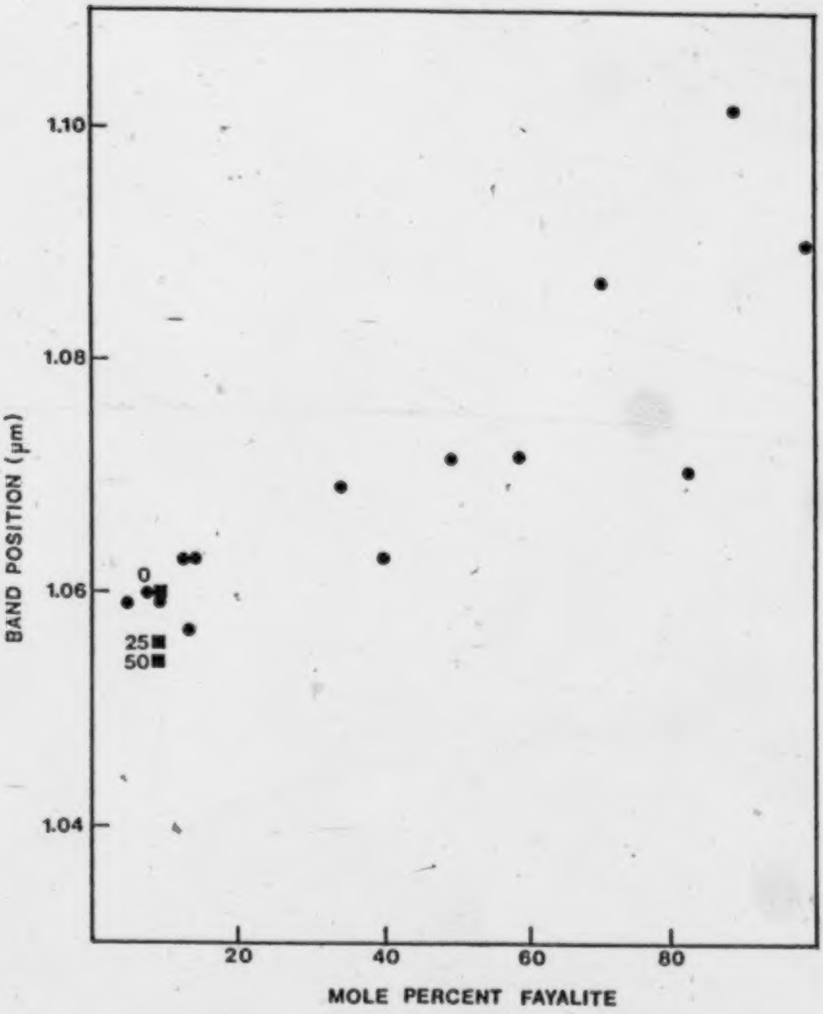

Figure II-4. Wavelength position of the continuum removed Band I center, as a function of olivine iron content. Symbols are the same as in Figure 2.

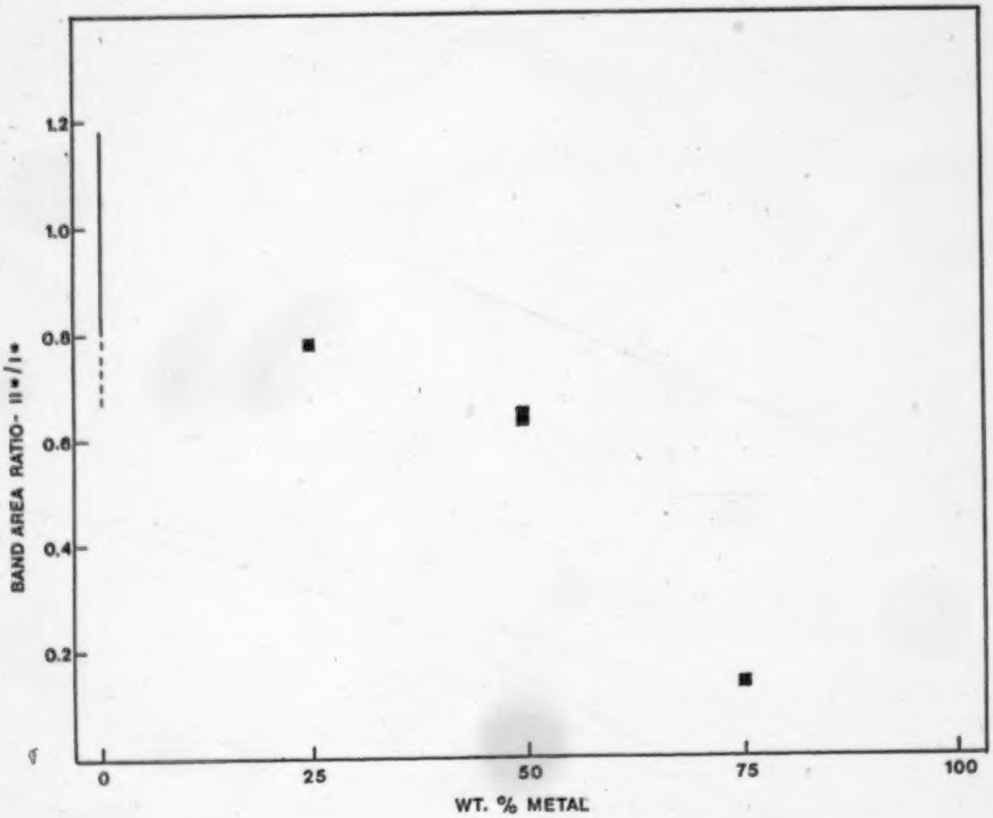

Figure II-5. Band area ratio as a function of metal abundance for pyroxene-metal mixtures. The range for pure pyroxenes is indicated by the vertical line. The dotted extension represents very fine-grained pyroxenes, which can be distinguished from the mixtures by other means.

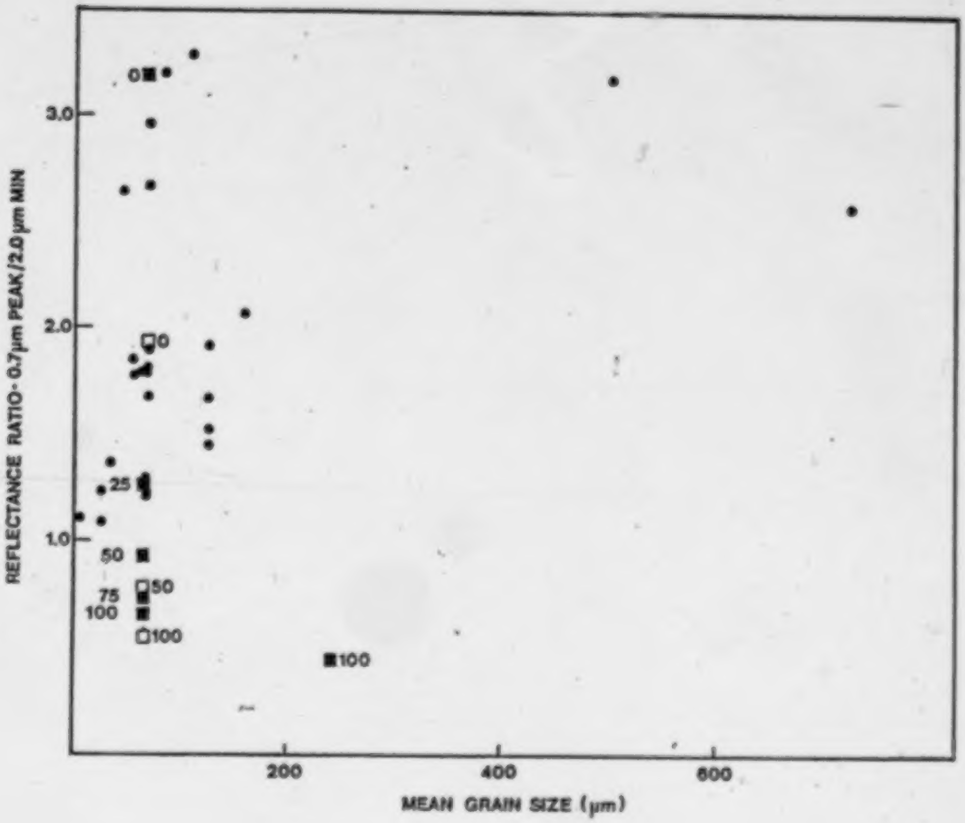

Figure II-6. Reflectance ratio of the local peak near 0.7μm to the Band II minimum near 2μm, as a function of grain size. The two different pyroxene-metal series are indicated by filled and open squares. Circles indicate pure orthopyroxenes. Numbers indicate weight percent metal in the mixtures.

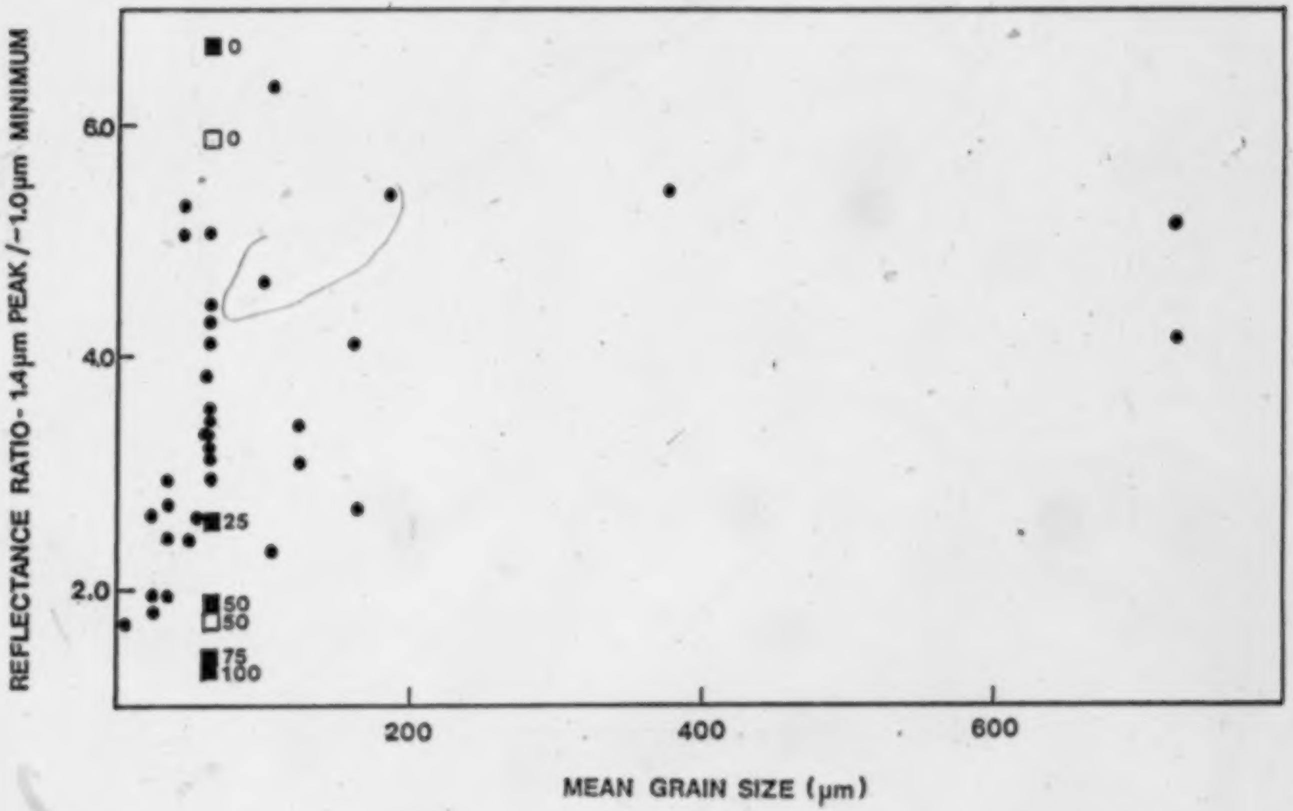

Figure II-7. Reflectance ratio of the interband peak near 1.4µm to the Band I minimum near 1µm, as a function of mean grain size. Symbols are the same as in Figure 6.

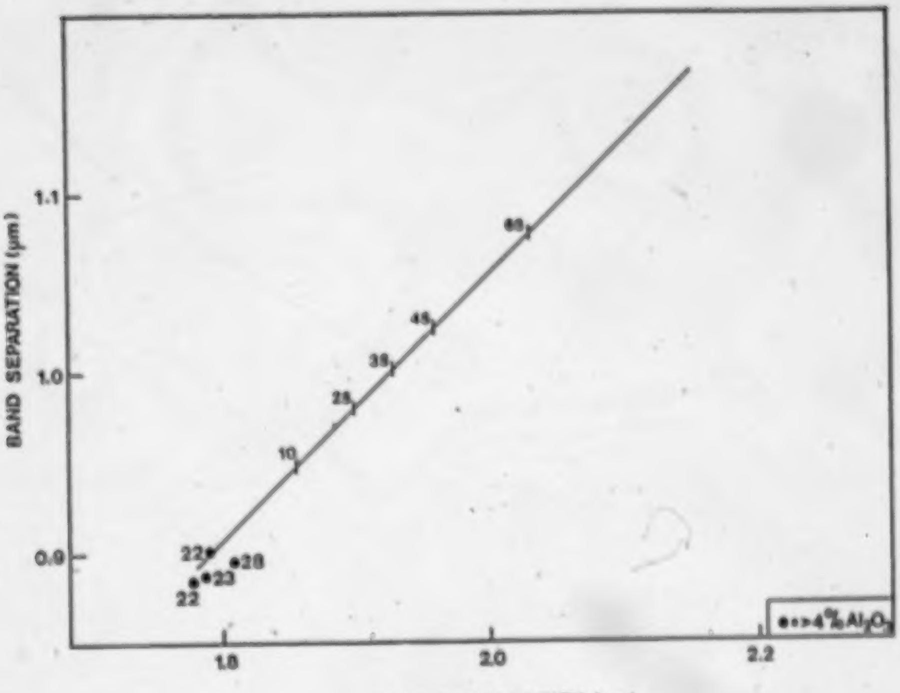

Figure II-8. Separation of the Band I and Band II minima as a function of wavelength position of the Band II minimum for orthopyroxenes show a linear trend. Both parameters increase with increasing iron content. The numbers along the trend indicate where the Fs content of low-aluminum pyaoxenes should lie. Four high-aluminum content pyroxenes are shown as circles along with their molar Fs contents.

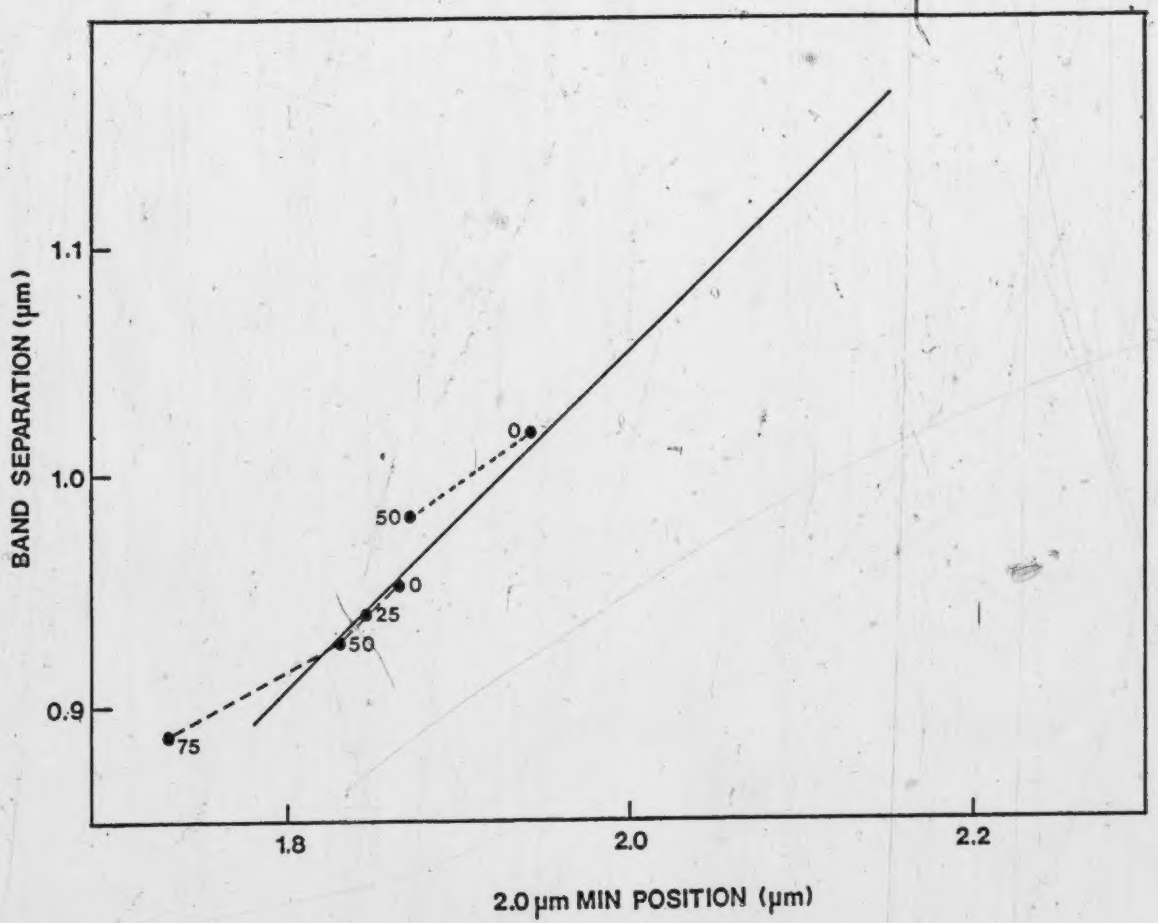

Figure II-9. Same as Figure 8 with the two orthopyroxene-metal series plotted. Numbers indicate the weight percent of metal in the mixtures.

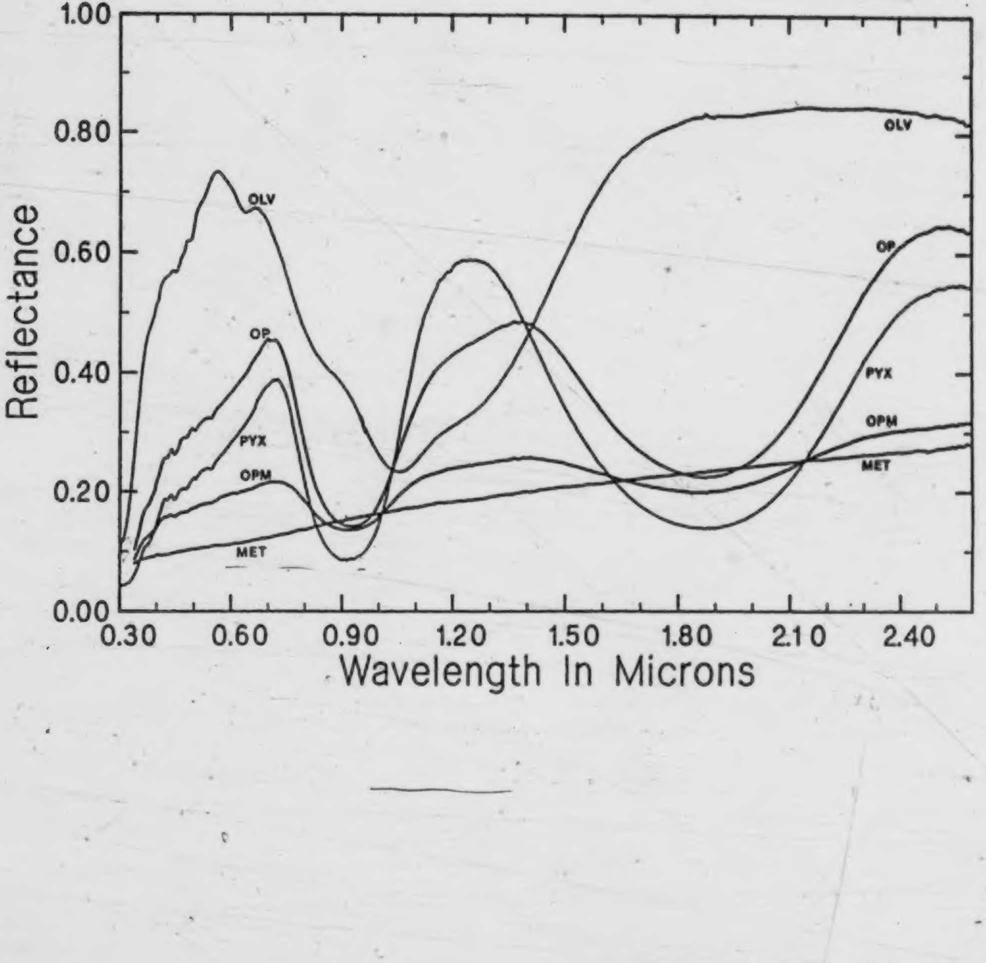

Figure II-10. Absolute reflectance spectra of 45-90μm sized ternary olivine-pyroxene-metal mixture (OPM), binary olivine-pyroxene mixture (OP), and pure end members- olivine (OLV), pyroxene (OPX), and meteoritic metal (MET).

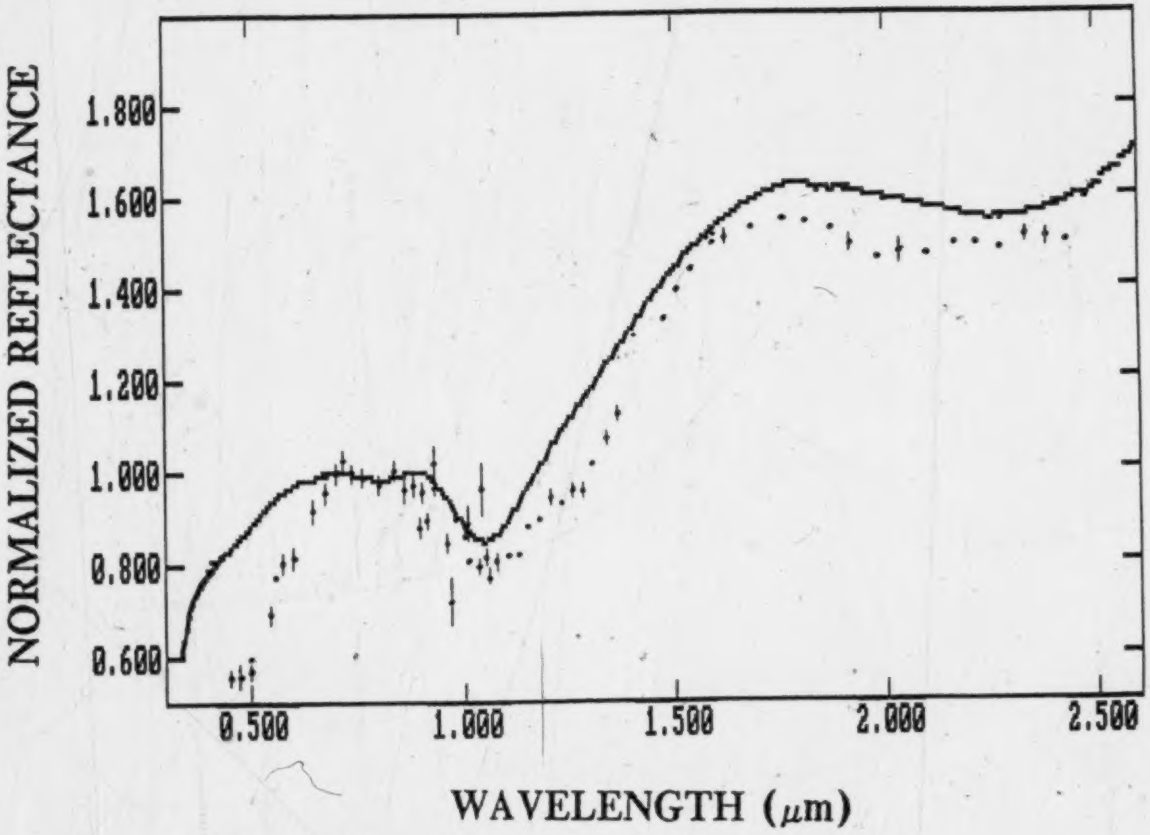

Figure II-11. Normalized reflectance spectra (scaled to 1 at 0.56μm) of asteroid (8) Flora (points) and a computer-generated additive assemblage of 30 % 50/50 OLV/MET, 60 % 25/75 OLV/MET, and 10 % PYX117 (line). Flora spectrum adapted from Gaffey (1984).

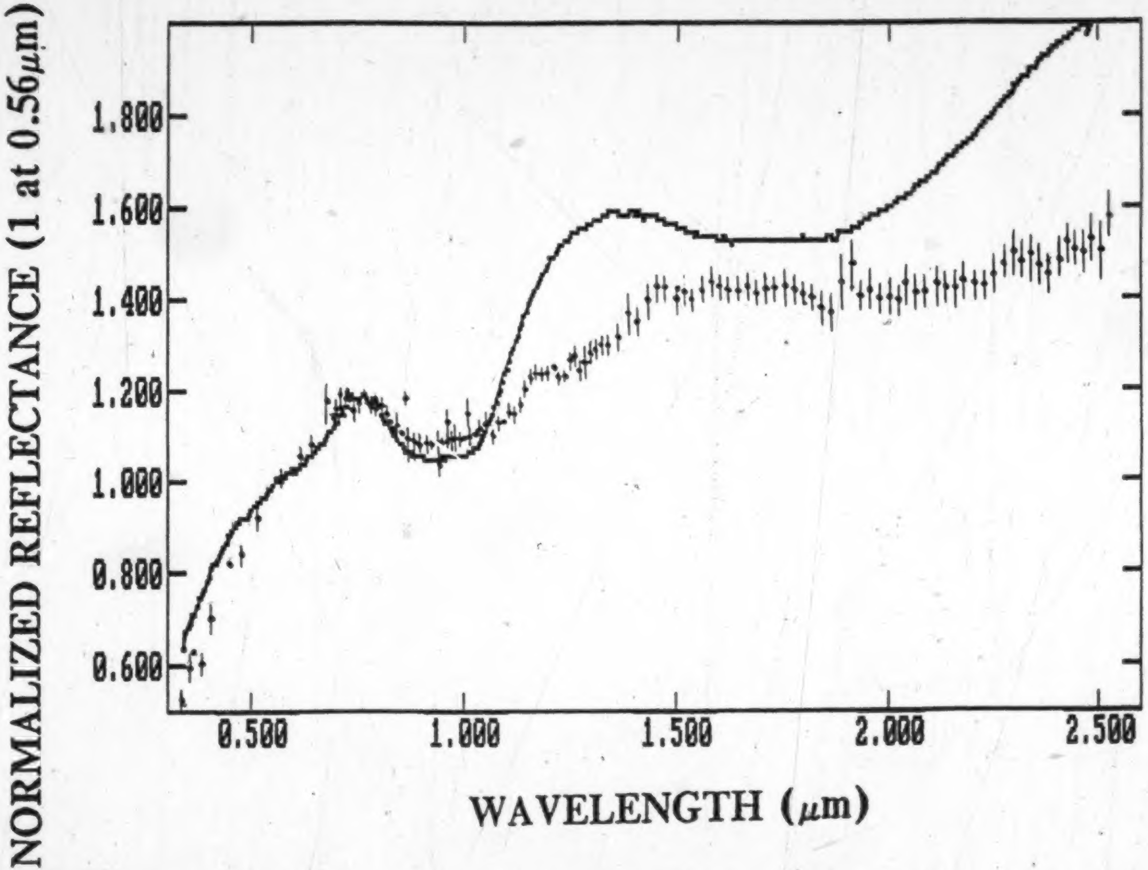

Figure II-12. Normalized reflectance spectra (scaled to 1 at 0.70μm) of asteroid (446) Aeternitas (points) and a computer-generated additive assemblage of 60 % 50/50 OLV/MET, 20 % 75/25 OLV/MET and 20 % clinopyroxene (line). Aeternitas spectrum adapted from Bell *et al.* (1984b).

A. REFERENCES

Adams, J.B., Lunar and martian surface materials: Petrologic significance of absorption bands in the near-infrared, *Science*, **159**, 1453-1455, 1968.

Adams, J.B., Visible and near-infrared diffuse reflectance spectra of pyroxenes as applied to remote sensing of solid objects in the solar system, *Jour. Geophys. Res.*, **79**, 4829-4836, 1974.

Adams, J.B., Interpretation of visible and near-infrared diffuse reflectance spectra of pyroxenes and other rock-forming minerals, in *Infrared and Raman Spectroscopy of Lunar and Terrestrial Minerals*, edited by C. Karr Jr., pp. 91-116, Academic Press, New York, 1975.

Adams, J.B., and T.B. McCord, Electronic spectra of pyroxenes and interpretation of telescopic spectral reflectivity curves of the Moon, *Proc. Third Lunar Sci. Conf.*, 3021-3034, 1972.

Adams, J.B., F. Horz, and R.V. Gibbons, Effects of shock-loading on the reflectance spectra of plagioclase, pyroxene, and glass (abstract), *Lunar Plan. Sci. Conf.* X, 1-3, 1979.

Anders, E., Most stony meteorites come from the asteroid belt, in *Asteroids: An Exploration Assessment*, edited by D. Morrison & W.C. Wells, pp.57-75, NASA CP-2053, 1978.

Aoyama, T., T. Hiroi, M. Miyamoto, and H. Takeda, Absorption spectra and bulk chemical composition of achondritic polymict breccias with reference to characterization of the surface of Vesta-like asteroids (abstract), *Lunar Plan. Sci. Conf.* XVIII, 27-28, 1987.

Auten, T.A., On the brittleness of Gibeon meteoritic iron, *Meteoritics*, **8**, 189-196, 1973.

Baldanza, B., and G. Pialla, Dynamically deformed structures in some meteorites, in *Meteorite Research*, edited by P.M. Millman, pp. 806-825, D. Reidel, Dordrecht, 1969.

Barucci, M.A., M. Fulchignoni, and R. Salvatori, Asteroid photometry simulated in the laboratory: Phase functions of some meteorites used as irregular asteroid models (abstract), *Lunar Plan. Sci. Conf.* XV, 35-36, 1984.

Bell, J.F., Mineralogical evolution of meteorite parent bodies (abstract), *Lunar Plan. Sci. Conf.* XVII, 985-986, 1986.

Bell, J.F., and K. Keil, Spectral alteration effects in chondritic gas-rich breccias: Implications for S-class and Q-class asteroids (abstract), *Lunar Plan. Sci. Conf.* **XVIII**, 58-59, 1987.

Bell, J.F., M.J. Gaffey, and B.R. Hawke, Spectroscopic identification of probable pallasite parent bodies (abstract), *Meteoritics*, **19**, 187-188, 1984a.

Bell, J.F., B.R. Hawke, and M.J. Gaffey, The olivine asteroids: discovery, mineralogy, and relationship to meteorites (abstract), *Lunar Plan. Sci. Conf.* **XV**, 48-49, 1984b.

Bell, J.F., P.D. Owensby, B.R. Hawke, and M.J. Gaffey, The 52-color asteroid survey: Final results and interpretation (abstract), *Lunar Plan. Sci. Conf.* **XIX**, 57-58, 1988.

Blodgett Jr., A.J., and W.E. Spicer, Experimental determination of the optical density states of iron, *Phys. Rev.*, **158**, 514-523, 1967.

Britt, D.T., and C.M. Pieters, The optical effects of small-scale surface processes on small bodies (abstract), *Meteoritics*, **22**, 340-342, 1987.

Britt, D.T., and C.M. Pieters, Bidirectional reflectance properties of iron-nickel meteorites, *Proc. 18th Lunar Plan. Sci. Conf.*, 503-512, 1988.

Buchwald, V.F., *Handbook of Iron Meteorites*, University of California Press, Berkeley, 1975.

Burns, R.G., Crystal field spectra and evidence of cation ordering in olivine minerals, *Amer. Mineral.*, **55**, 1608-1632, 1970a.

Burns, R.G., *Mineralogical Applications of Crystal Field Theory*, Cambridge University Press, Cambridge, 1970b.

Burns, R.G., F.E. Huggins, and R.M. Abu-Eid, Polarized absorption spectra of single crystals of lunar pyroxenes and olivines, *Moon*, **4**, 93-102, 1972.

Burns, R.G., D.J. Vaughan, R.M. Abu-Eid, and M. Witner, Spectral evidence for Cr^{3+}, Ti^{3+}, and Fe^{2+} rather than Cr^{2+} and Fe^{3+} in lunar ferromagnesian silicates, *Proc. Fourth Lunar Sci. Conf.*, 983-994, 1973.

Buseck, P.R., Pallasite meteorites- mineralogy, petrology and geochemistry, *Geochim. Cosmochim. Acta*, *41*, 711-740, 1977.

Chapman, C.R., and M.J. Gaffey, Reflectance spectra for 277 asteroids, in *Asteroids*, edited by T. Gehrels, pp. 655-687, University of Arizona Press, Tucson, 1979.

Chapman, C.R., and J.W. Salisbury, Comparisons of meteorite and asteroid spectral reflectivities, *Icarus*, **19**, 507-522, 1973.

Cintala, M.J., J.W. Head, and L. Wilson, The nature and effects of impact cratering on small bodies, in *Asteroids*, edited by T. Gehrels, pp. 579-600, University of Arizona Press, Tucson, 1979.

Clark Jr., S.P., Absorption spectra of some silicates in the visible and near infrared, *Amer. Mineral.*, **42**, 732-742, 1957.

Clark, R.N., A large-scale interactive one dimensional array processing system, *Publ. Astron. Soc. Pac.*, **92**, 221-224, 1980.

Clark, R.N., Spectral properties of mixtures of montmorillonite and dark carbon grains: Implications for remote sensing minerals containing chemically and physically adsorbed water, *Jour. Geophys. Res.*, **88**, 10635-10644, 1983.

Cloutis, E.A., *Interpretive Techniques for Reflectance Spectra of Mafic Silicates*, M.Sc. Thesis, University of Hawaii, 1985.

Cloutis, E.A., Olivine-metal mixtures: Spectral reflectance properties and phase determinations (abstract), *Lunar Plan. Sci. Conf.* XX, 173-174, 1989.

Cloutis, E.A., M.J. Gaffey, R. St J. Lambert, and D.G.W. Smith, The quality of geological information derivable from high resolution reflectance spectra: Results for mafic silicates, *Proc. 10th Canadian Symp. Remote Sensing*, 309-318, 1986a.

Cloutis, E.A., M.J. Gaffey, T.L. Jackowski, and K.L. Reed, Calibrations of phase abundance, composition, and particle size distribution for olivine-orthopyroxene mixtures from reflectance spectra, *Jour. Geophys. Res.*, **91**, 11641-11653, 1986b.

Cloutis, E.A., M.J. Gaffey, D.G.W. Smith, and R. St J. Lambert, Reflectance spectra of "featureless" materials and the surface mineral assemblages of M- and E-class asteroids, submitted to Jour. Geophys. Res., 1989.

Cloutis, E.A., M.J. Gaffey, D.G.W. Smith, and R. St J. Lambert, Reflectance spectra of "featureless" materials and the surface mineralogies of M- and E-class asteroids, *submitted to Jour. Geophys. Res.*, 1989.

Comerford, M.F., Comparative erosion rates of stone and iron meteorites under small-particle bombardment, *Geochim. Cosmochim. Acta*, **31**, 1457-1471, 1967.

Comerford, M.F., Phosphide and carbide inclusions in iron meteorites, in *Meteorite Research*, edited by P.M. Millman, pp. 780-794, D. Reidel, Dordrecht, 1969.

Cruikshank, D.P., and W.K. Hartmann, The meteorite-asteroid connection: Two olivine-rich asteroids, *Science*, **223**, 281-283, 1984.

Doan Jr., A.S., and J.I. Goldstein, The formation of phosphides in iron meteorites, in *Meteorite Research*, edited by P.M. Millman, pp. 763-779, D. Reidel, Dordrecht, 1969.

Dodd, R.T., Accretion of the ordinary chondrites, *Earth Plan. Sci. Lett.*, **30**, 281-291, 1976.

Dodd, R.T., *Meteorites, A Petrologic-Chemical Synthesis*, Cambridge University Press, Cambridge, 1981.

Dollfus, A., and B. Zellner, Optical polarimetry of asteroids and laboratory samples, in *Asteroids*, edited by T. Gehrels, pp. 170-183, University of Arizona Press, Tucson, 1979.

Dollfus, A., J.-C. Mandeville, and M. Duseaux, The nature of the M-type asteroids from optical polarimetry, *Icarus*, **37**, 124-132, 1979.

Dollfus, A., A. Cailleux, B. Cervelle, C.T. Hua, and J.-C. Mandeville, Reflectance spectrophotometry extended to u.v. for terrestrial, lunar and meteoritic samples, *Geochim. Cosmochim. Acta*, **44**, 1293-1310, 1980.

Easton, A.J., Grain-size distribution and morphology of metal in E-chondrites, *Meteoritics*, **18**, 19-27, 1983.

Feierberg, M.A., H.P. Larson, and C.R. Chapman, Spectroscopic evidence for undifferentiated S-type asteroids, *Astrophys. Jour.*, **257**, 361-372, 1982.

Gaffey, M.J., Spectral reflectance characteristics of the meteorite classes, *Jour. Geophys. Res.*, **81**, 905-920, 1976.

Gaffey, M.J., Rotational spectral variations of asteroid (8) Flora: Implications for the nature of the S-type asteroids and for the parent bodies of the ordinary chondrites, *Icarus*, **60**, 83-114, 1984.

Gaffey, M.J., The spectral and physical properties of metal in meteorite assemblages: Implications for asteroid surface materials, *Icarus*, **66**, 468-486, 1986.

Gaffey, M.J., Thermal history of the asteroid belt: Implications for accretion of the terrestrial planets (abstract), *Lunar Plan. Sci. Conf.* **XIX**, 369-370, 1988.

Gaffey, M.J., The abundance of metal on S-asteroid surfaces: Indications from IRAS 12 and 25 micron flux ratios (abstract), *Lunar Plan. Sci. Conf.* **XX**, 321-322, 1989.

Gaffey, M.J., J.F. Bell, and D.P. Cruikshank, Reflectance spectroscopy and asteroid surface mineralogy, papers presented at Asteroids II, Tucson, Arizona, March 8, 1988.

Geake, J.E., and A. Dollfus, Planetary surface texture and albedo from parameter plots of optical polarization data, *Mon. Not. R. astr. Soc.*, **218**, 75-91, 1986.

Gorban, N.Y., and V.S. Stashchuk, Optical absorption of Ni-Fe alloys, *Optic. Spectrosc.*, **37**, 202-203, 1974.

Gorban, N.Y., V.S. Stashchuk, A.V. Shirin, and A.A. Shishlovskii, Optical properties of nickel-iron alloys in the region of interband transitions, *Optic. Spectrosc.*, **35**, 295-298, 1973.

Gradie, J., and E. Tedesco, Compositional structure of the asteroid belt, *Science*, **216**, 1405-1407, 1982.

Hazen, R.M., H.K. Mao, and P.M. Bell, Effects of compositional variation on absorption spectra of lunar olivines, *Proc. Lunar Sci. Conf. 8th*, 1081-1090, 1977.

Hiroi, T., M. Miyamoto, and Y. Takano, An assignment of photon absorptions to Fe^{3+} and Cr^{3+} in pyroxenes and olivine by crystal field theory (abstract), *Lunar Plan. Sci. Conf.* **XVI**, 356-357, 1985.

Housen, K.R., and L.L. Wilkening, Regoliths on small bodies in the solar system, *Ann. Rev. Earth Plan. Sci.*, **10**, 355-376, 1982.

Housen, K.R., L.L. Wilkening, C.R. Chapman, and R. Greenberg, Asteroidal regoliths, *Icarus*, **39**, 317-351, 1979a.

Housen, K.R., L.L. Wilkening, C.R. Chapman, and R.J. Greenberg, Regolith development and evolution on asteroids and the Moon, in *Asteroids*, edited by T. Gehrels, pp. 601-627, University of Arizona Press, Tucson, 1979b.

Hunt, G.R., and R.C. Evarts, The use of near-infrared spectroscopy to determine the degree of serpentinization of ultramafic rocks, *Geophys.*, **46**, 316-321, 1981.

Hunt, G.R., and J.W. Salisbury, Visible and near-infrared spectra of minerals and rocks: I. Silicate minerals, *Mod. Geol.*, **1**, 283-300, 1970.

Johnson, T.V., and F.P. Fanale, Optical properties of carbonaceous chondrites and their relationship to asteroids, *Jour. Geophys. Res.*, **78**, 8507-8518, 1973.

Keil, K., Mineralogical and chemical relationships among enstatite chondrites, *Jour. Geophys. Res.*, **73**, 6945-6976, 1968.

King, E.A., E. Jarosewich, and F.W. Daugherty, Tierra Blanca: An unusual achondrite from west Texas, *Meteoritics*, **16**, 229-237, 1981.

King, T.V.V., and W.I. Ridley, Relation of the spectroscopic reflectance of olivine to mineral chemistry and some remote sensing implications, *Jour. Geophys. Res.*, **92**, 11457-11469, 1987.

King, T.V.V., M.J. Gaffey, and L.A. McFadden, Evidence for regolith maturation on asteroids (abstract), *Lunar Plan. Sci. Conf.* XV, 429-430, 1984.

Mao, H.K., and P.M. Bell, Interpretation of the pressure effect on the optical absorption bands of natural fayalite to 20 kb, *Carnegie Inst. Wash. Yearb.*, **71**, 524-527, 1972.

Marcus, H.L., and L.H. Hackett Jr., The low temperature fracture behavior of iron-nickel meteorites, *Meteoritics*, **9**, 371-376, 1974.

Mason, B., *Meteorites*, Wiley, New York, 1962.

Mason, B., The enstatite chondrites, *Geochim. Cosmochim. Acta*, **30**, 23-39, 1966.

Mason, B., and E. Jarosewich, The Barea, Dyarrl Island, and Emery meteorites, and a review of the mesosiderites, *Mineral. Mag.*, **39**, 204-215, 1973.

Matsui, T., and P.H. Schultz, On the brittle-ductile behavior of iron meteorites: New experimental constraints, *Proc. 15th Lunar Plan. Sci. Conf.*, in *Jour. Geophys. Res.*, **89**, C323-C328, 1984.

McFadden, L.A., M.J. Gaffey, H. Takeda, T.L. Jackowski, and K.L. Reed, Reflectance spectroscopy of diogenite meteorite types from Antarctica and their relationship to asteroids, *Proc. Seventh Symp. Antarctic Meteorites-Mem. Nat. Inst. Polar Res. Spec. Iss.* **25**, 188-206, 1982.

McFadden, L.A., *Spectral Reflectance of Near-Earth Asteroids: Implications for Composition, Origin and Evolution*, Ph.D. thesis, University of Hawaii, Honolulu, 1983.

Miyamoto, M., Diffuse reflectance from 0.25μm to 25μm of the Yamato-691 enstatite chondrite, *Proc. Eleventh Symp. Antarctic Meteorites-Mem. Nat. Inst. Polar Res. Spec. Iss.* **46**, 123-130, 1987.

Miyamoto, M., A. Mito, Y. Takano, and N. Fujii, Spectral reflectance (0.25-2.5μm) of powdered olivines and meteorites, and their bearing on surface materials of asteroids, *Proc. Sixth Symp. Antarctic Meteorites-Mem. Nat. Inst. Polar Res. Spec. Iss.* **20**, 345-361, 1981.

Miyamoto, M., M. Kinoshita, and Y. Takano, Spectral reflectance (0.25-2.5μm) of olivine and pyroxene from an ordinary chondrite, *Proc. Eighth Symp. Antarctic Meteorites-Nat. Inst. Polar Res. Spec. Iss.* **30**, 367-377, 1983.

Moore, C.B., and C.F. Lewis, Total carbon content in ordinary chondrites, *Jour. Geophys. Res.*, **72**, 6289-6292, 1967.

Mori, H., H. Takeda, M. Prinz, and G.E. Harlow, Mineralogical and crystallographic studies of lodranite and primitive achondrite groups bearing on their genetic link (abstract), *Lunar Plan. Sci. Conf.* XV, 567-568, 1984.

Morrison, D., and L. Lebofsky, Radiometry of asteroids, in *Asteroids*, edited by T. Gehrels, pp.184-205, University of Arizona Press, Tucson, 1979.

Morrison, B., and B. Zellner, V. Polarimetry and radiometry of the asteroids, in *Asteroids*, edited by T. Gehrels, pp. 1090-1097, University of Arizona Press, Tucson, 1979.

Mustard, J.F., C.M. Pieters, and S.F. Pratt, Deconvolution of spectra for intimate mixtures (abstract), *Lunar Plan. Sci. Conf.* XVII, 593-594, 1986.

Nash, D.B., and J.E. Conel, Spectral reflectance systematics for mixtures of powdered hypersthene, labradorite, and ilmenite, *Jour. Geophys. Res.*, **79**, 1615-1621, 1974.

Ostro, S.J., D.B. Campbell, and I.I. Shapiro, Main belt asteroids: Dual-polarization radar observations, *Science*, **229**, 442-446, 1985.

Papike, J.J., F.N. Hodges, A.E. Bence, M. Cameron, and J.M. Rhodes, Mare basalts:

Crystal chemistry, mineralogy, and petrology, *Rev. Geophys. Space Phys.*, **14**, 475-540, 1976.

Pieters, C.M., Polarization in a mineral absorption band, in *Planets, Stars and Nebulae Studied with Photopolarimetry*, edited by T. Gehrels, University of Arizona Press, Tucson, 1974.

Pieters, C.M., Strength of mineral absorption features in the transmitted component of near-infrared light: First results from RELAB, *Jour. Geophys. Res.*, **88**, 9534-9544, 1983.

Pieters, C.M., and J.F. Mustard, Exploration of crustal/mantle material for the Earth and Moon using reflectance spectroscopy, *Remote Sens. Envir.*, **24**, 151-178, 1988.

Powell, B.N., Petrology and chemistry of mesosiderites- I. Textures and composition of nickel-iron, *Geochim. Cosmochim. Acta*, 33, 789-810, 1969.

Powell, B.N., Petrology and chemistry of mesosiderites- II. Silicate textures and compositions and metal silicate relationships, *Geochim. Cosmochim. Acta*, 35, 5-34, 1971.

Prinz, M., D.G. Waggoner, and P.J. Hamilton, Winonaites: a primitive achondrite group related to silicate inclusions in IAB irons (abstract), *Lunar Plan. Sci. Conf.* XI, 902-904, 1980.

Remo, J.L., and A.A. Johnson, A preliminary study of the ductile-brittle transition under impact conditions in material from an octahedrite, *Jour. Geophys. Res.*, **80**, 3744-3748, 1975.

Robinson, P., the compositional space of terrestrial pyroxenes, In *Reviews in Mineralogy. Volume 7, Pyroxenes*, edited by C.T. Prewitt, pp. 419-494, Mineralogical Society of America, Washington, D.C., 1980.

Roush, T.L., *Effects of Temperature on Remotely Sensed Mafic Mineral Absorption Features*, M.Sc. Thesis, University of Hawaii, 1984.

Runciman, W.A., D. Sengupta, and J.T. Gourley, The polarized spectra of iron in silicates. II. Olivine, *Amer. Mineral.*, **58**, 451-456, 1973.

Salisbury, J.W., G.R. Hunt, and C.J. Lenhoff, Visible and near-infrared spectra: X. Stony meteorites, *Mod. Geol.*, 5, 115-126, 1975.

Singer, R.B., Near-infrared spectral reflectance of mineral mixtures: Systematic combinations of pyroxenes, olivine, and iron oxides, *Jour. Geophys. Res.*, **86**, 7967-7982, 1981.

Veeder, G.J., D.L. Matson, and J.C. Smith, Visual and infrared photometry of asteroids, *Astron. Jour.*, **83**, 651-663, 1978.

Veeder, G.J., D.L. Matson, and E.F. Tedesco, The R asteroids reconsidered, *Icarus*, **55**, 177-180, 1983.

Veverka, J., Photopolarimetric observations of the minor planet Flora, *Icarus*, **15**, 454-458, 1971.

Veverka, J., Photopolarimetric observations of 9 Metis, 15 Eunomia, 89 Julia, and other asteroids, *Icarus*, **19**, 114-117, 1973.

Wagner, J.K., B.W. Hapke, and E.N. Wells, Atlas of reflectance spectra of terrestrial, lunar, and meteoritic powders and frosts from 92 to 1800nm, *Icarus*, **69**, 14-28, 1987.

Watson, F.G., Reflectivity and color of meteorites, *Proc. Nat. Acad. Sci.*, **24**, 532-537, 1938.

Watters, T.R., and M. Prinz, Aubrites: Their origin and relationship to enstatite chondrites, *Proc. Lunar Plan. Sci. Conf. 10th*, 1073-1093, 1979.

Weidner, V.R., and J.J. Hsia, Reflection properties of pressed polytetrafluoroethylene powder, *Jour. Opt. Soc. Amer.*, **71**, 856-861, 1981.

White, W.B., and K.L. Keester, Selection rules and assignments for the spectra of ferrous iron in pyroxenes, *Amer. Mineral.*, **52**, 1508-1514, 1967.

Wilkening, L.L., What meteorites can tell us about regoliths (abstract), *Meteoritics*, **18**, 421-422, 1983.

Williams, C.V., K. Keil, A.E. Rubin, and A. San Miguel, Petrology of some ordinary chondrite regolith breccias: Implications for parent body history (abstract), *Meteoritics*, **19**, 338, 1984.

Williams, C.V., E.R.D. Scott, G.J. Taylor, K. Keil, L. Schultz, and R. Wieler, Histories of ordinary chondrite parent bodies: Clues from regolith breccias (abstract), *Meteoritics*, **21**, 541, 1986.

Yanai, K., and H. Kojima, A new stony-iron meteorite collection in the Yamato meteorites (abstract), *Meteoritics*, **18**, 429, 1983.

Yolken, H.T., and J. Kruger, Optical constants of iron in the visible region, *Jour. Opt. Soc. Amer.*, 55, 842-844, 1965.

Zellner, B., M. Leake, T. Lebertre, M. Duseaux, and A. Dollfus, The asteroid albedo scale. I. Laboratory polarimetry of meteorites, *Proc. Lunar Plan. Sci. Conf. 8th*, 1091-1110, 1977.

Zukas, E.G., Metallurgical results from shock-loaded iron alloys applied to a meteorite, *Jour. Geophys. Res.*, 74, 1993-2001, 1969.

III. REFLECTANCE SPECTRA OF "FEATURELESS" MATERIALS AND THE SURFACE MINERALOGIES OF M- AND E-CLASS ASTEROIDS

[1]

INTRODUCTION

Telescopic spectral studies of asteroids provide the best means for determining the surface compositions of these objects. There have been a number of notable successes in this area (e.g. McCord *et al.*, 1970; Bell *et al.*, 1984; Cruikshank & Hartmann, 1984; Gaffey, 1984). A significant proportion of the main-belt asteroids lack diagnostic features in the 0.3-2.5μm wavelength region (Gaffey, 1978; Gaffey & McCord, 1978). A number of "featureless" materials were spectrally characterized in order to search for diagnostic spectral parameters which can be used to overcome this difficulty. Among the materials examined were a number of iron-nickel alloys (both artificial and natural), meteoritic enstatite, amorphous carbon, iron oxides, and various mixtures of these phases with various mafic silicates.

That different meteorites possess unique spectral properties over even limited wavelength ranges has been known for some time (Watson, 1938). As the wavelength range examined has been increased, improved discrimination of different materials has resulted (Gaffey, 1976; Bell *et al.*, 1988). Most of the materials covered in this study have generally been ascribed to the featureless, and hence indistinguishable, class. For the sake of convenience they have been grouped into metals, silicates, carbon, and Fe-oxides. These materials are a chemically heterogeneous group, and positive identification of any one of them, either singly or in conjunction with other minerals, would have important implications for understanding the evolution of a particular body.

The controversy over one group of asteroids, the M class, involves a debate over whether they are differentiated metal-dominated bodies (e.g. Dollfus *et al.*, 1979; Britt & Pieters, 1988) or primitive objects similar to enstatite chondrites (Chapman & Salisbury, 1973;

---

[1] A version of this chapter has been submitted for publication. Cloutis, E.A., Gaffey, M.J., Smith, D.G.W., and Lambert, R. St J. 1989. Journal of Geophysical Research.

Chapman, 1976). Resolution of such a basic issue would have important implications for understanding the origin and early history of the asteroid belt and perhaps the solar system (Chapman, 1979; Bell, 1986; Gaffey, 1986; 1988).

EXPERIMENTAL

A number of natural and synthetic materials were spectrally characterized. The metals category includes synthetic Fe powder (IRO101, <63μm grain size), synthetic nickel powder (NIC101, <37μm grain size), synthetic pre-alloyed 50:50 iron:nickel powder (NIF101, <63μm grain size), and a number of different size fractions of the Odessa, Texas coarse octahedrite (MET101), which is predominantly composed of kamacite. The carbon is a synthetic amorphous carbon (LCA101, <0.023μm grain size). The iron oxide group is represented by natural magnetite from the Jacupiranga Mine, Sao Paulo State, Brazil (MAG101) in various size fractions. The lone spectrally featureless silicate is a metal-free sample of the Happy Canyon E7 enstatite chondrite (PYX205; Table III-1). Carbon and magnetite were incorporated into various mixtures with orthopyroxenes and olivine. The orthopyroxenes are from an unspecified locality in India (PYX117), and Ekersund, Norway (PYX032), and the olivine is from San Carlos, Arizona (OLV003).

The compositions of OLV003, PYX117, MET101, and MAG101 were obtained by electron microprobe analysis at the University of Calgary SEMQ facility and are averages of 6-8 point analyses and area scans (Table III-1). The data were reduced using Bence-Albee α and β corrections. The Fe^{2+} values were obtained by wet chemical methods, and Fe^{3+} as the difference between total and ferrous iron. For the iron meteorite, only the kamacite, which forms the bulk of the sample (Buchwald, 1975) was analyzed (MET101). The analysis of the pyroxene in Happy Canyon is from Watters & Prinz (1979).

The Happy Canyon E7 sample was prepared by crushing the sample in an alumina mortar and pestle, and acid treated to remove the pervasive iron oxide contaminants and metal. The magnetite and silicate samples were obtained by crushing in the same way. The required phases were separated through a combination of magnetic separation and hand picking. The cleaned samples were repeatedly wet sieved with acetone to obtain well-sorted size ranges. The meteoritic metal was obtained by grinding an unweathered, interior sample of the meteorite with an emery grinder and magnetically separating the grinding wheel contaminants. A portion of this powder was beaten in the alumina mortar and pestle in order to obtain a more equidimensional grain shape, and wet sieved with acetone. The 45-90μm beaten portion of the powder will be referred to as MET101b to distinguish it from the unbeaten 45-90μm sample. The 0-45μm and 125-355μm fractions are the unbeaten samples. Immediately following the sieving, the meteoritic metal powders were transferred to a dry nitrogen environment, separated into splits for X-ray diffraction and spectral analysis, and sealed. The artificial metal powders were opened in the nitrogen environment, split, and resealed.

The reflectance spectra were acquired at the RELAB spectrometer facility at Brown University and at the U.S. Geological Survey facility in Denver, CO. Details of the instrumentation can be found in Pieters (1983), and King & Ridley (1987). The spectra measured at the RELAB facility were acquired at 0° incidence and 15° emission. All but the three size fractions of MET101 (unbeaten) were measured at the RELAB facility. The spectra measured at the U.S. Geological Survey were acquired using an integrating sphere arrangement. All the spectra were measured relative to halon, a near-perfect diffuse reflector in the 0.3-2.7μm region (Weidner & Hsia, 1981), corrected for minor (~2%) irregularities in halon's absolute reflectance in the 2μm region, as well as for dark current offsets. The reflectance spectra were processed using the Gaffey Spectrum Processing System- a PC-compatible version of SPECPR (Clark, 1980).

RESULTS

The various reflectance spectra have been subdivided on the same basis used earlier- metals, silicates, carbon, and iron oxides, since the presence of each group has important genetic implications for remote sensing analysis. The pure metal and metal-silicate spectra provide information on the detection limits for silicates in these types of assemblages.

Carbon-silicate and magnetite-silicate mixtures were also examined to determine silicate detection limits and whether the opaque phases possess diagnostic spectral features.

Metal

Metallic nickel-iron is the dominant component in iron meteorites (Buchwald, 1975), and can comprise a substantial portion of many other meteorite classes (e.g. Mason, 1962). The spectral properties of meteoritic metal and the detection limits for silicates in metal-silicate mixtures are important for determining whether the parent bodies of various metal-rich meteorites can be identified. The principal meteoritic metal phase in almost all iron meteorites and achondrites is kamacite, whose brittle-ductile transition temperature is approximately equal to the temperatures present in the main asteroid belt, and hence may be subject to comminution during impacts (Auten, 1973; Marcus & Hackett, 1974; Remo & Johnson, 1975; Matsui & Schultz, 1984). The presence of various exsolved and included phases in iron meteorites such as schreibersite/rhabdite, troilite, graphite, and cohenite (Baldanza & Pialla, 1969; Comerford, 1969; Doan & Goldstein, 1969; Buchwald, 1975) may serve as zones of structural weakness and facilitate comminution. Laboratory studies of high velocity impacts on meteoritic metal show the development of irregular surfaces and spallation products even at temperatures well within the ductile deformation regime (Matsui & Schultz, 1984; Britt & Pieters, 1988).

There are a number of lines of evidence to suggest that metal-rich bodies possess particulate surfaces. Polarization data for M-type asteroids, presumed to be metal-rich, can be matched by those from 20-40μm sized metal powders (Dollfus & Mandeville, 1977; Dollfus *et al.*, 1979). Radar observations of the asteroid 16 Psyche are also interpreted as a nearly pure metallic surface with lunar surface-like porosities (Ostro *et al.*, 1985). M-asteroid reflectance spectra also seem to be consistent with particulate metal (Britt & Pieters, 1988). The interpretation of the observational data is dealt with at length in a later section.

The vast majority of iron meteorites and nickel-iron alloys show a gradual increase in reflectance from 0.20-2.7μm. The only exception seems to be flat plates with a surface roughness less than the wavelength of light (Britt & Pieters, 1988). Other flat, polished alloys and iron meteorites show the expected red slope (reflectance increasing towards longer wavelengths) (Yolken & Kruger, 1965; Blodgett & Spicer, 1967; Gorban *et al.*, 1973; Gorban & Stashchuk, 1974; Miyamoto, 1987). All powdered specimens show a red slope (Johnson & Fanale, 1973; Gaffey, 1974; Dollfus *et al.*, 1980; Britt & Pieters, 1988). This applies to even very fine-grained specimens with particle diameters of a few 10's of microns or less (Feierberg *et al.*, 1982; McFadden *et al.*, 1984; Gaffey, 1986; Wagner *et al.*, 1987), and metal-coated particles (Bell & Mao, 1977).

The reflectance properties of metal are a function of the composition and grain size/surface roughness of the sample. In order to understand the relative importance of these parameters better, the reflectance spectra of a series of well-characterized meteorite and artificial metals were measured. The compositional dependence of the spectra was investigated using metal powders with roughly equivalent grain sizes-IRO101 (<63μm), NIC101 (<37μm), NIF101 (<63μm), and the MET101 samples. The effect of grain size on spectral reflectance was determined from the four size fractions of the Odessa iron meteorite- 0-45μm, 45-90μm, 45-90μm beaten, and 125-355μm. A mixture of 99.5:0.5 meteoritic metal:amorphous carbon was also spectrally characterized in order to investigate the effect of opaque phases on metal spectra. The absolute and normalized reflectance spectra of some of the metals are shown in Figures 1 and 2. All show a red slope with no well-defined absorption bands. The slopes of the artificial metals (Figure III-1) show differences in spectral slope presumably due to composition since the grain sizes are all comparable. The reflectance decline towards shorter wavelengths is more pronounced in the nickel than in the iron, as expected (Gaffey, 1974). The two nickel-iron alloys (NIF101, MET101) are not intermediate between the two end members, suggesting that free electron densities, which affect spectral reflectance, are sensitive to crystallographic structure. No simple correlation exists between reflectance ratios and iron:nickel abundances. Different metals all show the red slope but quantitative analysis of metal-rich target spectra will require the use of spectrally compatible materials.

The effects of grain size variations on metal spectra are illustrated in Figure II-2. The different size samples of MET101 are metal shavings, hence spectral differences may not be as extreme as would be present for samples containing more equidimensional particles. Increasing the grain size results in a reduction in albedo at shorter wavelengths. At longer wavelengths, the increase in reflectance with increasing wavelength (red slope) is less for the finer-grained than the coarse-grained sample spectra, resulting in cross-overs in absolute reflectance. Absolute reflectance is then not only a function of grain size but also of wavelength. Although every effort was made to minimize exposure of the metal powders to air, the absolute reflectance of the spectra (4-9 % at 0.56μm) is low compared to other reflectance spectra of iron meteorite powders, slabs, and roughened surfaces, where absolute reflectances of up to 29 % at 0.56μm have been measured (Johnson & Fanale, 1973; Gaffey, 1976; Britt & Pieters, 1988). The reason for the large range in absolute albedos appears to be a complex function of grain size, sample preparation, and viewing geometry (Britt & Pieters, 1988).

The normalized reflectance spectra of the metal powders (Figure II-2) show that the relative increase in reflectance with increasing wavelength is greatest for the largest grain sizes. The 1.6μm/0.56μm reflectance ratio was selected to examine these changes in overall slope. For the metal powder spectra presented in Figure II-2, this reflectance ratio increases from 1.66 to 2.12 with increasing grain size. The investigators have measured reflectance ratios between 1.22 and 1.65, but again, there is not a simple dependency between this ratio and grain size or surface roughness dimensions of the samples. For metal slabs with surface roughness dimensions that are roughly equal to, or less than, the wavelength of light, the reflectance ratio may be less than one (Britt & Pieters, 1988).

Iron meteorites contain variable amounts of other minerals such as schreibersite, graphite, troilite, and silicates (Buchwald, 1975). The addition of a small amount of a spectrally distinct opaque phase was investigated by measuring the reflectance spectrum of a 99.5:0.5 MET101:LCA101 mixture. The overall reflectance of this spectrum is less than one half that of the metal spectrum but both spectra possess the same degree of redness (Figure III-3). Amorphous carbon is not spectrally equivalent to graphite, but shows that the metal red slope is not affected by the presence of a very dark, opaque phase at this abundance level in absolute reflectance. A further implication is that the small amount of carbon found in ordinary chondrites is probably not the cause of the flat slope of the metal-rich fraction (Gaffey, 1986).

Reflectance spectra of mafic silicate-metal mixtures were measured in order to determine what minimum abundance of silicate is required to be spectrally resolvable. The most metal-rich assemblages measured were 25:75 weight percent mixtures of olivine:metal and pyroxene:metal. At these abundances, olivine is barely resolvable as a narrow reflectance plateau near 1μm superimposed on the red metal slope, while the pyroxene:metal mixture retains two clearly resolved absorption bands. This may pose a problem in identifying the parent bodies of the pallasites, although olivine-metal asteroids have been identified (Bell *et al.*, 1984; Cruikshank & Hartmann, 1984). Pyroxene- and metal-rich asteroids similar to mesosiderites and siderophyres will be easier to identify because the minimum threshold for detecting ferrous-iron-bearing pyroxene is ~10 wt. %.

Enstatite

Very low-iron content enstatite (<1% FeO) is the most abundant mineral in enstatite chondrites and aubrites (Mason, 1966; Keil, 1968; Watters & Prinz, 1979). Aubrites are nearly pure enstatite with almost no carbon (Grady *et al.*, 1986). Their mineralogy is approximately 75-98% enstatite, 0-16% plagioclase, 0-8% diopside, 0-10% olivine, 0-4% metal, and 0-7% troilite (Olsen *et al.*, 1977; Watters & Prinz, 1979; Watters *et al.*, 1980).

Spectrally, enstatite shows no well-resolved absorption features because of the almost complete absence of transition series elements. The reflectance spectrum of the Happy Canyon acid-insoluble fraction is nearly flat with a slight downturn in reflectance at wavelengths less than ~0.4μm and a weak absorption band near 0.9μm (Figure III-4). The weak absorption band near 1.9μm is probably due to the presence of a small amount of a hydrated phase. This contrasts with meteoritic metal, the second most abundant phase in enstatite chondrite, which has a red slope even when the metal is finely divided (Figure III-2). There appears to be little chance of confusing metal with enstatite.

Enstatite+Metal

Difficulties in spectral interpretation may arise for enstatite+metal assemblages such as enstatite chondrites. Their spectral slopes are transitional between pure metal and pure enstatite (Salisbury & Hunt, 1974; Salisbury *et al.*, 1975; Gaffey, 1976; Dollfus *et al.*, 1980; Miyamoto, 1987). Some enstatite chondrite spectra show a slope break near 0.6μm whose cause is uncertain. The average grain size of the metal is <30μm in lower petrologic grades increasing to ~50μm in higher grades (Easton, 1983). It is reasonable to use the 0-45μm metal fraction as an end member in investigating these meteorites.

The enstatite chondrites contain a small amount (0.25-0.5 wt. %) of carbon (Moore & Lewis; 1965; Grady *et al.*, 1986), with the lower abundances in the higher petrologic grades. The carbon is largely in the form of graphite, cohenite, and other unspecified forms (Keil, 1968; Deines & Wickman, 1985), and is more ordered in the higher petrologic types (Grady *et al.*, 1986). This amount of carbon should not affect the overall reflectance slope. The less-equilibrated specimens have more diverse silicate compositions, with a few percent of the mafic silicates containing appreciable amounts of iron (Lusby *et al.*, 1987).

Lower petrologic grade enstatite chondrites should show some evidence of mafic silicate absorption bands, have a less red slope, and a higher overall albedo, than the more equilibrated meteorites on the basis of these properties. The available reflectance spectra show that the lower petrologic grade specimens exhibit variable evidence of mafic silicate absorption bands, a more red slope, and a lower overall albedo (e.g. Salisbury *et al.*,1975). The increased red slope of the lower grades may be due to the more efficient dispersal of metal throughout the matrix due to its smaller grain size (Easton, 1983), the presence of both oxidized and unoxidized metal grains, versus the higher petrologic grade meteorites (Gaffey, 1986), or differences in sample preparation. Some of the spectra show weak absorption features which may be due to minor amounts of iron-bearing silicates (Figure III-4; Gaffey, 1976; Miyamoto, 1987). Additional spectral complexities will appear if the mineralogy of enstatite-rich bodies is more diverse than previously believed (Grossman *et al.*, 1988).

The 1.8/0.7μm reflectance ratio was selected to highlight spectral differences between the aubrites, enstatite chondrites, and iron meteorites. This portion of the spectrum is fairly linear in all three groups, and avoids the ultraviolet-visible spectral region which can be strongly affected by intense charge transfer absorptions in accessory phases. A plot of this ratio versus the non-silicate content of the available spectra and those measured in this study shows a roughly linear correlation with the notable exception of Abee (Figure III-5). The increased red slope of this meteorite is likely due to some combination of the differences highlighted above. Other spectra of Abee and another low-grade enstatite chondrite (Y-691) show a much flatter slope (Salisbury & Hunt, 1974; Salisbury *et al.*, 1975; Miyamoto, 1987) more in line with the E6 chondrites. The 2.5/0.6μm reflectance ratio (available for all specimens) is variously ~1.2 (Salisbury & Hunt, 1974), 1.56 (Salisbury *et al.*, 1975), and 1.69 (Gaffey, 1976). Other low-petrologic grade enstatite chondrites have 2.5/0.6μm ratios of 1.28 (Yamato 691- Miyamoto, 1987) and 1.56 (Indarch- Salisbury *et al.*, 1975). Regardless of the cause of this excess reddening, the 1.8/0.7μm ratio of Abee (1.37) from Gaffey (1976) is less than the fine-grained pure metal (1.55).

Carbon

A series of carbon-mafic silicate and magnetite-mafic silicate mixtures was spectrally characterized. Only the most opaque-rich samples are dealt with here, as the intention is to establish spectral detection limits for the mafic silicates. Carbon is present in varying amounts and forms in all chondritic meteorites and the ureilites. Its abundance and form will determine the degree to which the mafic silicates are resolvable. The most carbon-rich meteorite classes are the ureilites (2-5 wt. %) and the carbonaceous chondrites (0.1-5 wt. %) (e.g. Gibson *et al.*, 1971; Gibson, 1976). The carbon is largely in the form of submicron, dispersed grains, commonly with an amorphous or semi-amorphous structure (Vdovykin, 1970; Baumann *et* *al.*, 1973; Van Der Stap *et al.*, 1986; Blake *et al.*, 1988). Fine-grained amorphous carbon was chosen as a worst case spectral scenario-a highly absorbing, dispersable material. The carbon used has a slightly blue slope with an overall reflectance of <1% (Figure III-6).

The lowest mafic silicate:carbon ratio measured was 98:2, which is in the mid-range of the carbonaceous chondrites and ureilites. At this abundance, carbon greatly reduces the spectral reflectance of the olivine (Figure III-6) and pyroxene (Figure III-7), but their major Fe^{2+} absorption bands are still resolvable. The effect of mafic silicate grain size on the detection limit was investigated for the olivine. A 99.5:0.5 by weight olivine:carbon mixture using 0-45μm size olivine has a reflectance spectrum with an almost completely obscured 1μm absorption band. The mixture containing the same proportions but with a 45-90μm size olivine has a well-defined 1μm absorption band (Figure III-6).

An overall red slope is introduced to the mafic silicate spectrum by the carbon. This seems to be a common feature in mafic silicate-amorphous carbon mixtures (Miyamoto *et al.*, 1981; 1982). A similar reddening is seen in the spectra of the finest fractions of carbonaceous chondrites, perhaps due to the more effective dispersal of the opaque phase (Johnson & Fanale, 1973). The redness seems to diminish at higher carbon abundances. An opposite effect (blue slope) is seen in fine-grained mixtures of montmorillonite-carbon, even though both phases are slightly red (Clark, 1983). This is presumably due to Rayleigh scattering.

The spectral effect of adding carbon to a mafic silicate is to reduce the overall albedo, but major absorption bands remain resolvable. Although no more than 2 wt. % carbon was used, the available data for the carbon-silicate mixtures suggests that olivine and pyroxene absorption bands may be resolvable up to 5-6 wt. % carbon if the silicates retain a mean grain size in the 10's of microns range. For finer-grained materials, the detection limit is substantially lower- perhaps 1-2 wt. % carbon. It would appear that the parent bodies of the carbon-rich meteorites should be identifiable by the presence of weak mafic silicate absorption bands, or if the silicates are finely comminuted, by a red spectral slope of low albedo. Re-examination of dark meteorite spectra has shown that Fe^{2+} silicate absorption features are more widespread than expected (Gaffey, 1978; 1980; Vilas & Gaffey, 1989). Dark, flat reflectance spectra cannot be attributed to the presence of amorphous carbon alone if the host materials consists of mafic silicates. The carbon must be in some other structural form or an additional opaque phase must be present.

Iron Oxides

Magnetite is the other opaque phase which is most prevalent in carbonaceous chondrites. A series of olivine-magnetite mixtures was spectrally characterized to confirm that magnetite-mafic silicate mixtures have dark, relatively flat reflectance spectra (Singer, 1981; Miyamoto *et al.*,1982). A 45-90μm size magnetite was used in most cases, although the bulk of the magnetite in carbonaceous chondrites is much finer-grained (e.g. Kerridge, 1970). Magnetite reflectance spectra show a reflectance maximum near 0.8μm and a weak absorption band near 1μm (Hunt *et al.*, 1971a; Adams, 1975; Gradie & Veverka, 1980; Singer, 1981; Wagner *et al.*, 1983). Beyond 1μm the spectrum may remain constant, decline slightly or increase slightly. The absence of a reflectance increase seems to be characteristic of cation-deficient and fine-grained specimens (Morris *et al.*, 1985). The magnetite in carbonaceous chondrites is fine-grained and probably not stoichiometric Fe_3O_4 (Kerridge, 1970; Nagy, 1975). The magnetite spectra in Morris *et al.* (1985) are the most reasonable spectral analogues for the magnetite in carbonaceous chondrites.

At the highest magnetite abundance measured, 50:50 magnetite:olivine both 45-90μm size, the Fe^{2+} absorption band is still clearly resolvable (Figure III-8). Coarse-grained magnetite is clearly not a viable candidate for the darkening agent in carbonaceous chondrites and C-class asteroids. Fine-grained magnetite provides more desirable spectral features. It imparts a much bluer slope to the reflectance spectrum. Magnetite alone is probably not sufficient to account for the low contrast or lack of mafic silicate absorption bands, but in combination with carbon can probably provide all the necessary spectral modifications. Unfortunately ternary carbon-magnetite-mafic silicate spectra were not measured in this study.

APPLICATION TO ASTEROID SPECTRA

The spectral detection limits for mafic silicates mixed with various featureless materials depends greatly on a number of factors. Particle size, mineral chemistry, degree of dispersion, and abundance are all significant parameters. This complicates interpretation of the reflectance spectra of dark, nearly featureless objects. The situation for enstatite and metal is more straightforward. A representative member of the M- and E-class asteroids was selected for reanalysis of the available data in light of the laboratory results.

M-Class Asteroid (16) Psyche

Asteroid (16) Psyche has been variously interpreted as possessing either an iron meteorite-like surface assemblage (Johnson & Fanale, 1973; Dollfus *et al.*, 1979; Ostro *et al.*, 1985), or an enstatite chondrite-like surface assemblage (Chapman & Salisbury, 1973; Chapman, 1976). The 0.3-1.1μm reflectance spectrum of Psyche (Gaffey & McCord, 1978) shows a gradual increase in reflectance towards longer wavelengths with an apparent reflectance minimum at 0.4μm, a weak, broad absorption feature near 0.6μm and a weak, narrow absorption feature near 0.9μm. The 52-color asteroid survey spectrum (Bell *et al.*, 1988) covers the wavelength range from 0.8μm to 2.5μm, and shows no other well-defined absorption bands (Figure III-9). The competing interpretations of Psyche's surface assemblage have largely been based on the overall slope of the reflectance spectrum. The 1.6μm/0.56μm and 2.2μm/0.56μm reflectance ratios for Psyche (Veeder *et al.*, 1978; Larson & Veeder, 1979; Gaffey *et al.*, 1988), enstatite chondrites, aubrites (Gaffey, 1976; Miyamoto, 1987), iron meteorite slabs and powders (Johnson & Fanale, 1973; Gaffey, 1976; Britt & Pieters, 1988) and the acid-insoluble fraction of the Happy Canyon E7 chondrite are shown in Figure III-10. The reflectance ratios for Psyche fall well within the enstatite chondrite field. Even the finest-grained metal spectrum (0-45μm size), which has a mean grain size similar top that derived for Psyche on the basis of polarimetry (Dollfus *et al.*, 1979) is significantly redder than Psyche. The absolute reflectance of Psyche (9-11 % at 0.56μm) is not diagnostic of a particular assemblage. The available enstatite chondrite spectra have absolute reflectances at 0.56μm of between 8 and 18%, while for iron meteorites the absolute reflectance ranges from 7 to 29 %. Variations in particle size and the presence of opaque, but spectrally neutral accessory phases could increase the ranges of absolute reflectance, further complication spectral interpretation based on absolute albedos.

The 0.3μm to 2.6μm normalized reflectance spectrum of Psyche is shown overlain with the normalized reflectance spectra of the Happy Canyon sample and the 45-90μm-sized iron meteorite powder (Figure III-9). Psyche's reflectance spectrum is intermediate between the two laboratory spectra and exhibits a change in slope near 1μm. The reason for this slope change is not known, but it appears to varying degrees in the iron meteorite powder spectra and is most apparent for the finest grain size spectrum. A similar change in slope is present in many of the enstatite chondrite spectra but occurs near 0.7μm in these cases (Gaffey, 1974; 1976). This suggests that enstatite chondrite and metal spectra may be distinguishable on the basis of the wavelength position of the slope change. On this basis, Psyche is similar to the iron meteorite spectra. The slopes of the iron meteorite spectra on either side of the slope change decreases with decreasing grain size. The slopes for Psyche (as measured by the 1.0μm/0.35μm and 2.5μm/1.0μm reflectance ratios) are less than for the 0-45μm-sized metal, but fall along a trend for the metal powders, suggesting that if the surface of Psyche is composed predominantly of metal, a significant portion of this metal is extremely fine-grained (Figure III-11).

The polarimetric parameters P_{min} and V_0 (or α_0) for enstatite chondrites plot outside the range for metal powders and M-asteroids with the exception of the E4 chondrite, Abee (Dollfus *et al.*, 1971; Zellner, 1975; Zellner *et al.*, 1977a; 1977b; Dollfus *et al.*, 1979). The reason for this discrepancy may be related to the fact that the Abee powdered sample was obtained from a cut slab, whereas the other enstatite chondrite samples were obtained from broken pieces. Saw cut chondrites are visibly different from broken surfaces because cutting a meteorite exposes the interior of metal grains which are otherwise not seen on broken surfaces (Gaffey, 1986). It is possible that this may also have an effect on the polarimetric properties of the sample.

The polarimetric data for metal powders suggest that the surface of Psyche possesses predominantly fine-grained metal particles of ~20μm size (Dollfus *et al.*, 1979). A fine-grained surface would also be in agreement with the radar albedo data suggesting a predominantly metallic surface of fine-grained particles with lunar regolith-like porosities (Ostro *et al.*, 1985). A reduction in metal content must be accompanied by a reduction in porosity in order to reconcile with the radar data.

The weak absorption bands seen in Psyche's reflectance spectrum are not particularly diagnostic. Psyche shows an apparent reflectance increase at wavelengths shorter than ~0.4μm, and broad absorption features near 0.6 and 0.9μm. The possible absorption feature near 0.4μm is also seen in troilite reflectance spectra (Egan & Hilgeman, 1977), but not in metal (Dollfus *et al.*, 1980) or enstatite (Figure III-4). The broad absorption near 0.6μ is seen as a reflectance break in meteoritic metal spectra (Figure III-2; Dollfus *et al.*, 1980), in troilite (Egan & Hilgeman, 1977), and in Abee (Gaffey, 1976; Dollfus *et al.*, 1980). It does not appear to be uniquely characteristic of a a particular phase.

The weak feature near 0.9μm is not characteristic of metal, but a similar feature is seen in the E7 reflectance spectrum (Figure III-4), other enstatite chondrites (Gaffey, 1976), and iron sulphides (Hunt *et al.*, 1971b). It is commonly ascribed to ferrous iron crystal field transitions and could be due to either sulphides or silicates.

The 3-4μm spectrum of Psyche (Eaton *et al.*, 1983) does not show the red slope expected for metal and appears to be even flatter than the E chondrite spectrum (Miyamoto, 1987). Fine-grained metal may account for the flatter than expected slope.

The observational data tend to support a fine-grained metal surface assemblage for Psyche, although an enstatite chondrite-like assemblage cannot be conclusively excluded. Minor accessory phases such as troilite are probably the cause of the various weak absorption bands which seem to be present. An iron-bearing mafic silicate component, if present, is constrained to <20 wt. % by spectroscopic and radar considerations.

E-Class Asteroid (44) Nysa

Asteroid (44) Nysa was selected for analysis because it is the best-characterized member of the E-class of asteroids. Visible and near-infrared spectra (Chapman & Gaffey, 1979; Bell *et al.*, 1988; Gaffey *et al.*, 1988), infrared photometry (Veeder *et al.*, 1978) and photopolarimetry (Zellner, 1975; Zellner *et al.*, 1978) are available forr this object.

Nysa is a bright object. Its geometric albedo has been determined to be ~38 % (Zellner, 1975), while the absolute albedo at 0.56μm has been determined to be ~49 % (Gaffey *et al.*, 1988). The high albedo strongly suggests that a transition metal-free silicate such as forsterite, plagioclase feldspar, or enstatite is a dominant surface component. Enstatite is the likeliest candidate on the basis of meteoritical evidence. The two main enstatite-rich meteorite groups, enstatite chondrites and aubrites, vary primarily in the amount of metal and sulphides they contain. Enstatite chondrites normally contain 25-30 wt. % metal+troilite versus <2 wt. % in the aubrites (Keil, 1968; Watters & Prinz, 1979). The reflectance spectra of these two groups differ in terms of overall reflectance and degree of spectral reddening.

The 1.6μm/0.56μm and 2.2μm/0.56μm reflectance ratios of Nysa from photometry and spectroscopy fall in or near the field occupied by the aubrites (Figure III-10). The 0.56μm to 0.35μm wavelength interval for Nysa (Figure III-12) shows a ~10 % reflectance decrease, comparable to the aubrites (Gaffey, 1974; 1976) and metal-free Happy Canyon spectrum (Figure III-4), but much less than the ~30 % decrease seen in most of the enstatite chondrites and metal (Gaffey, 1974; 1976; Salisbury *et al.*, 1975; Miyamoto, 1987; Figure III-2). The absolute reflectance of Nysa also suggests a close affinity to the aubrites. The absolute reflectance of aubrites and Happy Canyon at 0.56μm varies between 23 and 44 %. For enstatite chondrites the range is 6-18 %, even for very fine-grained samples. The difference in absolute reflectance between the Happy Canyon 45-90μm-sized sample spectrum (44 % at 0.56μm) and Nysa (49 % at 0.56μm) can be reconciled by decreasing the grain size of the laboratory sample. By analogy to plagioclase, another low transition metal content silicate, a <25μm-sized sample of Happy Canyon would have an absolute reflectance of ~55 %

at 0.56μm (Crown & Pieters, 1987). The reflectance spectrum of Nysa is redder than the Happy Canyon spectrum, but not as red as meteoritic metal (Figure III-12). The red slope and the weak absorption bands near 0.9μm, 1.4μm, and 1.8-1.9μm present in the spectrum of Nysa must be due to some other material because aubritic pyroxene is nearly flat and featureless (Figure III-4). The small amounts of metal present in aubrites (Watters & Prinz, 1979) could conceivably provide a slight red slope to enstatite without drastically reducing overall reflectance. The absorption features present in Nysa's spectrum are weak, with band depths (D_b- Clark & Roush, 1984) of 2-3 %. The wavelength positions of the bands near 0.9μm (0.905μm) and 1.8μm (1.808μm) correspond almost exactly with the band positions expected for very low iron (Fs=5) orthopyroxene, but not for low iron olivine, clinopyroxene, or plagioclase (Cloutis, 1985; Adams & Goullaud, 1978). Again using plagiocalse as a spectral analogy for enstatite, 5-10 wt. % of an iron bearing pyroxene added to the iron-free material either intimately or areally would be sufficient to produce two absorption bands comparable to those seen in Nysa's spectrum, in terms of wavelength position and intensity. This abundance would also not excessively reduce the absolute albedo. The lowest petrologic grade enstatite chondrites (E3) contain sufficient amounts of higher iron pyroxene to produce such absorption bands (Lusby *et al.*, 1987), but these bands are not apparent in E3 reflectance spectra (Miyamoto, 1987) perhaps because of the presence of accessory opaque components.

The absorption bands present in Nysa's spectrum near 1.4μm and 1.9μm are commonly associated with some form of water, either molecular or structural. If these bands are real, they suggest that a hydrated silicate is probably present on the surface of Nysa. Because of the high transparency of enstatite, a small amount of a spectrally featured material mixed in with, or adjacent to, enstatite will be detectable. Readily apparent compositional variations in meteorites over small scales are not unknown (Nininger, 1979). More significantly, distinct light and dark lithologies are present in the Cumberland Falls and Allan Hills 78113 aubrites (Lovering, 1962; Binns, 1969; Neal & Lipschutz, 1981; Verkouteren

& Lipschutz, 1983; Lipschutz *et al.*, 1988). The dark portions of these meteorites contain abundant low iron pyroxene which could account for the absorption bands in Nysa's spectrum at 0.9μm and 1.8μm. The dark xenoliths are a low petrologic grade chondritic material, and at least some are highly shocked (Binns, 1969; Verkouteren & Lipschutz, 1983; Lipschutz *et al.*, 1988). Reflectance spectra are not available for these xenoliths but other highly shocked ordinary chondrites show many desirable spectral features including a red slope similar to Nysa, weak mafic silicate absorption bands and a weak absorption band near 1.4μm, which may however be due to terrestrial weathering (Gaffey, 1976). Low petrologic grade meteorites that are mineralogically similar to the aubrite xenoliths, such as Renazzo and ALH85085, contain abundant hydrated silicates (Mason & Wiik, 1962; Van Schmus & Hayes, 1974; Weisberg *et al.*, 1988). While hydrated silicates have not been documented for aubrites, they may potentially possess all the spectral characteristics necessary to account for all of the absorption features seen in the reflectance spectrum of Nysa.

The polarimetric data for Nysa can be matched by either aubrites or enstatite chondrites. Consequently a small amount of a dark component added to an aubrite would not drastically affect the match between Nysa and the aubrites. The polarimetric data for Nysa also suggest a largely fine-grained surface, in agreement with the spectral interpretation (Dollfus *et al.*, 1971; Zellner, 1975; Zellner *et al.*, 1977a; Dollfus *et al.*, 1979).

The observational data for Nysa are all consistent with an aubrite-like surface assemblage with <10 % areally distributed or intimately mixed material similar to the Cumberland Falls chondritic inclusions. A significant portion of the surface is composed of fine-grained (<45μm-size) materials.

SUMMARY

The spectral detectability of mafic silicates associated with metal, carbon, and magnetite is strongly dependent on the particle sizes of the phases, their chemistries, crystal structures, and abundances. Metal from an iron meteorite has an essentially linear reflectance spectrum with a red slope (increasing reflectance towards longer wavelengths). The 1.8/0.7μm reflectance ratio can be used to highlight differences due to grain size and chemical variations. The smallest grain size of meteoritic metal measured (0-45μm) has a reflectance ratio of 1.55, which seems to be the approximate lower limit for metal powders and surfaces with roughnesses greater than the wavelength of light. There appears to be no simple correlation between metal content (nickel:iron ratio) and spectral slope. The detection limit for silicates in metal-silicate mixtures is strongly dependent on grain size. For olivine:metal powders a lower limit of ~20 wt. % olivine seems reasonable. Orthopyroxene has a lower detection limit of ~10 wt. %.

The acid-insoluble fraction of an E7 chondrite is predominantly enstatite, has a flat reflectance spectrum at >0.4μm with high overall reflectance,and a 1.8/0.7μm reflectance ratio of ~1. This material is a good spectral analogue to the aubrites.

Fine-grained carbon is very effective at suppressing mafic silicate absorption bands. Fine-grained olivine (0-45μm) is almost completely obscured by 0.5 wt. % carbon, while a coarser fraction (45-90μm) retains a well-defined Fe^{2+} absorption band when mixed with the same amount of carbon. If the olivine has a mean grain size in the 10's of microns, the olivine absorption band will be resolvable for carbon abundances present in all known meteorite types. Pyroxene-carbon mixtures have similar detection limits.

Magnetite is not very effective at suppressing olivine absorption features. A 50:50 mixture of olivine:magnetite shows absorptrion features due to ferrous iron. Finer-grained magnetite imparts a bluer slope to reflectance spectra. A combination of carbon and magnetite would probably be required to mimic the reflectance spectra of olivine-bearing carbonaceous chondrites with flat or blue slopes.

The reflectance spectrum of the M-class asteroid Psyche is not directly comparable to those of iron meteorite powders. However, the overall shape of Psyche's spectrum more closely resembles that of iron meteorites than enstatite chondrites, and lies on a trend suggesting an appreciable fine-grained surface component. This interpretation is also consistent with the constraints imposed by radar and polarimetric observations.

The reflectance spectrum of the best-characterized E-classasteroid, 44 Nysa, is interpreted to indicate an aubrite-like surface for this asteroid. The slight red slope and weak absorption bands present in the asteroid spectrum can probably be accounted for by a minor (<10 %) additional component similar to the dark inclusions found in the Cumberland Falls aubrite. The reflectance spectra also suggest that a significant portion of the surface materials on Nysa are fine-grained ($<45\mu m$).

The M- and E-class asteroids are concentrated in the inner part of the main asteroid belt (Gradie & Tedesco, 1982). If the interpretations of the surface assemblages for representative members of these groups can be extended to their entire respective groups, then the case for pervasive and widespread early heating of inner part of the main asteroid belt is strengthened (Bell, 1986).

Table III-1. Chemical composition of the minerals used in this study.

Wt. %	OLV003	PYX117	MAG101	Wt. %	MET101
SiO_2	40.64	53.54	N.D.	Si	N.D.
FeO	9.25	16.17	26.52	Fe	93.39
Fe_2O_3	0.59	1.02	63.71	--	--
MgO	49.13	27.53	3.63	Mg	0.00
CaO	0.07	0.35	N.D.	Ca	N.D.
Al_2O_3	<0.01	1.54	0.33	Al	0.03
NiO	0.33	0.05	N.D.	Ni	6.07
TiO_2	0.00	0.03	3.04	Ti	0.00
MnO	0.09	0.44	0.60	Mn	0.00
Cr_2O_3	0.01	0.07	0.03	Cr	0.18
Na_2O	0.00	0.00	N.D.	Na	0.00
ZnO	0.00	N.D.	N.D.	Zn	0.11
CoO	0.04	0.01	N.D.	Co	0.50
V_2O_5	0.00	0.00	N.D.	V	0.00
K_2O	0.00	N.D.	N.D.	K	N.D.
ZrO_2	N.D.	0.00	N.D.	Zr	N.D.
				S	0.00
				P	0.02
				Cu	0.00
				Pb	0.87
TOTAL	100.15	100.75	97.87	--	101.17

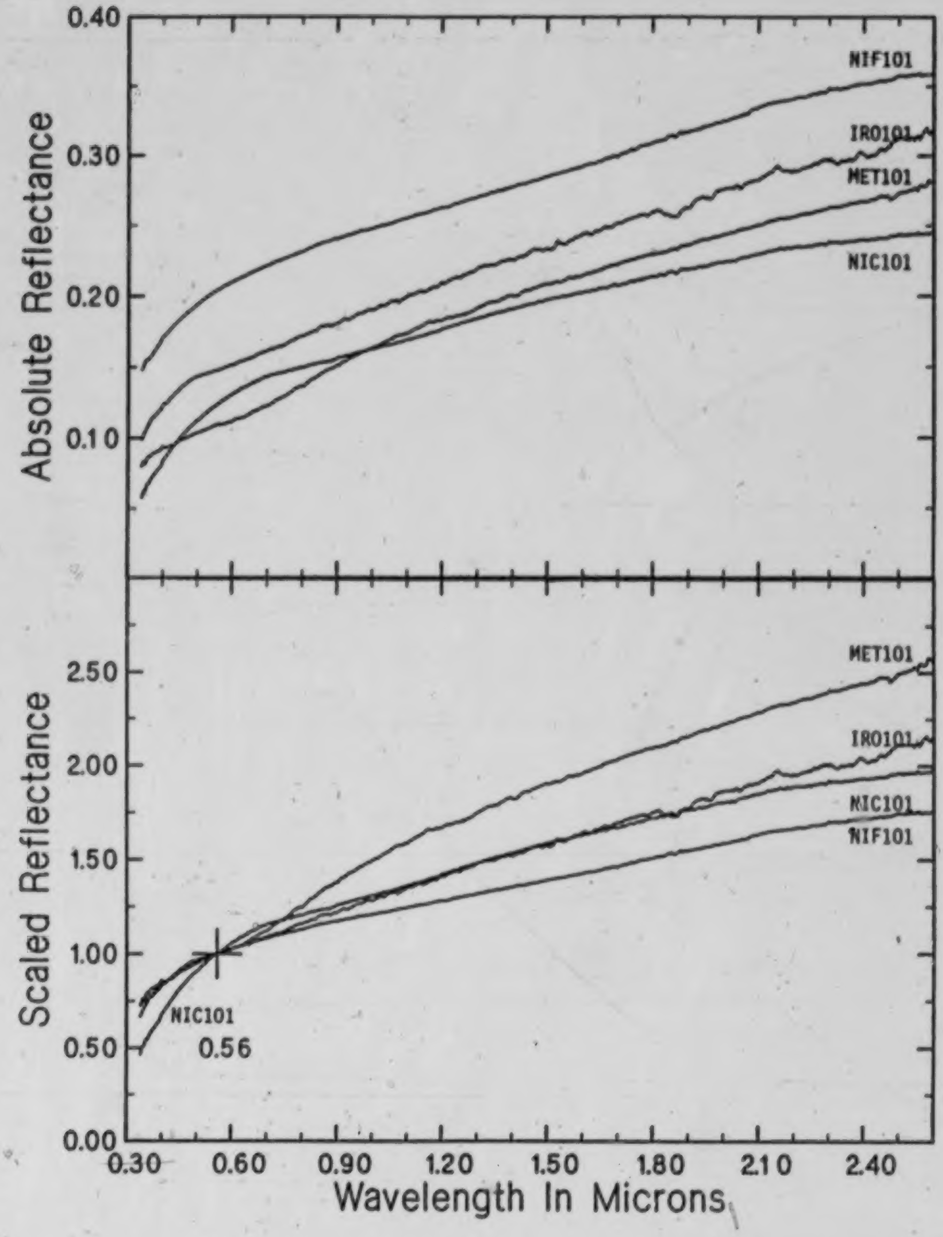

Figure III-1. Absolute (upper) and normalized (lower) reflectance spectra of various small-sized metal powders- nickel (NIC101, <37μm), iron (IRO101, <63μm), 50:50 pre-alloyed iron:nickel powder (NIF101, <63μm), and meteoritic metal (MET101b, 45-90μm). The normalized spectra are scaled to 1 at 0.56μm.

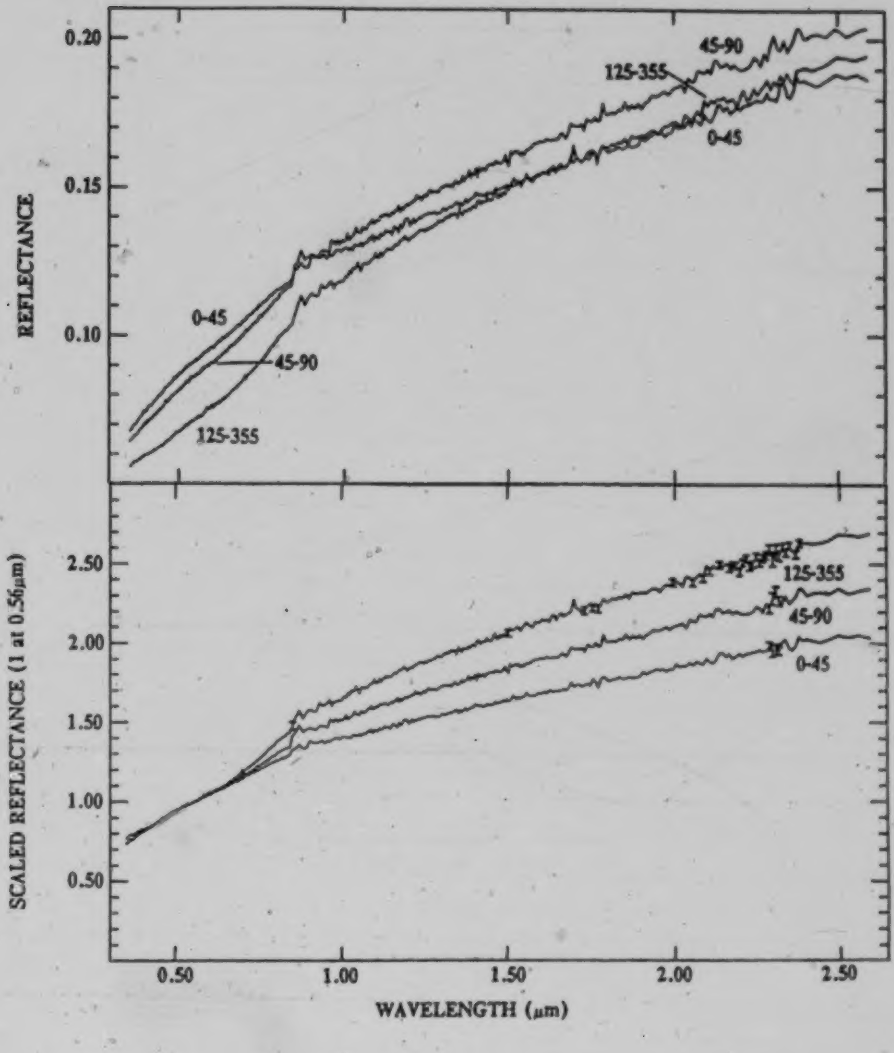

Figure III-2. Absolute (upper) and normalized (lower) reflectance spectra of various sizes of the Odessa octahedrite powdered sample. Grain size ranges are indicated for each spectrum. The normalized spectra are scaled to 1 at 0.56μm.

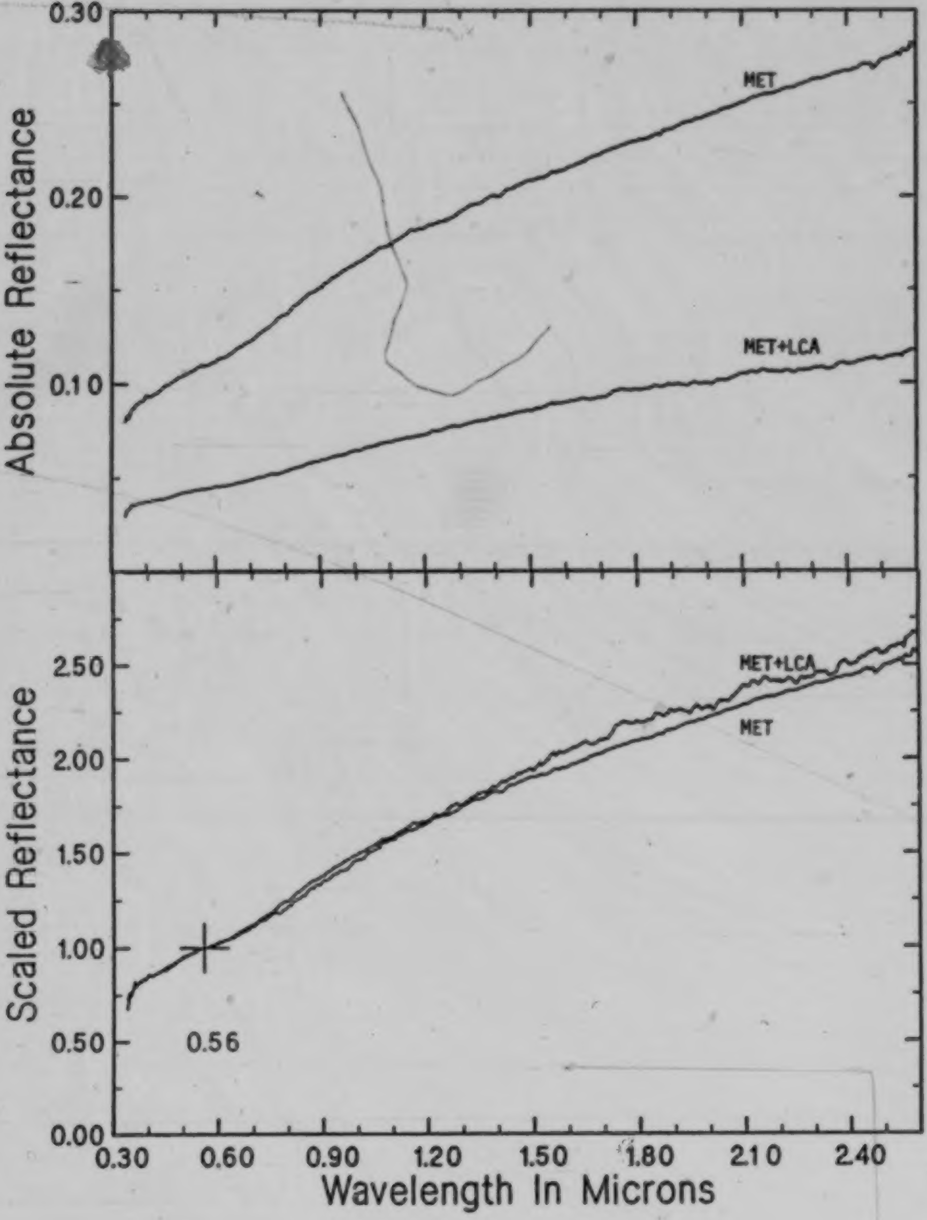

Figure III-3. Absolute (upper) and normalized (lower) reflectance spectra of 45-90μm beaten MET101 (MET) and a 99.5:0.5 weight percent mixture of MET101:LCA101 (MET+LCA). The normalized spectra are scaled to 1 at 0.56μm.

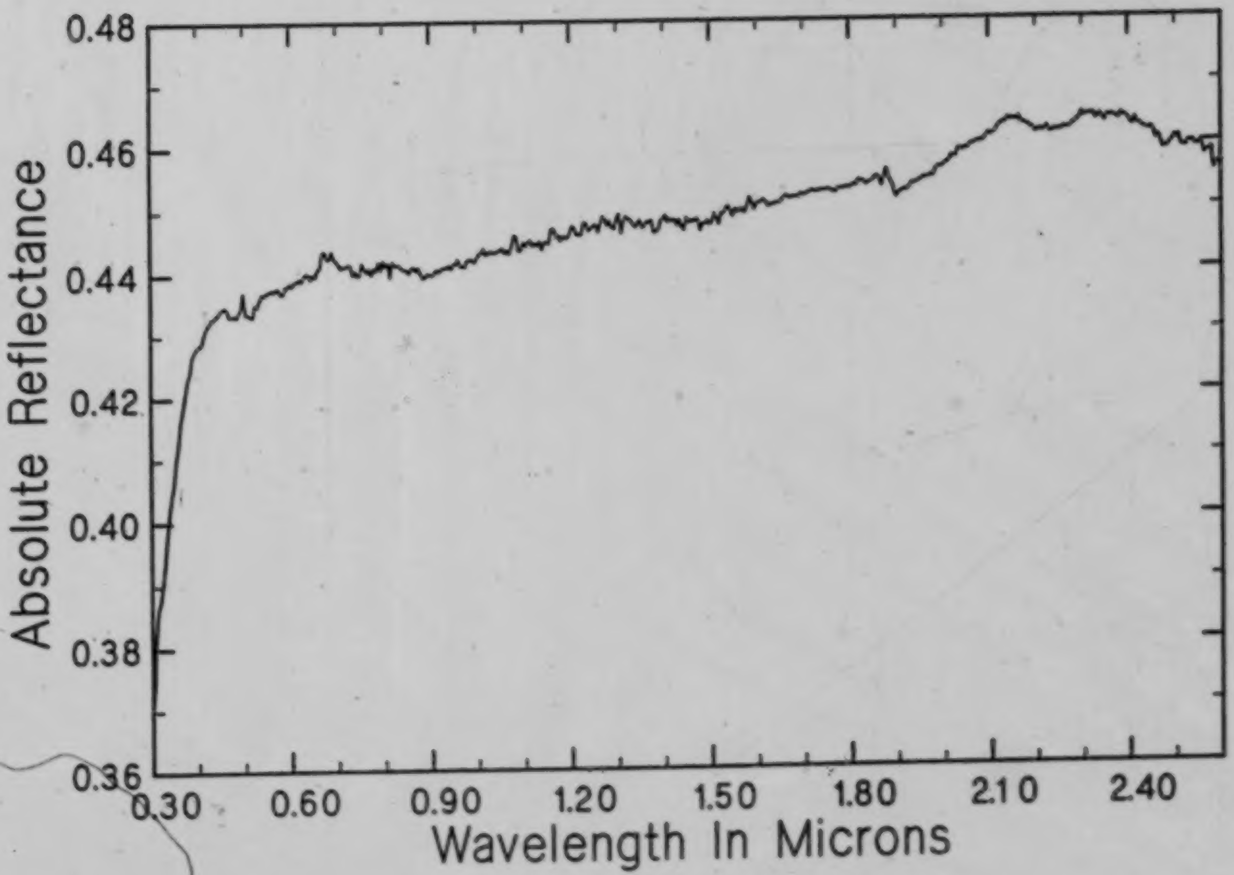

Figure III-4. Absolute reflectance spectrum of the acid-insoluble fraction of the Happy Canyon E7 enstatite chondrite.

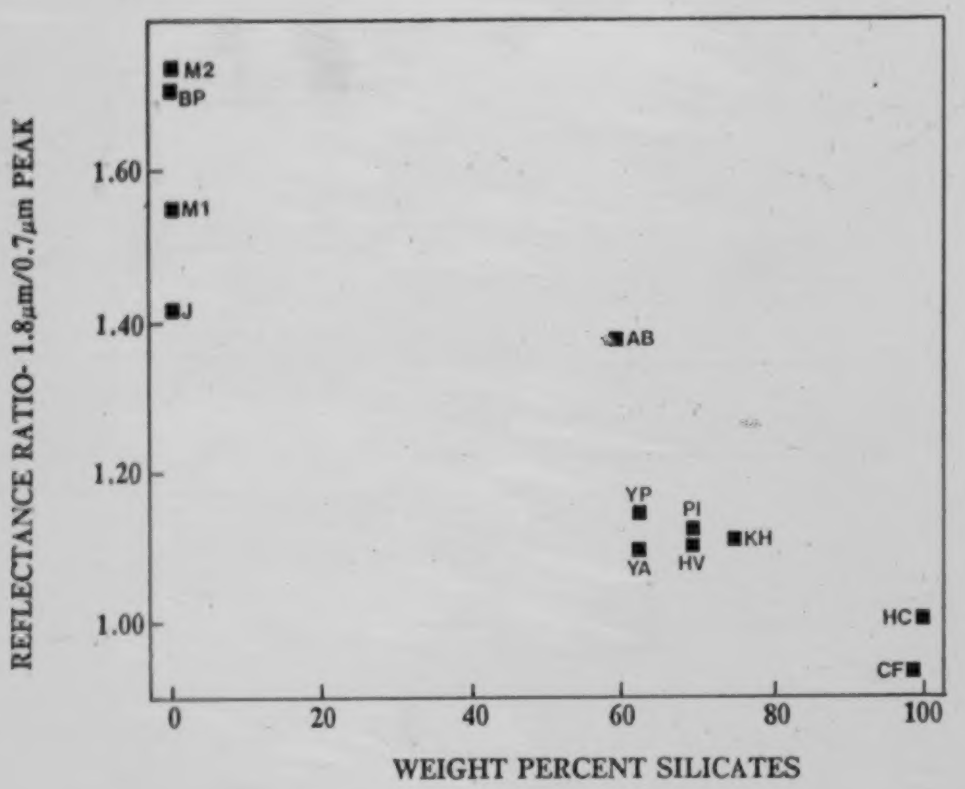

Figure III-5. Plot of the 1.8μm/0.7μm reflectance ratio versus the silicate abundance for the iron meteorite (MET101), acid-insoluble fraction of the Happy Canyon enstatite chondrite and various aubrites and enstatite chondrites adapted from the literature. M1=MET101:0-45μm, M2=MET101:45-90μm (this study); J=Odessa (adapted from Johnson & Fanale, 1973); AB=Abee, CF=Cumberland Falls, HV=Hvittis, KH=Khairpur, PI=Pillistfer (adapted from Gaffey, 1974, 1976); YP=Yamato-691 plate, YA=Yamato-691 powder (adapted from Miyamoto, 1987); BP=10μm-1mm size iron meteorite filings (adapted from Britt & Pieters, 1988).

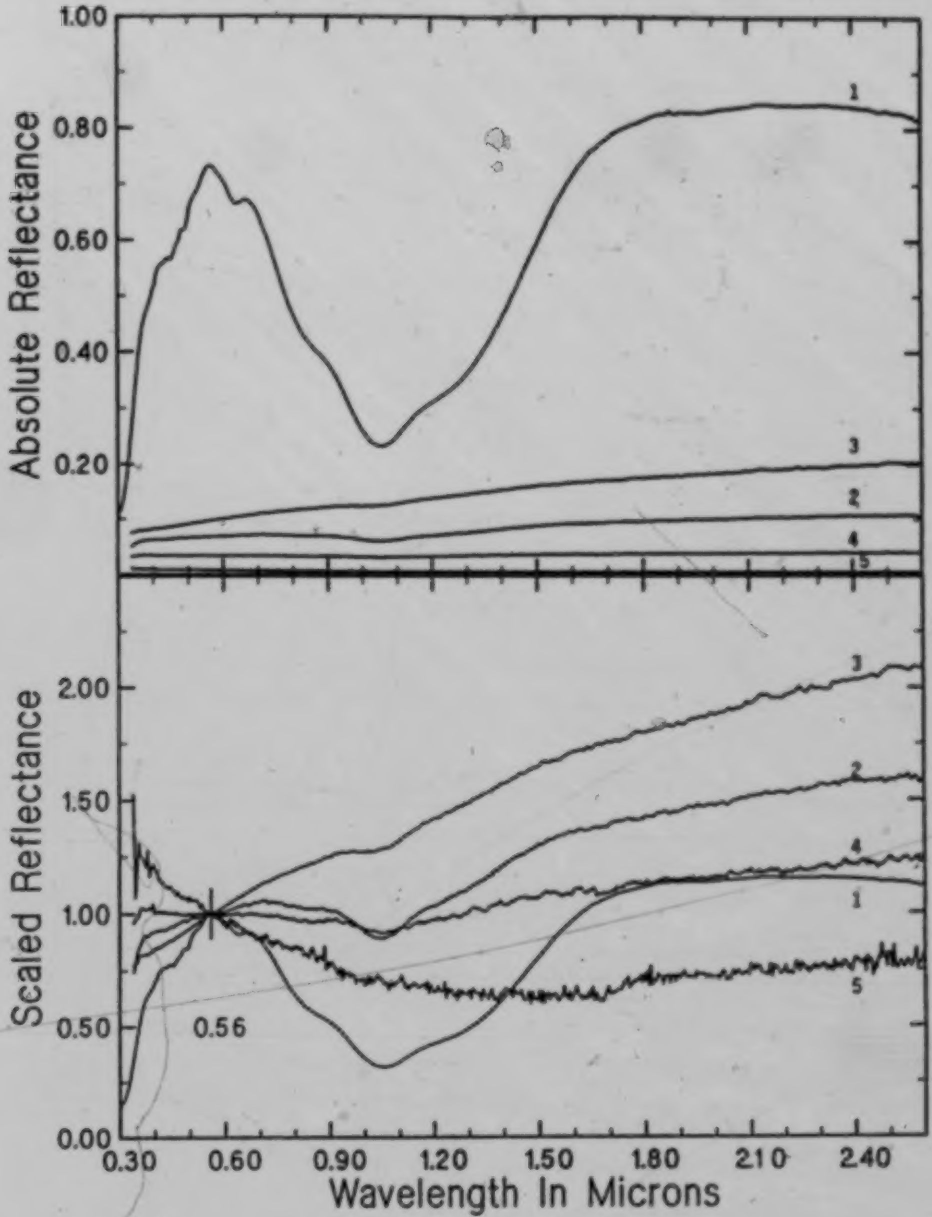

Figure III-6. Absolute (upper) and normalized (lower) reflectance spectra of various mixtures of olivine (OLV003) and amorphous carbon (LCA101). Olivine:carbon ratios- 1=100:0, 2=99.5:0.5, 3=99.5:0.5, 4=98:2, 5=0:100. Sample 3 contains <45μm grain size olivine. All other samples contain 45-90μm sized olivine. The normalized spectra are scaled to 1 at 0.56μm.

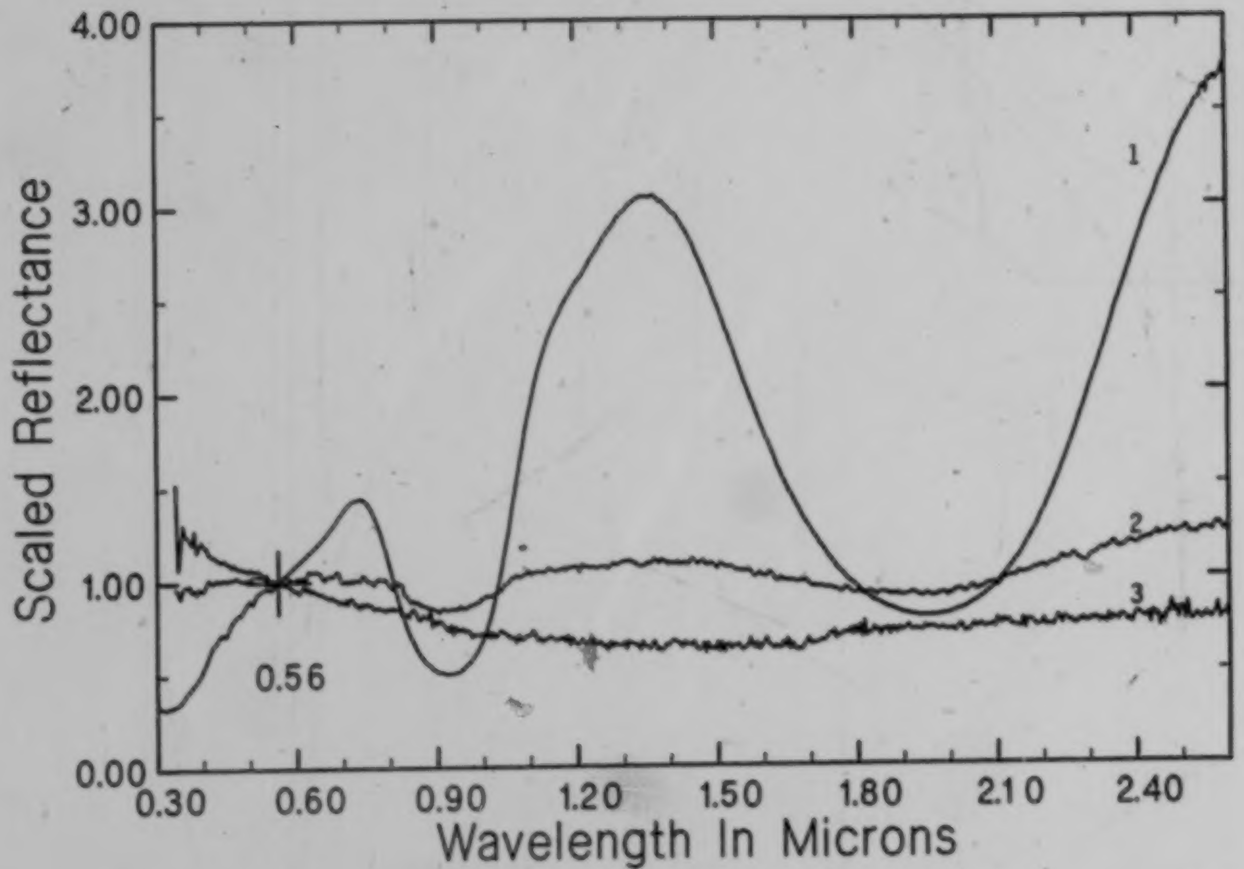

Figure III-7. Normalized reflectance spectra (scaled to 1 at 0.56μm) of mixtures of pyroxene (PYX117) and amorphous carbon (LCA101). The weight percentages of pyroxene/carbon and absolute reflectances at 0.56μm are: 1- 100/0, 0.080; 2- 98/2, 0.017; 3- 0/100, 0.0076.

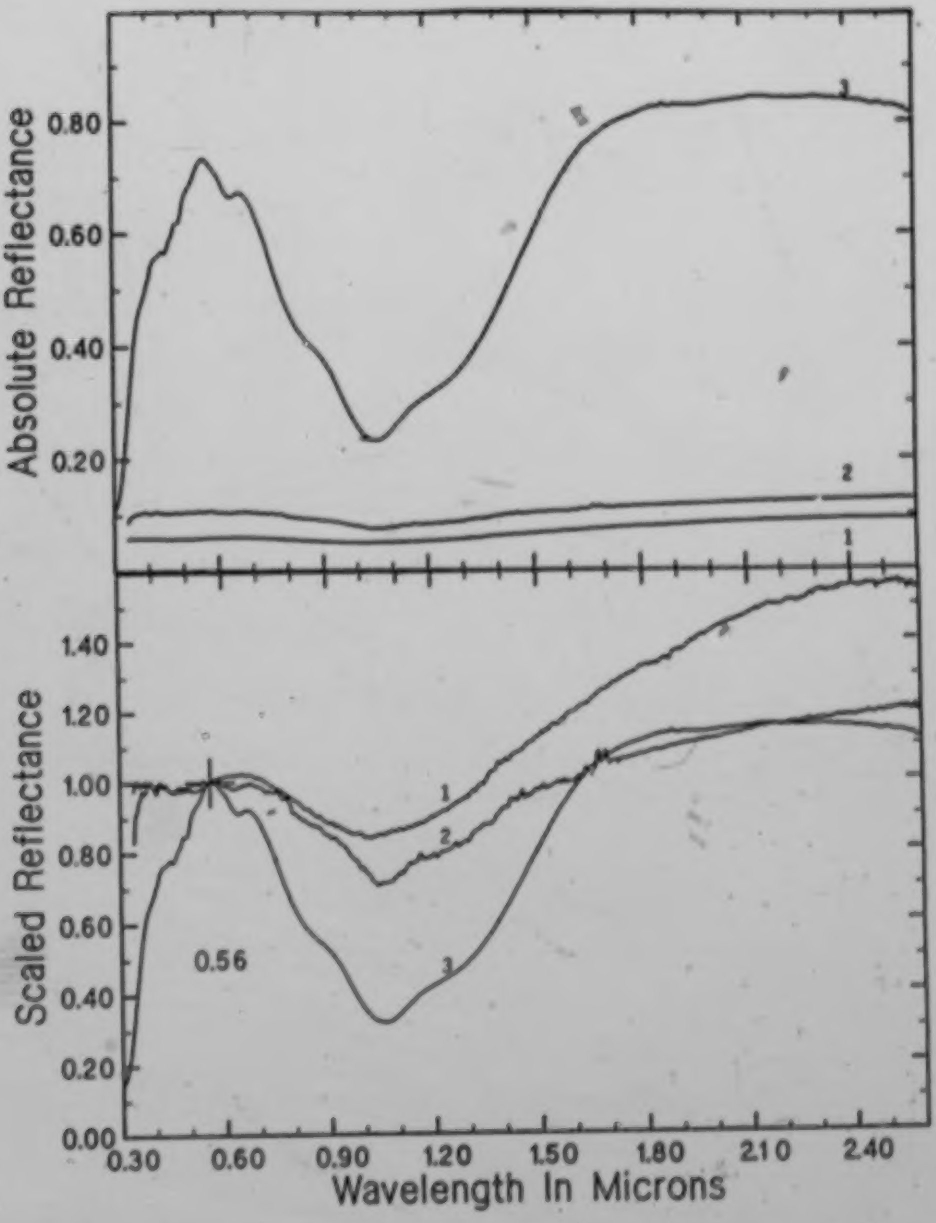

Figure III-8. Absolute (upper) and normalized (lower) reflectance spectra of: (1) olivine (OLV003, 45-90μm size), (2) magnetite (MAG101, 45-90μm), and (3) a 50:50 mixture of the two. The normalized spectra are scaled to 1 at 0.56μm.

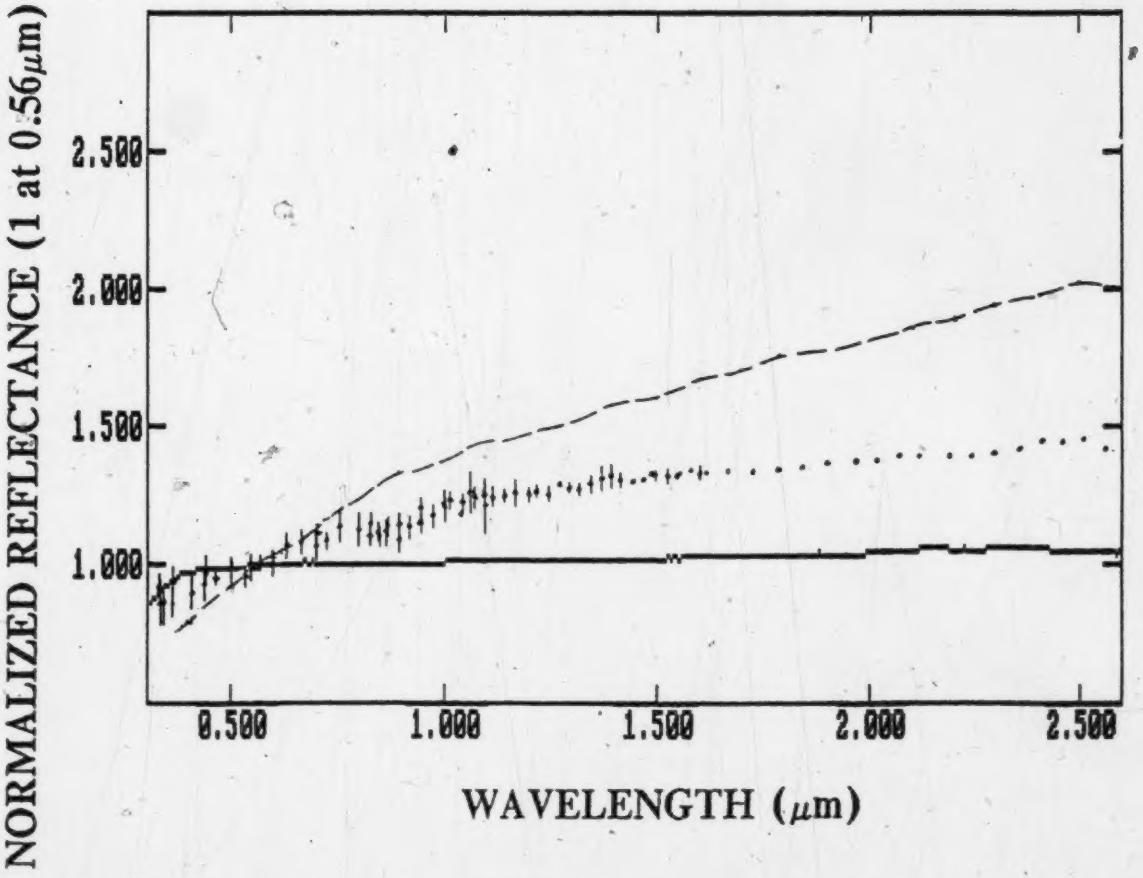

Figure III-9. Normalized reflectance spectra (scaled to 1 at 0.56μm) of the 0-45μm-sized meteoritic metal, MET101 (dotted line), the acid-insoluble fraction of the Happy Canyon enstatite chondrite (line), and asteroid (16) Psyche (points, adapted from Gaffey *et al.*, 1988).

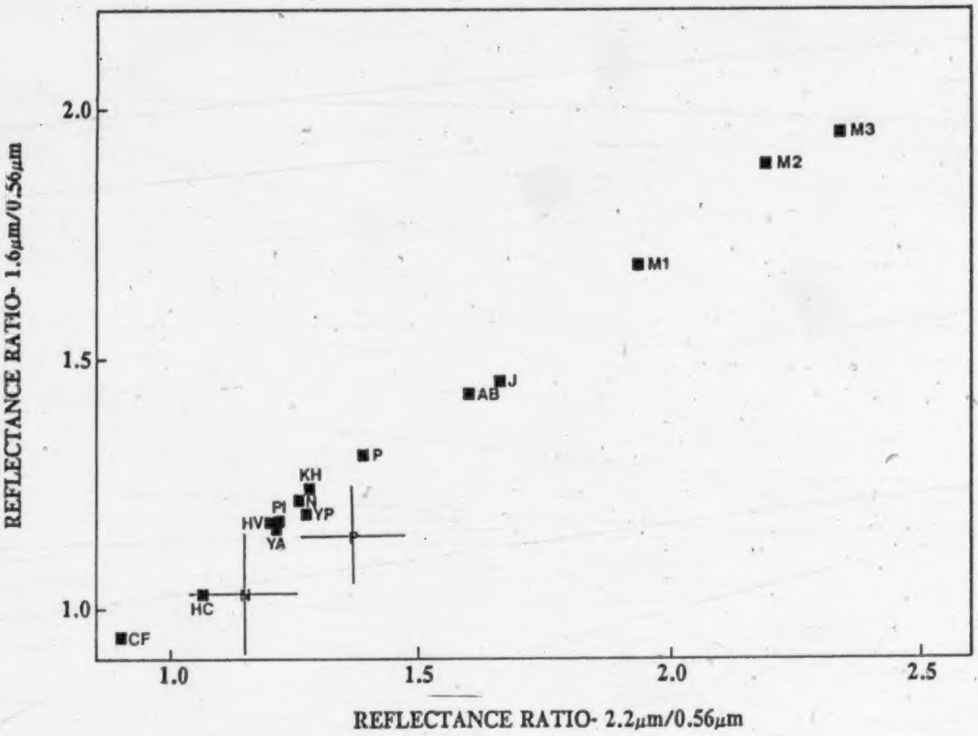

Figure III-10. Plot of the 1.6/0.56μm reflectance ratio versus the 2.2/0.56μm reflectance ratio for the various enstatite- and metal-rich meteorites. M3=MET101 125-355μm grain size; other symbols are the same as in Figure 5. The average values and error bars are also shown for the asteroids Psyche (P), and Nysa (N) (adapted from Veeder et al., 1978; Gaffey *et al.*, 1988).

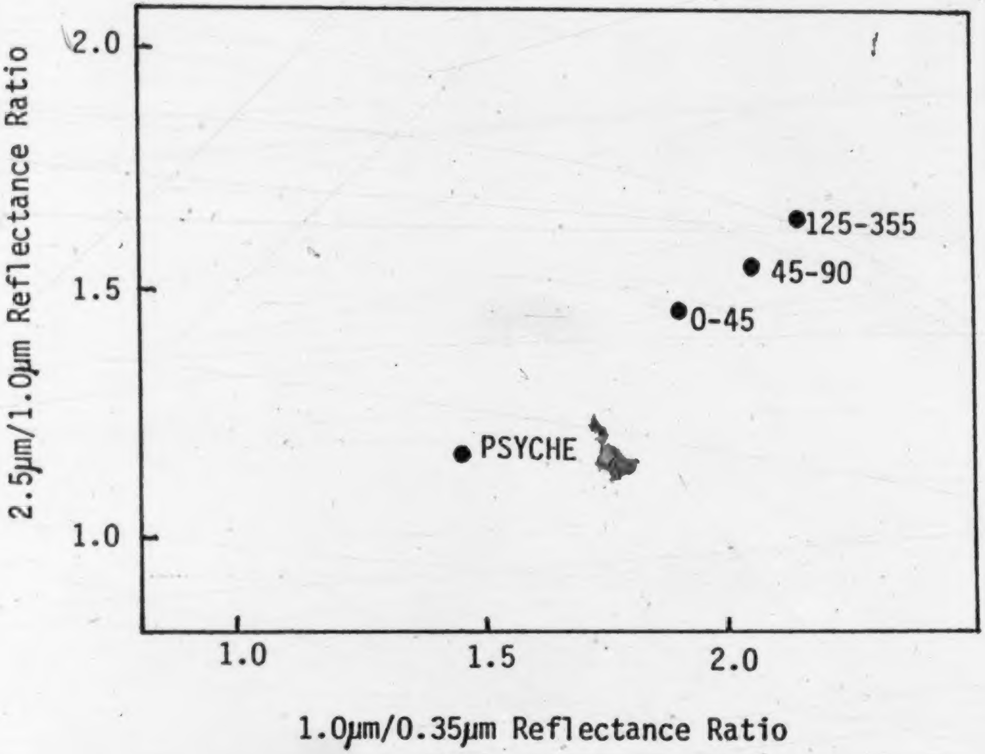

Figure III-11. 2.5µm:1.0µm versus 1.0µm:0.35µm reflectance ratios for the various MET101 iron meteorite powders and asteroid (16) Psyche. The numbers indicate the grain size range of the powders (µm).

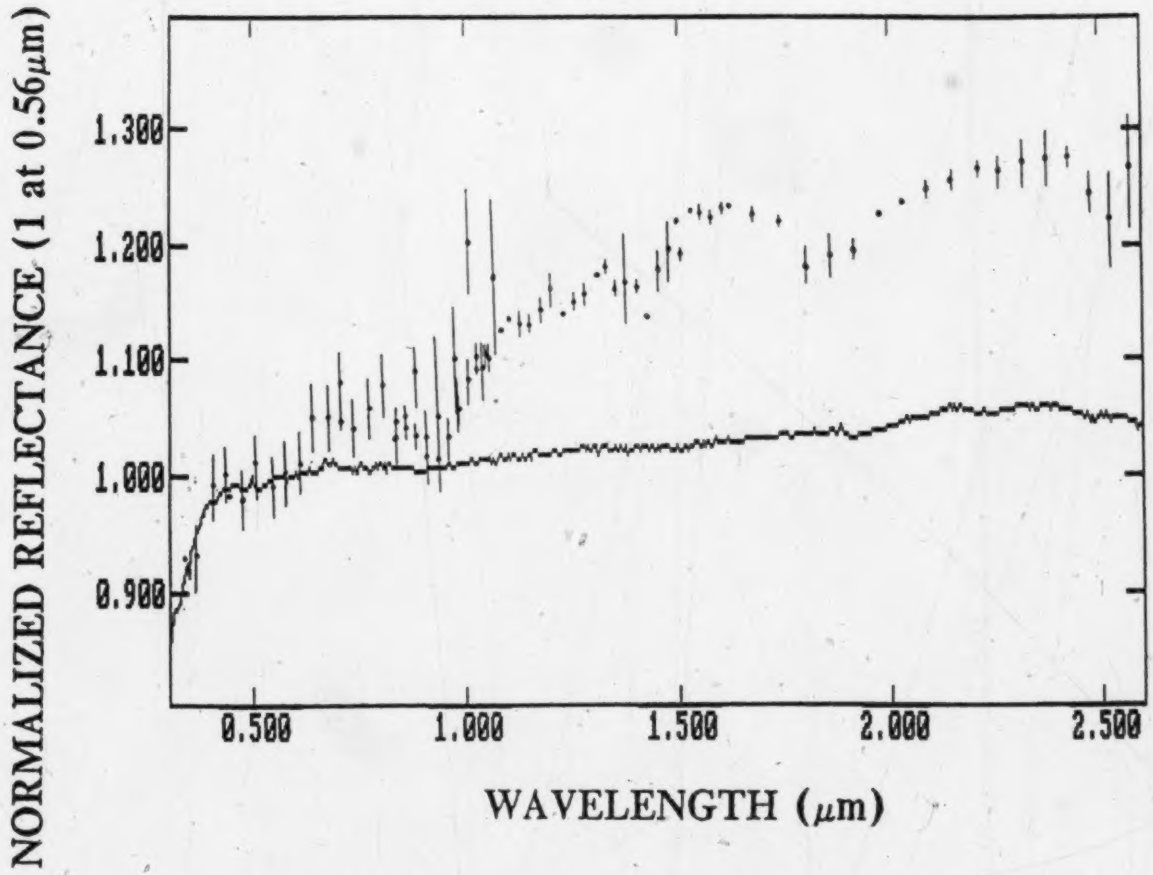

Figure III-12. Normalized reflectance spectra (scaled to 1 at 0.56μm) of the acid-insoluble fraction of the Happy Canyon enstatite chondrite (line) and asteroid (44) Nysa (adapted from Gaffey *et al.*, 1988).

A. REFERENCES

Adams, J.B., Interpretation of visible and near-infrared diffuse reflectance spectra of pyroxenes and other rock-forming minerals, in *Infrared and Raman Spectroscopy of Lunar and Terrestrial Minerals*, edited by C. Karr Jr., pp. 91-116, Academic Press, New York, 1975.

Adams, J.B., and L.H. Goullaud, Plagioclase feldspars: Visible and near infrared diffuse reflectance spectra as applied to remote sensing, *Proc. Lunar Plan. Sci. Conf. 9th*, 2901-2909, 1978.

Auten, T.A., On the brittleness of Gibeon meteoritic iron, *Meteoritics*, **8**, 189-196, 1973.

Baldanza, B., and G. Pialla, Dynamically deformed structures in some meteorites, in *Meteorite Research*, edited by P.M. Millman, pp. 806-825, D. Reidel, Dordrecht, 1969.

Bauman, A.J., J.R. Devaney, and E.M. Bollin, Allende meteorite carbonaceous phase: Intractable nature and scanning electron morphology, *Nature*, **241**, 264-267, 1973.

Bell, J.F., Mineralogical evolution of meteorite parent bodies (abstract), *Lunar Plan. Sci. Conf. XVII*, 985-986, 1986.

Bell, P.M., and H.K. Mao, Optical spectra of thin metallic coatings with applications to the spectra of lunar soil samples (abstract), *Lunar Sci. Conf. VIII*, 88-90, 1977.

Bell, J.F., M.J. Gaffey, and B.R. Hawke, Spectroscopic identification of probable pallasite parent bodies (abstract), *Meteoritics*, **19**, 187-188, 1984.

Bell, J.F., P.D. Owensby, B.R. Hawke, and M.J. Gaffey, The 52-color asteroid survey: Final results and interpretation (abstract), *Lunar Plan. Sci. Conf. XIX*, 57-58, 1988.

Binns, R.A., A chondritic inclusion of unique type in the Cumberland Falls meteorite, in *Meteorite Research*, edited by P.M. Millman, pp. 696-704, D. Reidel, Dordrecht, 1969.

Blake, D. F., F. Freund, K.F.M. Krishnan, C.J. Echer, R. Shipp, T.E. Bunch, A.G. Tielens, R.J. Lipari, C.J.D. Hetherington, and S. Chang, The nature and origin of interstellar diamond, *Nature*, **332**, 611-613, 1988.

Blodgett Jr., A.J., and W.E. Spicer, Experimental determination of the optical density of states in iron, *Phys. Rev.*, *158*, 514-523, 1967.

Britt, D.T., and C.M. Pieters, Bidirectional reflectance properties of iron-nickel meteorites, *Proc. Eighteenth Lunar Plan. Sci. Conf.*, 503-512, 1988.

Buchwald, V.F., *Handbook of Iron Meteorites*, University of California Press, Berkeley, 1975.

Chapman, C.R., Asteroids as meteorite parent bodies: The astronomical perspective, *Geochim. Cosmochim. Acta*, **40**, 701-719, 1976.

Chapman, C.R., The asteroids: Nature, interrelations, origin, and evolution, in *Asteroids*, edited by T. Gehrels, pp. 25-60, University of Arizona Press, Tucson, 1979.

Chapman, C.R., and M.J. Gaffey, Reflectance spectra for 277 asteroids, in *Asteroids*, edited by T. Gehrels, pp. 655-687, University of Arizona Press, Tucson, 1979.

Chapman, C.R., and Salisbury, J.W., Comparisons of meteorite and asteroid spectral reflectivities, *Icarus*, **19**, 507-522, 1973.

Clark, R.N., A large-scale interactive one dimensional array processing system, *Publ. Astron. Soc. Pacific*, **92**, 221-224, 1980.

Clark, R.N., Spectral properties of mixtures of montmorillonite and dark carbon grains: Implications for remote sensing minerals containing chemically and physically adsorbed water, *Jour. Geophys. Res.*, **88**, 10635-10644, 1983.

Clark, R.N., and T.L. Roush, Reflectance spectroscopy: Quantitative analysis techniques for remote sensing applications, *Jour. Geophys. Res.*, **89**, 6329-6340, 1984.

Cloutis, E.A., *Interpretive Techniques for Reflectance Spectra of Mafic Silicates*, M.Sc. thesis, University of Hawaii, Honolulu, 1985.

Comerford, M.F., Phosphide and carbide inclusions in iron meteorites, in *Meteorite Research*, edited by P.M. Millman, pp. 780-794, D. Reidel, Dordrecht, 1969.

Crown, D.A., and C.M. Pieters, Spectral properties of plagiocalse and pyroxene mixtures and the interpretation of lunar soil spectra, *Icarus*, **72**, 492-506, 1987.

Cruikshank, D.P., and W.K. Hartmann, The meteorite-asteroid connection: Two olivine-rich asteroids, *Science*, **223**, 281-283, 1984.

Deines, P., and F.E. Wickman, The stable carbon isotopes in enstatite chondrites and Cumberland Falls, *Geochim. Cosmochim. Acta*, **49**, 89-95, 1985.

Doan Jr., A.S., and J.I. Goldstein, The formation of phosphides in iron meteorites, in *Meteorite Research*, edited by P.M. Millman, pp. 763-779, D. Reidel, Dordrecht, 1969.

Dollfus, A., and J.-C. Mandeville, The M-type asteroids and the origin of iron meteorites (abstract), *Meteoritics*, **12**, 206-207, 1977.

Dollfus, A., E. Bowell, and C. Titulaer, Polarimetric properties of the lunar surface and its interpretation. Part II. Terrestrial samples in orange light, *Astron. Astrophys.*, **10**, 450-466, 1971.

Dollfus, A., J.-C. Mandeville, and M. Duseaux, The nature of the M-type asteroids from optical polarimetry, *Icarus*, **37**, 124-132, 1979.

Dollfus, A., A. Cailleux, B. Cervelle, C.T. Hua, and J.-C. Mandeville, Reflectance spectrophotometry extended to u.v. for terrestrial, lunar and meteoritic samples, *Geochim. Cosmochim. Acta*, *44*, 1293-1310, 1980.

Easton, A.J., Grain-size distribution and morphology of metal in E-chondrites, *Meteoritics*, **18**, 19-27, 1983.

Eaton, N., S.F. Green, R.S. McCheyne, A.J. Meadows, and G.J. Veeder, Observations of asteroids in the 3- to 4-μm region, *Icarus*, **55**, 245-249, 1983.

Egan, W.G., and T. Hilgeman, The rings of Saturn: A frost-coated semiconductor?, *Icarus*, **30**, 413-421, 1977.

Feierberg, M.A., H.P. Larson, and C.R. Chapman, Spectroscopic evidence for undifferentiated S-type asteroids, *Astrophys. Jour.*, **257**, 361-372, 1982.

Gaffey, M.J., *A Systematic Study of the Spectral Reflectivity Characteristics of the Meteorite Classes with Applications to the Interpretation of Asteroid Spectra for Mineralogical and Petrological Information*, Ph.D. Dissertation, Massachusetts Institute of Technology, 1974.

Gaffey, M.J., Spectral reflectance characteristics of the meteorite classes, *Jour. Geophys. Res.*, **81**, 905-920, 1976.

Gaffey, M.J., Optical and spectral properties of the low albedo meteorites: Applications to the interpretation of the spectra of dark asteroids (abstract), *Lunar Plan. Sci. Conf. IX*, 362-364, 1978.

Gaffey, M.J., Mineralogically diagnostic features in the visible and near-infrared reflectance spectra of carbonaceous chondrite assemblages (abstract), *Lunar Plan. Sci. Conf. XI*, 312-313, 1980.

Gaffey, M.J., Rotational spectral variations of asteroid (8) Flora: Implications for the nature of the S-type asteroids and for the parent bodies of the ordinary chondrites, *Icarus*, **60**, 83-114, 1984.

Gaffey, M.J., The spectral and physical properties of metal in meteorite assemblages: Implications for asteroid surface materials, *Icarus*, **66**, 468-486, 1986.

Gaffey, M.J., Thermal history of the asteroid belt: Implications for accretion of the terrestrial planets (abstract), *Lunar Plan. Sci. Conf. XIX*, 369-370, 1988.

Gaffey, M.J., and T.B. McCord, Asteroid surface materials: Mineralogical characterizations from reflectance spectra, *Space Sci. Rev.*, **21**, 555-628, 1978.

Gaffey, M.J., J.F. Bell, and D.P. Cruikshank, Reflectance spectroscopy and asteroid surface mineralogy, papers presented at Asteroids II, Tucson, Arizona, March 8, 1988.

Gibson Jr., E.K., Nature of the carbon and sulphur phases and inorganic gases in the Kenna ureilite, *Geochim. Cosmochim. Acta*, **40**, 1459-1464, 1976.

Gibson, E.K., C.B. Moore, and C.F. Lewis, Total nitrogen and carbon abundances in carbonaceous chondrites, *Geochim. Cosmochim. Acta*, **35**, 599-604, 1971.

Gorban, N.Y., and V.S. Stashchuk, Optical absorption of Ni-Fe alloys, *Opt. Spectrosc.*, **37**, 202-203, 11974.

Gorban, N.Y., V.S. Stashchuk, A.V. Shirin, and A.A. Shishlovskii, Optical properties of nickel-iron alloys in the region of interband transitions, *Opt. Spectrosc.*, **35**, 295-298, 1973.

Gradie, J., and E. Tedesco, Compositional structure of the asteroid belt, *Science*, **216**, 1405-1407, 1982.

Gradie, J., and J. Veverka, The composition of the Trojan asteroids, *Nature*, **283**, 840-842, 1980.

Grady, M.M., I.P. Wright, L.P. Carr, and C.T. Pillinger, Compositional differences in enstatite chondrites based on carbon and nitrogen stable isotope measurements, *Geochim. Cosmochim. Acta*, 50, 2799-2813, 1986.

Grossman, J.N., A.E. Rubin, and G.J. MacPherson, Allan Hills 85085: An out-of-the-ordinary enstatite-rich carbonaceous chondrite (abstract), *Lunar Plan. Sci. Conf. XIX*, 433-434, 1988.

Hunt, G.R., J.W. Salisbury, and C.J. Lenhoff, Visible and near-infrared spectra of minerals and rocks: III. Oxides and hydroxides, *Mod. Geol.*, 2, 195-205, 1971a.

Hunt, G.R., J.W. Salisbury, and C.J. Lenhoff, Visible and near-infrared spectra of minerals and rocks: IV. Sulphides and sulphates, *Mod. Geol.*, 3, 1-14, 1971b.

Johnson, T.V., and F.P. Fanale, Optical properties of carbonaceous chondrites and their relationship to asteroids, *Jour. Geophys. Res.*, 78, 8507-8518, 1973.

Keil, K., Mineralogical and chemical relationships among enstatite chondrites, *Jour. Geophys. Res.*, 73, 6945-6976, 1968.

Kerridge, J.F., Some observations on the nature of magnetite in the Orgueil meteorite, *Earth Plan. Sci. Lett.*, 9, 299-306, 1970.

King, T.V.V., and W.I. Ridley, Relation of the spectroscopic reflectance of olivine to mineral chemistry and some remote sensing implications, *Jour. Geophys. Res.*, 92, 11457-11469, 1987.

Larson, H.P., and G.J. Veeder, Infrared spectral reflectances of asteroid surfaces, in *Asteroids*, edited by T. Gehrels, pp. 724-744, University of Arizona Press, Tucson, 1979.

Lipschutz, M.E., R.M. Verkouteren, D.G.W. Sears, F.A. Hasan, M. Prinz, W.K. Weisberg, C.E. Nehru, J.S. Delaney, L. Grossman, and M. Boily, Cumberland Falls chondritic inclusions: III. Consortium study of relationship to inclusions in Allan Hills 78113 aubrite, *Geochim. Cosmochim. Acta*, 52, 1835-1848, 1988.

Lovering, J.F., The evolution of the meteorites- Evidence for the co-existence of chondritic, achondritic and iron meteorites in a typical parent meteorite body, in *Researches on Meteorites*, edited by C.B. Moore, pp. 179-197, Wiley, New York, 1962.

Lusby, D., E.R.D. Scott, and K. Keil, Ubiquitous high-FeO silicates in enstatite chondrites, *Proc. Seventeenth Lunar Plan. Sci. Conf.*, in *Jour. Geophys. Res.*, 91, E679-E695, 1987.

Marcus, H.L., and L.H. Hackett Jr., The low temperature fracture behavior of iron-nickel meteorites, *Meteoritics*, **9**, 371-376, 1974.

Mason, B., *Meteorites*, Wiley, New York, 1962.

Mason, B., The enstatite chondrites, *Geochim. Cosmochim. Acta*, **30**, 23-39, 1966.

Mason, B., and H.B. Wiik, The Renazzo meteorite, *Amer. Mus. Novit.*, **2106**, 1-11, 1962.

Matsui, T., and P.M. Schultz, On the brittle-ductile behavior of iron meteorites: New experimental constraints, *Proc. Fifteenth Lunar Plan. Sci. Conf.*, in *Jour. Geophys. Res.*, **89**, C323-C328, 1984.

McCord, T.B., J.B. Adams, and T.V. Johnson, Asteroid Vesta: Spectral reflectivity and compositional implications, *Science*, **168**, 1445-1447, 1970.

McFadden, L.A., *Spectral Reflectance of Near-Earth Asteroids: Implications for Composition, Origin and Evolution*, Ph.D. thesis, University of Hawaii, Honolulu, 1983.

Miyamoto, M., Diffuse reflectance from 0.25μm to 25μm of the Yamato-691 enstatite chondrite, *Proc. Eleventh Symp. Antarctic Meteorites-Mem. Nat. Inst. Polar Res. Spec. Iss.* **46**, 123-130, 1987.

Miyamoto, M., A. Mito, Y. Takano, and N. Fujii, Spectral reflectance (0.25-2.5μm) of powdered olivines and their bearing on surface materials of asteroids, *Proc. Sixth Symp. Antarctic Meteorites-Mem. Nat. Inst. Polar Res. Spec. Iss.* **20**, 345-361, 1981.

Miyamoto, M., A. Mito, and Y. Takano, An attempt to reduce the effects of black material from the spectral reflectance of meteorites or asteroids, *Proc. Seventh Symp. Antarctic Meteorites-Mem. Nat. Inst. Polar Res. Spec. Iss.* **25**, 291-307, 1982.

Moore, C.B., and C. Lewis, Carbon abundances in chondritic meteorites, *Science*, **149**, 317-318, 1965.

Morris, R.V., H.V. Lauer Jr., C.A. Lawson, E.K. Gibson Jr., G.A. Nace, and C. Stewart, Spectral and other physicochemical properties of submicron powders of hematite (α-Fe_2O_3), maghemite (γ-Fe_2O_3), magnetite (Fe_3O_4), goethite (α-FeOOH), and lepidocrocite (γ-FeOOH), *Jour. Geophys. Res.*, **90**, 3126-3144, 1985.

Nagy, B., *Carbonaceous Meteorites*, Elsevier, Amsterdam, 1975.

Neal, C.W., and M.E. Lipschutz, Cumberland Falls chondritic inclusions: Mineralogy/petrology of a forsterite chondrite suite, *Geochim. Cosmochim. Acta*, **45**, 2091-2107, 1981.

Nininger, H.H., The Bondoc meteorite: A one-ton sample of an asteroid? (abstract), *Meteoritics*, **14**, 498-499, 1979.

Olsen, E.J., T.E. Bunch, E. Jarosewich, A.F. Noonan, and G.I. Huss, Happy Canyon: A new type of enstatite achondrite, *Meteoritics*, **12**, 109-123, 1977.

Ostro, S.J., D.B. Campbell, and I.I. Shapiro, Mainbelt asteroids: Dual-polarization radar observations, *Science*, **229**, 442-446, 1985.

Pieters, C.M., Strength of mineral absorption features in the transmitted component of near-infrared light: First results from RELAB, *Jour. Geophys. Res.*, **88**, 9534-9544, 1983.

Remo, J.L., and A.A. Johnson, A preliminary study of the ductile-brittle transition under impact conditions in material from an octahedrite, *Jour. Geophys. Res.*, **80**, 3744-3748, 1975.

Salisbury, J.W., and Hunt, G.R., Meteorite spectra and weathering, *Jour. Geophys. Res.*, **79**, 4439-4441, 1974.

Salisbury, J.W., G.R. Hunt, and C.J. Lenhoff, Visible and near-infrared spectra: X. Stony meteorites, *Mod. Geol.*, **5**, 115-126, 1975.

Singer, R.B., Near-infrared spectral reflectance of mineral mixtures: Systematic combinations of pyroxenes, olivine, and iron oxides, *Jour. Geophys. Res.*, **86**, 7967-7982, 1981.

Van Der Stap, C.C.A.H., D. Heymann, R.D. Vis, and H. Verheul, Mapping of carbon concentrations in the Allende meteorite with the ^{12}C(d,p)^{13}C method, *Proc. Sixteenth Lunar Plan. Sci. Conf.*, D373-D377, 1986.

Van Schmus, W.R., and J.M. Hayes, Chemical and petrographic correlations among carbonaceous chondrites, *Geochim. Cosmochim. Acta*, **38**, 47-64, 1974.

Vdovykin, G.P., Ureilites, *Space Sci. Rev.*, **10**, 483-510, 1970.

Veeder, G.J., D.L. Matson, and J.C. Smith, Visual and infrared photometry of asteroids, *Astron. Jour.*, **83**, 651-663, 1978.

Verkouteren, R.M., and M.E. Lipschutz, Cumberland Falls chondritic inclusions- II. Trace element contents of forsterite chondrites and meteorites of similar redox state, *Geochim. Cosmochim. Acta,* **47**, 1625-1633, 1983.

Vilas, F., and M.J. Gaffey, Weak Fe^{2+}-Fe^{3+} charge transfer absorption features seen in CM2 carbonaceous chondrites and narrowband reflectance spectra of primitive asteroids (abstract), *Lunar Plan. Sci. Conf. XX*, 1156-1157, 1989.

Wagner, J.K., B.W. Hapke, and E.N. Wells, Atlas of reflectance spectra of terrestrial, lunar, and meteoritic powders and frosts from 92 to 1800 nm, *Icarus*, **69**, 14-28, 1987.

Watson, F.G., Reflectivity and color of meteorites, *Proc. Nat. Acad. Sci.*, **24**, 532-537, 1938.

Watters, T.R., and M. Prinz, Aubrites: Their origin and relationship to enstatite chondrites, *Proc. Lunar Plan. Sci. Conf. 10th*, 1073-1093, 1979.

Watters, T.R., M. Prinz, E.R. Rambaldi, and J.T. Wasson, ALHA78113, Mt. Egerton and the aubrite parent body, *Meteoritics*, **15**, 386, 1980.

Weidner, V.R., and J.J. Hsia, Reflection properties of pressed polytetrafluoroethylene powder, *Jour. Opt. Soc. Amer.*, **71**, 856-861, 1981.

Weisberg, M.K., M. Prinz, and C.E. Nehru, Petrology of ALH85085: A chondrite with unique characteristics, *Earth Plan. Sci. Lett.*, **91**, 19-32, 1988.

Yolken, H.T., and J. Kruger, Optical constants of iron in the visible region, *Jour. Opt. Soc. Amer.*, **55**, 842-844, 1965.

Zellner, B., 44 Nysa: An iron-depleted asteroid, *Astrophys. Jour.*, **198**, L45-L47, 1975.

Zellner, B., M. Leake, D. Morrison, and J.G. Williams, The E asteroids and the origin of the enstatite chondrites, *Geochim. Cosmochim. Acta,* **41**, 1759-1767, 1977a.

Zellner, B., M. Leake, T. Lebertre, M. Duseaux, and A. Dollfus, The asteroid albedo scale: I. Laboratory polarimetry of meteorites, *Proc. Lunar Sci. Conf. 8th*, 1091-1110, 1977b.

IV. REFLECTANCE SPECTRA OF MAFIC SILICATE-OPAQUE ASSEMBLAGES WITH APPLICATIONS TO METEORITE SPECTRA [1]

INTRODUCTION

Reflectance spectroscopy is one of the most powerful tools in remote sensing. It can provide accurate mineralogical information about inaccessible targets- information which is often not available by other techniques. As part of a comprehensive study of the spectral reflectance properties of mafic silicate-bearing assemblages, a series of mixtures involving mafic silicates and opaque phases (carbon, iron oxides, and metal) have been spectrally characterized. The spectra of mafic silicate+metal mixtures were the subject of an earlier paper (Cloutis *et al.*, 1989). References to these spectra are included when appropriate.

The reasons for the choice of these materials is threefold- mafic silicates are widespread in meteorites (Mason, 1962a), the surface mineralogies of many asteroids probably involve mafic silicates (Gaffey, 1978), and small amounts of the various opaque phases can drastically alter mafic silicate reflectance spectra (Miyamoto *et al.*, 1981; 1982). The various mixtures have been subdivided into mafic silicate+carbon and olivine+iron oxides.

Mafic silicates are the most common minerals in all meteorite classes except the iron meteorites and the CI and CM carbonaceous chondrites. The spectral properties of mafic silicates and olivine-pyroxene mixtures have been extensively studied. The reflectance spectrum of olivine in the 0.3 to 2.6μm range is dominated by a broad absorption feature near 1μm (Band I) due to crystal field transitions in ferrous iron located in the M1 and M2 crystallographic sites. The wavelength position of this band shifts to longer wavelengths with increasing iron content and can be used to determine ferrous iron content (King & Ridley, 1987). Olivine shows a strong reflectance decrease towards wavelengths shorter than ~0.5μm due to intense charge transfer absorptions, and a weak band near 0.65μm of uncertain origin. The reflectance spectrum is essentially flat at wavelengths beyond 1.8μm (e.g., Burns, 1970a;

---

[1] A version of this chapter has been submitted for publication. Cloutis, E.A., Gaffey, M.J., Smith, D.G.W., and Lambert, R. St J. 1989. Icarus.

Cloutis, 1985; King & Ridley, 1987).

Orthopyroxenes (OPX) will be used here to refer to low-calcium pyroxenes. Orthopyroxenes are spectrally distinct from olivine in that they exhibit two strong absorption bands near 1μm (Band I) and 2μm (Band II) due to crystal field transitions in ferrous iron located in the M2 crystallographic site. The centers of both bands move systematically to longer wavelengths with increasing iron content (Burns, 1970b; Adams & McCord, 1972; Adams, 1974; Cloutis, 1985; Cloutis *et al.*, 1986a; 1986b).

In spite of the widespread presence of mafic silicates in meteorites, most asteroids remain mineralogically uncharacterized, with a few notable exceptions (e.g., McCord *et al.*, 1970; Bell *et al.*, 1984; Cruikshank & Hartmann, 1984; Gaffey, 1984). Part of the problem is undoubtedly due to the lack of laboratory spectral data on possible asteroidal mineral assemblages. Dark, spectrally featureless, opaque phases can be very effective at suppressing the major Fe^{2+} silicate absorption bands (Miyamoto *et al.*, 1981; 1982). Carbon, magnetite, and metal are the most common opaque materials in meteorites, and are present in a range of abundances, morphologies, and grain sizes. The laboratory spectra should help to constrain possible mineral assemblages for some classes of asteroids and help to establish the validity of compositional variations in the asteroid belt (Bell, 1986).

The most numerous asteroid class is the C-type, which exhibit dark, relatively featureless, reflectance spectra. The surface assemblages of members of this group are poorly known (Gradie & Tedesco, 1982). Laboratory spectral data may help to determine whether these asteroids are related to carbonaceous chondrites or whether they possess mineral assemblages unrelated to known meteorites. Similar compositional uncertainties exist for other, less numerous, asteroid classes such as the F, P, and D groups (Gradie & Veverka, 1980; Bell, 1986).

Powdered mixtures were spectrally characterized in the laboratory because the weight of the evidence suggests that asteroids, which are the main focus of this study, possess comminuted surfaces. Solar gas-rich brecciated meteorites that resided at or near the surfaces of their parent bodies for extended periods of time show evidence of comminution (Wilkening, 1983; Williams *et al.*, 1984; 1986; Bell & Keil, 1988; Britt *et al.*, 1988). Radar albedo measurements of the dark asteroids Ceres and Bamberga are best modeled as a layer of dust overlying a more compacted material with a surface bulk density comparable to lunar values (Dickel, 1979; Ostro *et al.*, 1985). The optical polarimetry data for the vast majority of asteroids are consistent with "microscopically intricate surfaces" (Veverka, 1973; Zellner *et al.*, 1977; Dollfus & Zellner, 1979). Widespread development of asteroidal surface regoliths is also suggested by thermal radiometry (Morrison & Lebofsky, 1979), and predicted on theoretical and experimental grounds (Comerford, 1967; Cintala *et al.*, 1979; Housen *et al.*, 1979a; 1979b; Housen & Wilkening, 1982; King *et al.*, 1984).

EXPERIMENTAL PROCEDURE

Both natural and synthetic samples were used in this study. The mafic silicates include olivine (OLV003) from San Carlos, Arizona, and pyroxene from Ekersund, Norway (PYX032). The opaque phases include amorphous carbon (LCA101, $<0.023\mu m$ grain size from Johnson Matthey), natural magnetite from Jacupiranga Mine, Sao Paulo State, Brazil (MAG101), and artificial wüstite (stoichiometric FeO, WUS101, $<63\mu m$ grain size, from Morton Thiokol). The various samples were selected on the basis of the availability of compositional information, spectral similarities to extraterrestrial samples, low degree of alteration, and availability of sufficient quantities of material. The chemical analyses of the mafic silicates and magnetite were acquired at the University of Calgary microprobe facility and are an average of 4-8 point analyses. The data were reduced using Bence-Albee α and β correction factors. The ferrous iron contents were determined by wet chemical methods, and ferric iron as the difference between total and ferrous iron. The chemical analyses of the mafic silicates and the magnetite are listed in Table IV-3-2I-1.

Powders of the mafic silicates and magnetite were obtained by crushing the samples in an alumina mortar and pestle. Purified fractions were obtained through a combination of magnetic separation and hand picking. The powders were repeatedly wet sieved with acetone to produce well-constrained size ranges. A portion of each mineral was retained for X-ray diffraction analysis. The wüsite was opened only in a dry nitrogen environment chamber to prevent oxidation, and exposed to atmosphere only during the course of acquiring the reflectance spectrum. The mafic silicates and magnetite were sieved into two size fractions- 0-45μm, and 45-90μm. All mixtures were made on a weight percentage basis (e.g. a mixture of 98 wt. % pyroxene and 2 wt. % carbon is expressed as 98/2 PYX/LCA).

The reflectance spectra were measured at the RELAB spectrometer facility at Brown University. Details of the instrument can be found in Pieters (1983). The spectra were acquired in the bidirectional reflectance mode with an incidence angle of 0° and an emission angle of 15°. All spectra were measured relative to halon, which is a near-perfect diffuse reflector in the 0.3-2.6μm range (Weidner & Hsia, 1981). The spectra were corrected for minor irregularities in halon's absolute reflectance in the 2μm region, as well as for dark current offsets. The reflectance spectra were analyzed using the Gaffey Spectrum Processing System, which is a PC-compatible version of SPECPR (Clark, 1980). Continuum removal was used in some cases to isolate specific absorption features. This was accomplished by dividing the reflectance spectrum by a straight line tangent to the spectrum on either side of an absorption band. Band minima and band centers were determined by fitting a quadratic equation to ~10 data points on either side of a visually determined band minimum or center. Band depths (D_b) were calculated using equation (32) of Clark & Roush (1984).

RESULTS

The various laboratory reflectance spectra have been subdivided into groups on the basis of the opaque phase present. This helps to highlight the spectrum-altering properties of a particular opaque phase. The two types of assemblages are carbon-bearing and iron oxide-bearing mafic silicate mixtures.

Iron Oxide-Bearing Mixtures

Miyamoto *et al.* (1982) noted that magnetite+mafic silicate mixtures can have dark, relatively flat reflectance spectra. Magnetite is the most, or second most, abundant opaque phase in carbonaceous chondrites (Table IV-3-21-II). Some carbonaceous chondrite spectra are amenable to analysis on the basis of the laboratory spectra because they contain unhydrated mafic silicates, magnetite, and carbon (McSween, 1977a; 1977b). The magnetite in the carbonaceous chondrites occurs in two major forms- as submicron aggregates and as irregular isolated grains (Kerridge, 1970; Fredriksson *et al.*, 1981; Hyman *et al.*, 1985). The submicron variety comprises a substantial portion or most of the total magnetite (Bostrom & Fredriksson, 1966; Davy *et al.*, 1978; Kerridge *et al.*, 1979; Wdowiak & Agresti, 1984). The chemistry of the magnetite is not precisely known but the analytical data do not correspond exactly to terrestrial magnetite or stoichiometric Fe_3O_4 (Mason, 1962b; Mason & Wiik, 1962; Sztrokay *et al.*, 1962; Kerridge,1970; Nagy, 1975; Kerridge *et al.*, 1979).

The reflectance spectra of terrestrial magnetite show a reflectance maximum near 0.8μm and either a weak Fe^{2+} absorption band near 1μm, or an overall reflectance decrease beyond 0.8μm. (Hunt *et al.*, 1971; Adams, 1975; Gradie & Veverka, 1980; Singer, 1981; Wagner *et al.*, 1987). The reflectance decline beyond 0.8μm seems to be most characteristic of fine-grained and cation-deficient magnetites (Morris *et al.*, 1985). Fine-grained magnetites also show decreases in reflectance with decreasing particle size. The magnetite spectra in Morris *et al.* (1985) are probably the best representatives of the magnetite in the carbonaceous chondrites.

A series of magnetite+olivine spectra were acquired in order to gauge the effect of adding magnetite to olivine. The 45-90μm fraction of the magnetite was used in all but one of the mixtures, for which the 0-45μm fraction was used (Figures IV-1 and IV-2). The pure magnetite spectrum shows a clear absorption band near 1μm and no downturn in reflectance towards the ultraviolet. At the highest magnetite abundance (50 wt. %) an absorption band near 1μm is still clearly resolvable and the spectrum shows an overall red slope. Coarse-grained magnetite alone cannot completely suppress mafic silicate absorption bands. Fine-grained magnetite mixed with olivine (90/10 OLV/MAG) imparts a less red slope to the overall spectrum than does the coarse-grained magnetite (Figure IV-2). The average reflectance of the plateau in the 1.8 to 2.6μm region relative to the local peak near 0.6μm is also less than the coarse-grained magnetite-bearing sample. The equivalent mixture of olivine+coarse-grained magnetite retains a prominent 1μm absorption band and the longer wavelength plateau is not suppressed relative to the short wavelength peak. If the magnetite were even finer-grained (<<45μm) the decrease in the redness of the overall slope may become even more pronounced. The overall slopes of the magnetite-olivine spectra were assessed by determining the intersection point of a horizontal continuum tangent to the spectrum at the peak near 0.6μm with the longer wavelength side of the spectrum. In the pure olivine this point occurs at 1.61μm and is relatively constant for 10 wt. % (1.64μm) and 50 wt. % (1.62μm) coarse-grained magnetite. The intersection point is shifted to ~2.3μm for the fine-grained magnetite mixture versus 1.64μm for the equivalent mixture containing the coarse-grained magnetite. The overall spectral slope measured in this way seems to be most sensitive to the grain size rather than the abundance of magnetite.

The absorption feature seen near 1μm is due to Fe^{2+} crystal field transitions in both the magnetite and the olivine. The band depth criterion (D_b; Clark & Roush, 1984) allows the relative effects of the two minerals on this feature to be assessed (Table IV-3-2I-1II). The band depth is strongly influenced by both the abundance and grain size of the magnetite. The 50/50 OLV/MAG spectrum has a band depth of 32%. A simple average of the pure end member band depths is 48%. The lower value for the mixture indicates that magnetite dominates the expression of this absorption band. The finer-grained magnetite is even more effective at reducing the band depth.

The band centers (continuum removed) of the olivine and magnetite occur at 1.060μm and 1.101μm, respectively. The magnetite seems to have little influence on the position of the band center (Table IV-3-2I-1II). It would appear that a simple straight line continuum removal procedure is adequate for determining the wavelength position of the Band I center, and from this the iron content of the olivine. At least 10 wt. % fine-grained magnetite is required to dominate the Band I center position. This is much greater than the magnetite abundance in the CV and CO meteorites. The indications are that the magnetite in the carbonaceous chondrites will impart a blue slope to the spectrum, lower the overall reflectance, reduce band depths, and have very little effect on the wavelength position of the Band I center.

Carbon

Carbon is present in varying amounts and forms in all the chondritic meteorite classes and the ureilites (Table IV-3-2I-1I). The abundance and structure of the carbon will strongly affect the degree to which associated silicates will be spectrally detectable (Miyamoto *et al.*, 1982). The structural state of the carbon in the various meteorite classes is still not fully known. Most of the carbon in the carbonaceous chondrites is present as highly-polymerized acid- and solvent-insoluble molecules (e.g. Hayes, 1967; Hayatsu & Anders, 1981; Nuth, 1985). The non-organic fraction exists in a partially amorphous macromolecular form (Buseck & Bo-Jun, 1985; Blake *et al.*, 1988), and a small amount of diamond is also present (Lewis *et al.*, 1987). Physically, some of the carbon is finely dispersed in the matrix (Bauman *et al.*, 1973; Heymann *et al.*, 1985; Van Der Stap *et al.*, 1986), some coats olivine grains and chondrules (Sztrokay *et al.*, 1962; Bunch & Chang, 1980), and some is concentrated in dark inclusions (Heymann *et al.*, 1987). The carbon in ordinary chondrites is largely in the form of macromolecules (Mason, 1979). The bulk of the carbon in ureilites occurs in ordered forms-primarily as graphite and diamond (Ramdohr, 1972; Begemann & Ott, 1983; Goodrich & Berkley, 1986; Wacker, 1986). Both phases occur as micron-sized grains, but the genetic relationship of the diamond to the graphite has not been fully resolved (Lipschutz, 1964; Vdovykin, 1970; 1972; Berkley *et al.*, 1976; 1980; Shindo *et al.*, 1985; Berkley, 1986; Fukunaga *et al.*, 1987).

The spectral properties of different carbon polymorphs are quite variable. Amorphous carbon has low overall reflectance with an overall blue slope (Figure IV-3; Miyamoto *et al.*, 1981). Amorphous carbon is a semiconductor and is increasingly transparent towards longer wavelengths (Mizushima & Fujibayashi, 1968). Graphite, by virtue of its semi-metallic nature, has a relatively neutral slope with low overall reflectance and a reflectance minimum near 0.4μm (Gilbert, 1960; Taft & Philipp, 1965; Foster & Howarth, 1968; Hunt & Salisbury, 1976; Kelly, 1981). Diamond is spectrally similar to graphite but with higher overall reflectance (Orlov, 1977). Charcoal, coal mascerals, chars and bitumens are all carbon-rich organic materials which may be suitable analogues for the organic fraction of the carbonaceous chondrites. All these organic materials have dark, red-sloped reflectance spectra with a reflectance minimum in the ultraviolet-visible spectral region (Kmetko, 1951; Foster & Howarth, 1968; Gradie & Veverka, 1980; Clark, 1983; Nelson, 1986; Andronico *et al.*, 1987; Ito *et al.*, 1988). Lonsdaleite has also been identified in some meteorites (Berkley & Jones, 1982), but its spectral properties have not been determined.

Very fine-grained amorphous carbon was used in the mineral mixtures for a number of reasons. This type of material is present in most of the carbon-rich meteorites (Lumpkin, 1981; Smith & Buseck, 1981; Buseck & Bo-Jun, 1985; Blake *et al.*, 1988). Amorphous carbon may be spectrally similar to the finest-grained particles of more ordered carbon forms (Blake *et al.*, 1988). The grain size of the amorphous carbon ($<0.023\mu$m) is roughly consistent with that of meteoritic carbon.

Both orthopyroxene-carbon (OPX-LCA) and olivine-carbon (OLV-LCA) mixtures were spectrally characterized. The presence of even small amounts of carbon greatly reduces the overall reflectance of both the orthopyroxene (Figure IV-4) and the olivine (Figure IV-5). At the highest carbon abundance (2 wt. %) the mafic silicate Fe^{2+} absorption bands are still resolvable. Band depth was again selected to quantify the effect of the carbon on absorption band resolution. The depth of the olivine absorption band (Band I) shows a high initial rate of decline followed by a more gradual decrease with increasing carbon content. The rate of band depth decline for the pyroxene Band I is more gradual (Figure IV-6), probably because an apparent red slope is already present in the pure pyroxene as evidenced by the low reflectance of the peak near 0.7μm relative to the interband peak near 1.4μm. Extrapolating from these results, it would appear that a band depth of 5%, which may be at the limit of detectability, would require ~4-6 wt. % carbon. If the carbon is not thoroughly dispersed, the silicate absorption bands would be resolvable at even higher carbon abundances.

The effect of amorphous carbon on absorption band positions was also examined. The Band I centers for the OLV-LCA spectra involving the 45-90μm-sized olivine vary by ±3 nm from that of pure olivine (Table IV-3-2I-1II). This variation is less than the wavelength resolution of the spectra (5 nm) and much less than the range of olivine band center variations as a function of iron content (~40 nm). The band center determined for the 99.5/0.5 OLV/LCA spectrum involving the 0-45μm sized olivine is 10 nm higher than the pure olivine. The 0.9-1.2μm range of this spectrum shows that the absorption feature in this region is quite complex (Figure IV-7). The quadratic fit to the data obscures this complexity and provides only a smoothed average band center value. The detailed spectrum shows that a local minimum may be present near the expected location for the pure olivine (1.06μm).

The band minima variations for the PYX-LCA mixtures are greater than for OLV-LCA. Both the Band I and Band II minima (no continuum removal) show non-systematic variations as a function of carbon content (Table IV-3-2I-1II). Band minima were measured for the PYX-LCA spectra because the low reflectance of the local pyroxene peak near 0.7μm is atypical of most meteoritic pyroxenes (Gaffey, 1976; Miyamoto *et al.*, 1983). It was felt that a straight line continuum removal would not yield a true determination of the Band I center. The Band II center was also not determined because the long wavelength wing of this band is incomplete and a linear continuum could not be constructed. The maximum variation in Band I minimum wavelength position (11 nm) corresponds to a deviation in pyroxene ferrous iron content of 15 mole % (Cloutis *et al.*, 1986a). Band area ratios have proven to be a useful method for separating pure orthopyroxenes from orthopyroxene-olivine and orthopyroxene-metal mixtures (Cloutis *et al.*, 1986b; Cloutis *et al.*, 1989). The band area ratio (II*/I*- Cloutis *et al.*, 1986b) for the PYX-LCA spectra is fairly constant, varying by only 7% over the range of carbon concentrations measured.

The amorphous carbon used in the mixtures is not the ideal material for simulating the effects of the meteoritic carbonaceous phase. Ordinary chondrites, CV and CO carbonaceous chondrites which contain <1 wt. % carbon do not show the red slope found in the laboratory spectra (Johnson & Fanale, 1973; Gaffey, 1976; Britt *et al.*, 1988). Even though most of the carbon in meteorites occurs as small grains, the fact that it is in a structurally ordered form should cause its reflectance spectrum to be flat and similar to graphite, a semi-metal, and to be relatively opaque through the near-infrared (Mizushima & Fujibayashi, 1968; Hunt & Salisbury, 1976). Amorphous carbon is a semi-conductor and is increasingly transparent towards the infrared. This behavior is evident in the reflectance spectra of the mixtures containing 0.1 and 0.5 wt. % amorphous carbon (Figures IV-4 and IV-5). The mineral mixtures containing 2 wt. % carbon are less red-sloped probably because the carbon coats the mafic silicate grains more thickly, partially negating the transparency rise of the carbon towards longer wavelengths. Low abundances of amorphous carbon are therefore not suitable for simulating the spectral effects of more ordered carbon forms on mafic silicate spectra. These and other results for carbon-bearing mixtures (Miyamoto *et al.*, 1982; Clark, 1983) indicate that the parent bodies of all the known carbon-bearing meteorites should exhibit subdued, but potentially resolvable, mafic silicate Fe^{2+} absorption bands, provided that the mean grain size of the mafic silicates is greater than a few 10's of microns. In fact, weak silicate absorption bands seem to be more prevalent in dark meteorites than has commonly been believed (Gaffey, 1978; 1980; Vilas & Gaffey, 1989).

Carbon+Magnetite

Carbon and magnetite are both present in carbonaceous chondrites and unequilibrated ordinary chondrites (UOC) These materials occur as intimately associated aggregates in the latter group, and can comprise up to a few volume % of the meteorite (McKinley *et al.*, 1981; Scott *et al.*, 1981a; 1981b; Nagahara, 1984; Brearley *et al.*, 1987). Although carbon+magnetite+mafic silicate mixtures were not included in this study, their spectral properties can be anticipated in part from the binary mixture data.

Small amounts of fine-grained carbon lower overall reflectance, reduce band depths, and redden mafic silicate spectra. Fine-grained magnetite also lowers overall reflectance and reduces band depths but imparts a blue slope to mafic silicate spectra. The magnitude of the slope change can be evaluated by measuring the reflectance ratio of two widely separated poin~~ts in the~~ reflectance spectra whose ratio is approximately one in the pure minerals. The ratio chosen for the olivine-opaque spectra is the reflectance at 2.5μm to the reflectance of the peak in the 0.5-0.7μm region. For pyroxene-opaque mixtures, the reflectance ratio of the Band II minimum to the peak in the 0.5-0.7μm region was chosen. These ratios are listed in Table IV-3-2I-1II. The addition of the amorphous carbon to either mafic silicate causes an initial reddening of the spectra (increasing reflectance ratios) followed by a decrease. This is opposite to the trend observed for the olivine + magnetite spectra. If the finer-grained magnetite were used exclusively, the reflectance ratio should not exhibit this upturn in the reflectance ratio at higher magnetite abundances. The trends in reflectance ratios for the mafic silicates + magnetite are a function of the relative spectral contribution of the end members. If ordered carbon were used instead of the amorphous variety, the tendency of magnetite to impart a blue slope to the reflectance spectra would dominate. The slope of mafic silicate + opaque spectra will depend upon the chemistries, relative abundances and disposition of the opaques.

APPLICATION TO METEORITE SPECTRA

Mafic silicate-opaque assemblages are present in a number of meteorite classes. The ureilites, CV and CO carbonaceous chondrites, and the ordinary chondrites, including the unequilibrated and shock-blackened varieties, may be amenable to spectral analysis on the basis of the laboratory data. Each of these groups is discussed in reference to the laboratory spectral data.

Ureilites

The reflectance spectrum of the ureilite Novo Urei (Gaffey, 1976) shows many features characteristic of an olivine + opaque-rich assemblage. This meteorite is composed of

64 wt. % olivine, 28 wt. % pigeonite, 5 wt. % metal + troilite, and 2.5 wt. % carbon (Vdovykin, 1970; Berkley *et al.*, 1980). Its reflectance spectrum shows two weak absorption bands near 1μm (Band I) and 2μm (Band II). The wavelength position of the Band I minimum is 0.97μm. This corresponds to 25±5 wt. % pyroxene using the band minimum calibration of Cloutis *et al.* (1986a). The band area ratio criterion (Cloutis *et al.*, 1986b) suggests a much lower pyroxene abundance of 5±5 wt. %. This calibration is only strictly valid for olivine + orthopyroxene mixtures. Pigeonite and clinopyroxene have lower band area ratios than orthopyroxene. Consequently, the band area ratio for mixtures of olivine plus pigeonite/clinopyroxene provides only a lower limit on pigeonite/clinopyroxene abundance (Cloutis, 1985).

The carbon content of Novo Urei (2.5 wt. %) is comparable to that of some of the mineral mixtures (2 wt. %). The 2.5μm:0.5-0.7μm peak ratio of Novo Urei is 1.24, and is almost identical to both 98/2 mixtures of OLV/LCA (1.25) and PYX/LCA (1.21). The depth of Band I (16 %) is also comparable to the 45-90μm sized silicate-carbon mixtures (14-20 %). The most noticeable difference between the Novo Urei spectrum and the laboratory spectra is the abrupt decrease in reflectance below 0.5μm in the former is not present in the latter. The absolute reflectance of Novo Urei (0.079 at 0.56μm) is also appreciably higher than the mineral mixture spectra (0.017-0.034). Both of these discrepancies may be due to the spectral differences between graphite and amorphous carbon (Kelly, 1981). The other spectral features are consistent with an olivine-pigeonite-carbon assemblage.

CV and CO Carbonaceous Chondrites

CV and CO carbonaceous chondrites commonly contain between 0.1 and 0.6 wt. % carbon (Mason, 1962b). The major silicate phase is olivine, with minor amounts of pigeonite, oligoclase, sulfides, and calcium-aluminum inclusions (DuFresne & Anders, 1962; McSween, 1977a; 1977b). The laboratory reflectance spectra of 99.5/0.5 OLV/LCA should be the most similar to the CV and CO chondrite spectra (Johnson & Fanale, 1973; Gaffey, 1976). The CV and CO spectra show absorption bands near 1μm and 2μm due to the mafic silicates. The broadness of the absorption near 2μm may also be due in part to the calcium-aluminum inclusions, some of which have very broad absorption bands beyond 2μm (Rajan & Gaffey, 1984). The red slope characteristic of the olivine-carbon laboratory spectra is absent probably reflecting the spectral differences between amorphous carbon and the meteoritic carbonaceous phase.

The reflectance increase seen in carbonaceous chondrites with decreasing grain size has been attributed to more effective dispersal of the mafic silicates in the smaller-sized fractions. The average visible reflectance for the 99.9/0.1 and 99.5/0.5 mafic silicate carbon mixtures is between 4 and 13 %. The finest fractions of the carbonaceous chondrites have average visible reflectances of 11-17 %. This is further evidence that amorphous carbon is not a spectrally significant phase in carbonaceous chondrites and that the meteoritic carbonaceous phase is ordered and not as well dispersed as in the laboratory mixtures.

The reflectance spectrum of the CO3 carbonaceous chondrite Lancé (Johnson & Fanale, 1973) was examined in order to understand more fully the nature of the opaque phase. The Band I minimum occurs at 1.04±0.02μm. This corresponds to 90±10 wt. % olivine. Although the mineral abundances in this meteorite have not been determined, the CO3 group normally contains ~70 wt. % olivine (Mason, 1962b; McSween, 1977a). The band area ratio calibration yields an olivine content of 70±10 wt. %. The rather large error is due to the difficulty in selecting the precise position of the Band II minimum. The steep red slope characteristic of amorphous carbon is absent. Spectral analysis suggests that the carbonaceous phase in the carbonaceous chondrites does not appreciably affect band area ratio and band wavelength positions.

Ordinary Chondrites

The laboratory results from this and an earlier study (Cloutis *et al.*, 1989) on mafic silicate+metal spectra can be used to examine the nature of the opaque phases in ordinary chondrites, and whether ordinary chondrites can be related to specific asteroid classes. The telescopic spectra of S-class asteroids have been interpreted as being either modified ordinary chondrite spectra or representing differentiated assemblages. Resolution of this issue has important implications for understanding the origin and evolution of the asteroid belt and perhaps the inner solar system (Gaffey, 1984; Bell, 1986; Gaffey, 1986; 1988). Broadly, ordinary chondrite spectra show absorption bands due to mafic silicates, have low reflectance, but do not exhibit the overall red slope which is characteristic of S-class asteroids (Gaffey, 1976; Feierberg *et al.*, 1982; Gaffey, 1984).

All investigators agree that the S asteroids are likely metal-bearing (>20 %), mafic silicate assemblages. By this criterion alone, the H-type ordinary chondrites are the closest analogues. Gaffey (1984; 1986) examined a number of possible mechanisms by which ordinary chondrites may be modified to appear spectrally more like S-asteroids. The interpretation of ordinary chondrite spectra here will consider the nature of the neutral/opaque phases in ordinary chondrites, and whether they can be reconciled with the S-asteroid spectra.

Generally, H chondrites are composed of 15-20 wt. % metal, 0.07-0.6 wt. % carbon, 50-60 wt. % pyroxene, 25-40 wt. % olivine, 5-10 wt. % plagioclase, and 7-15 wt. % troilite (Mason, 1965; Moore & Lewis, 1967; Chapman & Salisbury, 1973; Dodd, 1981). The amount of metal present should be spectrally detectable by the distinct red slope it imparts to mafic silicate reflectance spectra (Cloutis *et al.*, 1989). The fact that it does not suggests that either the metal signature is suppressed by a very fine-grained dispersed material (carbon) or that the metal is not spectrally red. The first hypothesis was examined by measuring the reflectance spectrum of an iron meteorite powder (45-90μm grain size) and the same powder mixed with 0.5 wt. % of the amorphous carbon. This amount of carbon is within the range for H chondrites, but it has no effect on the red slope of the iron meteorite metal spectrum (Figure IV-8).

The second hypothesis was examined by Gaffey (1986) who found that the metal in ordinary chondrites is not spectrally red. The derived reflectance spectrum of ordinary chondrite metal differs from that of iron meteorites. He suggested that this may be due to a thin surface layer (<0.5μm) of an iron chloride (lawrencite-$FeCl_2$), or an iron oxide (wu¨stite). Lawrencite has been found in a variety of chondrites as a coating on metal grains or as minute inclusions (Krinov, 1960; Keil, 1968; Mason & Graham, 1970; Reed, 1971; Allen & Mason, 1973; Bryan & Kullerud, 1975; Sipiera *et al.*, 1980; Yabuki & El Goresy, 1986). Abundant chlorine has also been measured in some ordinary chondrite metal grains (Mason & Graham, 1970; Allen & Mason, 1973).

The major Fe^{2+} absorption band in lawrencite is quite broad and extends from ~1.3 to 2.0μm. The minimum reflectance occurs at about 1.33μm (Kuiper, 1969). The evidence for spectrally significant amounts of lawrencite is ambiguous. The reflectance spectra of the metal-rich magnetic fractions of ordinary chondrites, particularly the H4 chondrite Ochansk, show a weak absorption feature near 1.3μm which may be due to lawrencite (Gaffey, 1986). However, the 1.3μm absorption band in lawrencite shifts rapidly towards 1μm upon short exposure to air (Kuiper, 1969), as lawrencite readily oxidizes. It is unlikely that unoxidized, spectrally abundant lawrencite would remain in the crushed and separated meteorite fractions. Lawrencite also has high overall reflectance while the derived ordinary chondrite metal does not (Gaffey, 1986).

An absorption band near 1.3μm can also be attributed to plagioclase (Adams & Goullaud, 1978) or to the long wavelength wing of the major olivine absorption band (e.g. King & Ridley, 1987). This band is present in both the whole meteorite and the non-magnetic fractions as a weak shoulder on the long wavelength wing of the major Fe^{2+} absorption band present near 1μm. It seems likely that silicate minerals are the cause of this feature rather than lawrencite.

Some sort of iron oxide, such as wu¨stite (FeO) has also been suggested as a possible coating for the ordinary chondrite metal grains (Gaffey, 1986). The reflectance spectrum of wüstite (Figure IV-9) shows a number of desirable spectral features- low overall reflectance, a nearly flat reflectance spectrum and the lack of a prominent Fe^{2+} absorption band. An optically thick coating of wustite on ordinary chondrite metal grains could reduce the reflectance of unaltered metal and subdue its strong red slope.

Oxidized coatings on ordinary chondrite metal grains have been observed on a number of occassions. While some are undoubtedly due to terrestrial weathering (Knox, 1963; Ramdohr, 1963), others seem to be of preterrestrial origin (Rambaldi & Wasson, 1981; Scott & Rajan, 1981; Boctor *et al.*, 1982; Lambert *et al.*, 1984; Rambaldi & Wasson, 1984; Sears *et al.*, 1984). Some of these observations were made on shock-altered specimens which are expected to be more representative of the parent body surfaces than unshocked specimens. Models of ordinary chondrite metamorphism also predict the oxidation of the metal grains (Larimer, 1985).

Laboratory studies of metal oxidation show that it proceeds under a wide variety of conditions, including very low oxygen partial pressures, and in CO_2 and H_2-CH_4 atmospheres (Gibbs, 1973; Tomlinson & Menzies, 1978; Taylor, 1981; Smith *et al.*, 1985). Wustite is a common oxidation product of these reactions (Runk & Kim, 1970), and thin films of it can develop in a very short time (Kubaschewski & Hopkins, 1962). The presence of sulfur in an H_2-CH_4 atmosphere may inhibit the formation of iron oxides and instead result in iron carbide formation (Barnes *et al.*, 1985).

The thickness of a surface film on metal particles required to effect a spectral change depends on the chemistry of the film. An upper limit of 0.5μm (5000 Angstroms) for most ordinary chondrite metal grain coatings has been suggested (Gaffey, 1986). Substantial reflectivity changes are possible due to surface films of a few 100 Angstroms (McIntyre & Aspnes, 1971). Large reductions in iron reflectivity in the visible wavelength region have been documented for iron oxide films of ~500-1000Angstroms thickness (Constable, 1927). This is approximately an order of magnitude less than the maximum suggested thickness.

Ordinary chondrite reflectance spectra show absorption bands attributable to the mafic silicates. Mafic silicate band area ratios are strongly affected by the presence of red-sloped metal (Cloutis *et al.*, 1989). The pyroxene:olivine ratios determined for ordinary chondrites using band area ratios are very similar to the values determined independently (Britt *et al.*, 1988). Band minima wavelength positions also do not deviate in a systematic way from pure mafic silicates (Gaffey, 1976). This correspondence is expected to be retained only when the additional phases are spectrally neutral. Metal with a reflectance spectrum similar to that derived by Gaffey (1986) would not substantially affect the band area ratio, and band minima/center wavelength positions. Iron meteorite metal has measurable effects on these and other spectral parameters (Cloutis *et al.*, 1989).

S-class asteroids have been suggested as plausible parent bodies for the ordinary chondrites. However some surface modification process seems necessary in order to reconcile the spectral differences between the ordinary chondrites and the S-asteroids. A number of explanations have been suggested (e.g. Britt & Pieters, 1987).

Anders (1978) suggested that preferential erosion of brittle silicates on a silicate-metal surface would leave a deposit enriched in metal. It seems likely that kamacite, the primary metal phase in H chondrites (Smith, 1980) is brittle at the temperatures present in the main asteroid belt. When kamacite is in the ductile regime, its erosion rate is substantially less than brittle materials. However, when it is brittle, its erosion rate should not differ substantially from silicates (Comerford, 1967). Even assuming that erosion of silicates may be enhanced, a number of factors may preclude the development of a metallic red slope. Heavily shocked meteorites show some fracturing of metal grains, that seems to be accompanied by partial oxidation along metal grain boundaries (Boctor *et al.*, 1982; Sears *et al.*, 1984). Neither shock-blackened chondrites, nor gas-rich ordinary chondrites, which presumably resided at or near the surfaces of their parent bodies for some period of time, show unusually red-sloped reflectance spectra (Bell & Keil, 1988; Britt *et al.*, 1988).

Feierberg *et al.* (1982) measured the reflectance spectra of mixtures of metallic iron (37-74μm grain size) and a pyroxene (0-74μm grain size) in an attempt to simulate the reflectance spectrum of the S asteroid Flora. They noted that an intimate mixture of 20 wt. % metal and 80 wt. % pyroxene reproduces the absorption band depths of the Flora spectrum, but significantly, the red slope of the asteroid could not be reproduced. They attributed this discrepancy to the lack of olivine in their mineral mixtures, the addition of which they claimed would impart a red slope to the spectrum. However the addition of olivine will not cause a reddening of the spectral slope, since only achondritic meteorite metal or a small amount of effectively dispersed amorphous carbon can redden the slope (Cloutis *et al.*, 1989). Olivine has the opposite effect as measured by the peak:peak reflectance ratios (Cloutis *et al.*, 1986b).

The spectral parameters used by Feierberg *et al.* (1982)- wavelength position of the reflectance maximum between Band I and II, and ratio of the band depths (Band II/Band I) show that there is some overlap between the S-asteroid and ordinary chondrite fields. However, these parameters are not the most suitable for determining metal:pyroxene:olivine ratios because the trends for pyroxene+olivine, pyroxene+metal, orthopyroxene+clinopyroxene, and pyroxene+olivine+metal all overlap. Other more useful spectral characteristics have been identified for discriminating among these mixtures (Cloutis *et al.*, 1989). Based on the laboratory data for metal+mafic silicate mixtures, the spectrum of Flora has been interpreted as indicating a metal- and olivine-rich surface mineralogy, coinciding very well with an earlier independent analysis of the telescopic data (Gaffey, 1984). An approximate tenfold enrichment in metal abundance is required over that present in LL ordinary chondrites to reach the level of Flora (50 wt. %- Cloutis *et al.*, 1989). LL chondrites are the closest analogues to Flora on the basis of mafic silicate composition. A factor of ten enhancement of metal over silicate is not anticipated for even ductile metal. If the metal is ductile this level of enrichment is even less plausible (Comerford, 1967).

Red-sloped spectra are exhibited by some ordinary chondrites which contain abundant glass and/or agglutinates due to impact melting and perhaps space weathering (McFadden, 1983a; 1983b; King *et al.*, 1984; McFadden & Vilas, 1987). Artificial meteorite glass shows a strong red spectral slope similar to lunar agglutinates, and may account for the red slope seen in some asteroid telescopic spectra (King *et al.*, 1983; Pieters, 1984). However the development of a major glass/agglutinate component is not expected on asteroid surfaces (Housen & Wilkening, 1982), and the polarimetric data for almost 100 asteroids has failed to detect surface materials similiar to glassy lunar fines (Dollfus *et al.*, 1975; Zellner *et al.*, 1977; Dollfus & Zellner, 1979; Geake & Dollfus, 1986). The heavily shocked and gas-rich meteorites also do not contain appreciable quantities of glass or agglutinates (Basu & McKay, 1983) and are not spectrally reddened (Bell & Keil, 1988; Britt *et al.*, 1988). Artificially shock-loaded mafic silicates show a reduction in overall reflectance but no spectral reddening (Adams *et al.*, 1979). A simulation of space weathering using laser irradiation also failed to impart a red spectral slope to a dunite sample although overall reflectance was reduced (Fisenko *et al.*, 1989). The observed lack of agglutinates in meteorites may not be representative of asteroid surfaces, and a number of reasonable arguments can be made that true regolith samples of ordinary chondrite parent bodies would not survive the passage to Earth (King *et al.*, 1984).

A number of spectral parameters identified for mafic silicate-metal mixtures have been applied to strengthen the case for at least on S-class asteroid (Flora) having a metal+olivine-rich surface unlike ordinary chondrites (Cloutis *et al.*, 1989). At present it is unknown whether agglutinates added to mafic silicates will reproduce the reflectance spectrum of Flora or other red-sloped asteroids.

SUMMARY

Mafic silicate spectra can acquire an overall blue slope by the addition of fine-grained magnetite. Magnetite also reduces overall reflectance and band intensities. The reflectance spectra of magnetite-bearing meteorites (CV and CO carbonaceous chondrites) exhibit many of these features. The low band depths of these meteorites suggests that an additional dark, neutral phase such as ordered carbon is present. Carbon+mafic silicate spectra exhibit a red overall slope at low amorphous carbon concentrations. Amorphous carbon is not a suitable spectral analogue for the carbonaceous phase present in most meteorites.

The addition of carbon to mafic silicates has little effect on band center wavelength positions and band area ratios, both of which are key parameters for determining mafic silicate chemistries and abundances. The carbon does however greatly reduce band intensities.

The laboratory spectra suggest that the amount of carbon required to suppress mafic silicate absorption bands exceeds that found in all meteorite classes. The parent bodies of some of the darkest meteorites (shock-blackened ordinary chondrites, ureilites, CV and CO carbonaceous chondrites) should show spectral features attributable to mafic silicates. The reflectance spectra of ureilites are consistent with mafic silicates + carbon assemblages. Ordinary chondrite reflectance spectra do not show the strong red slope associated with unaltered metal or amorphous carbon. The ordinary chondrite metal seems to be spectrally distinct from that in iron meteorites. An optically thick, but largely undetected, coating on these metal grains can best explain the non-red spectral slope of the ordinary chondrites. The most plausible mechanism for the development of a red spectral slope in ordinary chondrites is the production of a significant glass/agglutinate component during regolith formation.

Table IV-1. Chemical analyses of the olivine (OLV003), pyroxene (PYX032) and magnetite (MAG101) used in this study.

Wt. %	OLV003	PYX032	MAG101
SiO_2	40.64	50.21	0.00
Al_2O_3	<0.01	1.24	0.33
Na_2O	0.00	0.00	N.D.
CaO	0.07	1.59	N.D.
FeO	9.25	23.65	26.52
Fe_2O_3	0.59	5.11	63.71
MgO	49.13	17.57	3.63
MnO	0.09	0.53	0.60
ZnO	0.00	N.D.	N.D.
NiO	0.33	0.01	N.D.
TiO_2	0.00	0.19	3.04
Cr_2O_3	0.01	0.04	0.03
CoO	0.04	0.06	N.D.
V_2O_5	0.00	<0.01	N.D.
TOTAL	100.15	100.20	97.86

N.D.= Not determined.

Table IV-2. Magnetite and carbon abundances in the H, L, and LL ordinary chondrite classes, the CV and CO carbonaceous chondrites and the ureilites (U).

Meteorite Class	Wt. % Magnetite[1]	Wt. % Carbon
H	0	0.02-0.03
L	0	0.01-0.50
LL	0	0.02-0.60
CV	1-13	0.20-1.50
CO	2-5	0.20-0.60
U	0	2.00-6.00

[1] Magnetite is present in some petrologic grade 3 ordinary chondrites (e.g., McKinley *et al.*, 1981; Scott *et al.*, 1981a; 1981b; Brearley *et al.*, 1987).

Sources of data: Mason, 1962b; Moore & Lewis, 1967; Gibson *et al.*, 1971; Gibson, 1976; Haggerty & McMahon, 1979; Gibson, 1980; Berkley & Jones, 1982; Hyman & Rowe, 1986.

Table IV-3. Band depth, band center and band minima wavelength positions, and reflectance ratios for the mafic silicate+carbon and mafic silicate+magnetite spectra. All ratios are in weight percents. Band positions are given in microns.

Sample	Band Depth (%)	Band I Center		Reflectance Ratio- 2.5/0.7
OLV:MAG				
100:0	70	1.060		1.137
90:10	50	1.058		1.077
90:10*	38	1.059		1.013
50:50	32	1.061		1.181
0:100	26	1.101		1.520
OLV:LCA				
100:0	70	1.060		1.137
99.9:0.1	31	1.059		1.734
99.5:0.5	24	1.058		1.500
99.5:0.5#	5	1.069		1.640
98.0:2.0	14	1.063		1.250
0:100	--	--		--
PYX:LCA		Band I Minimum	Band II Minimum	Ratio Band II/0.7
100:0	58	0.928	1.958	0.843
99.9:0.1	55	0.919	1.931	0.860
99.5:0.5	41	0.927	1.940	0.876
98.0:2.0	20	0.917	1.908	0.869
0:100	--	--	--	--

*= Mixture containing <45μm-sized magnetite.
#= Mixture containing <45μm-sized olivine.

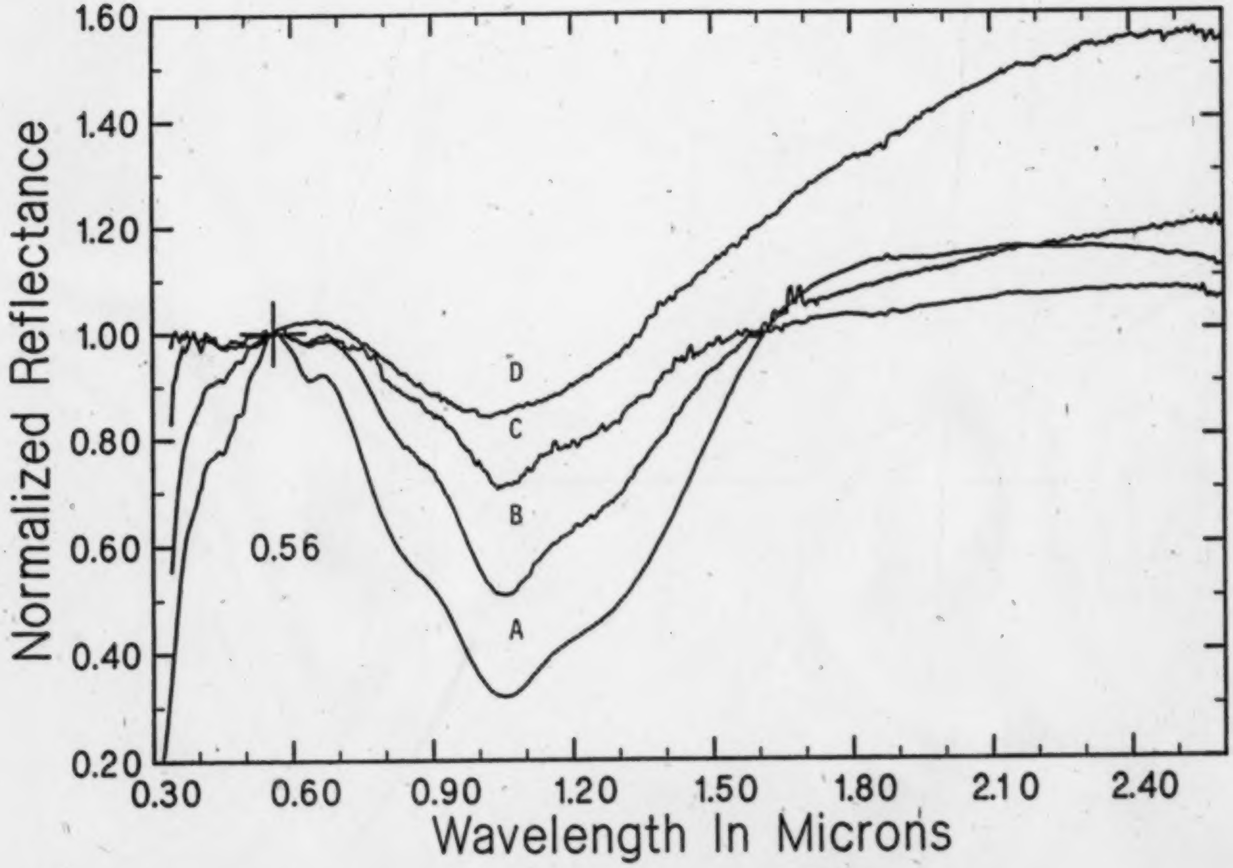

Figure IV-1. Normalized reflectance spectra (scaled to 1 at 0.56μm) of 45-90μm sized olivine+magnetite mixtures. The weight percentages of olivine/magnetite and absolute reflectances at 0.56μm are: A- 100/0, 0.732; B- 90/10, 0.362; C- 50/50, 0.106; D- 0/100, 0.059.

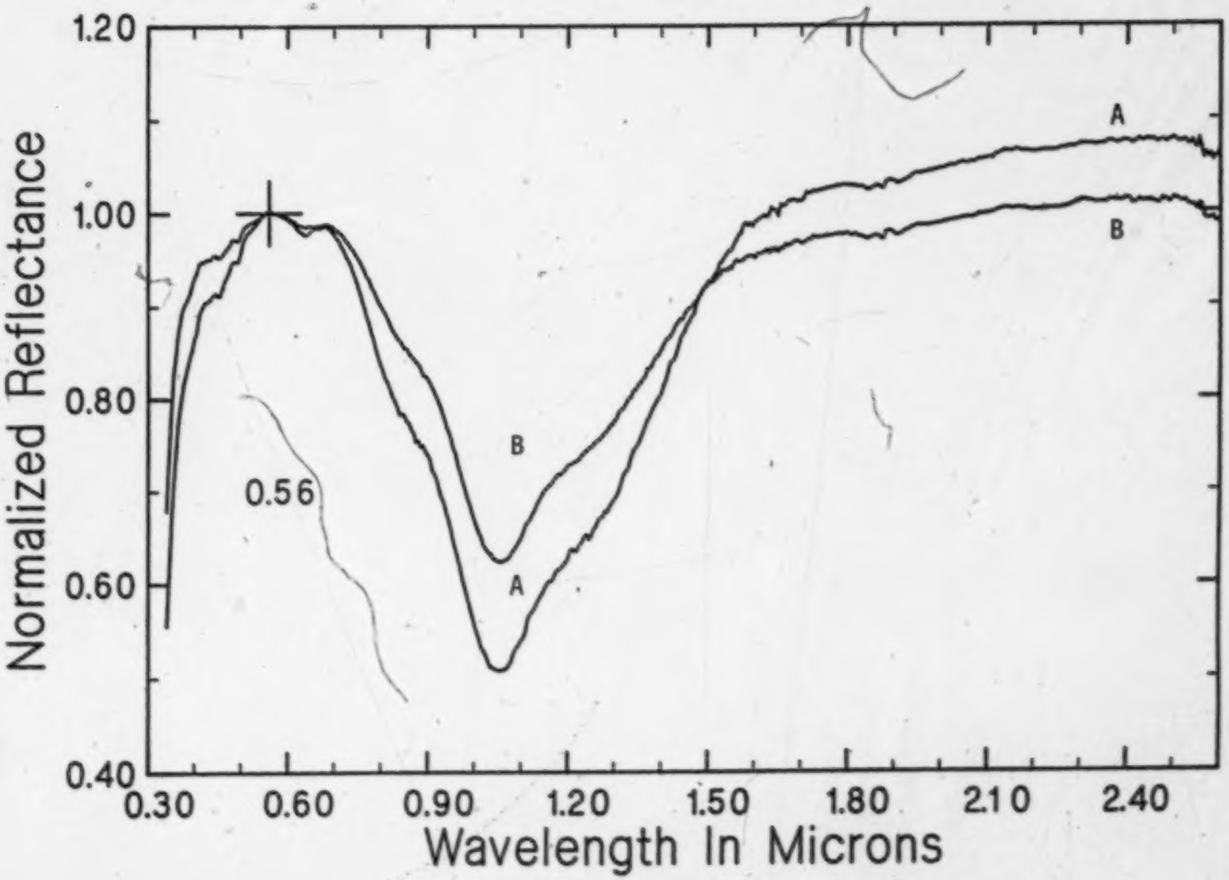

Figure IV-2. Normalized reflectance spectra of the 90/10 olivine/magnetite mixtures involving the 0-45μm (Spectrum A) and 45-90μm-sized magnetite (Spectrum B). The absolute reflectances at 0.56μm are 0.362 (A) and 0.214 (B).

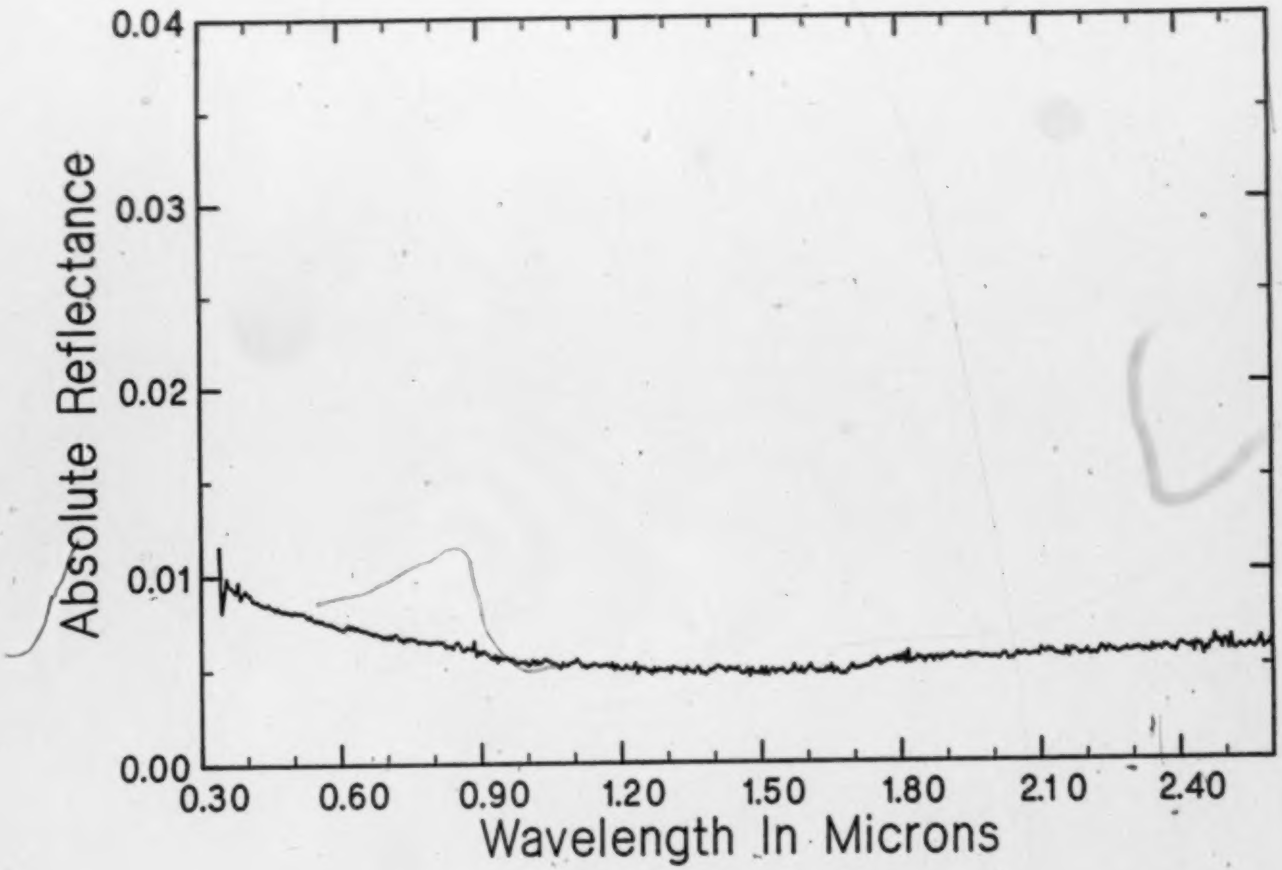

Figure IV-3. Absolute reflectance spectrum of the amorphous carbon used in some of the mineral mixtures.

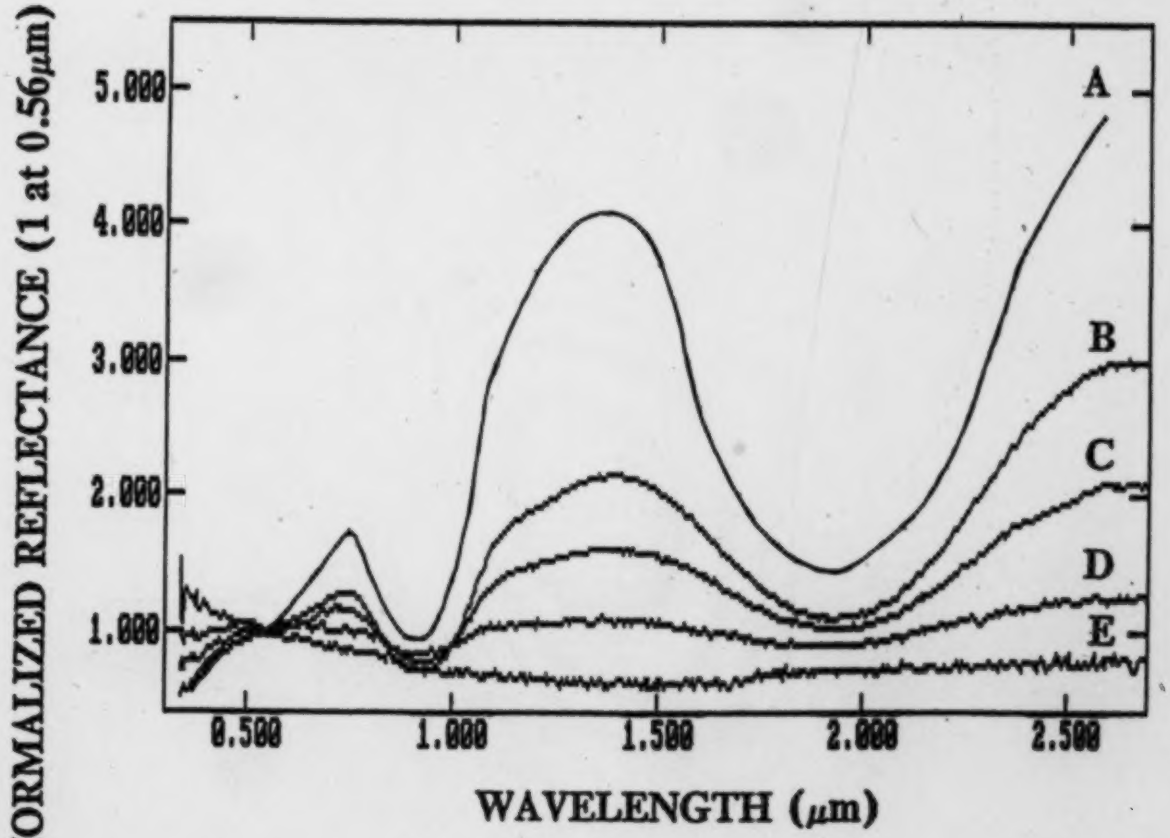

Figure IV-4. Normalized reflectance spectra (scaled to 1 at 0.56μm) of pyroxene+amorphous carbon mixtures. The weight percentages of pyroxene/carbon and absolute reflectances at 0.56μm are: A- 100/0, 0.080; B- 99.9/0.1, 0.058; C- 99.5/0.5, 0.033; D- 98.0/2.0, 0.017; E- 0/100, 0.0076.

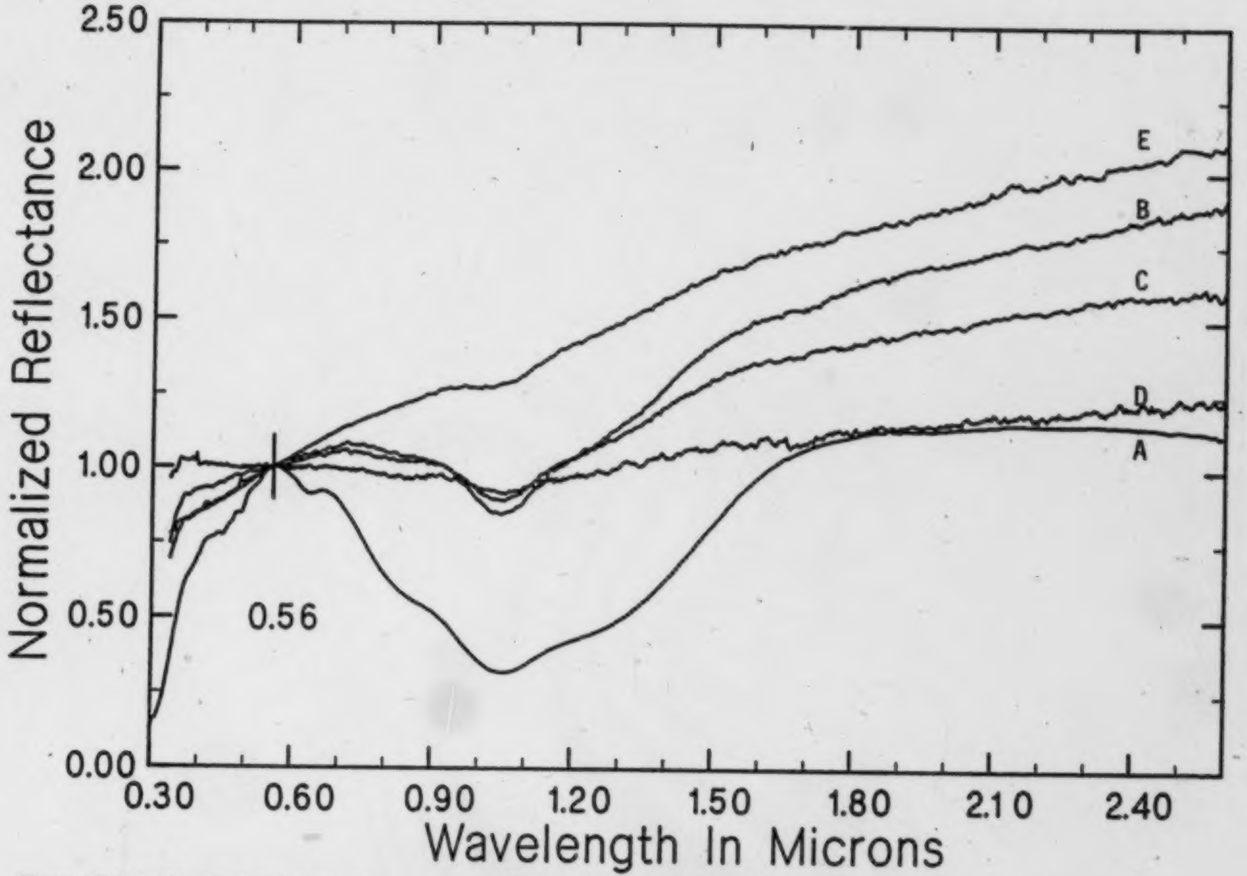

Figure IV-5. Normalized reflectance spectra (scaled to 1 at 0.56μm) of olivine+amorphous carbon mixtures. The weight percentages of olivine/carbon and absolute reflectances at 0.56μm are: A- 100/0, 0.732; B- 99.9/0.1, 0.129; C- 99.5/0.5, 0.068; D- 98.0/2.0, 0.033; E- 99.5/0.5, 0.097. Spectra A to D involve the 45-90μm sized olivine, while spectrum E involves the <45μm sized olivine.

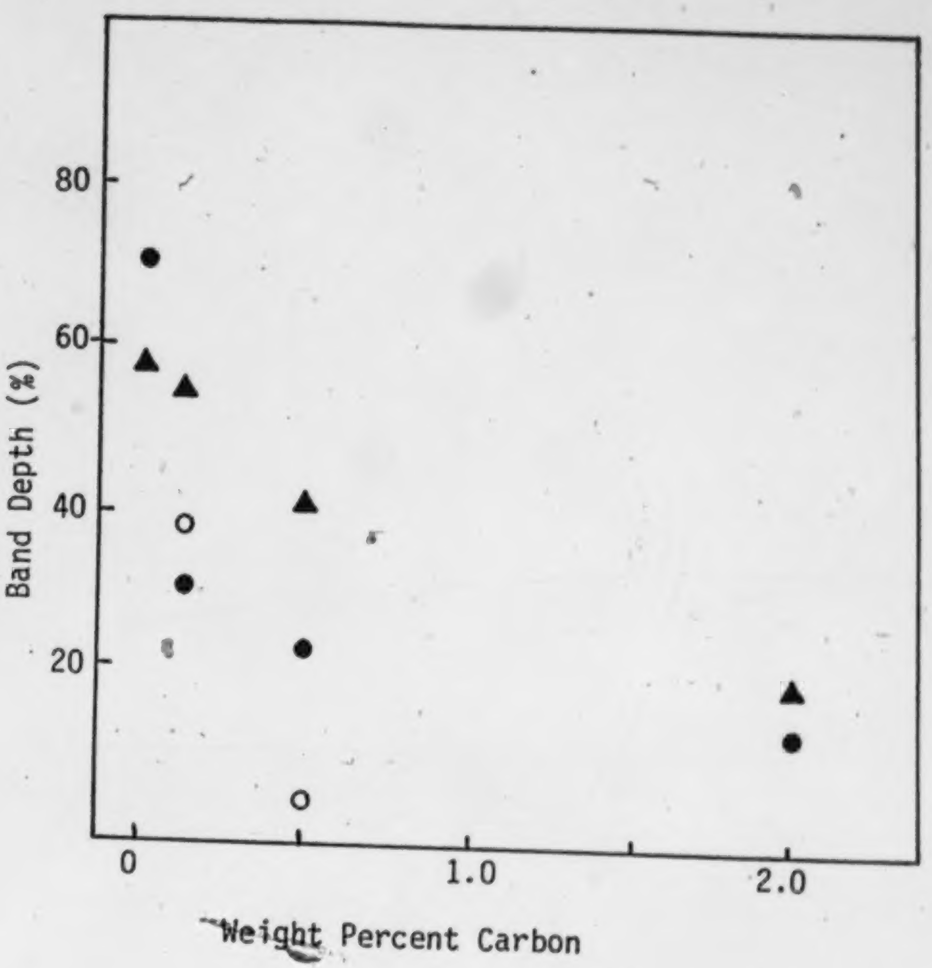

Figure IV-6. Band depth as a function of carbon content for the mafic silicate+carbon spectra of Figures 4 and 5. Triangles= PYX117+LCA101; filled circles= 45-90μm-sized OLV003+LCA101; open circles= <45μm-sized OLV003+LCA101.

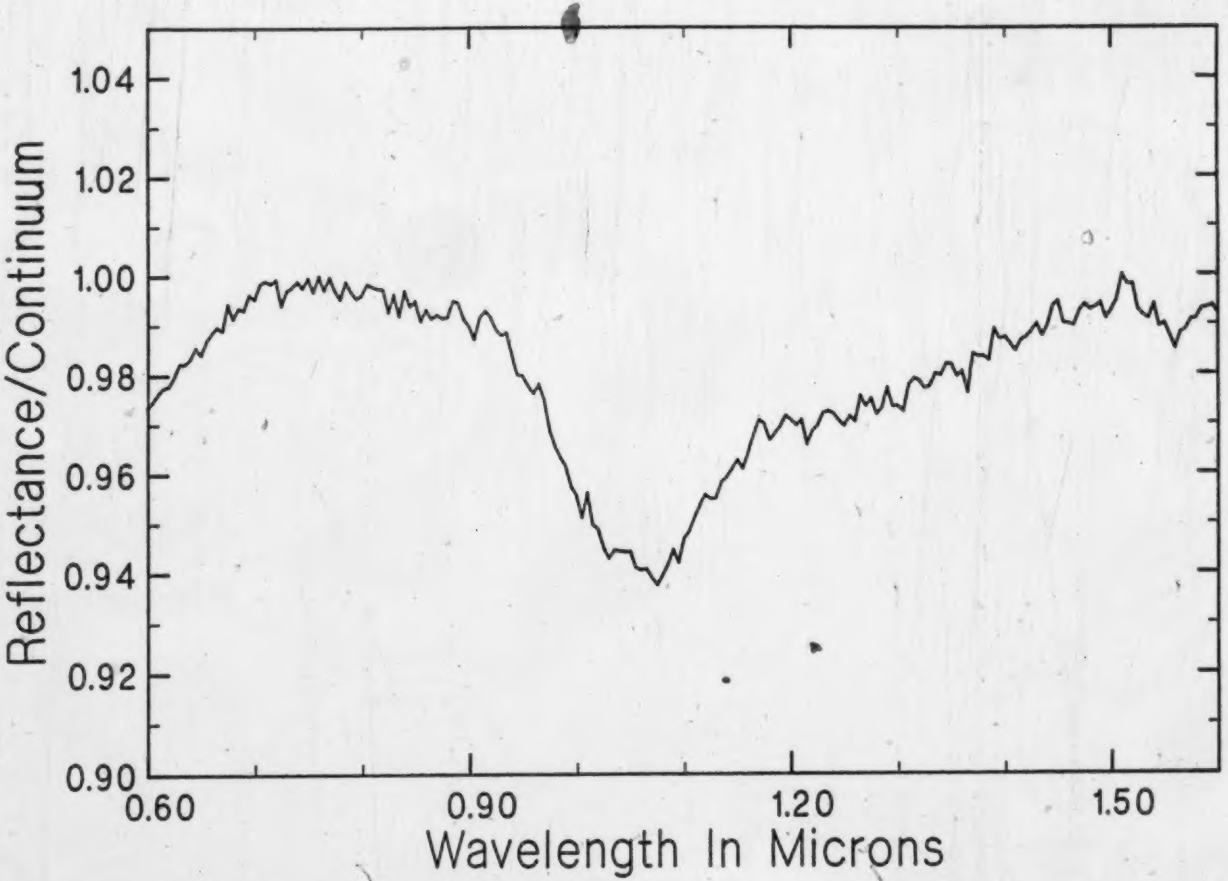

Figure IV-7. Straight line continuum removed spectrum (0.6-1.6μm) of the 99.5/0.5 olivine/carbon mixture involving the <45μm-sized olivine.

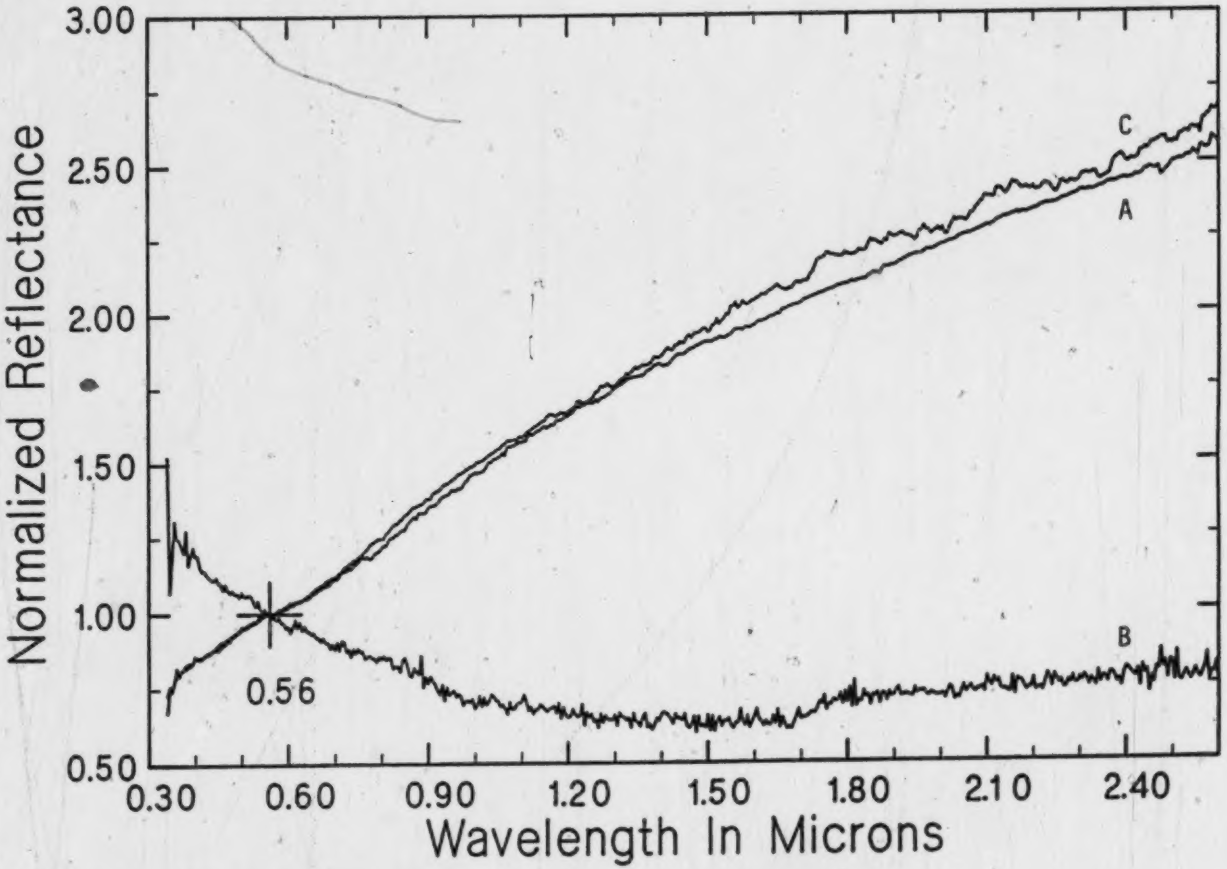

Figure IV-8. Normalized reflectance spectra of Odessa iron meteorite powder (45-90μ grain size; curve A), amorphous carbon (curve B), and a 99.5/0.5 mixture of this metal/carbon (curve C). The spectra have been scaled to one at 0.56μm and the absolute reflectance at this wavelength are 0.110 (A), 0.0076 (B), and 0.044 (C).

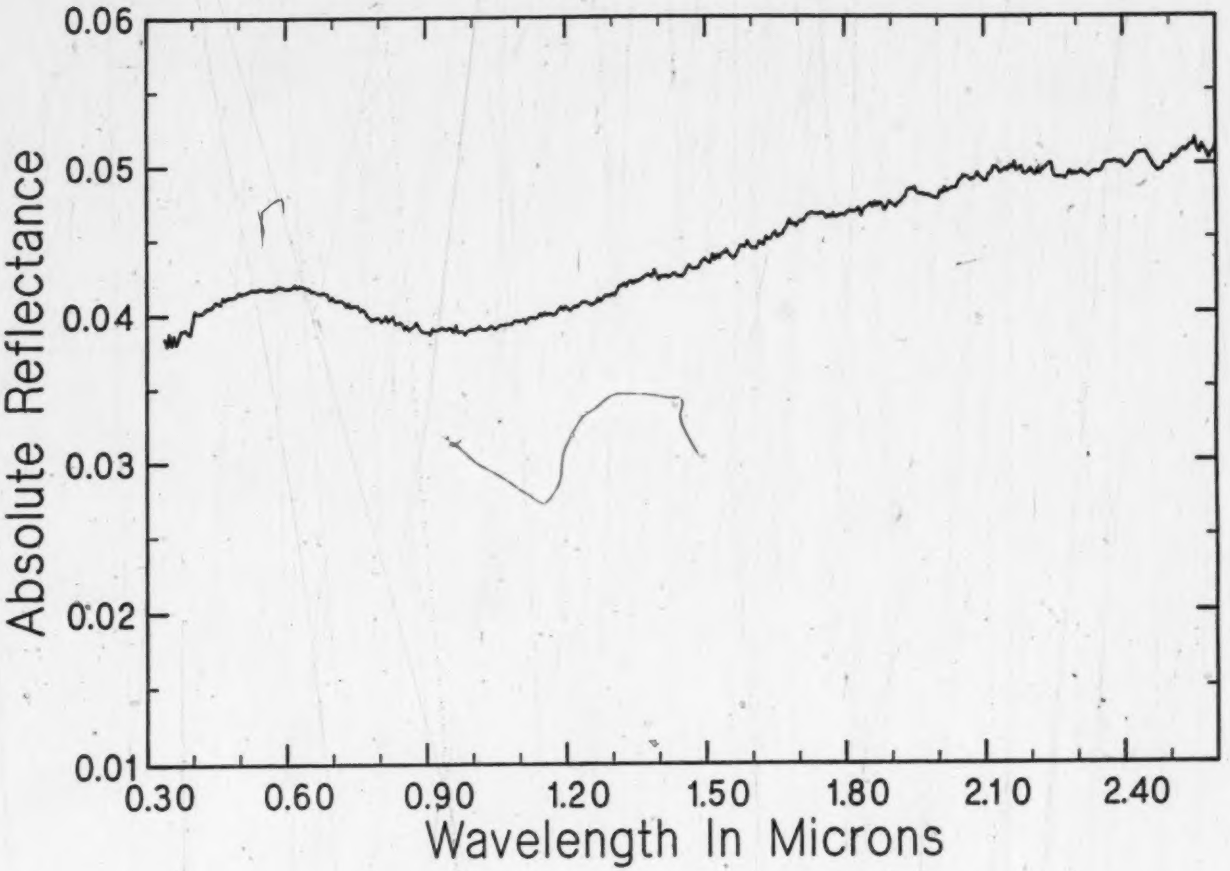

Figure IV-9. Absolute reflectance spectrum of $<63\mu m$-sized artificial wustite (stoichiometric FeO).

A. REFERENCES

Adams, J.B. 1974. Visible and near-infrared diffuse reflectance spectra of pyroxenes as applied to remote sensing of solid objects in the solar system. *Jour. Geophys. Res.* **79**, 4829-4836.

Adams, J.B. 1975. Interpretation of visible and near-infrared diffuse reflectance spectra of pyroxenes and other rock-forming minerals. In *Infrared and Raman Spectroscopy of Lunar and Terrestrial Minerals* (C. Karr Jr., Ed), pp. 91-116. Academic Press, New York.

Adams, J.B., and L.H. Goullaud 1978. Plagioclase feldspars: Visible and near infrared diffuse reflectance spectra as applied to remote sensing. *Proc. Lunar Plan. Sci. Conf. 9th*, 2901-2909.

Adams, J.B., and T.B. McCord 1972. Electronic spectra of pyroxenes and interpretation of telescopic spectral reflectivity curves of the Moon. *Proc. Third Lunar Sci. Conf.*, 3021-3034.

Adams, J.B., F. Horz, and R.V. Gibbons 1979. Effects of shock-loading on the reflectance spectra of plagioclase, pyroxene, and glass. *Lunar Plan. Sci. Conf. X*, 1-3.

Allen Jr., R.O., and B. Mason 1973. Minor and trace elements in some meteoritic minerals. *Geochim. Cosmochim. Acta* **37**, 1435-1456.

Anders, E. 1978. Most stony meteorites come from the asteroid belt. In *Asteroids: An Exploration Assessment* (D. Morrison and W.C. Wells, Eds.), pp. 57-75. NASA CP-2053.

Andronico, G., G.A. Baratta, F. Spinella, and G. Strazzulla 1987. Optical evolution of laboratory-produced organics: Applications to Phoebe, Iapetus, outer main belt asteroids and cometary nuclei. *Astron. Astrophys.* **184**, 333-336.

Barnes, J., J. Corish, F. Franck, and J.F. Norton 1985. Influence of sulfur on the nature and morphology of carbides formed on the surfaces of Fe-Ni-Cr alloys at high temperatures. *Oxid. Metals* **24**, 85-97.

Basu, A., and D.S. McKay 1983. Rarity of lunar soil analogs in meteorites. *Meteoritics* **18**, 263-264.

Bauman, A.J., J.R. Devaney, and E.M. Bollin 1973. Allende meteorite carbonaceous phase:

Intractable nature and scanning electron morphology. *Nature* **241**, 264-267.

Begemann, F., and U. Ott 1983. Comment on "The nature and origin of ureilites" by J.L. Berkley *et al. Geochim. Cosmochim. Acta* **47**, 975-977.

Bell, J.F. 1986. Mineralogical evolution of meteorite parent bodies. *Lunar Plan. Sci. Conf. XVII*, 985-986.

Bell, J.F., and K. Keil 1988. Spectral alteration effects on chondritic gas-rich breccias: Implications for S-class and Q-class asteroids. *Proc. Eighteenth Lunar Plan. Sci. Conf.*, 573-580.

Bell, J.F., M.J. Gaffey, and B.R. Hawke 1984. Spectroscopic identification of probable pallasite parent bodies. *Meteoritics* **19**, 187-188.

Berkley, J.L. 1986. Four Antarctic ureilites: Petrology and observations on ureilite petrogenesis. *Meteoritics* **21**, 169-189.

Berkley, J.L., and J.H. Jones 1982. Primary igneous carbon in ureilites: Petrological implications. *Proc. Thirteenth Lunar Plan. Sci. Conf.*, in *Jour. Geophys. Res.* **87**, A353-A364.

Berkley, J.L., H.G. Brown IV, K. Keil, N.L. Carter 1976. The Kenna ureilite: An ultramafic rock with evidence for igneous, metamorphic, and shock origin. *Geochim. Cosmochim. Acta* **40**, 1429-1437.

Berkley, J.L., G.J. Taylor, K. Keil, G.E. Harlow, and M. Prinz 1980. The nature and origin of ureilites. *Geochim. Cosmochim. Acta* **44**, 1579-1598.

Blake, D.F., F. Freund, K.F.M. Krishnan, C.J. Echer, R. Shipp, T.E. Bunch, A.G. Tielens, R.J. Lipari, C.J.D. Hetherington, and S. Chang 1988. The nature and origin of interstellar diamond. *Nature* **332**, 611-613.

Boctor, N.Z., P.M. Bell, H.K. Mao, and G. Kullerud 1982. Petrology and shock metamorphism of Pampa del Infierno chondrite. *Geochim. Cosmochim. Acta* **46**, 1903-1911.

Bostrom, K., and K. Fredriksson 1966. Surface conditions of the Orgueil parent body as indicated by mineral associations. *Smithsonian Misc. Coll.* **151**, 1-39.

Brearley, A.J., E.R.D. Scott, G.J. Taylor, and K. Keil 1987. Transmission electron microscopy of graphite-magnetite aggregates in the Sharps (H3) chondrite. *Lunar*

Plan. Sci. Conf. XVIII, 123-124.

Britt, D.T., and C.M. Pieters 1987. The optical effects of surface processes on small bodies. *Meteoritics* **22**, 340-342.

Britt, D.T., C.M. Pieters, M.I. Petaev, and N.I. Zaslavskaya 1988. The Tsarev meteorite: Petrology and bidirectional reflectance spectra. Submitted to Proc. Nineteenth Lunar Plan. Sci Conf.

Bryan, W.B., and G. Kullerud 1975. Mineralogy and chemistry of the Ashmore chondrite. *Meteoritics* **10**, 41-50.

Bunch, T.E., and S. Chang 1980. Carbonaceous chondrites- II. Carbonaceous chondrite phyllosilicates and light element geochemistry as indicators of parent body processes and surface conditions. *Geochim. Cosmochim. Acta* **44**, 1543-1577.

Burns, R.G. 1970a. Crystal field spectra and evidence of cation ordering in olivine minerals. *Amer. Mineral.* **55**, 1608-1632.

Burns, R.G. 1970b. *Mineralogical Applications of Crystal Field Theory*. Cambridge University Press, London.

Buseck, P.R., and H. Bo-Jun 1985. Structure of graphitic carbons: Terrestrial versus extraterrestrial origin. *Meteoritics* **20**, 619-620.

Chapman, C.R., and J.W. Salisbury 1973. Comparisons of meteorite and asteroid spectral reflectivities. *Icarus* **19**, 507-522.

Cintala, M.J., J.W. Head, and L. Wilson 1979. The nature and effects of impact cratering on small bodies. In *Asteroids* (T. Gehrels, Ed.), pp. 579-600. University of Arizona Press, Tucson.

Clark, R.N. 1980. A large-scale interactive one dimensional array processing system. *Publ. Astron. Soc. Pacific* **92**, 221-224.

Clark, R.N. 1983. Spectral properties of mixtures of montmorrilonite and dark carbon grains: Implications for remote sensing minerals containing chemically and physically adsorbed water. *Jour. Geophys. Res.* **88**, 10635-10644.

Clark, R.N., and T.L. Roush 1984. Reflectance spectroscopy: Quantitative analysis techniques for remote sensing applications. *Jour. Geophys. Res.* **89**, 6329-6340.

Cloutis, E.A. 1985. *Interpretive Techniques for Reflectance Spectra of Mafic Silicates*. M.Sc. Thesis, University of Hawaii.

Cloutis, E.A., M.J. Gaffey, R. St J. Lambert, and D.G.W. Smith 1986a. The quality of geological information derivable from high resolution reflectance spectra: Results for mafic silicates. *Proc. Tenth Canadian Symp. Remote Sensing*, 309-318.

Cloutis, E.A., M.J. Gaffey, T.L. Jackowski, and K.L. Reed 1986b. Calibration of phase abundance, composition, and particle size distribution for olivine-orthopyroxene mixtures from reflectance spectra. *Jour. Geophys. Res.* **91**, 11641-11653.

Cloutis, E.A., M.J. Gaffey, D.G.W. Smith, and R. St J. Lambert 1989. Metal-silicate mixtures: Spectral properties and applications to asteroid taxonomy. Submitted to *Jour. Geophys. Res.*, 36pp.

Comerford, M.F. 1967. Comparative erosion rates of stone and iron meteorites under small-particle bombardment. *Geochim. Cosmochim. Acta* **31**, 1457-1471.

Constable, F.H. 1927. Spectrophotometric observations on the growth of oxide films on iron, nickel, and copper. *Proc. Royal Soc. Series A* **117**, 376-387.

Cruikshank, D.P., and W.K. Hartmann 1984. The meteorite-asteroid connection: Two olivine-rich asteroids. *Science* **223**, 281-283.

Davy, R., S.G. Whitehead, and G. Pitt 1978. The Adelaide meteorite. *Meteoritics* **13**, 121-140.

Dickel, J.R. 1979. Radio observations of asteroids: Results and prospects. In *Asteroids* (T. Gehrels, Ed.), pp. 212-221. University of Arizona Press, Tucson.

Dodd, R.T. 1981. *Meteorites, A Peterologic-Chemical Synthesis*. Cambridge University Press, New York.

Dollfus, A., and B. Zellner 1979. Optical polarimetry of asteroids and laboratory samples. In *Asteroids* (T. Gehrels, Ed.), pp. 170-183. University of Arizona Press, Tucson.

Dollfus, A., J.E. Geake, J.C. Mandeville, and B. Zellner 1975. The nature of asteroid surfaces, from optical polarimetry. In *Comets, Asteroids, Meteorites- Interrelations, Evolution and Origin* (A.M. Delsemme, Ed.), pp. 243-251. University of Toledo Press, Toledo.

DuFresne, E.R., and E. Anders 1962. On the chemical evolution of the carbonaceous chondrites. *Geochim. Cosmochim. Acta* **26**, 1085-1114.

Feierberg, M.A., H.P. Larson, and C.R. Chapman 1982. Spectroscopic evidence for undifferentiated S-type asteroids. *Astrophys. Jour.* **257**, 361-372.

Fisenko, A.V., N.N. Kasanova, L.F. Semjonova, E.I. Chumak, Y.A. Surkov, and A.K. Lavrukhina 1989. Alteration of reflectance spectra for dunit processed by laser radiation. *Lunar Plan. Sci. Conf. XX*, 297-298.

Foster, P.J., and C.R. Howarth 1968. Optical constants of carbons and coals in the infrared. *Carbon* **6**, 719-729.

Fredriksson, K., B. Mason, R. Beauchamp, and G. Kurat 1981. Carbonates and magnetites in the Renazzo chondrite. *Meteoritics* **16**, 316.

Fukunaga, K., J. Matsuda, K. Nagao, M. Miyamoto, and K. Ito 1987. Noble-gas enrichment in vapour-growth diamonds and the origin of diamonds in ureilite. *Nature* **328**, 141-143.

Gaffey, M.J. 1976. Spectral reflectance characteristics of the meteorite classes. *Jour. Geophys. Res.* **81**, 905-920.

Gaffey, M.J. 1978. Optical and spectral properties of the low albedo meteorites: Applications to the interpretation of the spectra of dark asteroids. *Lunar Plan. Sci. Conf. IX*, 362-364.

Gaffey, M.J. 1980. Mineralogically diagnostic features in the visible and near-infrared reflectance spectra of carbonaceous chondrite assemblages. *Lunar Plan. Sci. XI*, 312-313.

Gaffey, M.J. 1984. Rotational spectral variations of asteroid (8) Flora: Implications for the nature of S-type asteroids and for the parent bodies of the ordinary chondrites. *Icarus* **60**, 83-114.

Gaffey, M.J. 1986. The spectral and physical properties of metal in meteorite assemblages: Implications for asteroid surface materials. *Icarus* **66**, 468-486.

Gaffey, M.J. 1988. Thermal history of the asteroid belt: Implications for accretion of the terrestrial planets. *Lunar Plan. Sci. Conf. XIX*, 369-370.

Geake, J.E., and A. Dollfus 1986. Planetary surface texture and albedo from parameter plots of optical polarization data. *Mon. Not. Royal Astron. Soc.* **218**, 75-91.

Gibbs, G.B. 1973. A model for mild steel oxidation in CO_2. *Oxid. Metals* 7, 173-184.

Gibson Jr., E.K. 1976. Nature of the carbon and sulfur phases and inorganic gases in the Kenna ureilite. *Geochim. Cosmochim. Acta* **40**, 1459-1464.

Gibson Jr. E.K. 1980. Carbon abundances in Antarctic meteorites. *Lunar Plan. Sci. Conf. XI*, 323-325.

Gibson, E.K., C.B. Moore, and C.F. Lewis 1971. Total nitrogen and carbon abundances in carbonaceous chondrites. *Geochim. Cosmochim. Acta* **35**, 599-604.

Gilbert, L.A. 1960. The reflectivity spectra of coal vitrains in the visible and ultra-violet. *Fuel* **39**, 393-400.

Goodrich, C.Y., and J.L. Berkley 1986. Primary magmatic carbon in ureilites: Evidence from cohenite-bearing metallic spherules. *Geochim. Cosmochim. Acta* **50**, 681-691.

Gradie, J., and E. Tedesco 1982. Compositional structure of the asteroid belt. *Science* **216**, 1405-1407.

Gradie, J., and J. Veverka 1980. The composition of the Trojan asteroids. *Nature* **283**, 840-842.

Haggerty, S.E., and B.M. McMahon 1979. Magnetite-sulfide-metalcomplexes in the Allende meteorite. *Proc. Lunar Plan. Sci. Conf. Tenth*, 851-870.

Hayatsu, R., and E. Anders 1981. Organic compounds in meteorites and their origins. *Topics Curr. Chem.* **99**, 1-37.

Hayes, J.M. 1967. Organic constituents of meteorites: A review. *Geochim. Cosmochim. Acta* **31**, 1395-1440.

Heymann, D., R. Vis, and C. Van Der Stap 1985. Carbon concentration mapping in a surface of the Allende meteorite. *Lunar Plan. Sci. Conf. XVI*, 348-349.

Heymann, D., C.C.A.H. Van der Stap, R.N. Vis, and H. Verheul 1987. Carbon in dark inclusions of the Allende meteorite. *Meteoritics* **22**, 3-15.

Housen, K.R., and L.L. Wilkening 1982. Regolith on small bodies in the solar system. *Ann. Rev. Earth Plan. Sci.* **10**, 355-376.

Housen, K.R., L.L. Wilkening, C.R. Chapman, and R. Greenberg 1979a. Asteroidal regoliths. *Icarus* **39**, 317-351.

Housen, K.R., L.L. Wilkening, C.R. Chapman, and R.J. Greenberg 1979b. Regolith development and evolution on asteroids and the Moon. In *Asteroids* (T. Gehrels, Ed.), pp. 601-627. University of Arizona Press, Tucson.

Hunt, G.R., and J.W. Salisbury 1976. Visible and near infrared spectra of minerals and rocks: XII. Metamorphic rocks. *Mod. Geol.* **5**, 219-228.

Hunt, G.R., J.W. Salisbury, and C.J. Lenhoff 1971. Visible and near-infrared spectra of minerals and rocks: III. Oxides and hydroxides. *Mod. Geol.* **2**, 195-205.

Hyman, M., and M.W. Rowe 1986. Saturation magnetization measurements of carbonaceous chondrites. *Meteoritics* **21**, 1-22.

Hyman, M., E.B. Ledger, and M.W. Rowe 1985. Magnetite morphologies in the Essebi and Haripura chondrites. *Proc. Fifteenth Lunar Plan. Sci. Conf.*, C710-C714.

Ito, O., H. Seki, and M. Iino 1988. Diffuse reflectance spectra in near-i.r. region of coals; a new index for degrees of coalification and carbonization. *Fuel* **67**, 573-578.

Johnson, T.V., and F.P. Fanale 1973. Optical properties of carbonaceous chondrites and their relationship to asteroids. *Jour. Geophys. Res.* **78**, 8507-8518.

Keil, K. 1968. Mineralogical and chemical relationships among enstatite chondrites. *Jour. Geophys. Res.* **73**, 6945-6976.

Kelly, B.T. 1981. *Physics of Graphite*. Applied Science Publishers, Essex, U.K.

Kerridge, J.F. 1970. Some observations on the nature of magnetite in the Orgueil meteorite. *Earth Plan. Sci. Lett.* **9**, 299-306.

Kerridge, J.F., A.L. McKay, and W.V. Boynton 1979. Magnetite in CI carbonaceous meteorites: Origin by aqueous activity on a planetesimal surface. *Science* **205**, 395-397.

King, T.V.V., and W.I. Ridley 1987. Relation of the spectroscopic reflectance of olivine to mineral chemistry and some remote sensing implications. *Jour. Geophys. Res.* **92**, 11457-11469.

King, T.V.V., M.J. Gaffey, and E.A. King 1983. Spectral reflectance measurements and surface characteristics of meteoritic condensates from solar furnace experiments. *Lunar Plan. Sci. Conf. XIV*, 371-372.

King, T.V.V., M.J. Gaffey, and L.A. McFadden 1984. Evidence for regolith maturation on asteroids. *Lunar Plan. Sci. Conf. XV*, 429-430.

Kmetko, E.A. 1951. Infrared absorption and intrinsic semiconductivity of condensed aromatic systems. *Phys. Rev.* **82**, 456-457.

Knox Jr., R. 1963. The microstructure of several stony meteorites. *Geochim. Cosmochim. Acta* **27**, 261-268.

Krinov, E.L. 1960. *Principles of Meteoritics*. Pergamon Press, Oxford.

Kubaschewski, O., and B.E. Hopkins 1962. *Oxidation of Metals and Alloys*. Butterworths Scientific Publications, London.

Kuiper, G.P. 1969. Identification of the Venus cloud layers. *Commun. Lunar Plan. Lab* **6**, 229-250.

Lambert, P., C. Lewis, and C.B. Moore 1984. Repeated shock and thermal metamorphism of the Abernathy meteorite. *Meteoritics* **19**, 29-48.

Larimer, J.W. 1985. Volatile behavior during thermal metamorphism. *Meteoritics* **20**, 691-692.

Lewis, R.S., M. Tang, J.F. Wacker, E. Anders, and E. Steel 1987. Interstellar diamonds in meteorites. *Nature* **326**, 160-162.

Lipschutz, M.E. 1964. Origin of diamonds in the ureilites. *Nature* **143**, 1431-1434.

Lumpkin, G.R. 1981. Electron microscopy of carbonaceous matter in Allende acid residues. *Proc. Lunar Plan. Sci. 12B*, 1153-1166.

Mason, B. 1962a. *Meteorites*. Wiley, New York.

Mason, B. 1962b. The carbonaceous chondrites. *Space Sci. Rev.* **1**, 621-646.

Mason, B. 1965. The chemical composition of olivine-bronzite and olivine-hypersthene chondrites. *Amer. Mus. Novit.* **2223**, 1-38.

Mason, B. 1979. *Data of Geochemistry*. Geol. Survey Prof. Pap. 440-B-1.

Mason, B., and A.L. Graham 1970. Minor and trace elements in meteoritic minerals. *Smiths. Contrib. Earth Sci.* 3, 1-17.

Mason, B., and H.B. Wiik 1962. The Renazzo meteorite. *Amer. Mus. Novit.* **2106**, 1-11.

McCord, T.B., J.B. Adams, and T.V. Johnson 1970. Asteroid Vesta: Spectral reflectivity and compositional implications. *Science* **168**, 1445-1447.

McFadden, L.A. 1983a. S-type asteroids and their relation to ordinary chondrites. *Meteoritics* **18**, 352-353.

McFadden, L.A. 1983b. Reflectance characteristics of some Antarctic meteorites and their relation to asteroid surface composition. *Bull. Amer. Astron. Soc.* **15**, 827.

McFadden, L.A., and F. Vilas 1987. The 3:1 Kirkwood Gap as a source of ordinary chondrites: Perspectives from spectral reflectance. *Lunar Plan. Sci. Conf. XVIII*, 614-615.

McIntyre, J.D.E., and D.E. Aspnes 1971. Differential reflection spectroscopy of very thin surface films. *Surface Sci.* **24**, 417-434.

McKinley, S.G., E.R.D. Scott, G.J. Taylor, and K. Keil 1981. A unique type 3 ordinary chondrite containing graphite-magnetite aggregates- Allan Hills A77011. *Proc. Lunar Plan. Sci. 12B*, 1039-1048.

McSween Jr., H.Y. 1977a. Carbonaceous chondrites of the Ornans type: A metamorphic sequence. *Geochim. Cosmochim. Acta* **41**, 477-491.

McSween Jr., H.Y. 1977b. Petrographic variations among carbonaceous chondrites of the Vigarano type. *Geochim. Cosmochim. Acta* **41**, 1777-1790.

Miyamoto, M., A. Mito, Y. Takano, and N. Fujii 1981. Spectral reflectance (0.25-2.5μm) of powdered olivines and meteorites, and their bearing on surface materials of asteroids. *Mem. Nat. Inst. Polar Res. Spec. Iss. 20*, 345-361.

Miyamoto, M., A. Mito, and Y. Takano 1982. An attempt to reduce the effects of black materials from the spectral reflectance of meteorites and asteroids. *Mem. Nat. Inst. Polar Res. Spec. Iss. 25*, 291-307.

Miyamoto, M., M. Kinoshita, and Y. Takano 1983. Spectral reflectance (0.25-2.5μm) of olivine and pyroxene from an ordinary chondrite. *Mem. Nat. Inst. Polar Res. Spec Iss. 30*, 367-377.

Mizushima, S., and Y. Fujibayashi 1968. Optical absorption edge of evaporated carbon films in the near infrared region. *Carbon* **6**, 123.

Moore, C.B., and C.F. Lewis 1967. Total carbon content of ordinary chondrites. *Jour. Geophys. Res.* **72**, 6289-6292.

Morris, R.V., H.V. Lauer Jr., C.A. Lawson, E.K. Gibson Jr., G.A. Nace, and C. Stewart 1985. Spectral and other physicochemical properties of submicron powders of hematite (α-Fe_2O_3), maghemite (γ-Fe_2O_3), magnetite (Fe_3O_4), goethite (α-FeOOH), and lepidocrocite (γ-FeOOH). *Jour. Geophys. Res.* **90**, 3126-3144.

Morrison, D., and L. Lebofsky 1979. Radiometry of asteroids. In *Asteroids* (T. Gehrels, Ed.), pp. 184-205. University of Arizona Press, Tucson.

Nagahara, H. 1984. Matrices of type 3 ordinary chondrites- primitive nebular records. *Geochim. Cosmochim. Acta* **48**, 2581-2595.

Nagy, B. 1975. *Carbonaceous Meteorites*. Elsevier, Amsterdam.

Nelson, M.L. 1986. *Application of Radiative Transfer Theory to the Spectra of Mixtures with Anisotropic Phase Functions*. M.Sc. Thesis, University of Hawaii.

Nuth, J.A. 1985. Meteoritic evidence that graphite is rare in the interstellar medium. *Nature* **318**, 166-168.

Orlov, Y.A. 1977. *The Mineralogy of the Diamond*. Wiley, New York.

Ostro, S.J., D.B. Campbell, and I.I. Shapiro 1985. Mainbelt asteroids: Dual polarization radar observations. *Science* **229**, 442-446.

Pieters, C.M. 1983. Strength of mineral absorption features in the transmitted component of near-infrared light: First results from RELAB. *Jour. Geophys. Res.* **88**, 9534-9544.

Pieters, C.M. 1984. Asteroid-meteorite connection: Regolith effects implied by lunar reflectance spectra. *Meteoritics* **19**, 290-291.

Rajan, S., and M.J. Gaffey 1984. Spectral reflectance characteristics of Allende white inclusions. *Lunar Plan. Sci. Conf. XV*, 659-660.

Rambaldi, E.R., and J.T. Wasson 1981. Metal and associated phases in Bishunpur, a highly unequilibrated ordinary chondrite. *Geochim. Cosmochim. Acta* **45**, 1001-1015.

Rambaldi, E.R., and J.T. Wasson 1984. Metal and associated phases in Krymka and Chainpur: Nebular formation processes. *Geochim. Cosmochim. Acta* **48**, 1885-1897.

Ramdohr, P. 1963. The opaque minerals in stony meteorites. *Jour. Geophys. Res.* **68**, 2011-2036.

Ramdohr, P. 1972. The highly reflecting and opaque components in the mineral content of the Havero meteorite. *Meteoritics* **7**, 565-571.

Reed Jr., G.W. 1971. Chlorine. In *Handbook of Elemental Abundances in Meteorites* (B. Mason, Ed.), pp. 143-148. Gordon & Breach, New York.

Runk, R.B., and H.J. Kim 1970. The oxidation of iron-carbon alloys at low temperatures. *Oxid. Metals* **2**, 285-306.

Scott, E.R.D., and R.S. Rajan 1981. Metallic minerals, thermal histories and parent bodies of some xenolithic, ordinary chondrite meteorites. *Geochim. Cosmochim. Acta* **45**, 53-67.

Scott, E.R.D., A.E. Rubin, G.J. Taylor, and K. Keil 1981a. New kind of type 3 chondrite with a graphite-magnetite matrix. *Earth Plan. Sci. Lett.* **56**, 19-31.

Scott, E.R.D., G.J. Taylor, A.E. Rubin, A. Okada, and K. Keil 1981b. Graphite-magnetite aggregates in ordinary chondritic meteorites. *Nature* **291**, 544-546.

Sears, D.W., J.R. Ashworth, C.P. Broadbent, and A.W.R. Bevan 1984. Studies of an artificially shock-loaded H group chondrite. *Geochim. Cosmochim. Acta* **48**, 343-360.

Shindo, H., M. Miyamoto, J. Matsuda, and K. Ito 1985. Vapor deposition of diamond from methane-hydrogen mixture and its bearing on the origin of diamond in ureilite: A preliminary report. *Meteoritics* **20**, 754.

Singer, R.B. 1981. Near-infrared spectral reflectance of mineral mixtures: Systematic combinations of pyroxenes, olivine and iron oxides. *Jour. Geophys. Res.* **86**, 7967-7982.

Sipiera, P.P., J. Tartar, C.B. Moore, B.D. Dod, and R.A. Johnston 1980. Gomez, Terry

County, Texas: A new meteorite find. *Meteoritics* **15**, 201-210.

Smith, D.G.W. 1980. The mineral chemistry of the Innisfree meteorite. *Canadian Mineral.* **18**, 433-442.

Smith, P.P.K., and P.R. Buseck 1981. Carbon in the Allende meteorite: Evidence for poorly graphitized carbon rather than carbyne. *Proc. Lunar Plan. Sci. 12B*, 1167-1175.

Smith, P.J., O. Van der Biest, and J. Corish 1985. The initial stages of high-temperature corrosion of Fe-Cr-Ni and Cr-Ni alloys in a carburizing atmosphere of low oxygen partial pressure. *Oxid. Metals* **24**, 47-83.

Sztrokay, K.I., V. Tolnay, and M. Foldvari-Vogl 1962. Mineralogical and chemical properties of the carbonaceous meteorite from Kaba, Hungary. *Acta Geol. Hungar.* **T7**, 57-103.

Taft, E.A., and H.R. Philipp 1965. Optical properties of graphite. *Phys. Rev.* **138**, A197-A202.

Taylor, M.F. 1981. The application of thermodynamics to the oxidation behavior of mild steels in carbon dioxide-based atmospheres. *Oxid. Metals* **16**, 1331-46.

Tomlinson, W.J., and I.A. Menzies 1978. Oxidation of an Fe-19 wt. % Ni alloy in CO_2 at 700-1000°C. *Oxid. Metals* **12**, 215-225.

Van Der Stap, C.C.A.H., D. Heymann, R.D. Vis, and H. Verheul 1986. Mapping of carbon concentrations in Allende meteorite with the $^{12}C(d,p)^{13}C$ method. *Proc. Sixteenth Lunar Plan. Sci. Conf.*, D373-D377.

Vdovykin, G.P. 1970. Ureilites. *Space Sci. Rev.* **10**, 483-510.

Vdovykin, G.P. 1972. Forms of carbon in the New Havero ureilite of Finland. *Meteoritics* **7**, 547-552.

Veverka, J. 1973. Photopolarimetric observations of 9 Metis, 15 Eunomia, 89 Julia, and other asteroids. *Icarus* **19**, 114-117.

Vilas, F., and M.J. Gaffey 1989. Weak Fe^{2+}-Fe^{3+} charge transfer absorption features seen in CM2 carbonaceous chondrites and narrowband reflectance spectra of primitive asteroids. *Lunar Plan. Sci. Conf. XX*, 1156-1157.

Wacker, J.F. 1986. Noble gases in the diamond-free ureilite, ALHA 78019: The role of shock and nebular processes. *Geochim. Cosmochim. Acta* **50**, 633-642.

Wagner, J.K., B.W. Hapke, and E.N. Wells 1987. Atlas of reflectance spectra of terrestrial, lunar, and meteoritic powders and frosts from 92 to 1800 nm. *Icarus* **69**, 14-28.

Wdowiak, T., and D. Agresti 1984. Presence of a superparamagnetic component in the Orgueil meteorite. *Nature* **311**, 140-142.

Weidner, V.R., and J.J. Hsia 1981. Reflection properties of pressed polytetrafluoroethylene powder. *Jour. Opt. Soc. Amer.* **71**, 856-861.

Wilkening, L.L. 1983. What meteorites can tell us about regoliths. *Meteoritics* **18**, 421-422.

Williams, C.V., K. Keil, A.E. Rubin, and A. San Miguel 1984. Petrology of some ordinary chondrite regolith breccias: Implications for parent body history. *Meteoritics* **19**, 338.

Williams, C.V., E.R.D. Scott, G.J. Taylor, K. Keil, L. Schultz, and R. Wieler 1986. Histories of ordinary chondrite parent bodies: Clues from regolith breccias. *Meteoritics* **21**, 541.

Yabuki, H., and A. El Goresy 1986. Phosphate-bearing microspherules in chondrules of unequilibrated ordinary chondrites. *Nat. Inst. Polar Res. Spec. Iss. 41*, 235-242.

Zellner, B., M. Leake, T. Lebertre, M. Duseaux, and A. Dollfus 1977. The asteroid albedo scale. I. Laboratory polarimetry of meteorites. *Proc. Lunar Sci. Conf. 8th*, 1091-1110.

V. REFLECTANCE SPECTRA OF GLASS-BEARING MAFIC SILICATE MIXTURES AND SPECTRAL DECONVOLUTION PROCEDURES[1]

INTRODUCTION

Of all the bodies in the solar system, only the Earth, the Moon, and perhaps some asteroids, provide the opportunity to compare spectroscopic remote sensing data directly with actual geological samples. However, the samples available for the Moon encompass only a tiny fraction of the total surface. Remote sensing remains the best method for conducting large-scale lunar surface exploration. Most meteorites are believed to be derived from asteroids, and reflectance spectroscopy provides the best method for identifying possible parent bodies. It is imperative therefore, that the amount of geological information derivable from spectral studies be maximized.

All lines of evidence suggest that the lunar surface is largely composed of plagioclase, pyroxene, olivine, ilmenite and impact-derived glass (Smith, 1974; Smith & Steele, 1976; Taylor, 1982). Telescopic reflectance spectra of many areas on the Moon show absorption features attributable to these minerals (e.g. Bell & Hawke, 1984; Lucey *et al.*, 1986; Pieters, 1986). Invariably, the spectra are reddened (generally increasing reflectance towards longer wavelengths) relative to spectra from pristine minerals, and often show subdued mafic silicate absorption bands because of the presence of variable amounts of opaques, glasses and agglutinates. Some asteroids also show red-sloped reflectance spectra which may be attributable to the presence of significant amounts of glass and/or agglutinates (King *et al.*, 1983; McFadden, 1983a; 1983b; King *et al.*, 1984; Pieters, 1984). The subdued mafic silicate absorption bands can, potentially, be analyzed to provide information on the relative abundances and compositions of the mafic silicates. This requires an accurate knowledge of how the various opaque and amorphous components alter the mafic silicate reflectance spectra.

---

[1] A version of this chapter has been submitted for publication. Cloutis, E.A., Gaffey, M.J., Smith, D.G.W., and Lambert, R. St J. 1989. Icarus.

Spectral reflectance properties of the major lunar and meteoritic minerals have been studied extensively. The reflectance spectrum of olivine is dominated by an absorption band near 1μm (Band I) due to Fe^{2+} crystal field transitions, shows a weaker band of uncertain origin near 0.65μm, and exhibits a steep drop-off in reflectance at wavelengths shorter than ~0.5μm due to charge transfer absorptions. The wavelength position of Band I moves systematically towards longer wavelengths with increasing iron content (Burns, 1970a; Cloutis, 1985; King & Ridley, 1987). Low calcium pyroxene shows two absorption bands due to Fe^{2+} crystal field transitions near 1μm (Band I) and near 2μm (Band II). The wavelength positions of both Band I and Band II minima show systematic shifts in their positions as a function of iron content (Burns, 1970b; Adams & McCord, 1972; Adams, 1974; Cloutis, 1985; Cloutis *et al.*, 1986a; 1986b). High-calcium pyroxene spectra are subdivided into two types: those that show two absorption bands, akin to low calcium pyroxenes (Type A), and those that exhibit three or more shallow absorption bands (Type B- Adams, 1975; Cloutis, 1985). Plagioclase feldspar spectra have high overall reflectance, a weak Fe^{2+} absorption band near 1.25μm, and a charge transfer-related reflectance decrease towards the ultraviolet (Hunt & Salisbury, 1970; Adams & Goullaud, 1978). The major lunar opaque phase, ilmenite, has a reflectance spectrum exhibiting a broad iron-titanium charge transfer band near 0.5μm, and a broad Fe^{2+} absorption feature near 1.2μm (Hunt *et al.*, 1971; Adams, 1974; Nash & Conel, 1974; Adams, 1975; Pieters, 1983). Natural and artificial lunar glasses show nearly featureless red-sloped reflectance spectra (Conel & Nash, 1970; Adams & McCord, 1971; Nash & Conel, 1973; Adams *et al.*, 1974; Farr *et al.*, 1980).

Laboratory reflectance spectra of lunar regolith fines are usually very similar to the glass and agglutinate spectra rather than whole rock or fresh powder spectra (e.g. Adams & Charette, 1975). The products produced by evaporation and condensation of meteorites in a vacuum also show a strong red slope (King *et al.*, 1983). Reflectance spectra of a series of well-characterized glass-mineral mixtures were measured in the laboratory in order to provide information on the spectrum-altering properties of glass and ilmenite on mafic silicate reflectance spectra.

EXPERIMENTAL PROCEDURE

Terrestrial minerals were used in this study because of the large quantities of pure separates required for the various mixtures. They were selected on the basis of a number of criteria - the availability of chemical analyses, key elemental abundances comparable to lunar minerals, availability of sufficient quantities, and spectral similarities to lunar minerals. Unfortunately, no single mineral could meet all these requirements and consequently emphasis was placed on the need for spectral similarities between the laboratory and lunar samples. The minerals finally selected for use in this work were a high-iron orthopyroxene (PYX032) from Ekersund, Norway, a high-calcium plagioclase feldspar (PLG108 - bytownite) from the Stillwater Complex, Montana, and an ilmenite (ILM101) from Kragerøø, Telemark, Norway. The samples were analyzed at the University of Calgary SEMQ electron microprobe facility and the compositions given are an average of 4-8 point analyses. The data were reduced using Bence-Albee α and β correction factors. The ferrous iron contents were determined by wet chemical methods, and ferric iron as the difference between total and ferrous iron. Chemical analyses of the mineral samples are listed in Table V-1.

Powdered samples were obtained by crushing the minerals in an alumina mortar and pestle. Clean fractions were obtained by a combination of magnetic separation and hand picking. Well-constrained size ranges were acquired by repeated wet sieving with acetone. They were sieved into 0-45μm and 45-90μm size fractions. The glasses used in the various mineral mixtures were produced from the same mineral proportions as the mixtures into which they were incorporated. The 0-45μm sizes of the various minerals were used in making the glasses. These samples were placed in platinum crucibles and heated at 1000°C for 15-30 minutes to drive off any water. They were then transferred to a DELTECH DT-31-VT furnace and held at 1400°C for 15 minutes in a CO-CO_2 atmosphere at an oxygen fugacity of 10^{-9} atmospheres, except for glass sample L31 which was fused for 90 minutes. The samples were quenched by immersing the lower half of the crucible in a water bath. This prevented the water from coming in contact with the sample. The glass powders were prepared in the same way as the mineral powders, and were examined under a petrographic microscope for homogeneity. The chemical analyses of the glasses were obtained at the University of Alberta SEMQ microprobe facility and are an average of four area scans. The data were reduced using the Applied Research Laboratory version of the MAGIC IV program. Ferrous iron contents were determined in the same way as the minerals. The chemical analyses of the glasses are listed in Table V-1.

All samples were made on a weight percentage basis. For example, a mixture prepared with 40 wt. % pyroxene, 30 wt. % plagioclase, 5 wt. % ilmenite, and 25 wt. % glass would be expressed as 40/30/5/25 PYX/PLG/ILM/GLA. The various samples that were spectrally characterized are listed in Table V-2. The starting composition of the glass was the same as the glass-free equivalent sample it is paired with. The mineral abundances used in making glasses L2, L31, and L32, are the same as for samples L3, L3, and L28, respectively.

Reflectance spectra were acquired at the NASA RELAB spectrometer facility at Brown University and details of the instrument can be found in Pieters (1983). Bidirectional reflectance spectra of flat sample surfaces were measured at an incidence angle of 30° and an emission angle of 0°. Sample spectra were measured relative to halon, a near-perfect diffuse reflector in the 0.34μm to 2.7μm wavelength range (Weidner & Hsia, 1981). Spectra were corrected for dark current offsets, as well as for minor irregularities in the absolute reflectance of halon in the 2μm region. The spectra were processed using the Gaffey Spectrum Processing System, a PC-compatible version of SPECPR (Clark, 1980). Band minima and band center wavelength positions were determined by fitting a quadratic equation to ~10 data points on either side of a visually determined minimum or center. Band depths (D_b) were calculated using equation (32) in Clark & Roush (1984).

SAMPLE VARIATION EFFECTS ON SPECTRAL REFLECTANCE

A number of factors can affect the spectral reflectance properties of minerals and mineral mixtures (Adams & Filice, 1967). The major concern here is with the spectrum-altering effects of glass. Lunar telescopic spectra are almost invariably characterized by an increase in reflectance towards longer wavelengths (red slope) upon which are superimposed mineral absorption bands of variable intensities (e.g. McCord *et al.*, 1981; Lucey *et al.*, 1986; Pieters, 1986). This red slope is attributable to the presence of glasses and/or glass-bonded aggregates (agglutinates), present as either primary products or formed by micrometeoroid impacts (Delano, 1986; Hughes *et al.*, 1988). The impact-generated glass/agglutinate component is derived largely from fusion of the finest fraction of the lunar soil- the so-called F^3 model (Laul & Papike, 1980; Papike *et al.*, 1981; 1982; Laul *et al.*, 1987). In turn, the finest soil fraction tends to be enriched in plagioclase feldspar (Papike *et al.*, 1982) because it is more comminutable than the other major components in lunar crust (Hörz *et al.*, 1985; Simon *et al.*, 1986; See & Hörz, 1988). The formation and composition of possible agglutinates on asteroidal surfaces is less well understood (Housen & Wilkening, 1979; Housen *et al.*, 1979a, 1979b; King *et al.*, 1983; 1984; Pieters, 1984).

The primary goal of lunar remote sensing is to determine surface mineralogies. This task is complicated by the red slope often present in the telescopic data. Mineral absorption bands are frequently extremely subdued, and spectral deconvolution techniques designed for determining mineral compositions and abundances which rely on spectral parameters such as band centers and band areas cannot be applied to uncorrected data. The agglutinate component is probably the cause of the red slope and it is commonly removed by dividing the reflectance spectrum by a straight line continuum tangent to the spectrum. Usually, one line segment, tangent to two points on the reflectance spectrum, is used (Farr et al., 1980; McCord *et al.*, 1981), although two line segments tangent at three or four points are also applied (Pieters, 1982).

In order to investigate the spectrum altering effects of various parameters, a "standard sample" was created, along with a glass made from this material, and a glass-bearing version of the "standard sample" ("standard mix"). These samples are labeled as L3, L2, and L1, respectively (Table V-2), and are used to investigate the spectrum-altering effects of glass. Secondary considerations include the effects of plagioclase grain size and ilmenite abundance. Reflectance spectra of the constituent phases (plagioclase, pyroxene and ilmenite) are shown in Figures V-1 and V-2.

Addition of Glass. Reflectance spectra of samples L1, L2, and L3 are shown in Figure V-3. The major difference between sample L1 and L3 is the presence of 25 wt. % glass in the former. The glass itself has no well-defined absorption bands but shows weak inflections near 0.9μm and 1.8μm likely attributable to Fe^{2+} crystal field transitions. These features, the absolute reflectance, and the overall red slope of the glass, are also seen in natural lunar glasses, agglutinates, and laboratory produced glasses (Adams & McCord, 1971b; 1973; Nash & Conel, 1973; Adams *et al.*, 1974).

Addition of glass to the mineral mixtures causes a reduction in the overall reflectance of sample L1 relative to sample L3 and a decrease in band depths (Figure V-3). A straight line continuum was divided out from the reflectance spectra in an attempt to overcome the spectrum-altering effects of the glass. The continuum-removed L1 and L3 spectra are shown in Figure V-4. The reduction of band depths due to the glass can clearly be seen in the L1 spectrum. The spectral deconvolution techniques designed for mafic silicates are useful for assessing the validity of the straight line continuum removal.

Band centers are useful indicators of mafic silicate ferrous iron content. The continuum-removed wavelength positions of the Band I and Band II centers are given in Table V-3. It can be seen that the Band I position varies by only 1 nm while the Band II variation is 16 nm. It appears that a straight line continuum is a reasonable approximation to the actual glass continuum at shorter wavelengths.

An alternative to the straight line continuum was also examined. The glass spectrum (L2) was multiplied by a factor sufficient to increase its reflectance to the same value as that of the samples L1 and L3 at their interband peaks near 1.4μm. The L3 and L1 spectra were then divided by the scaled L2 spectra (Figure V-5). The band centers obtained in this way show a much smaller deviation- 0 nm for Band I and 6 nm for Band II (Table V-3). The advantage of the straight line continuum, however, is that no prior knowledge of the spectral properties of the glass phase is required.

Band area ratios are useful indicators of mafic silicate abundances (Cloutis *et al.*, 1986b). The two continuum removal procedures (straight line division versus glass spectrum division) can be compared by how well each reproduces band area ratios. The band area ratio II*/I* (Cloutis *et al.*, 1986b) for the L3 and L1 spectra are listed in Table V-3. The straight line continuum method shows the lesser amount of variation between the band area ratios of samples L1 and L3. While the straight line method is better at reproducing band areas, the glass continuum method is more effective at providing consistent band center wavelength positions.

Plagioclase Grain Size Variations. The effect of plagioclase grain size on spectral reflectance was examined by comparing the L1 spectrum to an equivalent assemblage containing 0-45μm-sized plagioclase (L8), and their glass-free equivalents (L3 and L9, respectively). The plagioclase used in the mixtures shows a prominent absorption band near 1.25μm (Figure V-2) due to Fe^{2+} crystal field transitions, and is spectrally similar to lunar plagioclases (Adams & McCord, 1971b; Adams & Goullaud, 1978; Pieters & Mustard, 1988). The overall composition of the plagioclase is also comparable to plagioclase from lunar mare basalts (Smith, 1974). The 1.25μm region is obviously the best region to search for evidence of plagioclase, by its effect on the wavelength position of the pyroxene interband peak near 1.4μm (Nash & Conel, 1974; McFadden & Gaffey, 1978; Crown & Pieters, 1987).

The smaller-sized plagioclase causes an increase in overall reflectance in both the glass-bearing (Figure V-6) and glass-free samples (Figure V-7). The wavelength position of the interband peak near 1.4μm is similar in the glass-bearing and glass-free groups, suggesting that the glass can effectively overide any variations in peak position due to plagioclase grain size variations. As expected, the band centers wavelength positions of the mafic silicates are unaffected by changes in plagioclase grain size.

These results suggest that it will be difficult to develop spectral deconvolution procedures for determining plagioclase abundances at the few tens of percent level for anything but the most simple systems. While plagioclase causes a shoulder to appear on the long wavelength side of Band I, there does not seem to be any other systematic spectral variation which can be uniquely attributed to plagioclase (Nash & Conel, 1974; Crown & Pieters, 1987). In any case, spectral calibration procedures developed for plagioclase determinations will represent an optimum scenario because impact-shocked feldspars are even more weakly featured than unshocked samples (Adams *et al.*, 1979; Bruckenthal & Pieters, 1984).

Glass Abundance Variations. Measurable spectral differences are found between mature and immature lunar soils which are related to the agglutinate content of the samples (Adams & McCord, 1973; Charette *et al.*, 1974). Reflectance spectra from a series of samples of increasing glass content were measured to determine whether these effects could be reproduced in the laboratory. Five standard sample+glass mixtures were created with 0 wt. % glass (L3), 25 wt. % glass (L1), 50 wt. % glass (L26), 75 wt. % glass (L27) and 100 wt. % glass (L2). The most noticeable effects of increasing glass content are the decrease in overall reflectance and subduction of absorption bands (Figure V-8), and a generally increasingly red slope (Figure V-9).

Charette *et al.* (1974) found that the 0.402μm to 0.565μm slope can serve as a measure of soil maturity. They found a consistent trend for soils containing 60-70 wt. % glass+agglutinates (Figure V-10). Immature soils fall to the right of the trend. Data for the laboratory spectra define a trend which actually moves away from the mature soil field with increasing glass content. This behavior must be due to either a structural or chemical difference between the laboratory and lunar samples. While the laboratory glass L2 reproduces the steep red overall slope of lunar samples, it tends to flatten significantly at shorter wavelengths.

Reflectance spectra of lunar-like glasses usually show weak absorption bands near 1μm and 2μm which are at least an order of magnitude less absorbing than similar pyroxene absorption bands. Straight line continuum removal seems to be adequate for neutralizing the effects of the glass and reconstructing mineral absorption band positions to within a few nm (Conel & Nash, 1970; Adams & McCord, 1971b; Nash & Conel, 1973; Farr *et al.*, 1980). The expected absorption band positions of the glass-free sample can serve as a standard for assessing continuum removal accuracies. The key spectral parameters used for determining mafic silicate abundances and chemistries are band area ratios, and band minimum/center wavelength positions (Cloutis *et al.*, 1986a; 1986b). Single straight line continua tangent to the spectra on either side of the absorption feature near 1μm were divided out of the curves in Figure V-8 (Figure V-11). Both Band I minima and Band I centers show small variations from the values of sample L3. The Band II minima and centers show larger variations because straight line continua do not reproduce the increasing red slope of the glass (Table V-3). The band minima show much larger variations than the band centers.

The "normalized" glass spectrum was also divided out from the L3-L1-L26-L27 sequence, as previously described (Figure V-12). The band centers determined for these spectra show less variation than the straight line continuum-removed spectra (Table V-3). For this sequence of samples, the range of variation in band position corresponds to differences in pyroxene molar iron content of 13% (Band I) and 37% (Band II) for the uncorrected spectra, 13% (Band I) and 17% (Band II) for the straight line continuum-removed spectra, and 3% (Bands I and II) for the glass spectrum divided curves (Adams, 1974; Cloutis, 1985; Aoyama *et al.*, 1987).

Band area ratio variations show opposite trends depending on the type of continuum removal procedure. While the values are not directly comparable to those derived for pure mafic silicate assemblages (Cloutis *et al.*, 1986b), the amount of variation is least for the glass spectrum divided curves. The eventual development of band area ratio calibrations for lunar data will be most effective if glass-like continua can be divided out.

Glass Grain Size Variations. Glasses produced in the laboratory often have higher reflectances than lunar agglutinates (Conel & Nash, 1970; Adams & McCord, 1971b). In order to investigate this difference, the spectrum of the standard mix (L1) is compared to that of an equivalent sample made with 0-45μm sized glass (L29). Spectrum L29 is more red-sloped than spectrum L1, has more subdued absorption bands, and lower visible reflectance (8.5% versus 10.6% at 0.56μm). All these characteristics are indicative of a higher apparent glass content (Figure V-13).

The band I centers determined after straight line continuum division, occur at 0.954μm (L29), and 0.938μm (L1- Table V-3). The raw spectra were divided by the glass spectrum L2, again multiplied by a factor to increase its reflectance to that of the interband peak of L1 and L29. Both band centers determined for L29 are substantially different from the values for L1. It appears that simple division of a glass spectrum does not always provide a reasonable correction. The spectrum of the 0-45μm sized glass was not measured but may provide a better correction to the L29 spectrum. These results suggest that the reflectance spectrum of the continuum must be known if band positions are to be accurately reconstructed. If such data are not available, a straight line continuum may serve as a reasonable approximation.

Ilmenite Content Variations. The spectral properties of a glass will clearly depend on its chemical composition. For impact-produced glasses, the minerals from which it forms are of primary importance. Ilmenite is the most common opaque phase in lunar mare basalts and its inclusion in the vitrification process causes a reduction in the overall reflectance of the glass (Adams & McCord, 1971a; 1971b). The reflectance spectra of the standard sample glass made with 6.7 wt. % ilmenite (L2) and an ilmenite-free glass (L32) show this effect (Figure V-14). The lower overall reflectance of L2 must be due to the inclusion of the ilmenite in the vitrification process, as all other mineral proportions are equal.

The correlation between the 0.402μm-0.565μm slope and TiO_2 content in mature soils (Charette *et al.*, 1974) fails to effectively delineate the two glasses. Their 0.400:0.565μm ratios fall well inside the field defining immature, glass-poor soils (Figure V-10). This discrepancy is probably related to the high degree of dependence between the oxidation state of the transition series elements (i.e. Ti) and the spectral properties of the glass (Bell *et al.*, 1976).

However the chemistry of the glass seems to have little effect on the spectrum of the mixtures into which it is incorporated. The sample mixtures made with glasses L2 and L32 (L1 and L28 respectively) show little variation in overall reflectance (Figure V-15). The straight line continuum removed band centers are nearly identical (Table V-3). As was the case with increasing glass content, the TiO_2 content of samples L1, L2, L28, and L32 do not show the same trends as lunar soils (Figure V-10). This reflects the chemical or structural differences between laboratory and lunar samples, and invalidates the use of the former as lunar analogues based on the 0.40-0.565μm reflectance ratio.

Glass Fusion Time Variations. The spectral properties of a glass are not only a function of the precursor materials, but also of the formation conditions (Nash & Conel, 1973). Progressively darker glasses can be made if the heating time is increased, probably due to an increase in the concentration of refractory elements or a change in the oxidation states of the transition series metals. This effect was investigated by preparing two glasses of identical starting composition melted for 15 minutes (L2) and 90 minutes (L31). The chemical analyses of the glasses show that a longer heating time had little effect on overall composition (Table V-1), except for a slight increase in Ti and Fe contents. The L31 glass shows a few regions of minute ($<2\mu$m) exsolved material. Because of the small size of the particles, a chemical analysis of the pure material could not be obtained. However, two point analyses centered on these grains show that these points are enriched in Ti and Fe relative to the bulk sample. If the slightly lower reflectance of L31 relative to L2 at longer wavelengths (Figure V-16) is a function of the higher Ti and Fe contents of the former, then glass composition may be a function of both starting materials and exposure time, perhaps leading to a postulated refractory-rich "ultimate glass" (Nash & Conel, 1973).

DISCUSSION

Simulations of lunar sample spectra in the laboratory are difficult to accomplish for a number of reasons. Terrestrial silicates with spectral properties comparable to lunar minerals are available, and were used in this study. Preparation of agglutinates is much more difficult because it is difficult to control compositions and abundances of glass welded aggregates. As a reasonable approximation, glasses were prepared, powdered, and mixed with the minerals. The structural differences between powdered glass-bearing mixtures and agglutinate-bearing mixtures are such that the albedos of the former are usually higher than the latter (Conel & Nash, 1970; Adams & McCord, 1971b). Mature soils and agglutinate-rich samples commonly show a four- to fivefold increase in reflectance over the 0.5 to 2.5μm wavelength range, and a reflectance of between 3 and 16% at 0.5μm (Adams & Jones, 1970; Conel & Nash, 1970; Adams & McCord, 1971b; 1973; Nash & Conel, 1973; Adams *et al.*, 1974; Adams & Charette, 1975). The various glasses produced here (L2, L31, L32) all show a reflectance at 0.5μm of <3% and a four- to fivefold increase in reflectance from 0.5 to 2.5μm. It is felt that they are reasonable analogues to lunar materials in gross spectral properties. The 0.402-0.564μm reflectance ratio found by Charette *et al.* (1974) to be a useful parameter for separating mature from immature lunar soils, and for determining TiO_2 contents, cannot be applied to these laboratory spectra (Figure V-10). The absolute reflectances at 0.400 and 0.565μm decrease with increasing glass content in both the laboratory and lunar samples. However, the relative decrease in 0.565μm reflectance is greater than at 0.400μm in the laboratory samples and the ratio increases with increasing glass content, opposite to the trend for lunar samples.

The ultraviolet and shorter wavelength visible spectral regions are strongly affected by crystal field transitions (Abu-Eid, 1976). The differences in oxidation states of the most common transition series elements in lunar materials (Fe and Ti) may account for the spectral differences in this wavelength region (Burns *et al.*, 1972; Bell & Mao, 1974; Mao *et al.*, 1974; Bell *et al.*, 1976; 1978). Straight line continua, tangent to lunar telescopic reflectance spectra on either side of the absorption feature near 1μm, are commonly divided out in an effort to isolate and enhance mafic silicate absorption bands (e.g. Farr *et al.*, 1980; McCord *et al.*, 1981). The laboratory glass spectra, being broadly similar to lunar agglutinates/glasses are useful for evaluating different continuum removal procedures. Sample L3 was used as a baseline because it is glass-free. On the basis of no continuum removal, increasing glass content shifts both Band I and Band II minima towards shorter wavelengths. The shift is accelerated if the glass is fine-grained.

A single straight line continuum, divided out of the sample spectra, accurately reproduces the L3 Band I wavelength position for <75 wt. % 45-90μm sized glass, while the Band II position is shifted towards progressively shorter wavelengths with increasing glass content. The band centers determined in this way for the sample containing 0-45μm-sized glass (L29) are at higher than anticipated wavelengths (Table V-3). Overall, the sample spectra divided by the glass spectrum which has been scaled to tangency at the peak in the sample spectra near 1.4μm produce the most consistent band positions irrespective of glass abundance. The band position of the mafic silicates in the L29 spectrum cannot be reproduced. This suggests that the shape of the glass reflectance spectrum is sensitive to the particle size of the glass and continuum removal using glass spectra must be undertaken with an accurate knowledge of the glass spectrum.

Pyroxene is the most common lunar mafic silicate (Smith, 1974). The wavelength position of its absorption band centers are sensitive to iron and calcium content (Adams & McCord, 1972; Adams, 1974). In many lunar telescopic spectra, mafic silicate absorption bands do not show a reflectance minimum, instead appearing as inflections on an overall red slope. It is necessary to determine the absorption band centers in order to determine the mafic silicate compositions and abundances. A straight line continuum seems to work reasonably well because it is easily constructed and provides good estimates of Band I positions over a wide range of glass contents. A more complex continuum, based on glass spectra, is potentially more useful, but at this stage, not enough is known about the spectral properties of lunar glasses to permit its widespread application. Spectral deconvolution procedures based on absorption band areas cannot be applied at present to lunar remote sensing data because the variations seen in the laboratory spectra have not yet been correlated with the mafic silicates. All the samples measured are olivine-free and should have nearly identical II*/I* area ratios (Cloutis *et al.*, 1986b). The variability shows that further work is required to develop viable band area spectral calibrations.

If lunar agglutinates do not show spectral variability, except perhaps in overall reflectance, as a function of exposure time and chemistry, continuum removal procedures based on a common glass spectrum would be possible. The silicate absorption band centers could be reconstructed to within a few nanometers of the agglutinate- or glass-free samples, and from this, the abundances and ferrous iron contents of the mafic silicates could be determined (Adams & McCord, 1972; Adams, 1974; Cloutis, 1985; King & Ridley, 1987).

The available reflectance spectra of evaporated and recondensed meteorites show generally featureless red-sloped reflectance spectra with no evidence for crystal field absorption bands (King *et al.*, 1983). The spectra show a five-fold increase in reflectance from 0.5 to 2.5μm- similar to the laboratory glasses presented here. The flattening out of the laboratory glasses at shorter wavelengths is not seen in the meteoritic condensates which more closely resemble lunar glasses. The evidence for widespread agglutinates on asteroid surfaces is ambiguous (Cloutis *et al.*, 1989). If significant amounts of agglutinates are present, then the asteroidal spectra may be amenable to analysis using the techniques developed for lunar samples.

Table V-1. Chemical analyses of the pyroxene (PYX032), plagioclase (PLG108), ilmenite (ILM101), and glasses L2, L31, and L32 used in this study.

Wt. %	PYX032	PLG108	ILM101	L2	L31	L32
SiO_2	50.21	46.55	0.20	45.67	46.09	48.30
Al_2O_3	1.24	32.70	0.11	11.22	11.12	12.71
FeO	23.65	N.D.	45.20[2]	20.40[2]	20.53[2]	18.75[2]
Fe_2O_3	5.11	0.64[1]	----	----	----	---
MgO	17.57	0.04	0.02	11.14	11.02	11.33
CaO	1.59	17.28	0.11	6.44	6.39	7.11
Na_2O	0.00	1.71	0.08	0.71	0.55	0.71
TiO_2	0.19	0.05	51.49	3.59	3.66	0.57
Cr_2O_3	0.04	0.03	0.01	N.D.	N.D.	N.D.
V_2O_5	<0.01	0.01	N.D.	N.D.	N.D.	N.D.
CoO	0.06	0.03	0.02	N.D.	N.D.	N.D.
NiO	0.01	0.09	0.00	N.D.	N.D.	N.D.
MnO	0.53	0.01	0.01	0.28	0.26	0.31
K_2O	N.D.	0.02	0.00	N.D.	N.D.	N.D.
TOTAL	100.20	99.16	97.25	99.45	99.62	99.79
Number of Ions[3]						
Si	1.920	8.655				
Al	0.056	7.158				
V	<0.001	0.001				
Ti	0.005	0.007				
Cr	0.001	0.004				
Fe^{3+}	0.147	0.089				
Fe^{2+}	0.756	--				
Mg	1.002	0.011				
Ca	0.065	3.439				
Co	0.002	0.006				
Ni	tr.	0.013				
Mn	0.017	0.001				
Sr	--	0.003				
Ba	--	0.002				
Zn	--	0.002				
Na	--	0.616				
K	--	0.004				
Total	3.972	20.014				

N.D. = Not determined.

[1] - All Fe reported as Fe_2O_3

[2] - All Fe reported as FeO

[3] - Calculated on the basis of 6 oxygen for pyroxene, 32 oxygen for plagioclase. Structural formula not provided for ilmenite because of lack of Fe_2O_3 data.

Table V-2. Mineral and glass weight percentages in the various spectrally characterized samples. PYX= pyroxene, PLG= plagioclase, ILM= ilmenite, GLA= glass. For particular sample descriptions see the text.

Sample #	PYX	PLG	ILM	GLA
L1	50.0	20.0	5.0	25.0
L2	0.0	0.0	0.0	100.0
L3	66.7	26.7	6.7	0.0
L8	50.0	20.0	5.0	25.0
L9	66.7	26.7	6.7	0.0
L26	33.3	13.3	3.3	50.0
L27	16.7	6.7	1.7	75.0
L28	52.6	21.1	0.0	26.3
L29	33.3	13.3	3.3	50.0
L30	33.3	13.3	3.3	50.0
L31	0.0	0.0	0.0	100.0
L32	0.0	0.0	0.0	100.0

Table V-3. Spectral properties of selected samples. Columns 2 & 3 - Band I and Band II minima of uncorrected spectra; columns 4 & 5 - Band I and Band II centers after division by a straight line continuum; columns 6 & 7 - Band I and Band II centers after division by a scaled L2 glass spectrum; columns 8 - Band II*/Band I* area ratio (Cloutis *et al.*, 1986b) for straight line continuum removed spectra; and column 9 - same as column 8 for glass continuum removed spectra. All band positions are in microns.

Sample	Band Minima		Band Centers		Band Centers		Area	Area
	I	II	I	II	I	II	Ratio	Ratio
L3	0.925	1.946	0.937	1.991	0.925	2.037	2.02	2.73
L1	0.926	1.927	0.938	1.975	0.925	2.043	1.69	3.51
L26	0.919	1.907	0.938	1.952	0.926	2.046	1.20	3.97
L27	0.918	1.821	0.944	1.940	0.924	2.053	0.41	4.05
L29	0.902	1.844	0.954	2.003	0.904	2.235	--	--
L28	0.922	1.933	0.936	1.979	--	--	--	--

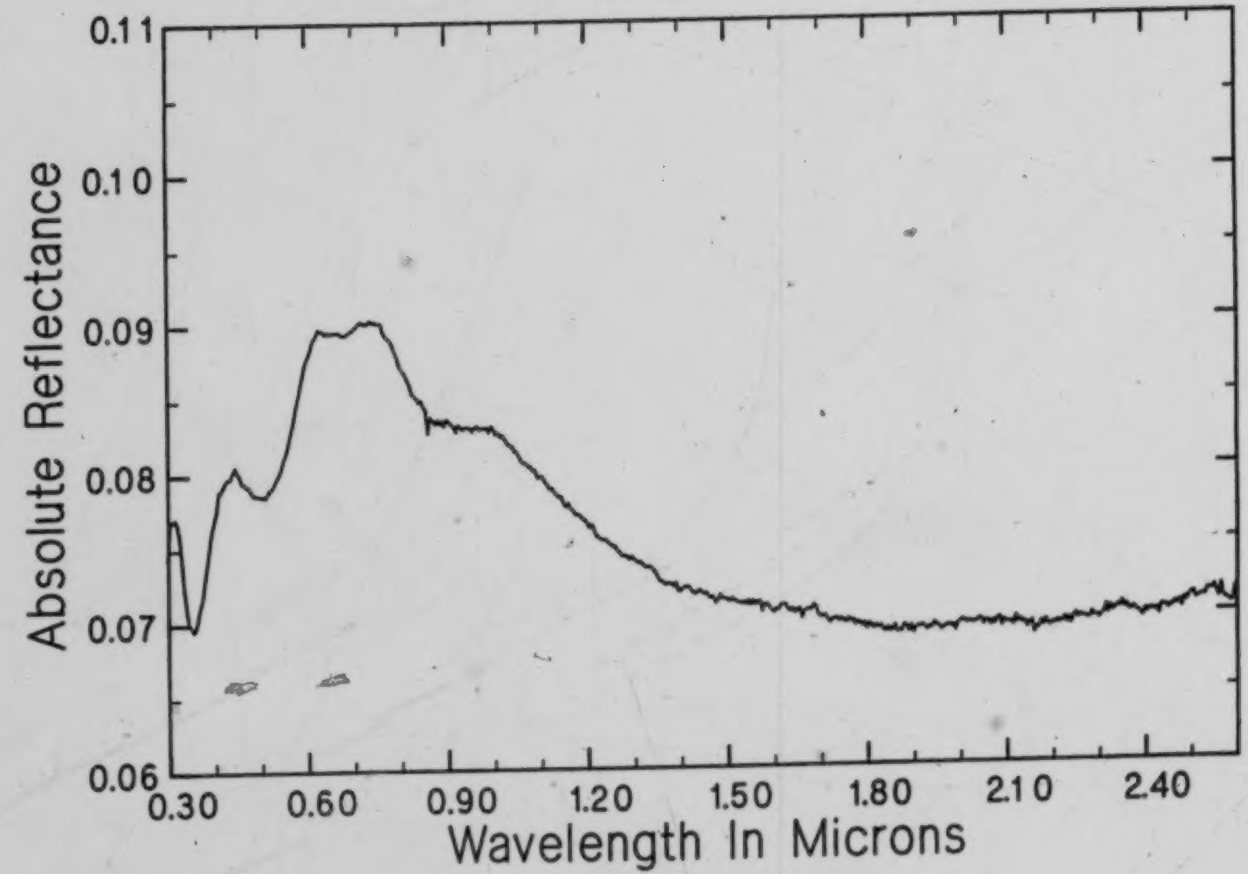

Figure V-1. Absolute reflectance spectrum of the 45-90μm-sized fraction of the ilmenite (ILM101) used in the mixtures.

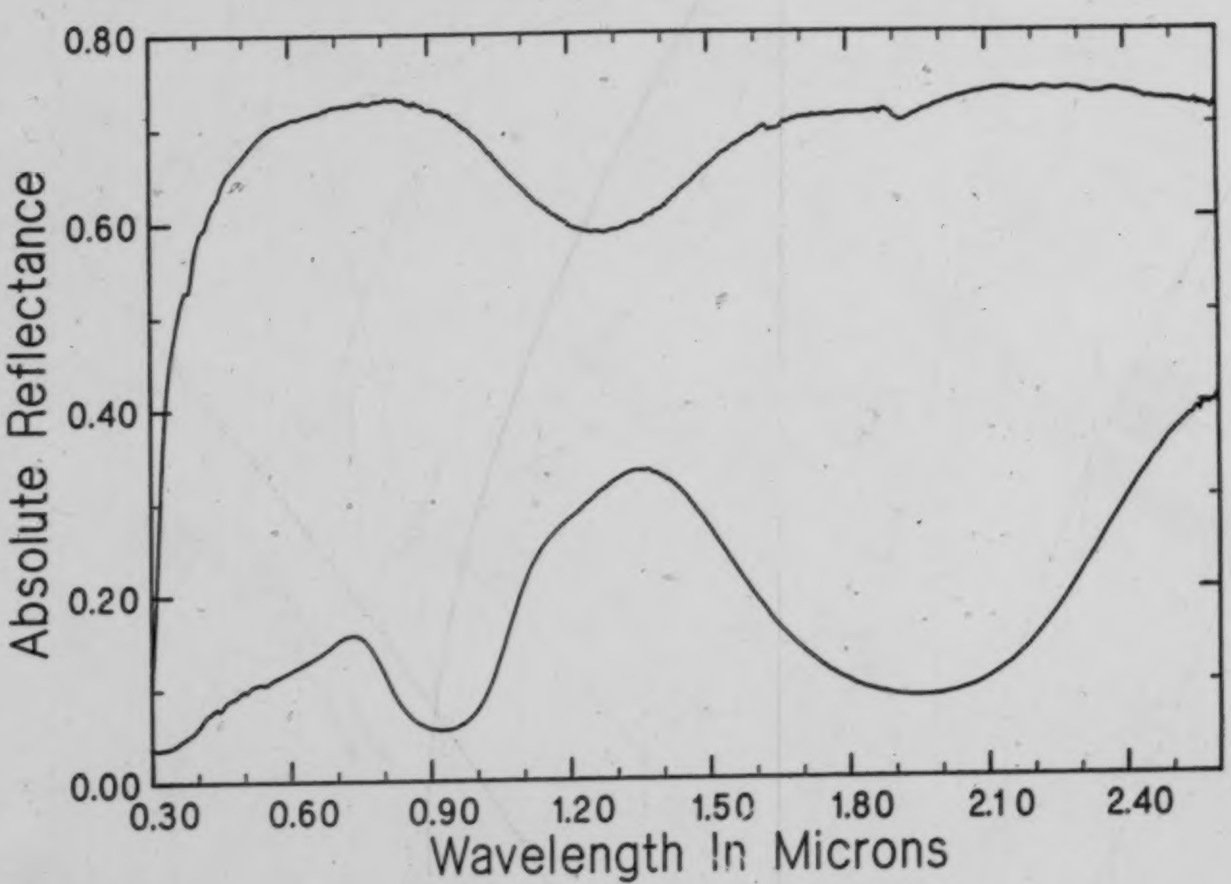

Figure V-2. Absolute reflectance spectra of the 45-90μm-sized fractions of the pyroxene (PYX032, lower curve) and plagioclase (PLG108, upper curve) used in the mixtures.

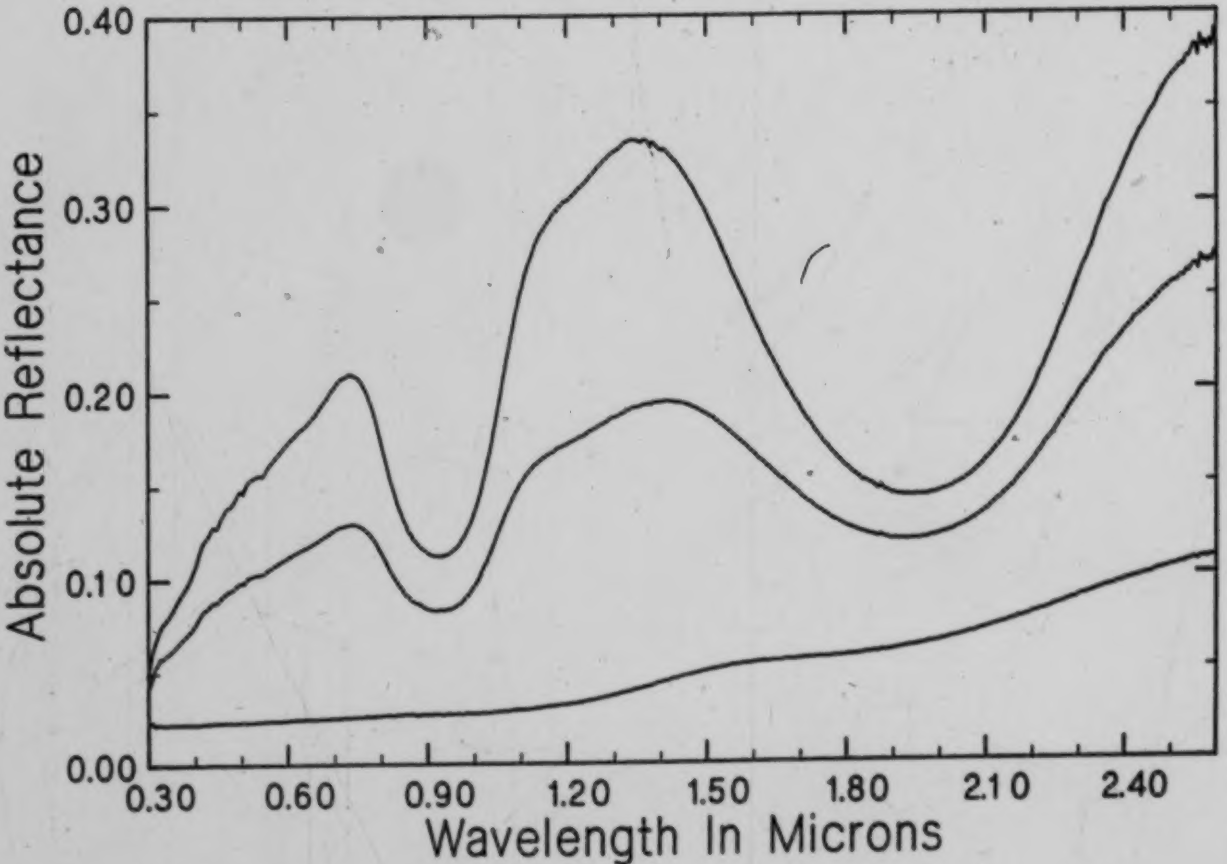

Figure V-3. Absolute reflectance spectra of the 45-90μm-sized samples L3 (upper), L1 (middle), and L2 (lower).

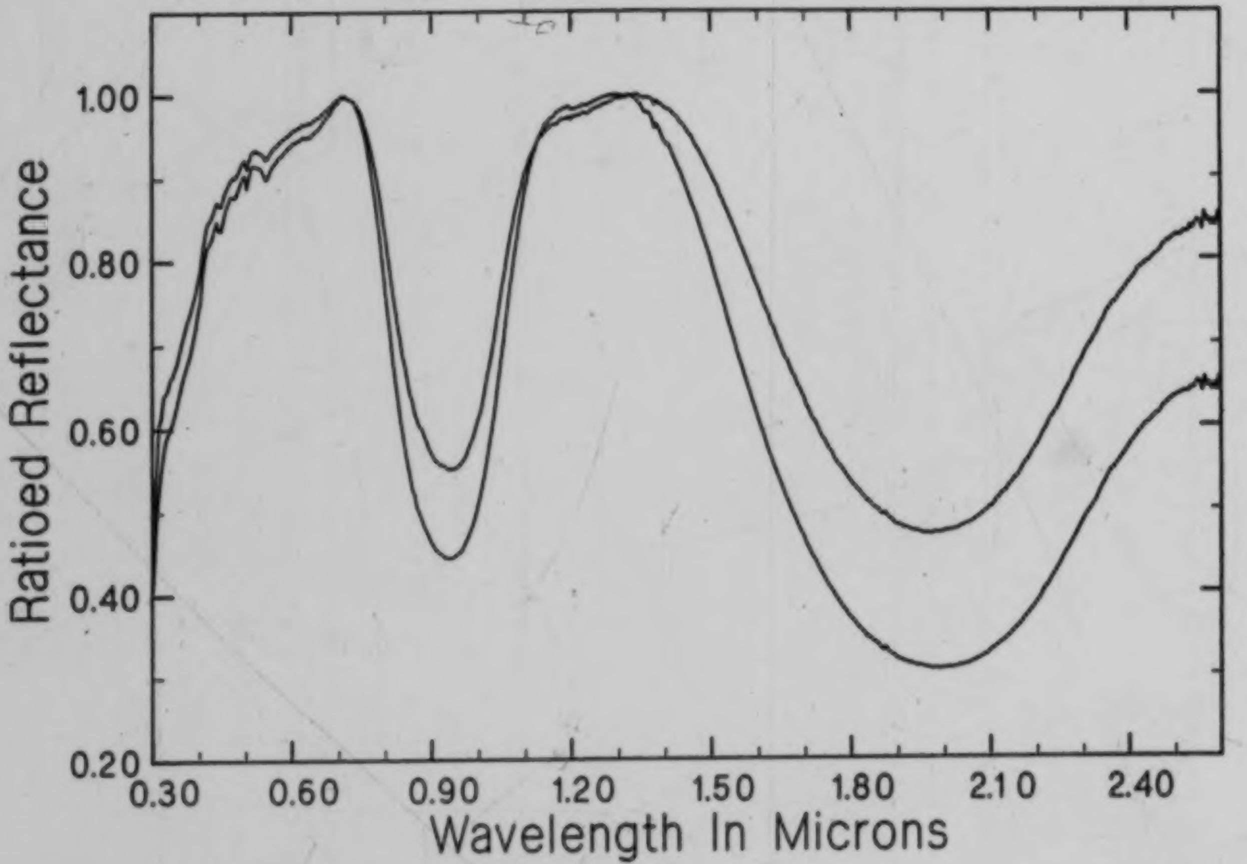

Figure V-4. Reflectance spectra of samples L1 (upper) and L3 (lower) after division by straight line continua.

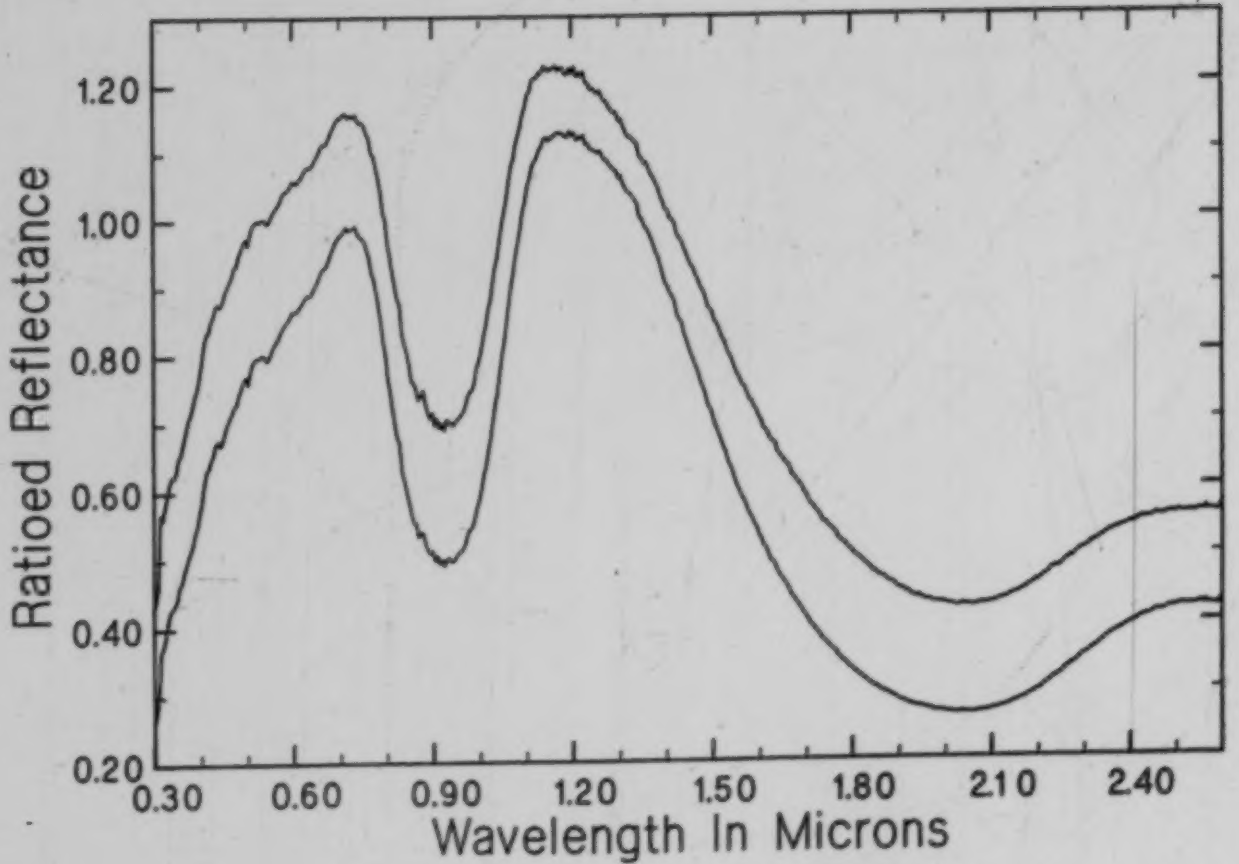

Figure V-5. Reflectance spectra of samples L1 (upper) and L3 (lower) after division by the scaled L2 spectrum (see text for details).

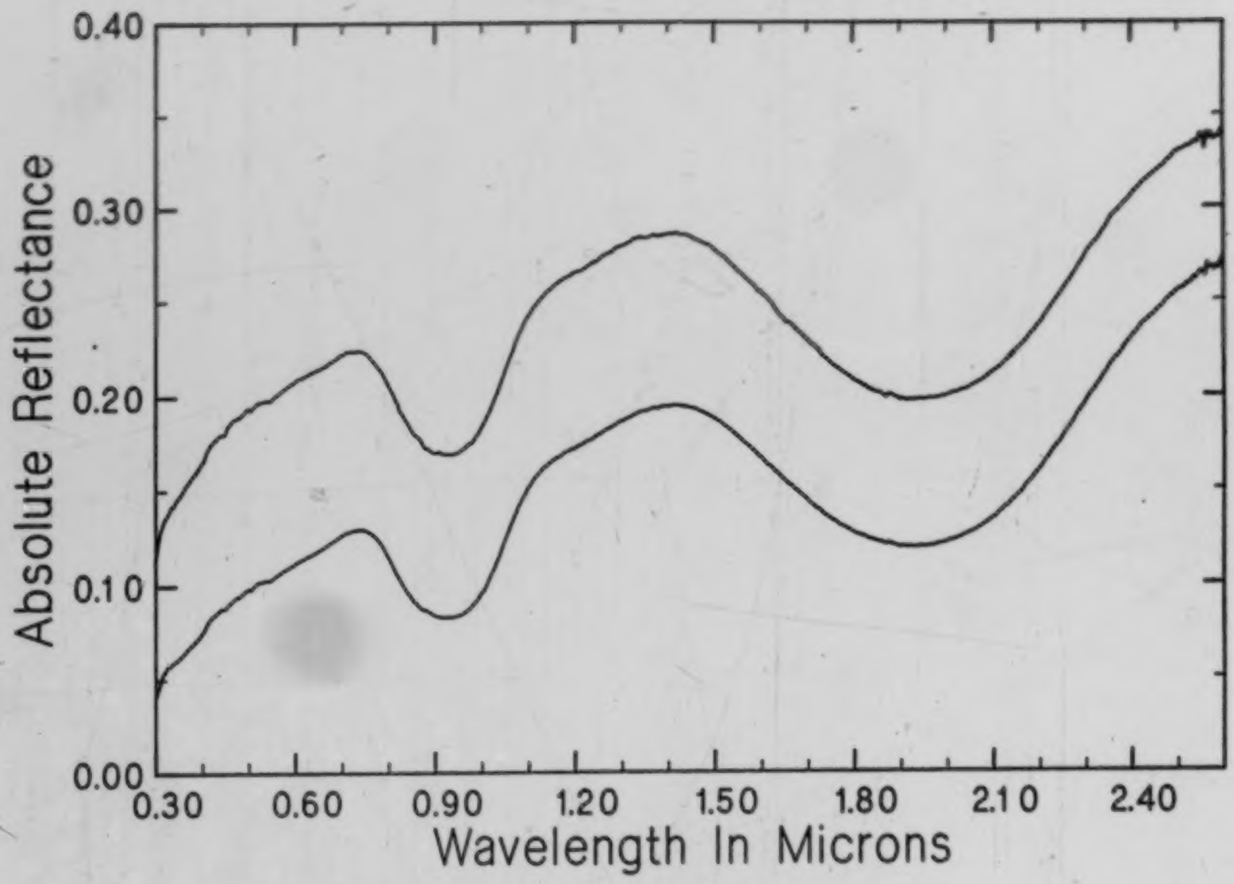

Figure V-6. Absolute reflectance spectra of samples L8 (upper) and L1 (lower).

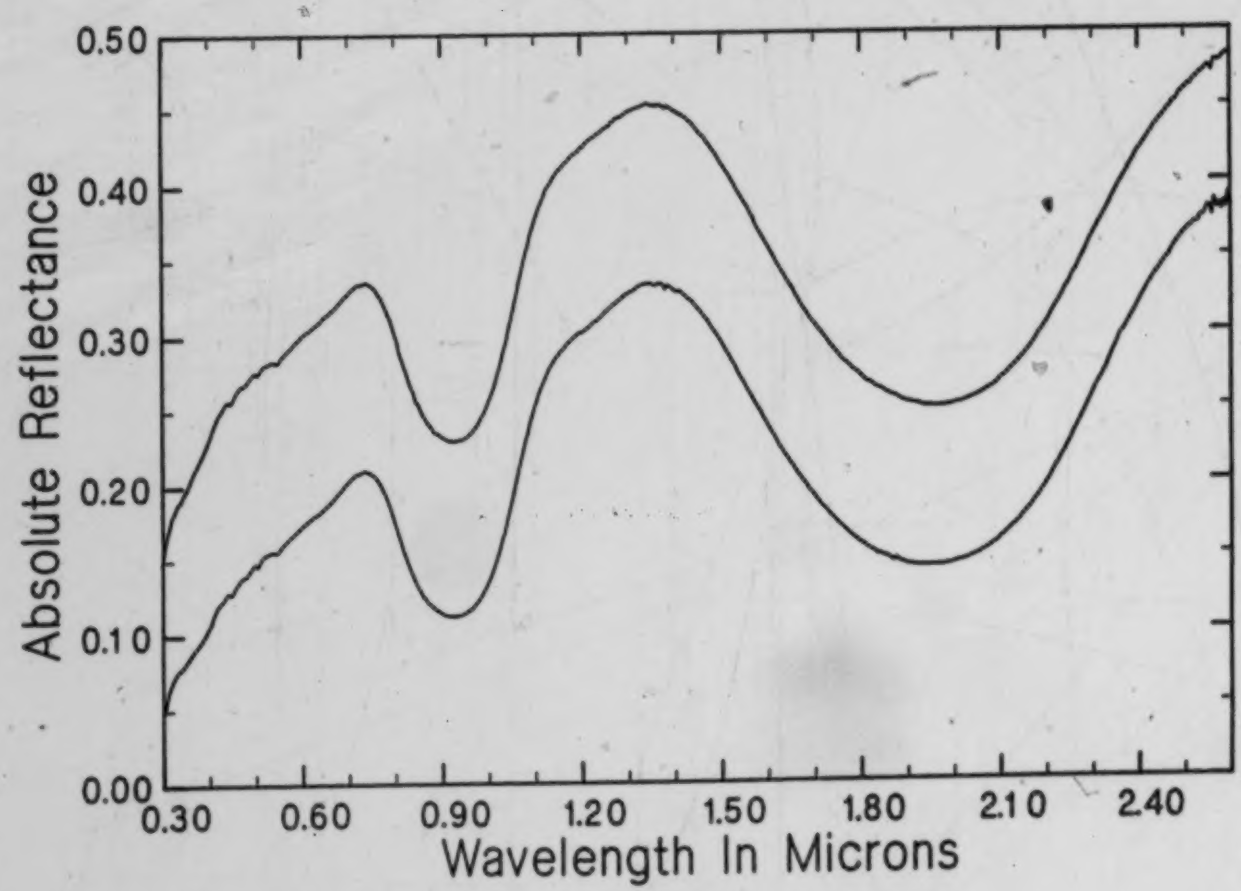

Figure V-7. Absolute reflectance spectra of glass-free samples L9 (upper) and L3 (lower).

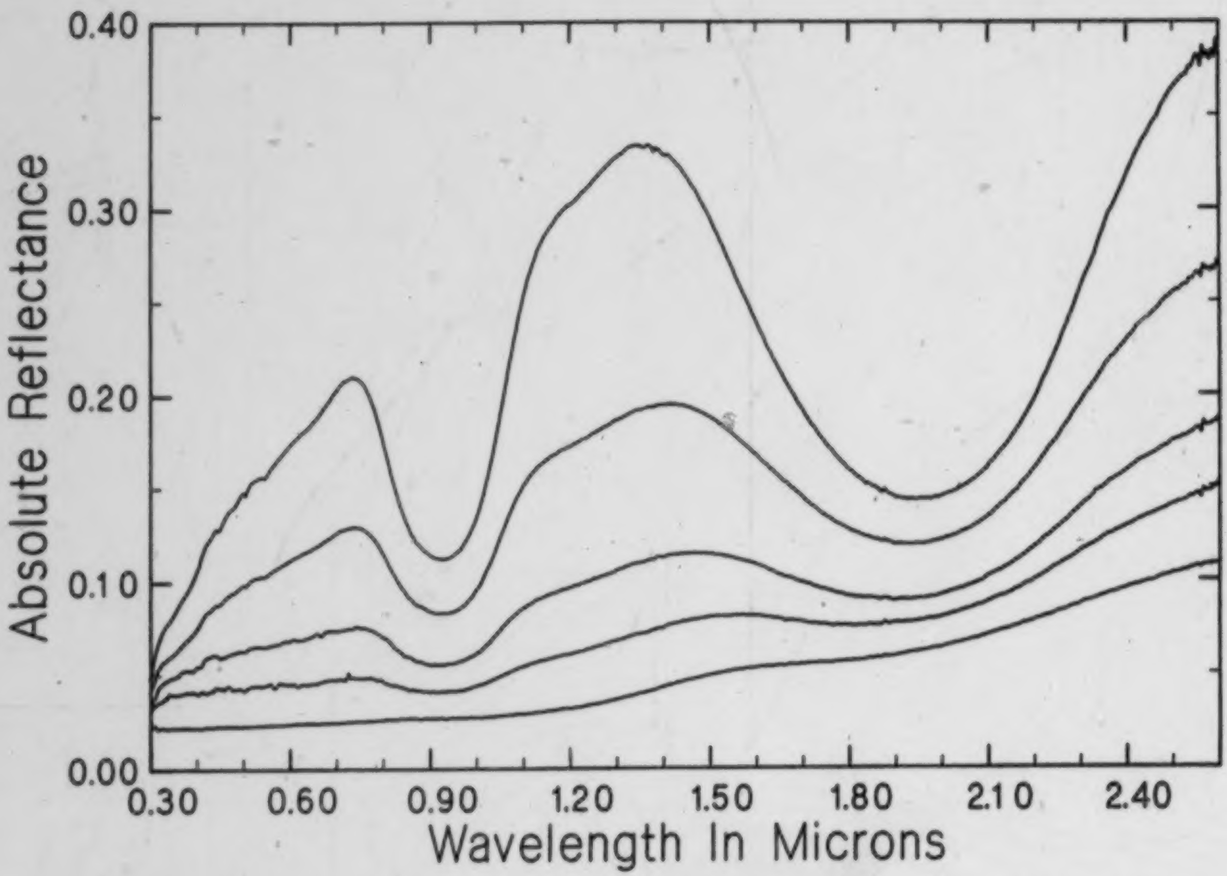

Figure V-8. Absolute reflectance spectra of samples with increasing glass content. Overall reflectance decreases in the sequence: L3 (0 wt. % glass)- L1 (25 wt. % glass)- L26 (50 wt. % glass)- L27 (75 wt. % glass)- L2 (100 wt. % glass).

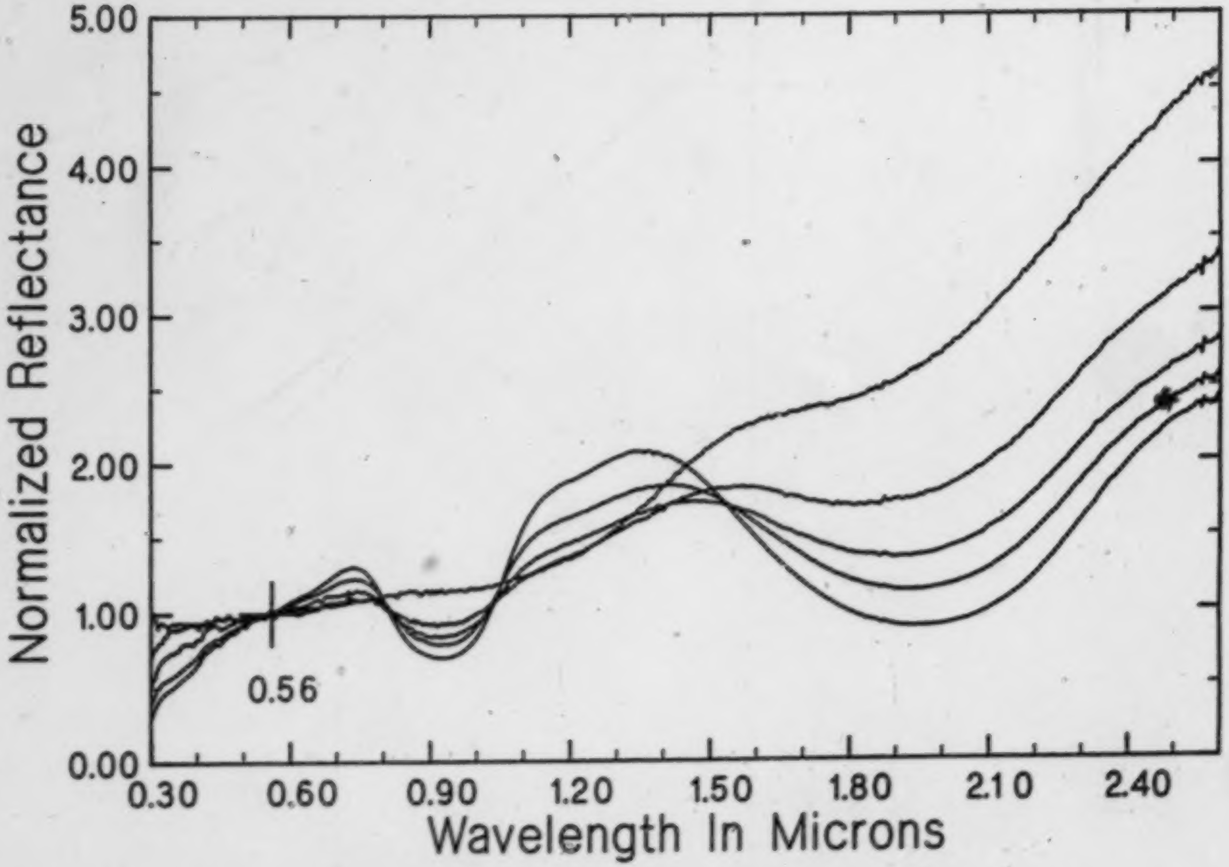

Figure V-9. Normalized reflectance spectra of samples L3, L1, L26, L27, and L2. The reflectance at the Band I and Band II minima decrease in the sequence L2-L27-L26-L1-L3.

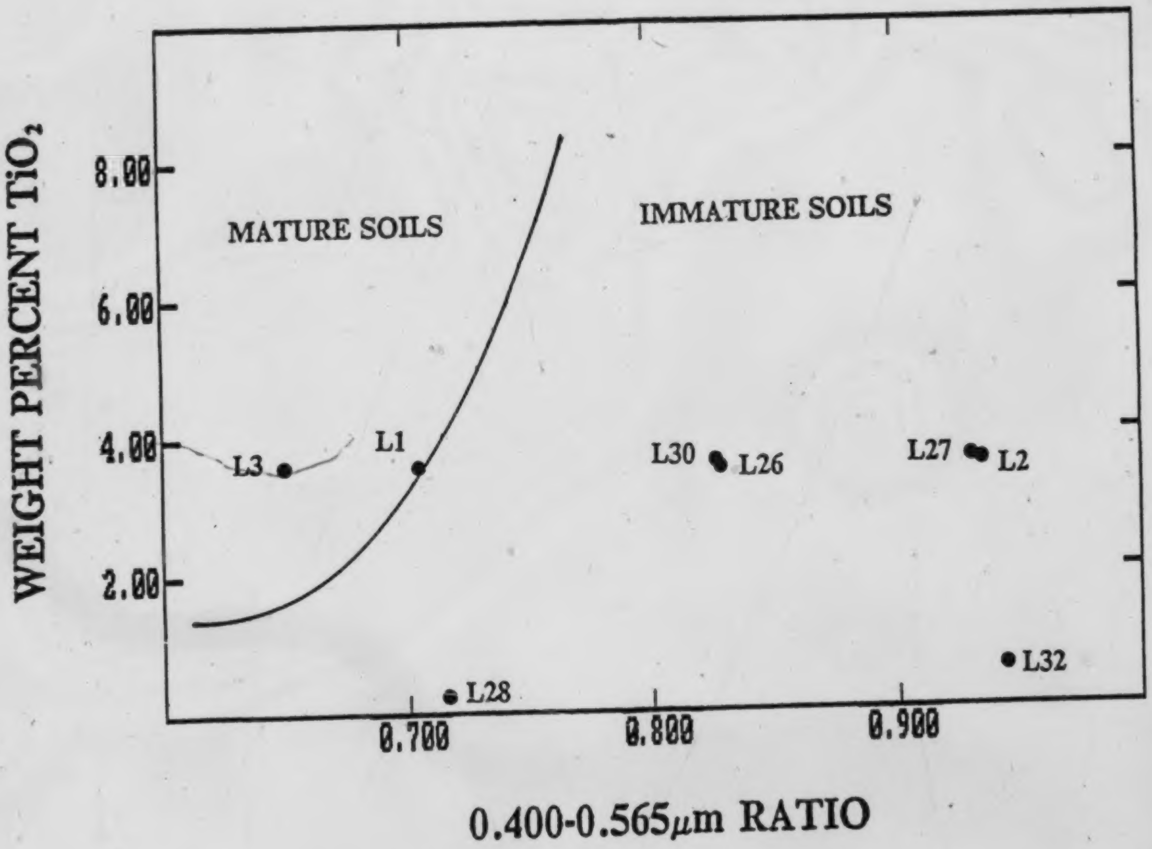

Figure V-10. Variation of 0.402:0.565μm reflectance as a function of TiO_2 and glass content with some points from this study superimposed (adapted from Charette *et al.*, 1974).

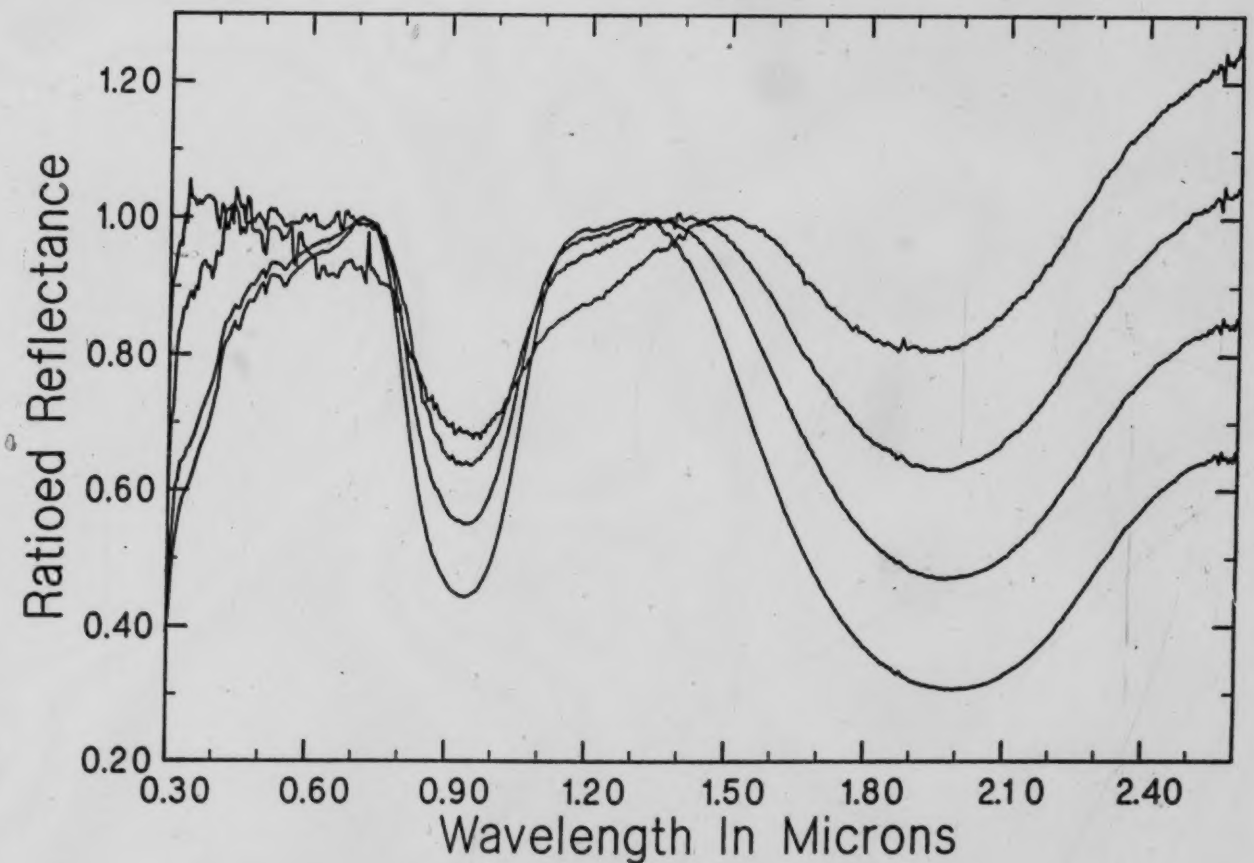

Figure V-11. Reflectance spectra of samples L3, L1, L26, and L27, after division by straight line continua. Reflectance at the band minima decreases in the sequence L27-L26-L1-L3.

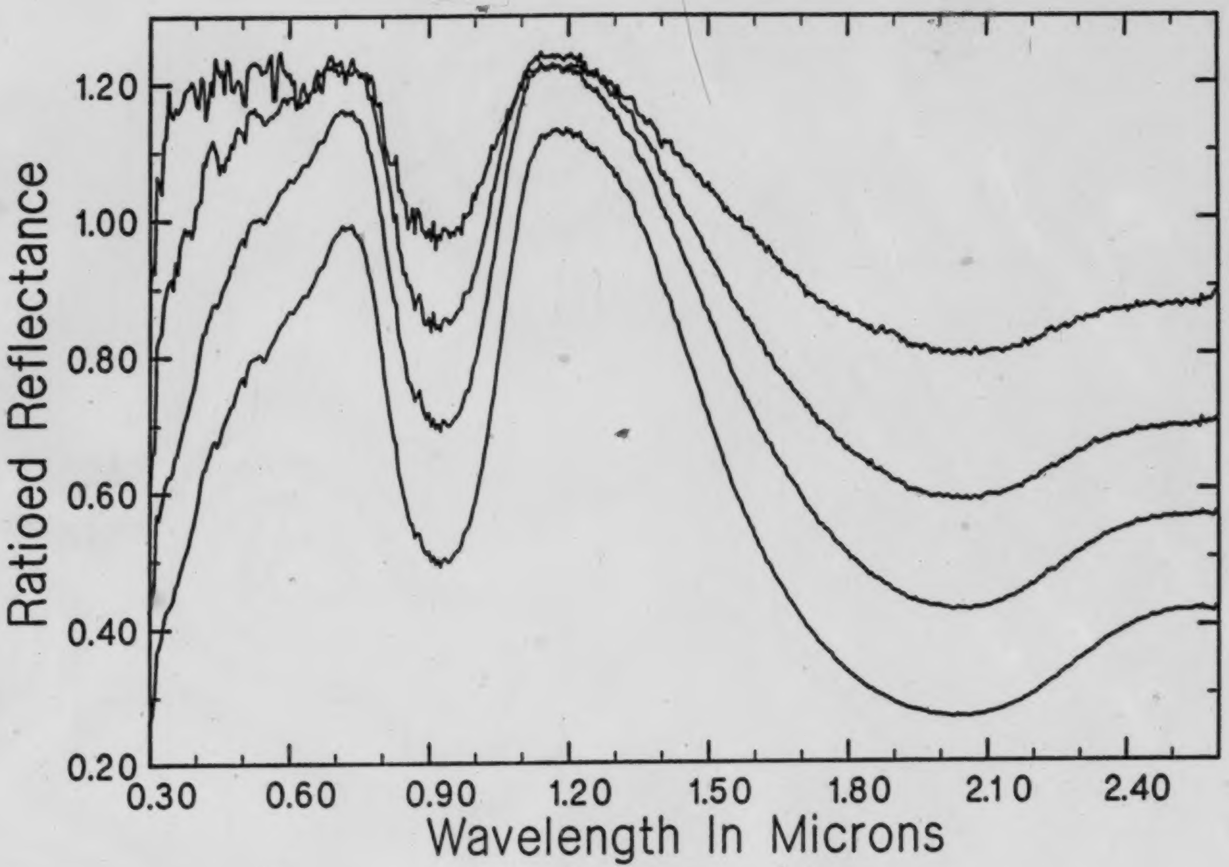

Figure V-12. Reflectance spectra of samples L3, L1, L26, and L27 after division by the scaled L2 glass spectrum- see text for details. Reflectance at the band minima decreases in the sequence L27-L26-L1-L3.

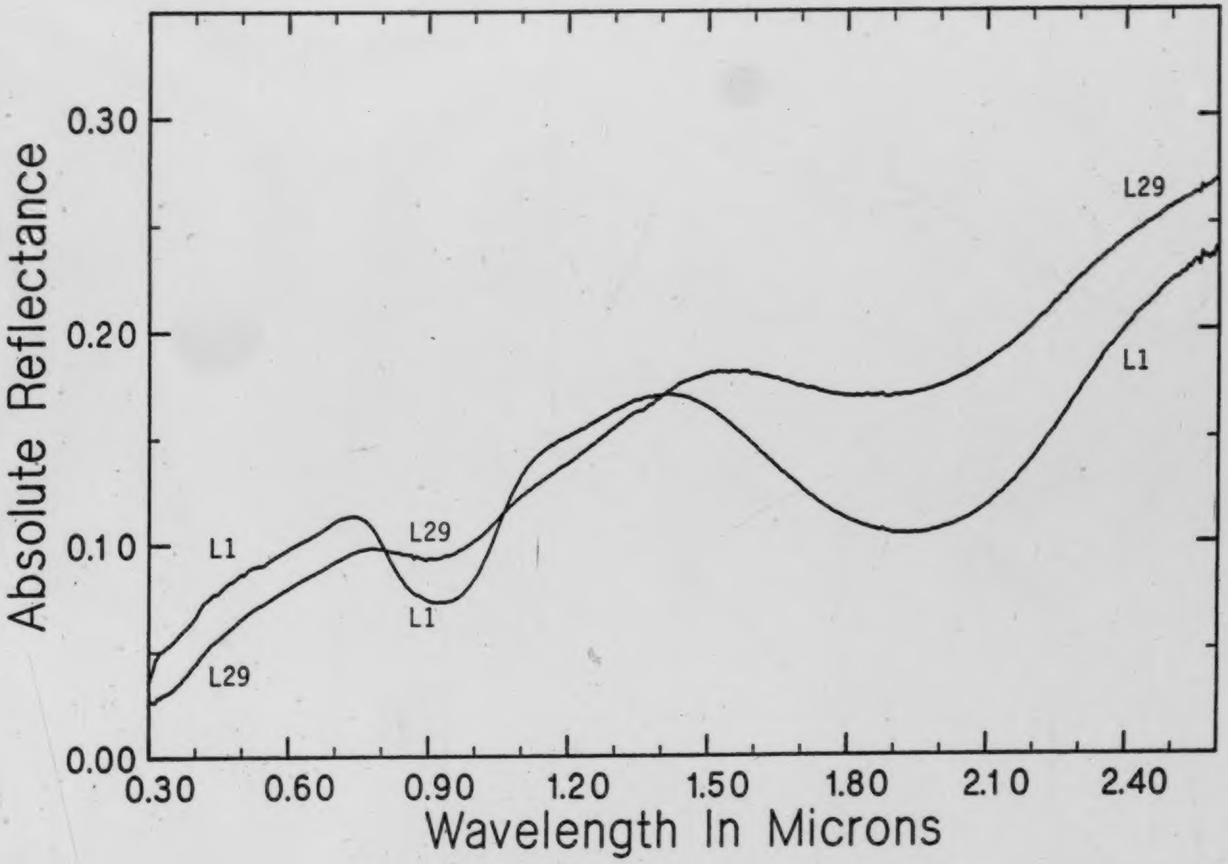

Figure V-13. Absolute reflectance spectra of samples L1 and L29.

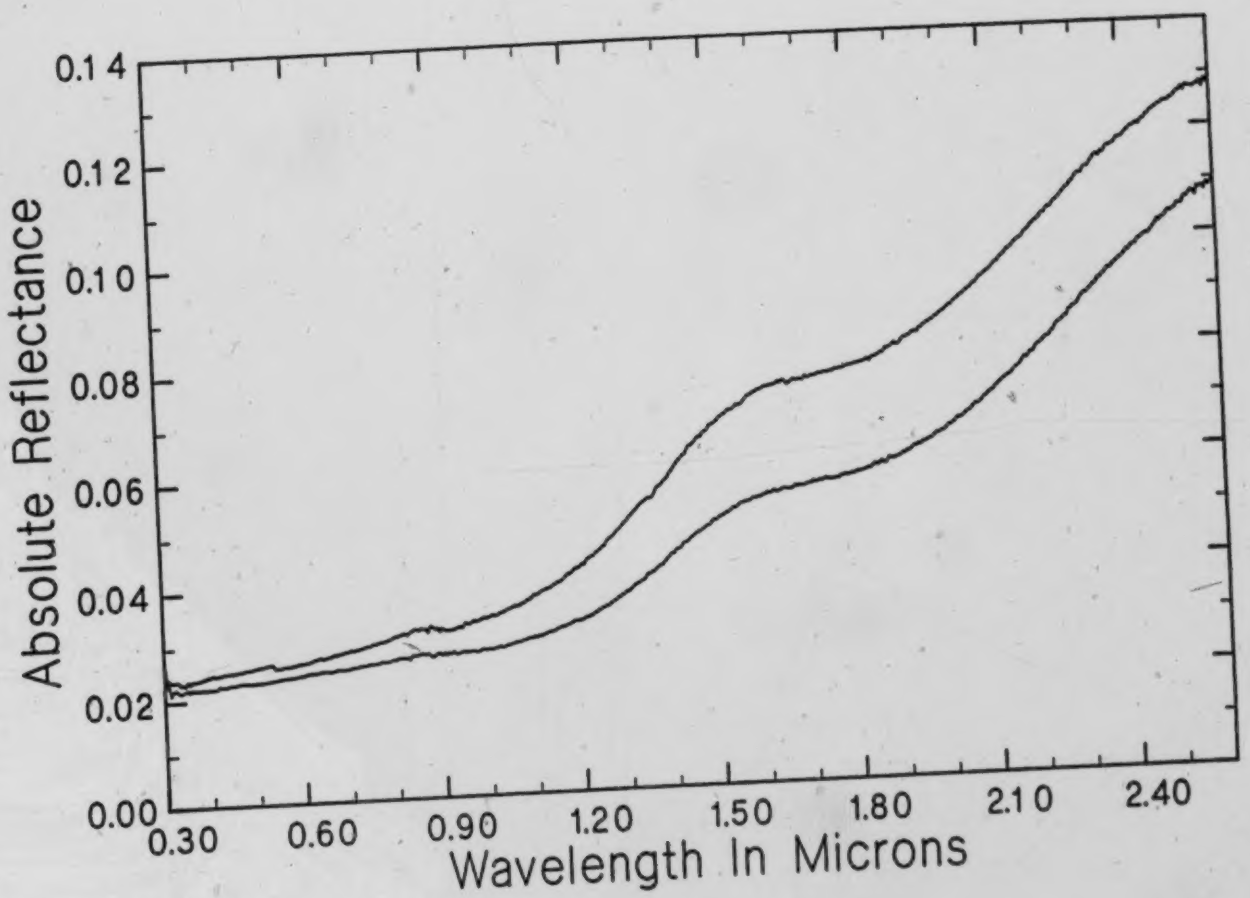

Figure V-14. Absolute reflectance spectra of samples L2 (lower) and L32 (upper).

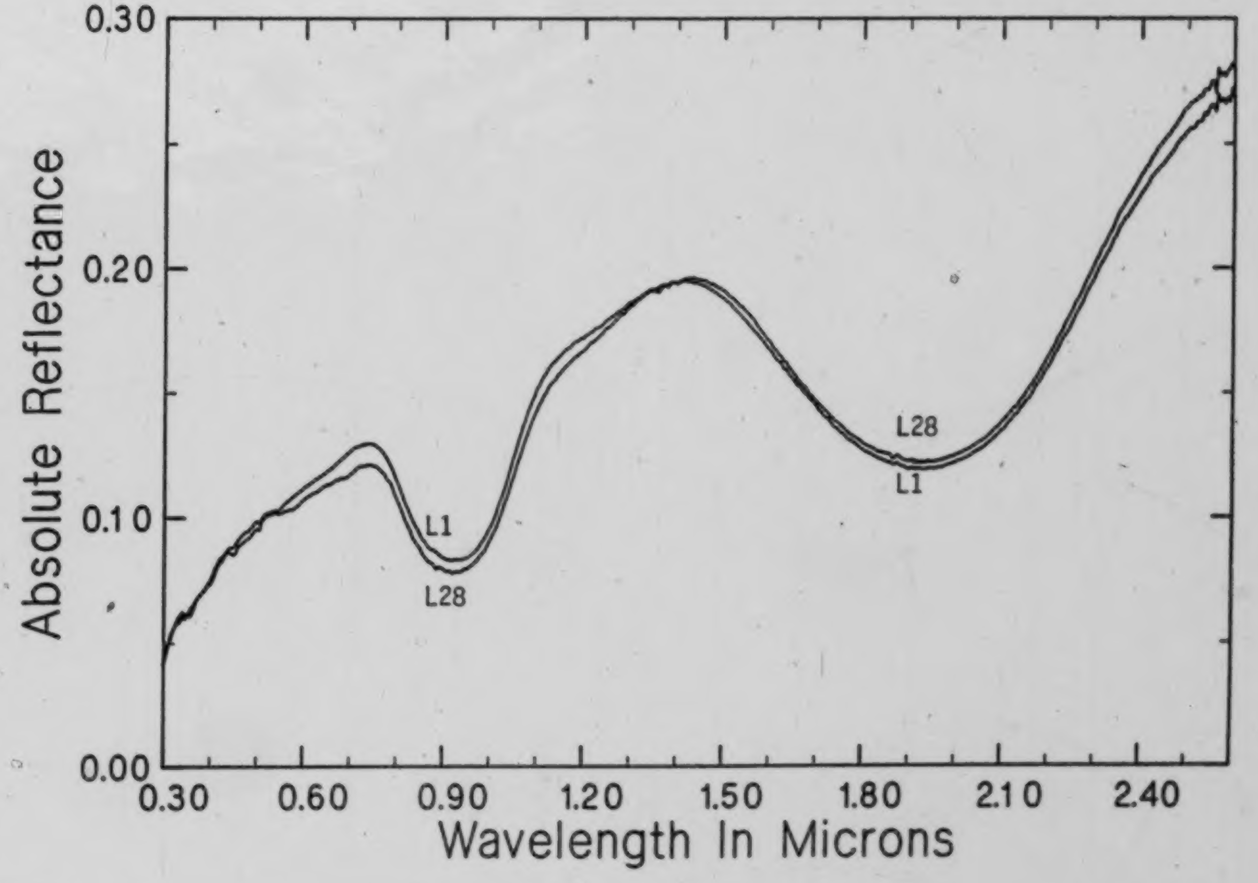

Figure V-15. Absolute reflectance spectra of samples L1 and L28.

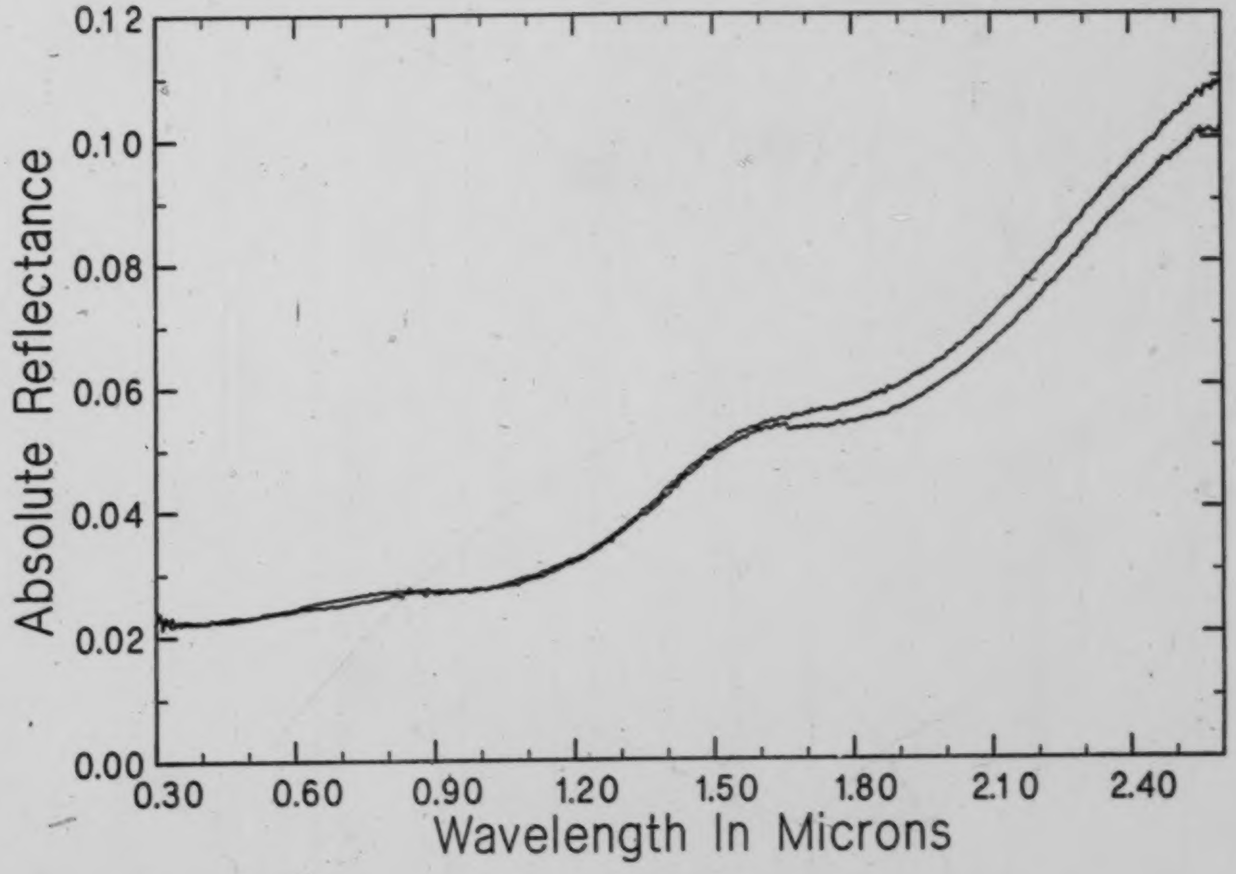

Figure V-16. Absolute reflectance spectra of samples L31 (lower) and L2 (upper).

A. REFERENCES

Abu-Eid, R.M. 1976. Absorption spectra of transition metal-bearing minerals at high pressures. In *The Physics and Chemistry of Minerals and Rocks* (R.G.J. Strens, Ed.), pp. 641-675. Wiley & Sons, London.

Adams, J.B. 1974. Visible and near-infrared diffuse reflectance spectra of pyroxenes as applied to remote sensing of solid objects in the solar system. *Jour. Geophys. Res.* **79**, 4829-4836.

Adams, J.B. 1975. Interpretation of visible and near-infrared diffuse reflectance spectra of pyroxenes and other rock-forming minerals. In *Infrared and Raman Spectroscopy of Lunar and Terrestrial Minerals* (C. Karr Jr., Ed.), pp. 91-116. Academic Press, New York.

Adams, J.B., and M.P. Charette 1975. Spectral reflectance of highland rock types at Apollo 17: Evidence from boulder 1, station 2. *The Moon* **14**, 483-489.

Adams, J.B., and A.L. Filice 1967. Spectral reflectance 0.4 to 2.0 microns of silicate rock powders. *Jour. Geophys. Res.* **72**, 5705-5715.

Adams, J.B., and L.H. Goullaud 1978. Plagioclase feldspars: Visible and near infrared diffuse reflectance spectra as applied to remote sensing. *Proc. Lunar Plan. Sci. Conf. 9th*, 2901-2909.

Adams, J.B., and T.B. McCord 1971a. Alteration of lunar optical properties: Age and composition effects. *Science* **171**, 567-571.

Adams, J.B., and T.B. McCord 1971b. Optical properties of mineral separates, glass, and anorthositic fragments from Apollo mare samples. *Proc. Second Lunar Sci. Conf.*, 2183-2195.

Adams, J.B., and T.B. McCord 1972. Electronic spectra of pyroxenes and interpretation of telescopic spectral reflectivity curves of the Moon. *Proc. Third Lunar Sci. Conf.*, 3021-3034.

Adams, J.B., and T.B. McCord 1973. Vitrification darkening in the lunar highlands and identification of Descartes material at the Apollo 16 site. *Proc. Fourth Lunar Sci. Conf.*, 163-177.

Adams, J.B., C. Pieters, and T.B. McCord 1974. Orange glass: Evidence for regional deposits of pyroclastic origin on the Moon. *Proc. Fifth Lunar Conf.*, 171-186.

Adams, J.B., F. Hörz, and R.V. Gibbons 1979. Effects of shock-loading on the reflectance spectra of plagioclase, pyroxene and glass. *Lunar Plan. Sci. Conf.* X, 1-3.

Aoyama, T., T. Hiroi, M. Miyamoto, and H. Takeda 1987. Absorption spectra and bulk chemical compositions of achondritic polymict breccias with reference to characterization of the surface of Vesta-like asteroids. *Lunar Plan. Sci. Conf.* XVIII, 27-28.

Bell, J.F., and B.R. Hawke 1984. Lunar dark-haloed impact craters: Origin and implications for early mare volcanism. *Jour. Geophys. Res.* **89**, 6899-6910.

Bell, P.M., and H.K. Mao 1974. Crystal-field spectra of Fe^{2+} and Fe^{3+} in synthetic basaltic glass as a function of oxygen fugacity. *Carnegie Inst. Wash. Yearb.* 73, 496-497.

Bell, P.M., H.K. Mao, and R.A. Weeks 1976. A study of the oxidation states of iron and titanium in synthetic glasses of lunar basalt composition. *Carnegie Inst. Wash. Yearb.* 75, 688-695.

Bell, P.M., H.K. Mao, and R.M. Hazen 1978. Luna 24 glass fragments: A study of soil samples recovered from the Russian Luna 24 mission to Mare Crisium. *Carnegie Inst. Wash. Yearb.* 77, 855-866.

Bruckenthal, E.A., and C.M. Pieters 1984. Spectral effects of natural shock on plagioclase feldspar. *Lunar Plan. Sci. Conf.* XV, 96-97.

Burns, R.G. 1970a. Crystal field spectra and evidence of cation ordering in olivine minerals. *Amer. Mineral.* 55, 1608-1632.

Burns, R.G. 1970b. *Mineralogical Applications of Crystal Field Theory*. Cambridge University Press, Cambridge.

Burns, R.G., F.E. Huggins, and R.M. Abu-Eid 1972. Polarized absorption spectra of single crystals of lunar pyroxenes and olivines. *Moon* 4, 93-102.

Charette, M.P., T.B. McCord, C. Pieters, and J.B. Adams 1974. Application of remote spectral reflectance measurements to lunar geology classification and determination of titanium content of lunar soils. *Jour. Geophys. Res.* **79**, 1606-1613.

Clark, R.N. 1980. A large-scale interactive one dimensional array processing system. *Publ. Astron. Soc. Pacific* **92**, 221-224.

Clark, R.N., and T.L. Roush 1984. Reflectance spectroscopy: Quantitative analysis techniques for remote sensing applications. *Jour. Geophys. Res.* **89**, 6329-6340.

Cloutis, E.A. 1985. *Interpretive Techniques for Reflectance Spectra of Mafic Silicates.* M.Sc. Thesis, University of Hawaii.

Cloutis, E.A., M.J. Gaffey, R. St J. Lambert, and D.G.W. Smith 1986a. The quality of geological information derivable from high resolution reflectance spectra: Results for mafic silicates. *Proc. 10th Canadian Symp. Rem. Sens.*, 309-318.

Cloutis, E.A., M.J. Gaffey, T.L. Jackowski, and K.L. Reed 1986b. Calibrations of phase abundance, composition, and particle size distribution for olivine-orthopyroxene mixtures from reflectance spectra. *Jour. Geophys. Res.* **91**, 11641-11653.

Cloutis, E.A., M.J. Gaffey, D.G.W. Smith, and R. St J. Lambert 1989. Reflectance spectra of mafic silicate-opaque assemblages with applications to meteorite spectra. *submitted to Icarus*, 49 pp.

Conel, J.E., and D.B. Nash 1970. Spectral reflectance and albedo of Apollo 11 lunar samples: Effects of irradiation and vitrification and comparison with telescopic observations. *Proc. Apollo 11 Lunar Sci. Conf.*, 2013-2023.

Crown, D.A., and C.M. Pieters 1987. Spectral properties of plagioclase and pyroxene mixtures and the interpretation of lunar soil spectra. *Icarus* **72**, 492-506.

Delano, J.W. 1986. Pristine lunar glass: Criteria, data, and implications. *Proc. Lunar Plan. Sci. Conf. 16th, Jour. Geophys. Res.* **91**, D201-D213.

Farr, T.G., B.A. Bates, R.L. Ralph, and J.B. Adams 1980. Effects of overlapping optical absorption bands of pyroxene and glass on the reflectance spectra of lunar soils. *Proc. Lunar Plan. Sci. Conf. 11th*, 719-729.

Hörz, F., M.J. Cintala, S. Olds, T.H. See, and F. Cardenas 1985. Experimental regolith evolution: Differential comminution of plagioclase, pyroxene and olivine. *Lunar Plan. Sci. Conf.* XVI, 362-363.

Housen, K.R., and L.L. Wilkening 1982. Regoliths on small bodies in the solar system. *Ann. Rev. Earth Plan. Sci.* **10**, 355-376.

Housen, K.R., L.L. Wilkening, C.R. Chapman, and R. Greenberg 1979a. Asteroidal regoliths. *Icarus* **39**, 317-351.

Housen, K.R., L.L. Wilkening, C.R. Chapman, and R.J. Greenberg 1979b. Regolith development and evolution on asteroids and the moon. In *Asteroids* (T. Gehrels, Ed.), pp. 601-627. University of Arizona Press, Tucson.

Hughes, S.S., J.W. Delano, and R.A. Schmitt 1988. Apollo 15 yellow-brown volcanic glass: Chemistry and petrogenetic relations to green volcanic glass and olivine normative mare basalts. *Geochim. Cosmochim. Acta* **52**, 2379-2391.

Hunt, G.R., and J.W. Salisbury 1970. Visible and near-infrared spectra of minerals and rocks: I Silicate minerals. *Mod. Geol.* **1**, 283-300.

Hunt, G.R., J.W. Salisbury, and C.J. Lenhoff 1971. Visible and near-infrared spectra of minerals and rocks: III. Oxides and hydroxides. *Mod. Geol.* **2**, 195-205.

King, T.V.V., and W.I. Ridley 1987. Relation of the spectroscopic reflectance of olivine to mineral chemistry and some remote sensing implications. *Jour. Geophys. Res.* **92**, 11457-11469.

King, T.V.V., M.J. Gaffey, and E.A. King 1983. Spectral reflectance measurements and surface characteristics of meteoritic condensates from solar furnace experiments. *Lunar Plan. Sci. Conf.* XIV, 371-372.

King, T.V.V., M.J. Gaffey, and L.A. McFadden 1984. Evidence for regolith maturation on asteroids. *Lunar Plan. Sci. Conf.* XV, 429-430.

Laul, J.C., and J.J. Papike 1980. The Apollo 17 drill core: Chemistry of size fractions and the nature of the fused soil components. *Proc. Lunar Plan. Sci. Conf. 11th*, 1395-1414.

Laul, J.C., O.D. Rode, S.B. Simon, and J.J. Papike 1987. The lunar regolith: Chemistry and petrology of Luna 24 grain size fractions. *Geochim. Cosmochim. Acta* **51**, 661-673.

Lucey, P.G., B.R. Hawke, C.M. Pieters, J.W. Head, and T.B. McCord 1986. A compositional study of the Aristarchus region of the Moon using near-infrared reflectance spectroscopy. *Proc. Sixteenth Lunar Plan. Sci. Conf.; Jour. Geophys. Res.* **91**, 344-354.

Mao, H.K., A. El Goresy, and P.M. Bell 1974. Evidence of extensive chemical reduction in lunar regolith samples from the Apollo 17 site. *Proc. Fifth Lunar Conf.*, 673-683.

McFadden, L.A. 1983a. S-type asteroids and their relation to ordinary chondrites. *Meteoritics* **18**, 352-353.

McFadden, L.A. 1983b. Reflectance characteristics of some Antarctic meteorites and their relation to asteroid surface composition. *Bull. Amer. Astron. Soc.* **15**, 827.

McFadden, L.A., and M.J. Gaffey 1978. Calibration of quantitative mineral abundances determined from meteorite reflection spectra and applications to solar system objects. *Meteoritics* 13, 556-557.

Nash, D.B., and J.E. Conel 1973. Vitrification darkening of rock powders: Implications for optical properties of the lunar surface. *The Moon* **8**, 346-364.

Nash, D.B., and J.E. Conel 1974. Spectral reflectance systematics for mixtures of powdered hypersthene, labradorite and ilmenite. *Jour. Geophys. Res.* **79**, 1615-1621.

Papike, J.J., S.B. Simon, C. White, and J.C. Laul 1981. The relationship of the lunar regolith <10μm fraction and agglutinates. Part I: A model for agglutinate formation and some indirect supportive evidence. *Proc. Lunar Plan. Sci. Conf. 12th*, 409-420.

Papike, J.J., S.B. Simon, and J.C. Laul 1982. The lunar regolith: Chemistry, mineralogy, and petrology. *Rev. Geophys. Space Phys.* **20**, 761-826.

Pieters, C.M. 1982. Copernicus crater central peak: Lunar mountain of unique composition. *Science* **215**, 59-61.

Pieters, C.M. 1983. Strength of mineral absorption features in the transmitted component of near-infrared light: First results from RELAB. *Jour. Geophys. Res.* **88**, 9534-9544.

Pieters, C.M. 1984. Asteroid-meteorite connection: Regolith effects implied by lunar reflectance spectra. *Meteoritics* **19**, 290-291.

Pieters, C.M. 1986. Composition of the lunar highland crust from near-infrared spectroscopy. *Rev. Geophys.* **24**, 557-578.

Pieters, C.M., and J.F. Mustard 1988. Exploration of crustal/mantle material for the Earth and Moon using reflectance spectroscopy. *Rem. Sens. Envir.* **24**, 151-178.

See, T.H., and F. Hörz 1988. Formation of agglutinate-like particles in an experimental regolith. *Proc. Eighteenth Lunar Plan. Sci. Conf.*, 423-434.

Simon, S.B., J.J. Papike, F. Hörz, and T.H. See 1986. An experimental investigation of agglutinate melting mechanisms: Shocked mixtures of Apollo 11 and 16 soils. *Proc. Seventeenth Lunar Plan. Sci. Conf., Jour. Geophys. Res.* **91**, E64-E74.

Smith, J.V. 1974. Lunar mineralogy: A heavenly detective story. Presidential Address, Part I. *Amer. Mineral.* **59**, 231-243.

Smith, J.V., and I.M. Steele 1976. Lunar mineralogy: A heavenly detective story. Part II. *Amer. Mineral.* **61**, 1059-1116.

Taylor, S.R. 1982. *Planetary Science: A Lunar Perspective*. Lunar & Planetary Institute, Houston.

Weidner, V.R., and J.J. Hsia 1981. Reflection properties of pressed polytetrafluoroethylene powder. *Jour. Opt. Soc. Amer.* **71**, 856-861.

VI. CONCLUSION

The analysis of remotely sensed reflectance spectra of many targets in the solar system is hampered by the lack of laboratory data on the spectral properties of candidate materials. Aside from the Earth, the only other body for which geological samples from a known locality are available is the Moon. Consequently, exploration of inaccessible targets is best accomplished through remote sensing. A number of candidate materials for various targets in the inner solar system were spectrally characterized in the laboratory.

One of the main goals of this study is to understand the spectral reflectance properties of asteroids. Main-belt asteroids generally reside in the region between Mars and Jupiter. This region is also the boundary between the small, rocky inner planets (Mercury, Venus, Earth, Mars) and the giant, outer, gas-rich planets (Jupiter, Saturn, Uranus, Neptune). Determining the compositional structure of the main asteroid belt has important implications for understanding the reasons for the difference between the inner and outer solar system, for theories concerning the origin of the asteroid belt, and for the origin and evolution of the solar system (Gaffey, 1984; Bell, 1986; Gaffey, 1986; 1988).

The surface mineralogies of the various asteroid classes are poorly known at present. Different interpretation have been advanced for most of the major asteroid classes. The laboratory reflectance spectra are an attempt to reduce some of the uncertainties in spectral interpretation and to reconcile the spectral data with other observational data such as photopolarimetry and radiometry.

The mafic silicate+metal spectra are most relevant to the interpretation of S- and A-class asteroid spectra (Bell *et al.*, 1984; Gaffey, 1984). These two classes comprise a substantial fraction of the inner main belt asteroids (Gradie & Tedesco, 1982). Asteroid (8) Flora was selected for spectral analysis because it is one of the most well characterized of the S-class asteroids. Its telescopic spectra, analyzed on the basis of the laboratory spectra, suggests a surface assemblage consisting of ~50 wt. % metal, ~40 wt. % olivine (Fa=35±30), ~10 wt. % orthopyroxene (Fs=$30^{[illegible]}_{[illegible]}$), and perhaps a few weight percent clinopyroxene. A significant portion of the optically active surface consists of fine-grained (<45μm size) material. Other observational data, such as radar and polarimetric observations, are compatible with such an assemblage. The closest meteorite analogues to Flora are the pallasites and lodranites. However, the pallasites contain less pyroxene than is indicated for Flora, while the most compatible lodranite is deficient in metal relative to Flora.

Less observational data are available for the A-class asteroids, but the best characterized member of this group is probably (446) Aeternitas. The reflectance spectrum of Aeternitas is interpreted as indicating a surface assemblage of ~35 wt. % metal, ~55 wt. % olivine (Fa=20±10), ~3 wt. % orthopyroxene (Fs<45), and 7 wt. % clinopyroxene (Fs<17). A substantial fine-grained (<45μm size) surface component is probably present. The Eagle Station sub-group of pallasites have similar metal:olivine ratios and olivine compositions to those derived for Aeternitas. These meteorites contain almost no pyroxene which seems to be a necessary surface component on Aeternitas.

The inner part of the main asteroid belt is dominated by the S, A, M and E classes of asteroids (Gradie & Tedesco, 1982). The reflectance spectra of the M- and E-classes are largely devoid of well-defined absorption bands. The laboratory reflectance spectra of a number of materials exhibiting no well-defined absorption bands, which are possible candidates for the surfaces of M- and E-class asteroids, were measured. In the absence of absorption bands, spectral features such as slopes and wavelength positions of inflection points can be used to distinguish the different materials. The closest spectral analogue to the largest M-class asteroid, (16) Psyche, is very fine-grained (<<45μm size) metal, although an enstatite chondrite-like surface assemblage for this asteroid cannot be ruled out. This assignment is based almost exclusively on the overall slope and inflection point present in the reflectance spectrum of Psyche. Polarimetric and radar data are entirely consistent with a metal-rich surface assemblage on Psyche.

Of the E-class asteroids, (44) Nysa, was selected for analysis because high-quality spectral data are available for this asteroid. The high absolute reflectance of this object is most consistent with a surface composed of materials similar to those found in aubrites. A number of weak absorption bands present in the spectrum of Nysa can perhaps be attributed to a material similar to the chondritic inclusions found in the Cumberland Falls and ALH78113 aubrites. However, this assignment is not definite because the reflectance spectra of these inclusions and similar carbonaceous chondrites have not been measured. The strength of the absorption bands and overall reflectance spectrum of Nysa suggests a surface composed of ~90 wt. % iron-poor enstatite ($Fs<1$), perhaps with minor metal and troilite, and up to 10 wt. % of a material similar to the Cumberland Falls dark, chondritic inclusions. The polarimetric data are consistent with this assignment. Both polarimetric and spectral data suggest that a substantial portion of the surface of Nysa is composed of fine-grained ($<45\mu m$ size) materials.

Mafic silicate + opaque laboratory spectra have different spectral properties than mafic silicate + metal assemblages, and their spectra can be analyzed using spectral deconvolution techniques developed for mafic silicates (Cloutis *et al.*, 1986a, 1986b). In cases where mafic silicate absorption bands are resolvable, which may be the case for many dark asteroids (Gaffey, 1978; 1980; Vilas & Gaffey, 1989), the abundances and major element compositions of the mafic silicate phases may be determinable.

Mafic silicate + glass laboratory spectra may be applicable to the analysis of some asteroid spectra that have features similar to glass-rich assemblages (King *et al.*, 1983; McFadden, 1983a, 1983b; King *et al.*, 1984; Pieters, 1984), and to lunar remote sensing. It may be possible to reconstruct mafic silicate absorption band positions if the glass spectrum can be accurately reproduced and divided out of the spectrum. Knowing the absorption band positions would place severe constraints on possible mafic silicate compositions and abundances.

The interpreted surface assemblages of the various representative members of the major inner main belt asteroid groups suggests that the abundances of meteorites on the Earth do not correspond to asteroidal abundances. The S-asteroids, and perhaps the A-asteroids, may be unrepresented in terrestrial meteorite collections. If the spectroscopic interpretations are relaxed slightly, the closest meteorite analogues are among the rarest groups- lodranites and pallasites. The M- and E-class asteroids seem to be related to the iron meteorites and enstatite achondrites (aubrites), respectively. The S-, A-, M- and E-class asteroids are all interpreted as differentiated assemblages although the differentiation process on S and A asteroids does not appear to have been of sufficient intensity to cause widepread differentiation and gravitational separation of materials. The interpretation of the observational data for one M-class asteroid does not definitively support its being a differentiated object. Current theories suggesting that inner main belt asteroids were severely heated (Bell, 1986) support the case for the M-class asteroids being differentiated objects.

Most lunar telescopic spectra, and a few asteroidal spectra, show a strong red slope (reflectance increasing towards longer wavelengths) due to the presence of glass or agglutinates (Bell & Hawke, 1984; Lucey *et al.*, 1986; Pieters, 1986). While the laboratory spectra of mafic silicates+glass fail to reproduce this effect at shorter wavelengths, the results suggest that current spectral deconvolution techniques are generally adequate for restoring mafic silicate absorption band positions to within a few nanometers of the unaltered spectra. Better results would be achieved by dividing out an accurate glass spectrum. This may be possible in the lunar case if, as suspected, all lunar agglutinates are spectrally quite similar. Final resolution of this issue will increase the quantity and quality of geological information derivable from lunar telescopic spectra.

Although not explicitly dealt with, the results of this study are potentially applicable to other bodies in the inner solar system. Reflectance spectra of Mercury have been interpreted as perhaps indicating the presence of mafic silicates, although thermal emission complicates the spectral interpretation (McCord & Clark, 1979). If future surface landers on Venus are equipped with spectrometers capable of imaging the surface at a number of wavelengths, it may be possible to derive mineralogical information from these data for regions inferred to possess basaltic surface assemblages (Surkov *et al.*, 1983). As spatial and spectral resolution of terrestrial remote sensing systems improves, detailed analysis of basaltic exposures will become more feasible (Pieters & Mustard, 1988). Near-Earth asteroid spectra are also amenable to analysis, particularly as the quality of the telescopic data improves (McFadden, 1983c). Meteoritical evidence, and telescopic and spacecraft data suggest that relatively unaltered basaltic regions may exist on Mars (Lucchitta, 1981; Wood & Ashwal, 1981; Singer, 1982; Huguenin, 1987). If high spectral and spatial resolution data become available from future missions it may be possible to identify these areas and derive compositional information on the nature of unaltered martian crust. The martian Moons, Phobos and Deimos, have dark, relatively featureless reflectance spectra (Veverka & Thomas, 1979). As the quality of the spectral data for these objects improves, weak mafic silicate bands may well be detected. If this is the case, the spectral deconvolution techniques developed for mafic silicates may be applicable to the analysis of these data. Clearly, the full applications of the spectral data have yet to be realized. However, the potential applications encompass all the major bodies of the inner solar system.

A. REFERENCES

Bell, J.F. 1986. Mineralogical evolution of meteorite parent bodies, *Lunar Plan. Sci. Conf. XVII*, 985-986.

Bell, J.F., and B.R. Hawke 1984. Lunar dark-haloed impact craters: Origins and implications for early mare volcanism. *Jour. Geophys. Res.* **89**, 6899-6910.

Bell, J.F., M.J. Gaffey, and B.R. Hawke 1984. Spectroscopic identification of probable pallasite parent bodies. *Meteoritics* **19**, 187-188.

Cloutis, E.A., M.J. Gaffey, R. St J. Lambert, and D.G.W. Smith 1986a. The quality of geological information derivable from high-resolution reflectance spectra: Results for mafic silicates. *Proc. 10th Canadian Symp. Rem. Sens.*, 309-318.

Cloutis, E.A., M.J. Gaffey, T.L. Jackowski, and K.L. Reed 1986b. Calibrations of phase abundance, composition, and particle size distribution for olivine-orthopyroxene mixtures from reflectance spectra. *Jour. Geophys. Res.* **91**, 11641-11653.

Gaffey, M.J. 1978. Optical and spectral properties of the low-albedo meteorites: Applications to the interpretation of the spectra of dark asteroids. *Lunar Plan. Sci. Conf. IX*, 362-364.

Gaffey, M.J. 1980. Mineralogically diagnostic features in the visible and near-infrared reflectance spectra of carbonaceous chondrite assemblages. *Lunar Plan. Sci. Conf. XI*, 312-313.

Gaffey, M.J. 1984. Rotational spectral variations of asteroid (8) Flora: Implications for the nature of the S-type asteroids and for the parent bodies of the ordinary chondrites. *Icarus* **60**, 83-116.

Gaffey, M.J. 1986. The spectral and physical properties of metal in meteorite assemblages: Implications for asteroid surface materials. *Icarus* **66**, 468-486.

Gaffey, M.J. 1988. Thermal history of the asteroid belt: Implications for accretion of the terrestrial planets. *Lunar Plan. Sci. Conf. XIX*, 369-370.

Gradie, J., and E. Tedesco 1982. Compositional structure of the asteroid belt. *Science* **216**, 1405-1407.

Hugeunin, R.L. 1987. The silicate component of martian dust. *Icarus* **70**, 162-188.

King, T.V.V., M.J. Gaffey, and E.A. King 1983. Spectral reflectance measurements and surface characteristics of meteoritic condensates from solar furnace experiments. *Lunar Plan. Sci. Conf. XIV*, 371-372.

King, T.V.V., M.J. Gaffey, and L.A. McFadden 1984. Evidence for regolith maturation on asteroids. *Lunar Plan. Sci. Conf. XV*, 429-430.

Lucchitta, B.K. 1987. Recent mafic volcanism on Mars. *Science* **235**, 565-567.

Lucey, P.G., B.R. Hawke, C.M. Pieters, J.W. Head, and T.B. McCord 1986. A compositional study of the Aristarchus region of the Moon using near-infrared reflectance spectroscopy. *Proc. Sixteenth Lunar Plan. Sci. Conf.; Jour. Geophys. Res.* **91**, 344-354.

McCord, T.B., and R.N. Clark 1979. The Mercury soil: Presence of Fe^{2+}. *Jour. Geophys. Res.* **84**, 7664-7668.

McFadden, L.A. 1983a. S-type asteroids and their relation to ordinary chondrites. *Meteoritics* **18**, 352-353.

McFadden, L.A. 1983b. Reflectance characteristics of some Antarctic meteorites and their relation to asteroid surface composition. *Bull. Amer. Astron. Soc.* **15**, 827.

McFadden, L.A. 1983c. *Spectral Reflectance of Near-Earth Asteroids: Implications for Composition, Origin and Evolution*. Ph.D. Dissertation, University of Hawaii.

Pieters, C.M. 1984. Asteroid-meteorite connection: Regolith effects implied by lunar reflectance spectra. *Meteoritics* **19**, 290-291.

Pieters, C.M. 1986. Composition of the lunar highland crust from near-infrared spectroscopy. *Rev. Geophys.* **24**, 557-578.

Pieters, C.M., and J.F. Mustard 1988. Exploration of crustal/mantle material for the Earth and Moon using reflectance spectroscopy. *Rem. Sens. Envir.* **24**, 151-178.

Singer, R.B. 1982. Spectral evidence for the mineralogy of high-albedo soils and dust on Mars. *Jour. Geophys. Res.* **87**, 10159-10168.

Surkov, Y.A., L.P. Moskalyeva, O.P. Shcheglov, V.P. Kharyukova, O.S. Manvelyan, V.S.

Kirichenko, and A.D. Dudin 1983. Determination of the elemental composition of rocks on Venus by Venera 13 and Venera 14 (Preliminary results). *Proc. 13th Lunar Plan. Sci. Conf.*, A481-A493.

Veverka, J., and P. Thomas 1979. Phobos and Deimos: A preview of what asteroids are like?. In *Asteroids* (T. Gehrels, Ed.), University of Arizona Press, Tucson, pp. 628-651.

Vilas, F., and M.J. Gaffey 1989. Weak Fe^{2+}-Fe^{3+} charge transfer absorption features seen in CM2 carbonaceous chondrites and narrowband reflectance spectra of primitive asteroids. *Lunar Plan. Sci. Conf. XX*, 1156-1157.

Wood, C.A., and L.D. Ashwal 1981. SNC meteorites: Igneous rocks from Mars?. *Proc. Lunar Plan. Sci. 12B*, 1359-1375.

VII. APPENDIX

EXPERIMENTAL PROCEDURES

One of the primary aims of this project was to obtain comprehensive chemical data for the various samples in order to strengthen potential relationships between their spectral and chemical properties. The procedures followed in attaining this goal are outlined below.

The various minerals used in this study were selected from a much larger suite of chemically characterized materials. The chemical analyses represent a combination of microprobe and wet chemical data. A number of fragments of each mineral were mounted in epoxy discs for microprobe analysis, polished, and carbon coated. The microprobe analyses of the olivine (OLV003), pyroxenes (PYX032, PYX117), plagioclase (PLG108), and magnetite (MAG101) were acquired at the University of Calgary microprobe facility. The electron microprobe was run with a beam current of 0.15μA and an operating voltage of 15 keV. Integration times were 20 seconds per point, with a nominal beam diameter of ~1μm. The standard samples were as similar to the minerals being analyzed as possible. The elements were analyzed using crystal spectrometers, four fixed crystals for Fe, Mg, Al, and Si, and four adjustable spectrometers for other elements. The average analyses given represent an average of 4-8 point analyses. The data were reduced using Bence-Albee α and β factors.

The lunar analogue glasses (L2, L31, L32) were analyzed at the University of Alberta electron microprobe laboratory, using silicates as standards whenever possible. Operating conditions were: 15keV operating voltage, 0.06μA probe current, and a nominal spot size of ~1μm. Integration times were 40 seconds on peaks and 10 seconds on backgrounds. Four adjustable crystal spectrometers were available at a time. Data reduction was performed using the Applied Research Laboratory version of the MAGIC IV program. The ilmenite sample (ILM101) was analyzed at both facilities as a check on interlaboratory reproducibility. The ferrous iron contents of the olivine, pyroxenes, glasses, and magnetite were determined by wet chemistry. Following standard procedures, a portion of each sample was dissolved in HF and sulfuric acid, stabilized, and titrated with a standard permanganate solution. The titrate was also calibrated against a known solution and a blank. A separate pyroxene sample was run as a standard to check for reproducibility. Ferrous iron contents were repeatedly reproducible to within ±0.2 mole % FeO, absolute. Ferric iron was calculated as the difference between total and ferrous iron.

The powders required for spectral analysis were ground in an alumina mortar and pestle and repeatedly wet sieved with acetone to produce well-constrained size fractions. The sample of the Happy Canyon E7 chondrite was contaminated with rust. It was initially crushed to $<325\mu m$ and soaked in an $HCl+HNO_3$ to dissolve the iron oxides. Once a visible reaction had ceased, the sample was crushed in the mortar and pestle and wet sieved with acetone. This material was found to be >99.5% free of visible contaminants. The meteoritic metal powder (MET101) was obtained from a visually unaltered portion of the interior of a slice of the Odessa, TX iron meteorite. The protective lacquer on the sample, and any signs of fusion crust or alteration were removed from the sample area with an emery grinding wheel. The cleaned area was then ground on the emery wheel (after cleaning the wheel of visible contaminants) and the powder retained. The metal was separated from the grinding wheel contaminants using a hand magnet. A visual inspection of the powder showed this to be an extremely effective procedure. The metal powder was largely in the form of filamentary shavings. A portion of this powder was swirled and gently beaten in the alumina mortar and pestle for several minutes. This resulted in a marked alteration of the largely filamentary particles to more equidimensional forms. Both beaten and unbeaten powders were separately wet sieved with acetone. Upon completion of the sieving, the samples were transferred to a dry nitrogen environment chamber, thoroughly purged, separated into required amounts, and sealed in vials. The meteoritic metal powders were exposed to atmosphere for <2 days while in the possession of the author. The artificial metal powders were received in sealed containers from the various suppliers, and opened only in the environment chamber. A portion of each sample (2-5 grams) was transfered to separate vials, and all containers were subsequently sealed before removal from the chamber.

The various mineral mixtures were all made on a weight percentage basis. Each sample totaled at least 750 mg, in order to obtain good signal:noise ratios during spectral measurements. The weighing of the samples was accomplished using a Mettler B5 Analytical Balance, to an accuracy of ±0.2mg. The mixtures involving the amorphous carbon were measured using a Mettler M5 microbalance, to an accuracy of ±0.02mg. All mineral mixtures were alternately gently stirred and shaken in order to homogenize them. In the case of the amorphous carbon mixtures, approximately 15-30 minutes were required to produce a homogeneous-appearing sample.

The glasses prepared for the lunar analogue samples were made with the 0-45μm sized mineral fractions in order to facilitate fusion. The constituents were weighed out using the Mettler B5 Analytical Balance. All mixtures were gently stirred using a glass rod and gently shaken in order to obtain a uniform sample. They were then placed in a platinum crucible and held at 1000°C for 15-30 minutes to drive off any water. They were then transferred to a Deltech DT-31-VT furnace and held at 1400°C for 15 minutes (90 minutes for sample L31) in a CO-CO_2 atmosphere at an oxygen fugacity of 10^{-9} atmospheres. After removal from the furnace, the lower half of the crucible was immersed in a water bath to prevent any water from coming in contact with the sample. The glasses were then powdered in the same way as the mineral samples, and examined under a petrographic microscope for homogeneity.

The reflectance spectra were measured at either the U.S. Geological Survey spectrometer facility in Denver, CO, or at the NASA RELAB facility at Brown University in Providence, RI. The U.S.G.S. instrument is a modified Beckman 5270 double-grating, double-beam instrument, custom interfaced to an IBM PC computer. The reflectance spectra of the standard and sample were measured using an integrating sphere. The 1x resolution program (standard slit program) provides spectral resolution (Δμm/μm) of 200. The sample spectra were measured relative to pressed polytetrafluoroethylene powder (halon) which is a near-perfect diffuse reflector in the 0.3-2.6μm region. The spectra were corrected for minor irregularities in the absolute reflectance of the standard in the 2μm region (Weidner & Hsia,

1981) and for dark current offsets. More complete details of the instrument can be found in King (1986) and King & Ridley (1987).

The NASA RELAB instrument measures bidirectional reflectance (spectrogoniometer) - both incidence and emission angles can be varied. The samples were measured at either $i=0°$ and $e=15°$, or $i=30°$ and $e=0°$. They are also measured relative to halon and corrected in a similar manner. More complete descriptions of the instrument and the facility can be found in Pieters (1983; 1987).

The corrected spectra were analyzed using the Gaffey Spectrum Processing System - a PC compatible version of SPECPR (Clark, 1980). A number of spectral parameters that are useful for quantifying various physical and chemical properties of the samples were examined. Among the most useful are band minima and band center wavelength positions, band depths, and band areas. Band minima were calculated by fitting a 3-term polynomial to 10-15 channels (~50-75nm) on either side of a visually determined minimum. Higher order polynomials were also looked at, but did not show any significant differences from the quadratic fits. Band centers and band depths were calculated after dividing the reflectance spectrum by a straight line continuum that was constructed as a straight line segment tangent to the reflectance spectrum on either side of an absorption band. The reflectance spectra were then divided by this continuum The band centers were determined after continuum division in the same way as the band minima.

Band depths D_b were calculated as:

$$D_b=1-R_b/R_c$$

where R_b is the reflectance at the band minimum or center, and R_c is the reflectance of the continuum at the same wavelength as R_b. This seems to be the best approach to calculating meaningful band depths (Clark & Roush, 1984). For some of the lunar analogue spectra, the L2 spectrum was used as a continuum. In these cases, the L2 spectrum was multiplied by the factor required to increase its reflectance to that of the local peak located near 1.4μm in the other spectrum, making the L2 spectrum tangent at one point. The sample spectra were then divided by the scaled L2 spectra and the band depths and band centers were calculated in the same way as for the other spectra.

A. REFERENCES

Clark, R.N. 1980. A large-scale interactive one dimensional array processing system. *Publ. Astron. Soc. Pacific* **92**, 221-224.

Clark, R.N., and T.L. Roush 1984. Reflectance spectroscopy: Quantitative analysis techniques for remote sensing applications. *Jour. Geophys. Res.* **89**, 6329-6340.

King, T.V.V. 1986. *Contributions Towards a Quantitative Understanding of Reflectance Spectroscopy: Phyllosilicates, Olivine and Shocked Materials.* Ph.D. Dissertation, University of Hawaii.

King, T.V.V., and W.I. Ridley 1987. Relation of the spectroscopic reflectance of olivine to mineral chemistry and some remote sensing implications. *Jour. Geophys. Res.* **92**, 11457-11469.

Pieters, C.M. 1983. Strength of mineral absorption features in the transmitted component of near-infrared reflected light: First results from RELAB. *Jour. Geophys. Res.* **88**, 9534-9544.

Pieters, C.M. 1987. *Reflectance Experiment Laboratory Description and Users Manual.* Brown University.

Weidner, V.R., and J.J. Hsia 1981. Reflection properties of pressed polytetrafluoroethylene powder. *Jour. Opt. Soc. Amer.* **71**, 856-861.